UNIVERSITÀ DELLA CALABRIA

UNIVERSITA' DELLA CALABRIA

Dipartimento di Farmacia e scienza della salute e della nutrizione

Dottorato di Ricerca

in

Biochimica cellulare ed attivita dei Farmaci in oncologia XXVI ciclo

Con il contributo di MIUR

Role of PPARγ in breast cancer cell death and in adipocyte differentiation

MED/05 PATOLOGIA CLINICA

Coordinatore

Ch.mo Prof. Diego Sisci

Supervisore/Tutor: Ch.mo

Prof.ssa Daniela Bonofiglio

Dottorando: Dott./ssa Daniela Rovito

Index

Introduction

Peroxisome Proliferator-Activated Receptors (PPARs), belonging to the nuclear receptor superfamily, include the three isotypes PPARα (NR1C1), PPARβ/δ (also referred to as NUC1; NR1C2), and PPARγ (NR1C3). All of them are composed of four functional domains called A/B, C, D and E/F. The A/B domain is located at N-terminus and presents an AF-1 region that is responsible for independent activation by ligands of the receptor, the domain C is implicated in DNA binding (DBD), the domain D is the docking region for cofactors and domain E/F is responsible for the ligand-dependent activation containing AF-2 (LBD). In Figure 1 is reported the structure and post-translational modifications of PPARγ.

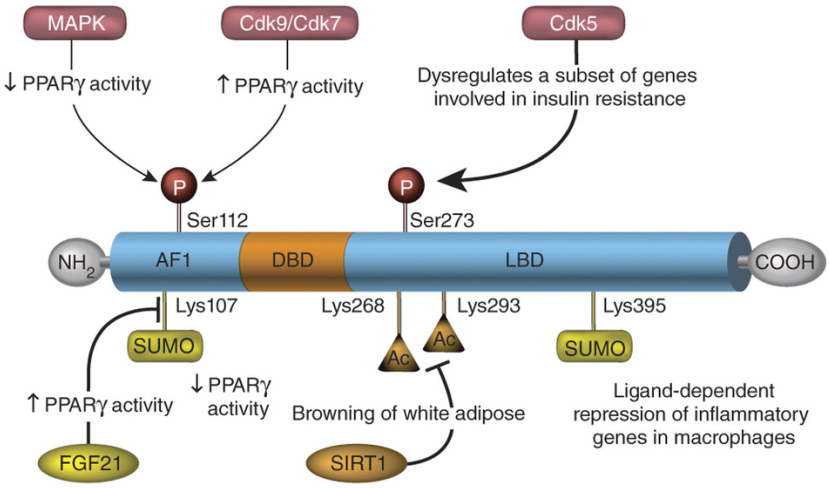

Figure 1: Nuclear receptor structure and post-translational modifications of PPARγ influence both its transcriptional activity and its protein stability in a cell- and context-dependent manner. Ac, acetylation; P, phosphorylation; Cdk9/Cdk7, Cyclin-dependent kinases 9 and 7.

PPARγ heterodimerizes with the Retinoid X Receptor (RXR) and regulates transcription of target genes through binding to specific response elements or PPREs, which consist of a direct repeat of the nuclear receptor hexameric DNA core recognition motif spaced by one nucleotide, to activate or repress gene transcription depending on its interaction with coactivators or corepressors, respectively (Figure 2) (Kondo Y et al. 2005).

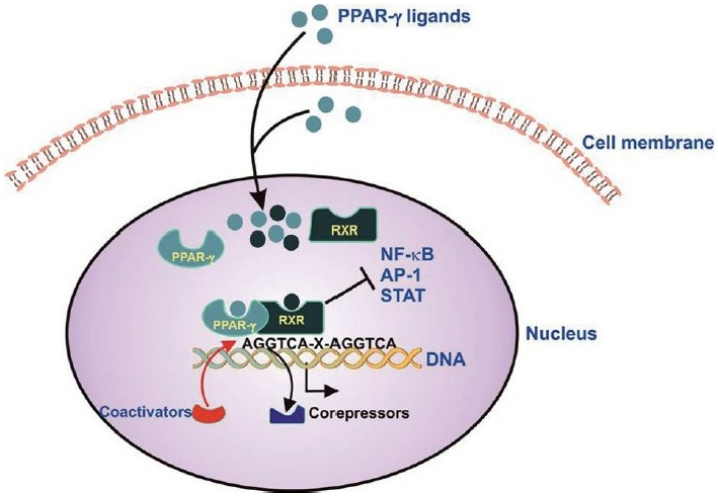

Figure 2: Schematic illustration of PPARγ-mediated gene regulation. PPAR-γ ligands originating from outside or inside the cell bind to the PPARγ, stimulating formation of a heterodimer with the retinoid X receptor (RXR). The PPAR-γ–RXR heterodimer binds to PPAR response elements (PPRE) comprising hexameric repeats of the sequence, AGGTCA-X-AGGTCA. This active heterodimer recruits coactivators to and/or derecruits corepressor molecules from the transcriptional start site, leading to increased transcription of selected genes. Activation of PPAR-γ can also inhibit the expression of genes regulated by specific proinflammatory transcription factors such as NF-kB, AP-1, and STAT.

In humans, the gene PPARγ is located on chromosome 3 in position 3p25 and is expressed as two isoforms, PPARγ1 and PPARγ2, generated by alternative promoter usage of the same gene, which gives rise to four distinct mRNAs. pparγ1, pparγ3, and pparγ4 mRNAs all encode the PPARγ1 polypeptide, while pparγ2 mRNA encodes the corresponding PPARγ2 polypeptide, which is identical to PPARγ1 with an additional 30 aminoacids present at the N terminus (Fajas et al., 1997; Meirhaeghe et al., 2003; Tontonoz et al., 1994b). PPARγ1 is expressed in many tissues, whereas PPARγ2 expression is restricted almost exclusively to adipose tissue.

Since its discovery in the 90's PPARγ has emerged as the prime regulator of adipocyte differentiation, a highly regulated process taking place from birth throughout adult life. The role in the adipogenesis is supported by overwhelming evidence from both in vivo and in vitro studies (Tontonoz et al., 1994a, 1994b, 1994c; Koutnikova et al., 2003). Its most notable function in regulating development of adipose tissue involves coordinating expression of many hundreds of genes responsible for establishment of the mature adipocyte phenotype. For example, PPARγ induces expression of the fat-specific adipocyte P2 (aP2) gene,

LPL, FATP, FABP, FAT, and ACS, the GLUT4 glucose transporter, c-Cbl-associated protein (CAP), glucokinase, uncoupling proteins 2 and 3 (UCP2 and UCP 3) and the mitochondrial citrate carrier (CIC) (Nagy L et al. 1998; Spiegelman B et al. 2001; Damiano F et al. 2012) (Fig.3).

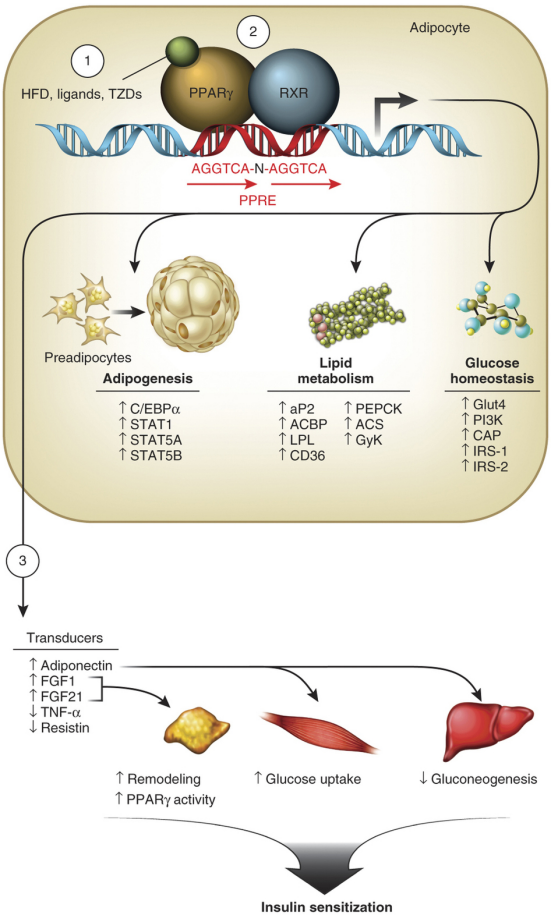

Figure 3: HFD, ligands or TZDs (1) activate PPARγ-RXR functional heterodimers (2) and maintain metabolic homeostasis through direct regulation of genes harboring PPAR response elements (PPREs) involved in adipocyte differentiation, lipid metabolism and glucose homeostasis, as well as the expression of adipose secreted factors that act as transducers for PPARγ (3). C/EBPα, CCAAT/enhancer-binding protein α; STAT1, STAT5A and STAT5B, signal transducer and activator of transcription 1, 5A and 5B, respectively; aP2, fatty acid binding protein 2; ACBP, acyl-CoA–binding protein; LPL, lipoprotein lipase; CD36, cluster of differentiation 36; PEPCK, phosphoenolpyruvate carboxykinase; ACS, acyl-CoA synthetase; GyK, glycerol kinase; Glut4, glucose transporter 4; PI3K, phosphoinositide 3 kinase; IRS-1 and IRS-2, insulin receptor substrate 1 and 2, respectively; HFD, high-fat diet.

CIC, a nuclear-encoded protein which belongs to the mitochondrial carrier family, is located in the inner membrane of mitochondria (Kaplan RS et al. 2001; Palmieri F et al. 2011; Palmieri F et al. 2012) and consists of three tandemly related domains of approximately 100 amino acids in length that span the membrane six times with both the N- and C-termini protruding toward the cytosol (Kaplan RS et al.1993; Capobianco L. et al. 1995). CIC exports citrate from the mitochondria to the cytosol where citrate is cleaved by ATP-citrate lyase to acetyl-CoA and

oxaloacetate. Acetyl-CoA is used for fatty acid and sterol biosynthesis, whereas oxaloacetate is reduced to malate, which in turn is converted to pyruvate via malic enzyme with production of NADPH plus H^+, underling the role of CIC also in glycolytic process (Fig.4).

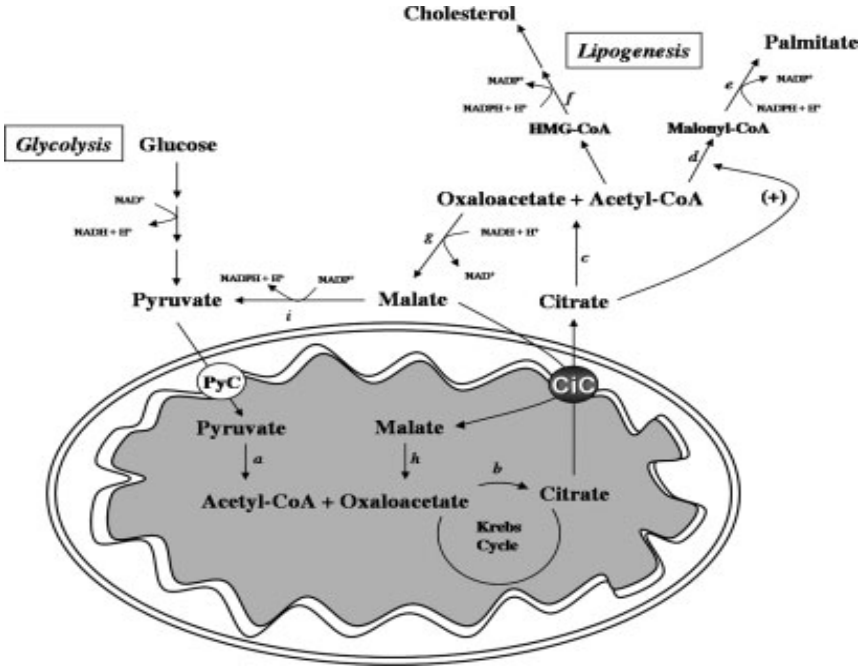

Figure 4: *Schematic model depicting the key role of the CiC in hepatic lipogenesis and its link with glycolysis. HMGCoA, 3-hydroxy-3-methylglutaryl-CoA; PyC, pyruvate carrier. (a) Pyruvate dehydrogenase, (b) citrate synthase, (c) ATP-citrate lyase, (d) acetyl-CoA carboxylase, (e) fatty acid synthase, (f) 3-hydroxy-3-methylglutaryl-CoA reductase, (g) cytosolic malate dehydrogenase, (h) mitochondrial malate dehydrogenase, (i) malic enzyme.*

On the basis of this knowledge, aim of the first part of our study was to define whether PPARγ may differently regulate CIC expression during the differentiation of 3T3-L1 fibroblasts into mature adipocyte cells.

We have provided evidences, for the first time, that activated PPARγ upregulates CIC expression in fibroblasts through binding Sp1 site present within CIC promoter region. The upregulation of CIC mediated by PPARγ disappears in mature adipocytes in which PPARγ/Sp1 complex recruits SMRT corepressor to the Sp1 site of the CIC promoter. Our results contribute to clarify the molecular mechanisms by which PPARγ during adipogenesis regulates CIC expression, which represents a crucial cross-point for several metabolic pathways.

In addition to the PPARγ's role mentioned above, its involvement in inflammation, atherosclerosis, cell cycle control, growth inhibition and apoptosis was demonstrated (Forman B et al. 1995; Wilson TM et al. 2000). In the last decade much research has focused on characterizing the role of this receptor in

cancer (Kubota T et al. 1998; Mueller E et al. 1998; Sarraf P et al. 1998; Tontonoz P et al. 1998). Several antineoplastic effects, such as induction of apoptosis and differentiation, have been described in a variety of cancer cells as a result of PPARγ-mediated action (Sarraf P et al. 1999; Mueller E et al. 2000; Kezoe T et al. 2001). Particularly, our previous studies in human cultured breast cancer cells have demonstrated that the synthetic PPARγ ligand Rosiglitazone (BRL) promotes antiproliferative effects and activates different molecular pathways leading to distinct apoptotic processes (Bonofiglio D. et al. 2005; Bonofiglio D. et al. 2006; Bonofiglio D. et al. 2009a-2010). Apoptosis, genetically controlled and programmed death, can be initiated by two major routes: the intrinsic and extrinsic pathways. The intrinsic pathway is triggered in response to a variety of apoptotic stimuli that produce damage within the cell, including anticancer agents, oxidative damage, UV irradiation, and is mediated through the mitochondria. The extrinsic pathway is activated by extracellular ligands able to induce oligomerization of death receptors, such as Fas, followed by the formation of the death inducing signaling complex, after which the caspases cascade can be activated. Previous data showed that the combination of PPARγ ligand Troglitazone with either all-trans retinoic acid or 9-cis-retinoic acid (9RA) can induce apoptosis in breast cancer cells (Elstner E. et al. 2002). Furthermore, Elstner et al. demonstrated that the combination of these drugs at micromolar concentrations reduced tumor mass without any toxic effects in mice (Elstner E. et al. 1998). However, in humans PPARγ agonists at high doses exert many side effects including weight gain due to increased adiposity, edema, hemodilution, and plasma-volume expansion, which preclude their clinical application in patients with heart failure (Arakawa K. et al. 2004; Rangwala SM and Lazar MA. 2004; Staels B. 2005). The undesirable effects of RXR-specific ligands on hypertriglyceridemia and suppression of the thyroid hormone axis have been also reported (Pinaire JA. et al. 2007). In an earlier work, Bonofiglio et al. demonstrated that combined treatment with nanomolar doses of BRL and 9RA induces a p53-dependent intrinsic apoptosis in MCF-7 breast cancer cells (Bonofiglio et al., 2009b). Of note, MCF-7 cells express the wild type p53 protein able to induce growth arrest and apoptosis mainly through the activation of a growing plethora of p53-responsive target genes.

In the present work, we aimed to extend previous results on p53-mediated apoptosis induced by low doses of BRL and 9RA also in SKBR3 and T47D breast cancer cells harboring endogenous mutant p53His175 and p53Phe194, respectively in order to elucidate the mechanism through which PPARγ and RXR ligands can trigger apoptotic processes independently of p53 transcriptional activity. Our results showed that BRL and 9RA induce apoptosis via an upregulation of Bid expression and a formation of p53/tBid/Bak multicomplex localized on mitochondria of breast carcinoma cells.

Due to the inhibitory role exerted by activated PPARγ in mammary carcinogenesis, in the last part of the work we aimed to identify natural compounds that potentially acting as PPARγ ligands can affect breast cancer growth.

It is well known that the development of breast cancer has been associated with genetic, environmental, hormonal, and nutritional factors. Among dietary factors, long chain fatty acids have been implicated in breast cancer risk, although their role in the promotion or prevention of breast cancer development and progression is not properly understood and remains still controversial. Polyunsatured fatty acids (PUFAs), for long time solely considered of as an energy source in our bodies, have been proven to be highly active molecules. They can act as transcription factors modulating protein synthesis, as ligands signal transduction, and as membrane components able to regulate the fluidity, permeability, and dynamics of cell membranes (Chapkin et al., 2008). Most fatty acids can be synthesized in the human body, but not all. In particular, essential fatty acids which are those required for biological processes, must be obtained from dietary sources (Williams and Burdge, 2006). The two major families of essential fatty acids are the omega-3 and omega-6 PUFAs, whose ratio in the body is believed to be of higher importance than the absolute levels of fatty acids (Gleissman et al., 2010). Existing reports suggest that omega-6 essential fatty acids are tipically proinflammatory and are linked with initiation and progression of carcinogenesis (Lanson et al., 1990; Cohen, 1997; Chapkin et al., 2007; Hyde and Missailidis, 2009); whereas omega-3 essential fatty acids have broad health benefits, including anti-cancer properties (Serini et al., 2011 and references therein). Indeed, consumption of the two main omega-3 fatty acids, eicosapentaenoic acid (EPA), and docosahexaenoic acid (DHA), naturally present in fish, is associated with decreased breast cancer risk (Fig.5) (Thiebaut et al., 2009).

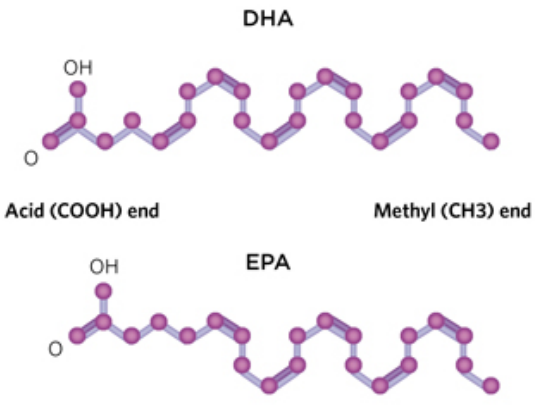

Figure 5: Polyunsaturated fatty acids (PUFAs) are characterized by the presence of carbon-carbon double bonds (C=C), which give them a kinked structure that makes them prime targets for oxygen or lipid radicals.

All PUFAs have two ends—an acid (COOH) end and a methyl (CH3) end—and the location of the first double bond (counted from the methyl, or omega, end) dictates the molecule's name. In the case of n-3 PUFAs from fish oil, also known as omega-3s, the first double bond falls after the third carbon atom. Docosahexaenoic acid (DHA) and eicosapentaenoic acid (EPA) are two common examples of n-3 PUFAs.

Three main anti-neoplastic activities of omega-3 fatty acids have been proposed: (i) alteration of membrane fluidity and cell surface receptor function; (ii) modulation of COX activity; and (iii) increased cellular oxidative stress. Besides, in breast cancer cells DHA strongly reduces cell viability and DNA synthesis promoting cell death via apoptosis (Kang et al., 2010); while EPA has been shown to inhibit mitogen activation of AKT enhancing the growth inhibitory response to the anti-estrogen tamoxifen (DeGraffenried et al., 2003). These findings are consistent with microarray studies revealing that both fatty acids are able to modulate the expression of genes involved in the regulation of apoptosis, defense immunity, and cell growth in several breast cancer cell lines (Hammamieh et al., 2007). The anti-cancer activities exerted by EPA and DHA are also due to their ability to bind PPARγ (Gani, 2008). In breast cancer DHA and EPA can be directly converted to N-acyl-ethanolamines, DHEA and EPEA, respectively (Brown et al., 2011), however to date their biological activities remain unexplored.

In the last of this study, we demonstrate, for the first time, that the DHEA and EPEA, through PPARγ activation, induce cell growth inhibition triggering autophagy in breast cancer cells.

Materials and methods

Reagents: BRL 49653 (BRL) was purchased from Alexis (San Diego, CA) and solubilized in_DMSO. 9-cis retinoic acid (9RA) was obtained from Sigma-Aldrich (Milan, Italy). 9RA was prepared just before use (Sigma-Aldrich) and diluted into medium at the indicated concentration. All experiments involving 9RA were performed under yellow light, and the tubes and culture plates containing 9RA were covered with aluminium foil. The irreversible PPARγ antagonist GW9662 (GW) and mithramycin (M) were purchased from Sigma-Aldrich.

Synthesis of DHEA and EPEA: N-Docosahexaenoylethanolamine (DHEA) and N-Eicosapentaenoylethanolamine (EPEA) were prepared from ethanolamine and their corresponding fatty acids, DHA, and EPA, respectively (Sigma–Aldrich) using an enzymatic procedure as described earlier (Plastina et al., 2009). Briefly, the method is based on a direct condensation reaction between ethanolamine and the fatty acid (molar ratio 1:1), carried out at 40°C in hexane, for 15 h, using Novozym1435 (consisting of immobilized Candida antarctica Lipase B) as the catalyst. Compounds were purified by column chromatography on silica gel. Authenticity of the products was verified by electrospray ionization-MS, 1H NMR, 13C NMR, and IR.

Cells: The 3T3-L1 fibroblasts were maintained in Dulbecco's modified Eagle's medium (DMEM) supplemented with 10% (v/v) fetal bovine serum, 2 mM L-glutamine, 100 U penicillin and 100 μg/ml streptomycin (Sigma) in an atmosphere of 5% CO2 at 37 °C. The cells were cultured until confluence had been reached, and then differentiation was induced 2 days thereafter (designated as “day 0”) by adding 3-isobutyl-1-methylxanthine, dexamethasone and insulin (Sigma) to make their final concentrations of 0.5mM, 1μM and 1 μg/ml, respectively. After 72h, the medium was changed to maturation medium supplemented with 1μM dexamethasone and 1μg/ml insulin. Cells were fed with maturation medium every 48h, obtaining adipocytes at an early stage of differentiation (preadipocytes) after 7 days and mature adipocytes after 14 days from day 0. Cell differentiation was monitored by evaluating cell morphology under phase-contrast microscopy. Cells were considered to be adipocytes when numerous lipid droplets were observed in the cytoplasm. More than 90% of cells expressed the adipocyte phenotype. Cells were switched to serum-free medium the day before each experiment and then treated as indicated. Wild-type human breast cancer MCF-7 cells were grown in Dulbecco’s modified Eagle’s medium-F12 plus glutamax containing 5% new-born calf serum (Invitrogen, Milan, Italy) and 1 mg/ml penicillinstreptomycin (P/S). SKBR3 breast cancer cells were grown in RPMI 1640 without red phenol plus glutamax containing 10% fetal bovine serum (FBS) and 1 mg/ml P/S. T47-D breast cancer cells were grown in RPMI 1640 with glutamax and red phenol containing 10% FBS, 1 mM sodium pyruvate, 10 mM HEPES, 2.5 g/L glucose, 0.2 U/ml insulin and 1

mg/ml P/S. MCF-10A normal breast epithelial cells were grown in Dulbecco's modified Eagle's medium-F12 plus glutamax containing 5% horse serum (Invitrogen), 1 mg/ml penicillin–streptomycin, 0.5 mg/ml hydrocortisone, and 10mg/ml insulin. Before each experiment, cells were grown in phenol red free media, containing 1% charcoal-stripped foetal bovine serum (cs-FBS) for 24 h and then treated as described.

Plasmids: The plasmid pCIC1437 containing the rat CIC gene promoter region spanning from −1473 to +35 bp was amplified from Rat Genomic DNA (Novagen, Merck Bioscience, Germany) by nested PCR as previously described using the following primers:
sense 5′-AGAGCTCCAGACCATGTGC-3′
and *antisense* 5′-AGTTTGGCTTTCCCGGACC-3′;

nestedsense (*pCIC1473for*) 5′-TGAGGTACCAACAAGCCCCTCAGAGGCTG-3′
and *nested-antisense* (*pCICrev*) 5′-TGAAAGCTTTCGACCTCGGGTCCGAGCC-3′.

The amplified DNA fragmentwas digestedwith KpnI and HindIII and then cloned into the pGL3 basic vector (Promega, Milan, Italy). The pCIC1473 plasmid was used as template to generate the different deleted constructs: pCIC284 (-284 to +35 bp), pCIC145 (-145 to +35 bp), pCIC115 (-115 to +35 bp) and pCIC82 (-82 to +35 bp). Forward primers are listed in Table 1; the reverse primer was pCICrev for all the constructs. The mutation of Sp1 site included from -115 to -82 region was obtained by site-directed mutagenesis using QuickChange kit (Stratagene, La Jolla, CA) performed on pCIC115 plasmid. The mutagenic primers to construct the pCIC115-Sp1mut are listed in Table 1. The plasmid pCIC-3xSp1, containing a threefold repeat of wild type responsive Sp1 site, was constructed by annealing between the following forward and reverse primers: forward
5′-CATGGTACCTAATGCGGGGCGGATGCGGGGCGGAAGCGGGGCGGATCCAAGCTG-3′;
reverse
5′-CTAAAGCTGGATCCGCCCCGCTTCCGCCCCGCATCCGCCCCGCATTAGGTACCT-3′.
The fragment obtained by annealing was used as template in a PCR reaction conducted with the following forward and reverse primers *5′-CATGGTACCTAATGCGGG-3′* and *5′-CTAAAGCTTGGATCCGCC-3′*, respectively. The DNA fragment was digested with KpnI and HindIII and then cloned into the pGL3 basic vector (Promega, Milan, Italy). The sequence of the different constructs was verified by nucleotide sequence analysis. The human wild-type $p21^{WAF1/Cip1}$ promoter-luciferase (luc) reporter was a kind gift from Dr. T. Sakai (Kyoto Prefectural University of Medicine, Kyoto, Japan). As an

internal transfection control, we co-transfected the plasmid pRL-CMV (Promega Corp., Milan, Italy), which expresses Renilla luciferase enzymatically distinguishable from firefly luciferase by the strong cytomegalovirus enhancer/promoter. The pGL3 vector containing three copies of a peroxisome proliferator response element sequence upstream of the minimal thymidine kinase promoter ligated to a luciferase reporter gene (3XPPRE-TK-pGL3) was a gift from Dr. R.Evans (The Salk Institute, San Diego, CA).

Transient transfection assay: 3T3-L1 fibroblasts were transiently transfected using the Lipofectamine 2000 reagent (Invitrogen, Milan, Italy) with the described rat CIC promoter constructs for 18 h. After transfection, cells were treated as described for 12 h. SKBR3 and T47D and MCF-7 cells were transferred into 24-well plates with 500 µl of regular growth medium/well the day before transfection. The medium was replaced with 1% CT-FBS on the day of transfection, which was performed using Fugene 6 reagent as recommended by the manufacturer (Roche Diagnostics, Mannheim, Germany), with a mixture containing 0.5µg of p21 promoter-luc plasmid for SKBR3 and T47D, and 0.5 mg of 3XPPRE-TK ligated to a luciferase reporter gene (PPRE) into the pGL3 vector for MCF-7 and 10ng of pRL-CMV. After transfection for 24 h, treatments were added in 1% CT-FBS, and cells were incubated for an additional 24 h. Firefly and Renilla luciferase activities were measured using the Dual Luciferase Kit (Promega, Madison, WI). The firefly luciferase data for each sample were normalized based on the transfection efficiency measured by Renilla luciferase activity and data were reported as fold induction.

Table 1: Oligonucleotides used for CIC promoter constructs.

Construct	*Oligonucleotide sequence*
pCIC1473	*5'-TGAGGTACCAACAAGCCCCTCAGAGGCTG-3'*
pCIC284	*5'-TGAGGTACCTACCCGCTTTGGCAAAGAGTTGC-3'*
pCIC145	*5'-TAGGGTACCAGTTTCCCGGCTGGCAC-3'*
pCIC115	*5'-TAGGGTACCGGCGGGGCTCAGCTCAG-3'*
pCIC82	*5'-TAGGGTACCCCGGGGAGCTGACGTGA-3'*
pCIC115Sp1mut For	*5'-GCTCAGGCCACGCGGATCCGAGCCGGGGAGCTGAC-3'*
pCIC115Sp1mut Rev	*5'-GTCAGCTCCCCGGCTCGGATCCGCGTGGCCTGAGC-3'*

Mitochondrial isolation: 3T3-L1 fibroblasts and mature adipocytes were grown in 10-cm dishes and exposed to treatments in serum-free medium as indicated before fractionation.Mitochondriawere isolated as described previously [37]. Briefly, cells

were washed with ice cold PBS, collected by scrapping in cold PBS and, after centrifugation (600 Å~g, 4 °C, 10min), resuspended in 200 mM sucrose, 10 mM Tris–MOPS and 1 mM EDTA/Tris, pH 7.4 (STE buffer). Cells were homogenized by glass Potter homogenization and mitochondria were then isolated by serial centrifugations. The mitochondrial pellet was resuspended in lysis buffer for immunoblotting analysis and in STE buffer for transport measurements.

Immunoblotting: Cells were grown in 6 cm dishes to 70–80% confluence and exposed to treatments in 1% charcoal-treated (CT)-FBS as indicated. Cells were harvested in cold phosphatebuffered saline (PBS) and resuspended in total ripa buffer containing 1% NP40, 0.5% Na-deoxycholate, 0.1% SDS and inhibitors (0.1 mM sodium orthovanadate, 1% phenylmethylsulfonylfluoride or PMSF, 20 mg/ml aprotinin). Protein concentration was determined by Bio-Rad Protein Assay (Bio Rad Laboratories, Hercules, CA). A 40 μg portion of total lysates was used for protein gel blotting, resolved on a 11% SDS-polyacrylamide gel, transferred to a nitrocellulose membrane and probed with an antibody directed against the C terminal-CIC, anti-PPARγ (cat#sc-7196), p53 (cat#sc-126), $p21^{WAF1/Cip1}$ (cat#sc-756), PARP (cat#sc-7150), Bid (cat#sc-11423), anti-RXRα (cat#sc-774) antibodies, anti-beclin-1, anti-PTEN, anti-phospho-AKT (ser473), anti-AKT (AKTtot), anti-phospho-Bcl-2 (ser70), anti-Bcl-2 (Santa Cruz Biotechnology, CA), anti-phospho-mTOR (Ser2448), anti-mTOR (mTORtot), anti-phospho-P38 MAPK (Thr180/Tyr182), anti-P38 (P38tot) (Cell Signaling, Denvers, MA). As internal control, all membranes were subsequently stripped (0.2 M glycine, pH 2.6, for 30 min at room temperature) of the first antibody and reprobed with anti-GAPDH antibody (cat#sc-25778, Santa Cruz Biotechnology). A mouse monoclonal antibody against the β-subunit of human F1-ATPase (β-ATPase) (BD Biosciences, San Josè, CA, USA) was used as a loading control to ensure that any differences in protein expression between pre- and post-differentiation cells were not due to the increase in number of mitochondria, typically occurring to mature adipocytes during differentiation. The antigen-antibody complex was detected by incubation of the membranes for 1 h at room temperature with peroxidase-coupled goat anti-mouse or anti-rabbit IgG and revealed using the enhanced chemiluminescence system (Amersham Pharmacia, Buckinghamshire UK). Blots were then exposed to film (Kodak film, Sigma). The intensity of bands representing relevant proteins was measured by Scion Image laser densitometry scanning program. To obtain cytosolic and total mitochondrial fraction of proteins, cells were grown in 10 cm dishes to 70–80% confluence and exposed to treatments as for 48h. Cells were harvested by centrifugation at 2,500 rpm for 10 min at 4°C. The pellets were suspended in 250 μl of RIPA buffer plus 10 μg/ml aprotinin, 50mM PMSF and 50 mM sodium orthovanadate, and then 0.1% digitonine (final concentration) was added. Cells were incubated for 15 min at 4°C and centrifuged at 3,000 rpm for 10min at 4°C. Supernatants were collected and further centrifuged at 14,000 rpm for 10min at 4°C. The supernatant, containing cytosolic fraction of proteins,

was collected, while the resulting mitochondrial pellet was resuspended in 3% Triton X-100, 20 mM Na2 SO4 , 10 mM PIPES and 1 mM EDTA, pH 7.2, incubated for 15 min at 4°C and centrifuged at 12,000 rpm for 10 min at 4°C. Alternatively, to provide matrix mitochondrial fraction of proteins, mitochondrial pellet was further solubilized in 6% of digitonine in RIPA buffer, for 10 min at 4°C then centrifuged at 14,000 rpm, 4°C, 10 min. The pellets (mitoplasts) were then lysed osmotically and centrifuged at 14,000 rpm 4°C for 10 min to discard the membrane residues and recover the soluble matrix content. Proteins of the mitochondrial and cytosolic fractions were determined by Bio-Rad Protein Assay (Bio-Rad Laboratories). Equal amounts of cytosolic and mitochondrial proteins (40 μg) were resolved by 11% SDS-PAGE, electrotransferred to nitrocellulose membranes and probed with antibodies directed against Bid, Bad (cat#sc-8044) and BCL-XL (cat#sc-7195) (Santa Cruz Biotechnology). For the internal loading, all membranes were stripped and reprobed with anti GAPDH (Santa Cruz Biotechnology) antibody. Blots shown are representative of two or three individual experiments and the intensity of bands representing relevant proteins was measured by Scion Image laser densitometry scanning program.

Mitochondria reconstitution and transport measurements: Isolated mitochondria from 3T3-L1 fibroblasts and mature adipocytes were solubilized in a buffer containing 3% Triton X-114, 4 mg/ml cardiolipin, 10 mM Na2SO4, 0.5 mM EDTA, and 5 mM PIPES, pH 7 using modifications of the method described previously by Jordens et al. [38]. After incubation for 20 min at 4 °C, the mixture was centrifuged at 138,000 Å~g for 10 min. The supernatantwas incorporated into phospholipid vesicles by cyclic removal of the detergent. The reconstitution mixture consisted of 0.04 mg protein solution, 10% Triton X-114, 10% phospholipids (egg lecithin from Fluka, Milan, Italy) as sonicated liposomes, 10 mM citrate, 0.85 mg/ml cardiolipin (Sigma) and 20 mM PIPES; pH 7.0. The mixture was recycled 13 times through an Amberlite column. All phases were performed at 4 °C, except for the passages through Amberlite, which were carried out at room temperature. To measure citrate transport, external substrate was removed from the proteoliposomes on Sephadex G-75 columns pre-equilibrated with buffer A (50 mM NaCl and 10 mM PIPES, pH 7.0). Transport at 25°C was started by the addition of 0.5 mM [^{14}C]citrate (Amersham) to the eluted proteoliposomes and terminated by the 'inhibitor-stop' method with the addition of 20 mM 1,2,3- benzene-tricarboxylate [40,41]. In control samples, the inhibitor was added simultaneously to the labeled substrate. Finally, the external radioactivitywas removed fromthe Sephadex G-75 columns and radioactivity in the liposomes was measured. Transport activitywas calculated by subtracting the control values from the experimental values.

Electrophoretic mobility shift assays (EMSA): Nuclear extracts from 3T3-L1 fibroblasts were prepared as above described. The probe was generated by annealing single-stranded oligonucleotides labeled with [^{32}P]ATP and tyrosine_polynucleotide kinase and then purified using Sephadex G-50 spin_columns (Sigma). The DNA

sequence used as probe or as cold competitor_was as follows (the nucleotide motif of interest is underlined and mutations are shown as lowercase letters):

Sp1 5'-AGGCCACGCGGGGCGGAGCCCGGGA-3',
mutated Sp1 5'-AGGCCACGCGattaGGAGCCCGGGA-3'.
The protein-binding reactions were carried out in 20 µl of buffer [20 mM HEPES (pH 8), 1 mM EDTA, 50 mM KCl, 10 mM dithiothreitol, 10% glycerol, 1 mg/ml BSA, 50 µg/ml poly(dI/dC)]with 50,000 cpm of labeled probe, and 5 µg of fibroblast nuclear protein. The mixtures were incubated at room temperature for 20 min in the presence or absence of unlabeled competitor oligonucleotides. For the experiments involving anti-PPARγ and anti-Sp1 antibodies (Santa Cruz Biotechnology), the reaction_mixture was incubated with these antibodies at 4 °C for 30 min_before addition of the labeled probe. The entire reaction mixture_was electrophoresed through a 6% polyacrylamide gel in 0.25Å~Tris-borate-EDTA for 3 h at 150 V. Gel was dried and subjected to autoradiography at -80 °C.

Chromatin immunoprecipitation (ChIP) and re–ChIP assays: 3T3-L1 fibroblasts and mature adipocytes were grown in 10-cm dishes to 50%–60% confluence, starved with serum-free medium for 24 h and then treated with BRL. Thereafter, cells were washed twice with PBS and cross-linked with 1% formaldehyde and sonicated. Supernatants were immunocleared with salmon sperm DNA/protein A agarose for 1h at 4 °C. The precleared chromatin was immunoprecipitated with specific anti-PPARγ, anti-Sp1, or anti-polymerase II (PolII) antibodies (Santa Cruz Biotechnology). The anti-PPARγ samples were reimmunoprecipitated with anti-Sp1, anti-ARA70, anti-PCG1α (Santa Cruz Biotechnology), anti-SMRT or anti-NCoR (Novus Biologicals, Milan, Italy) antibodies. The anti-Sp1 samples were reimmunoprecipitated with anti-SMRT antibody. A normal mouse serum IgG was used as negative control. Pellets were washed, eluted with elution buffer (1% SDS, 0.1 mol/l NaHCO3), and digested with proteinase K. DNA was obtained by phenol/chloroform/isoamyl alcohol extractions and was precipitated with ethanol. Five microliters of each sample and input were used for PCR with the primers flanking the Sp1 sequence present in the CIC promoter region:

5'-TAGCGTTGCTGTCCGGAGACCA-3'
and 5'-GAGACCACGACCAATTCTGGT-3'.

The amplification products obtained were analyzed in 2% agarose gel and visualized by ethidium bromide staining.

Immunoprecipitation: Three hundred micrograms of mitochondrial and cytosolic proteins were incubated overnight with anti-p53 (cat#sc-126) or anti-Bid (cat#sc-135847) antibodies (Santa Cruz Biotechnology) or Five hundred micrograms of total proteins were incubated overnight with 1mg of anti-beclin-1 antibody and 500 µL of HNTG (immunoprecipitation) buffer [50 mmol/L HEPES (pH 7.4), 50 mmol/L NaCl,

0.1% Triton X-100, 10% glycerol, 1 mmol/L phenylmethylsulfonyl fluoride, 10 μg/mL leupeptin, 10 μg/mL aprotinin, 2 μg/mL pepstatin]. Immunocomplexes were recovered by incubation with protein A/G-agarose. The immunoprecipitates were centrifuged, washed twice with HNTG buffer and then used for protein gel blotting. Membranes were probed with anti-p53 (cat#sc-6243), anti-Bid (cat#sc-11423), anti-Bak (cat#sc-832), anti-Bax (cat#sc-7480), anti-PPARγ (cat#sc-7196) and anti-RXRα (cat#sc-774) antibodies (Santa Cruz Biotechnology), Membranes were probed with anti-Bcl2 and anti-beclin-1 antibodies.

PCR assay: Total RNA was extracted from 3T3-L1 fibroblasts, pre-adipocytes and mature adipocytes using a Trizol reagent (Invitrogen, Milan, Italy) according to the manufacturer's protocol. RNA was quantified spectrophotometrically and its quality was checked by electrophoresis through agarose gels stained with ethidium bromide. CIC and PPARγ expression were performed using the following primers:

CIC forward 5'-CTGTCAGGTTTGGGATGTTC-3'
and reverse 5'-GTGGGTTCATAGGTTTGTTG-3';

PPARγ forward 5' GGTGAAACTCTGGGAGATTC-3'
and reverse 5'-CAACCATTGGGTCAGCTCTT-3';

β-actin forward 5'-AGGCATCCTGACCCTGAAGTAC-3'
and reverse 5'-TC TTCATGAGGTAGTCTGTCAG-3'.

PCR was performed for 34 cycles for CIC (94 °C 1 min, 66 °C 1 min, 72 °C 1 min), 32 cycles for PPARγ (94 °C 1 min, 67 °C 1 min, 72 °C 1 min) and 24 cycles for β-actin (94 °C 1 min, 60 °C 1 min, 72 °C 1 min).

MCF-7, SKBR3 and T47-D cells were grown in 10 cm dishes to 70–80% confluence and exposed to treatments in 1% CT-FBS as indicated. Total cellular RNA was extracted using TRIZOL reagent (Invitrogen) as suggested by the manufacturer. The RNA sample was treated with DNase I (Ambion, Austin, TX), and purity and integrity of the RNA was confirmed both spectroscopically and electrophoretically. RNA was then reversed transcribed with High Capacity cDNA Reverse Transcription Kit (Applied Biosystems, Applera Italia, Monza, Milano, Italy). The evaluation of p53, p21WAF1/Cip1, PPARg and the internal control gene 36B4 was performed using the RT-PCR method with the following primers: *5'-CCAGTGTGATGATGGTGAGG-3' (p53 forward) and 5-GCTTCATGCCAGCTACTTCC-3‘ (p53 reverse), 5'-CTGTGCTCACTTCAGGGTCA-3' (p21 forward) and 5'-CTCAAATCTCCCCC TTC-3' (p21 reverse), 5'-CTCAACATCTCCCCCTTCTC-3' (36B4 forward) and 5'-CAAATCCCATATCCTCGTCC-3' (36B4 reverse)* to yield, respectively, products of 190 bp with 18 cycles, 270 bp with 18 cycles and 408 bp with 18 cycles. The results

obtained as optical density arbitrary values were transformed to percentage of the control (percent control) taking the samples from untreated cells as 100%.

Real-time (RT)-PCR: Analysis of p53 gene expression was performed using Real-time reverse transcription PCR. cDNA was diluted 1:3 in nuclease-free water, and 5 μ l were analyzed in triplicates by realtime PCR in an iCycler iQ Detection System (Bio-Rad) using SYBR Green Universal PCR Master Mix with 0.1 mmol/l of each primer in a total volume of 30 μl reaction mixture following the manufacturer's recommendations. Each sample was normalized on its GAPDH mRNA content. Relative gene expression levels were normalized to the basal, untreated sample chosen as calibrator. Final results are expressed as folds of difference in gene expression relative to GAPDH mRNA and calibrator, calculated following the Δ Ct method, as follows:

Relative expression (folds) $= 2^{-(\Delta Ctsample - \Delta Ctcalibrator)}$ where ΔCt values of the sample and calibrator were determined by subtracting the average Ct value of the GAPDH mRNA reference gene from the average Ct value of the analyzed gene. For p53 and GAPDH the primers were:

p53 forward: *5′-GCTGCTCAGATAGCGATGGTC-3′*
and p53 reverse: 5′-CTCCCAGGACAGGCACAAACA-3′

GAPDH forward: 5′-CCCACTCCTCCACCTTTGAC-3′
and GAPDH reverse: 5′-TGTTGCTGTAGCCAAATTCGT-3′
Negative controls contained water instead of first strand cDNA.

RNA interference (RNAi): 3T3-L1 fibroblasts and mature adipocytes were transfected with RNA duplex of stealth siRNA targeted for the mouse SMRT mRNA sequence (Ambion, ID:s74031) or with a control siRNA used as a control for non-sequence-specific effects. After 5 h, the transfection medium was changed with complete 1% CT-FBS with P/S, in order to avoid Lipofectamine 2000 toxicity and cells were exposed to treatments. MCF-7, SKBR3 and T47-D cells were plated in 6 cm dishes with regular growth medium the day before transfection to 60–70% confluence. On the second day, the medium was changed with 1% CT-FBS without P/S, and cells were transfected with stealth RNAi targeted human Bid mRNA sequence *-5′-UGCGGUUGCCAUCAGUCUGCAGCUC-3′* (Invitrogen). In other sets of experiments MCF-7 cells were transfected with a stealth RNAi targeted human PPARγ mRNA sequence *5′-AGAAUAAUAAGGUGGAGAUGCAGGC-3′* (Invitrogen), a stealth RNAi targeted human RXRα mRNA sequence *5′-UCGUCCUCUUUA ACCCUGACUCCAA-3′* or with a stealth RNAi-negative control (Invitrogen) to a final concentration of 100 nM using Lipofectamine 2000 (Invitrogen) as recommended by the manufacturer. After 5 h, the transfection medium was changed with complete 1% CT-FBS with P/S and then cells were exposed to treatments and subjected to different experiments.

Immunofluorescence: MCF-7 cells were seeded on glass coverslips in complete growth medium. On the second day, the medium was changed with 1% cs-FBS and cells were treated with ligands , washed with PBS, and then fixed with 4% paraformaldehyde in PBS for 20 min at room temperature. Next, cells were permeabilized with 0.2% Triton X-100 in PBS for 5 min, blocked with 5% bovine serum albumin for 30 min, and incubated with anti-p53, anti-Bid, anti-beclin-1, anti-LC3 (Santa Cruz) and anti-PPARγ primary antibodies (1:100) in PBS overnight at 4°C. The day after the cells were washed three times with PBS and incubated with Alexa-fluo 350 (blue), Alexa-fluo 488 (green) (Invitrogen), anti-mouse or anti-rabbit secondary antibodies conjugated with FITC (fluorescein isothiocyanate; green; 1:200) for 1h at room temperature. 40,6-Diamidino-2-phenylindole (DAPI; Sigma) was used for the determination of the nuclei. Mitochondria were stained with MitoTracker mitochondrion selective probe (cat#MP07510, Invitrogen) according to manufacturer's instructions. To check the specificity of immunolabeling the primary antibody was replaced by normal mouse serum (negative control). The images were acquired using fluorescent microscopy (Leica Microsystems, Milan, Italy, AF6000).

JC-1 mitochondrial membrane potential detection assay: Alteration of mitochondrial membrane potential was detected using the dye 5,5',6,6'-tetra-chloro-1,1',3,3'-tetraethylbenzimidazolyl-carbocyanine iodide (JC-1) as recommended by the manufacturer's instruction (Biotium, Hayward). MCF-7, SKBR3 and T47D cells were grown in 10 cm dishes, transfected with control RNAi or Bid RNAi and then treated with BRL and 9RA for 56 h in 1% CT-FBS. Subsequently, cells were washed in ice-cold PBS and incubated with 10 mM JC-1 at 37°C in a 5% CO2 incubator for 20 min in darkness. Subsequently, cells were extensively washed with PBS and analyzed by fluorescence microscopy. The red form has an absorption/emission maxima of 585/590 nm. The green monomeric form has absorption/emission maxima of 510/527 nm.

TUNEL assay: Apoptosis was determined by enzymatic labeling of DNA strand breaks using terminal deoxynucleotidyl transferase- mediated deoxyuridine triphosphate nick end-labeling (TUNEL). TUNEL labeling was conducted using APO-BrdUTM TUNEL Assay Kit (Invitrogen) and performed according to the manufacturer's instructions. Briefly, cells were trypsinized after treatments and resuspended in 0.5 ml of PBS. After fixation with 1% paraformaldehyde for 15 min on ice, cells were incubated on ice-cold 70% ethanol overnight. After washing twice with washing buffer for 5 min, the labeling reaction was performed using terminal deoxynucleotidyl transferase end-labeling cocktail for each sample and incubated for 1 h at 37°C. After rinsing, cells were incubated with antibody staining solution prepared with Alexa Fluor 488 dye-labeled anti-BrdU for 30 min at room temperature. Subsequently 0.5 mL of propidium iodide/RNase A buffer were added for each sample. Cells were incubated 30 min at room temperature, protected from light, analyzed and photographed by using a fluorescent microscope.

Cell viability assay: Cell viability was determined with the 3-(4,5-dimethylthiazol- 2-yl)-2,5-diphenyltetrazolium (MTT) assay. MCF-7 cells (3_106 cells/ ml) were grown in 24-well plates and exposed to treatments as indicated, in 1% cs-FBS. Hundred microliter of MTT (2 mg/ml, Sigma, Milan, Italy) were added to each well, and the plates were incubated for 2 h at 378C followed by medium removal and solubilization in 500 ml DMSO. The absorbance was measured at a test wavelength of 570 nm in Beckman Coulter. The IC50 values were calculated using GraphPad Prism 4 (GraphPad Software, Inc., San Diego, CA).

Anchorage-independent soft agar growth assays: Cells (50,000/well) were plated in 2ml of 0.35% agarose with 5% cs-FBS in phenol red-free media, in a 1% agarose base in 24-well plates. Two days after plating, media containing control vehicle, or treatments was added to the top layer, and the media was replaced every 2 days. After 14 days, 200ml of MTT was added to each well and allowed to incubate at 378C for 4 h. Plates were then placed in 4°C overnight and colonies >50mm diameter from triplicate assays were counted. Data are the mean colony number of three plates and representative of two independent experiments, each performed in triplicate, analyzed for statistical significance ($P<0.05$) using a two-tailed Student's t-test, performed by Graph Pad Prism 4.

DNA fragmentation: DNA fragmentation was determined by gel electrophoresis. MCF-7 cells were grown in 10 cm dishes to 70% confluence and exposed to treatments as indicated. After 6 h cells were collected and washed with PBS and pelleted at 1,800 rpm for 5 min. The samples were resuspended in 0.5 ml of extraction buffer (50 mmol/L Tris–HCl, pH 8; 10 mmol/L EDTA, 0.5% SDS) for 20 min in rotation at 4°C.DNA was extracted three times with phenol–chloroform and one time with chloroform. The aqueous phase was used to precipitate nucleic acids with 0.1 volumes of 3M sodium acetate and 2.5 volumes cold ethanol overnight at_208C. The DNA pellet was resuspended in 15 ml of H2O treated with RNase A for 30 min at 378C. The absorbance of the DNA solution at 260 and 280 nm was determined by spectrophotometry. The extracted DNA (40 mg/lane) was subjected to electrophoresis on 1.5% agarose gels. The gels were stained with ethidium bromide and then photographed.

Mono-dansyl-cadaverine (MDC) staining: Mono-dansyl-cadaverine (MDC; Sigma–Aldrich; Biederbick et al.,1995) was used to visualize autophagic vacuoles. MCF-7 cells were plated six-well plates on coverslips in phenol-red DMEM-F12. Media was replaced the following day with DMEM-F12 containing 1% cs-FBS. After 12 h of treatment, cells were stained using 0.05mM MDC in PBS at 378C for 10 min. After incubation, cells were washed four times with PBS and immediately analyzed by fluorescence microscopy.

***Statistical analyses*:** Each datum point represents the mean ±SD of three different

experiments. Statistical analysis was performed using ANOVA followed by Newman-Keuls testing to determine differences in means. $p < 0.05$ was considered as statistically significant.

Results

1. Role of PPARγ in adipogenesis

1.1 Functional characterization of CIC in 3T3-L1 cells

Herein, we first aim to investigate the expression and activity of CIC in mitochondrial extracts from 3T3-L1 fibroblasts (F) and mature adipocytes (A, 14 days after differentiation induction). Immunoblot analysis, using an antibody raised against the carboxy-terminus of the mature CIC protein, revealed a weak immunoreactive band in fibroblasts at 34 kDa, corresponding to the mitochondrial CIC, while a 4.5-fold increase in band intensity was observed in mature adipocytes (Fig. 6A). A similar pattern of CIC expression was also found in total extracts of both fibroblasts and adipocytes (Fig. 6B). The activity of CIC in mitochondrial extracts from 3T3-L1 fibroblasts and mature adipocyte cells was tested by assaying the rate of the [^{14}C]citrate/citrate exchange in reconstituted liposomes (Bisaccia F et al., 1989-1990). As shown in Fig. 1C, the uptake of radioactive L-citrate in liposomes reconstituted with mitochondrial extracts from fibroblasts was approximately 45% lower compared to liposomes reconstituted with the mitochondrial extracts from mature adipocyte cells (132±14.4 versus 238±25.0 nmol citrate/mg protein, respectively).

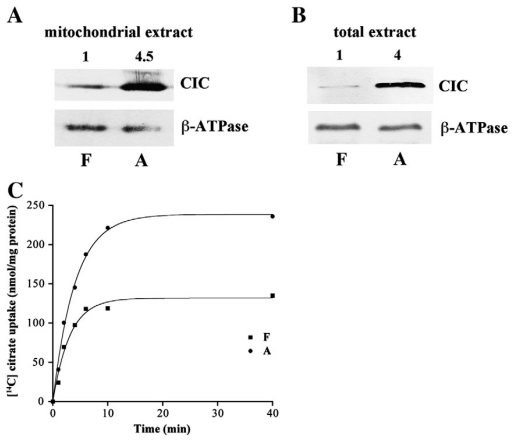

*Figure 6: CIC expression and activity in 3T3-L1 cells. Immunoblots for CIC expression from mitochondria (A) and total extracts (B) of fibroblasts (F) and mature adipocytes (A). Beta subunit of mitochondrial ATPase (**β**-ATPase) was used as loading control. Numbers represent the average fold change of CIC/**β**-ATPase levels. C: Rate of [^{14}C]citrate/citrate exchange in fibroblast and adipocyte mitochondria. Transport was initiated by adding 0.5 mM [^{14}C]citrate to proteoliposomes containing 10 mM citrate and reconstituted with mitochondria isolated from either fibroblasts (square) or mature adipocytes (circle). The transport reaction was stopped at the indicated times. The data represent means of three independent experiments.*

1.2 The PPARγ ligand BRL up-regulates CIC expression in 3T3-L1 fibroblasts

Since PPARγ is considered to be one of the master regulators of adipocyte differentiation, we evaluated the involvement of this nuclear receptor in the modulation of CIC expression during adipocyte differentiation. We tested the effects of BRL49653 (BRL), a synthetic and specific ligand of PPARγ, in 3T3-L1 fibroblasts (F), in pre-adipocytes (P), which are adipocytes at an early stage of differentiation, and in mature adipocytes (A). The results obtained demonstrated that BRL treatment up-regulated CIC mRNA expression in fibroblasts and to a lesser extent in pre-adipocytes, while it did not elicit any effects on mature adipocytes (Fig. 7A). As previously reported (Takamura T et al. 2001), the expression level of PPARγ mRNA was enhanced in BRL-treated fibroblasts and pre-adipocytes and reduced in BRL-treated mature adipocytes (Fig. 7A). Moreover, CIC protein content in fibroblasts increased 4-fold after treatment with BRL for 24h compared to untreated fibroblasts (Fig. 7B). This up-regulation was abrogated by GW9662 (GW), an irreversible PPARγ antagonist, demonstrating a direct involvement of PPARγ (Fig. 2B). As expected, in mature adipocytes BRL treatment did not modulate CIC protein levels, while it down-regulated PPARγ protein expression, which was reversed in the presence of GW (Fig. 7C). Finally, we investigated the effects of the PPARγ ligand BRL on CIC activity in mitochondrial extracts from fibroblasts and adipocytes. We found that the uptake of [^{14}C]citrate in BRL-treated fibroblasts was enhanced as compared to untreated cells (192±21.2 versus 130±15 nmol citrate/mg protein, respectively), reaching the CIC activity levels measured in mature adipocytes (235±24 nmol citrate/mg protein), while BRL did not exert any effects in mature adipocytes (Fig. 7D). Taken together, these data suggest that activated PPARγ is able to induce CIC expression and increase CIC activity only in fibroblasts.

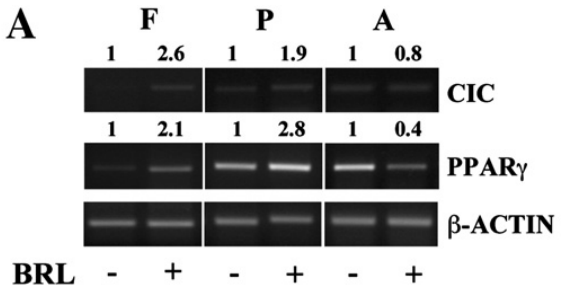

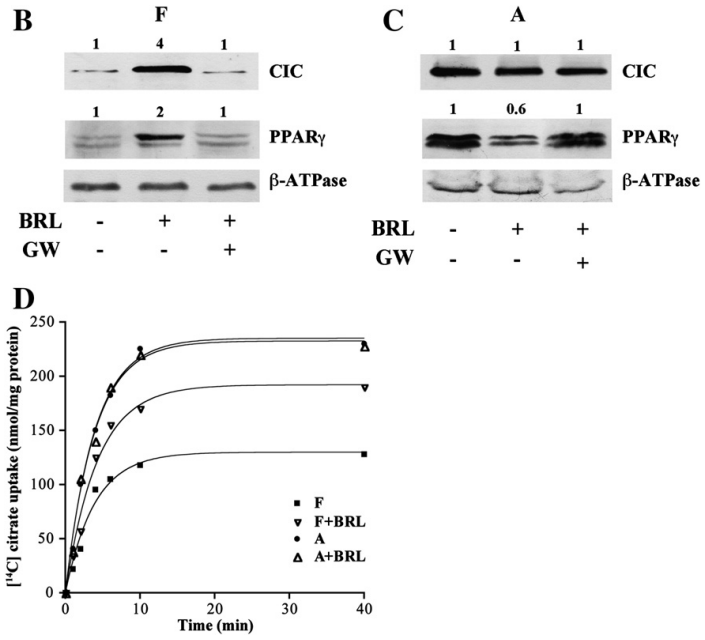

Figure 7: Activated PPARγ up-regulates CIC expression and activity in fibroblasts. A: CIC and PPARγ mRNA expression in 3T3-L1 fibroblasts (F), preadipocytes (P) and mature adipocytes (A) untreated (−) or treated with 10 μM BRL for 24 h. β-ACTIN was used as loading control. Numbers represent the average fold change of CIC or PPARγ/β-ACTIN levels. Immunoblots for CIC and PPARγ expression from total extracts of fibroblast (B) and mature adipocyte cells (C) untreated (−) or treated with 10 μM BRL in the presence or not of 10 μM GWfor 24 h. β-ATPase was used as loading control. Numbers represent the average fold change of CIC or PPARγ/β-ATPase levels. D: [14C]citrate/citrate exchange in fibroblast and adipocyte mitochondria untreated or treated with BRL. Transport was initiated by adding 0.5 mM [14C]citrate to proteoliposomes containing 10 mM citrate and reconstituted with mitochondria isolated from untreated fibroblasts (square), BRL-treated fibroblasts (down-pointing triangle), adipocytes (circle) and BRL-treated adipocytes (up-pointing triangle). The transport reaction was stopped at the indicated times. The data represent means of three independent experiments.

1.3 BRL transactivates CIC gene promoter in 3T3-L1 fibroblasts

The aforementioned observations prompted us to investigate whether BRL is able to modulate CIC transcriptional activity. Thus, we performed functional assays by transiently transfecting 3T3-L1 fibroblasts with a plasmid containing rat CIC regulatory sequence pCIC1473 (-1473/+35) and found that BRL significantly induced luciferase activity (Fig. 8A). This effect was no longer noticeable in the presence of GW, confirming that the transactivation of CIC by BRL occurred in a PPARγ-dependent manner (data not shown). The rat CIC promoter contains multiple responsive elements for different transcription factors, including glucocorticoid receptor (GR), estrogen receptor alpha (ERα), PPARγ and α, c/EBPα and Sp1 (Fig. 8A). To identify the region within the CIC promoter

responsible for the BRL-induced transactivation, the activity of the different CIC promoter-deleted constructs pCIC284 (-284/+35), pCIC145 (-145/+35), pCIC115 (-115/+35) and pCIC82 (-82/+35) was tested. In transfection experiments performed using the aforementioned plasmids pCIC284, pCIC145 and pCIC115, responsiveness to BRL was still observed (Fig. 8A). Of note, BRL was able to transactivate all tested constructs independently of the PPRE site, which was recently identified at -625 bp (Damiano F et al., 2012). In contrast, in cells transfected with the promoter-deleted construct pCIC82 we did not detect any increase in luciferase activity (Fig. 8A). Consequently, the region from -115 to -82, which contains the Sp1 motif, was the minimal region of CIC promoter responsible for BRL induction. Thus, we performed site-directed mutagenesis on the minimal responsive Sp1 domain (pCIC115-Sp1mut) within the CIC promoter (Fig. 8A). Mutation of this domain abrogated BRL effects (Fig. 8A) demonstrating that the integrity of Sp1-binding site is necessary for PPARγ modulation of CIC promoter activity. To strengthen the importance of the Sp1 site in CIC promoter modulation by BRL, we performed transfection experiments using a construct (pCIC-3xSp1) bearing threefold repeat of wild type responsive Sp1 site located in the minimal region of CIC promoter. BRL treatment induced a 1.7 fold increase in luciferase activity respect to untreated cells (Fig. 8B). In addition, functional experiments and RT-PCR analysis were performed using mithramycin that binds to GC boxes and prevents sequential Sp1 binding to its consensus sequence (Blume SW et al. 1991). Our results showed that mithramycin was able to abrogate the BRL-induced CIC transcriptional activity as well as its mRNA expression in fibroblast cells (Fig. 8C and D).

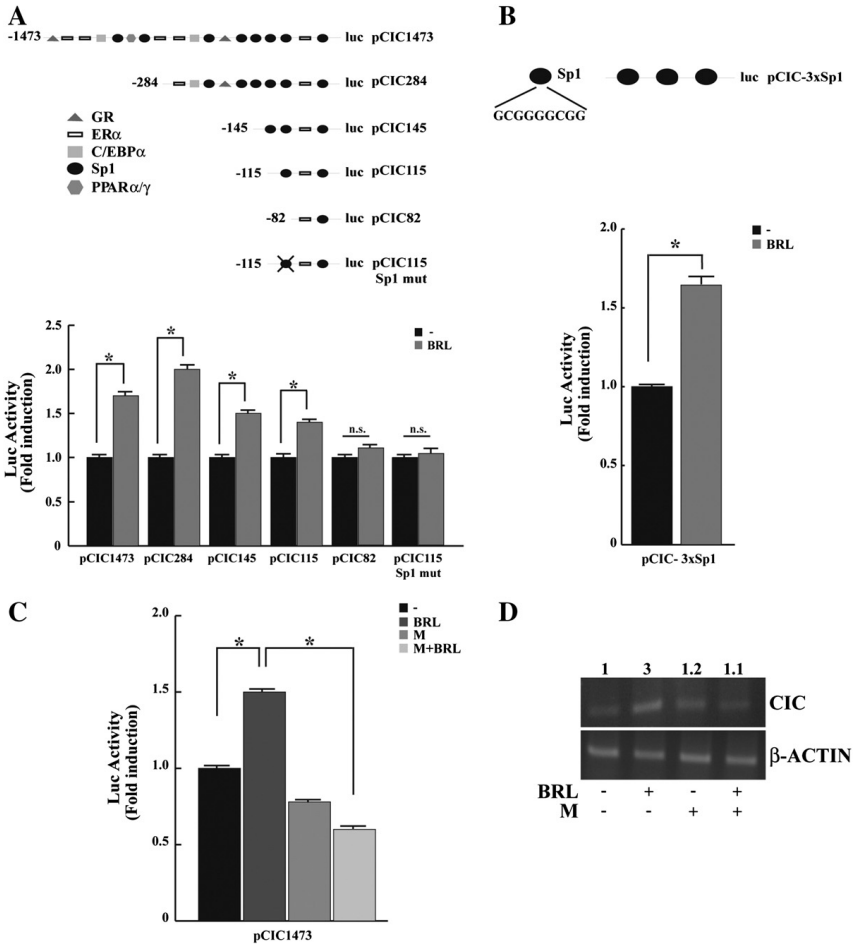

*Figure 8: BRL transactivates CIC transcriptional activity in fibroblasts. A:Upper panel, schematic representation of the CIC promoter constructs used in this study. Lower panel, 3T3-L1 fibroblasts were transiently transfected with luciferase plasmids containing the CIC promoter (pCIC1473), its deletions (pCIC284, pCIC145, pCIC115 and pCIC82) or pCIC115-Sp1mut mutated in Sp1 site and then untreated (−) or treated with 10μM BRL for 12h. B: Upper panel, schematic representation of the pCIC-3xSp1 construct used in this study. Lower panel, cells transiently transfected with pCIC-3xSp1were untreated (−) or treated with 10μM BRL for 12h. C: Cells transiently transfected with pCIC1473 were untreated (−) or treated with 10μM BRL and/or 100nM mithramycin (M) for 12h. Luciferase activity of untreated cells was set as 1-fold induction, upon which treatments were calculated. Columns are the means±S.D. of three independent experiments performed in triplicate.*P<0.05, n.s.=non significant. D: CIC mRNA expression in 3T3-L1 fibroblasts untreated (−) or treated with 10μM BRL and/or 100nM mithramycin (M) for 24h. Numbers represent the average fold change of CIC/β-ACTIN levels.*

1.4 BRL enhances recruitment of PPARγ and Sp1 to the CIC promoter in 3T3-L1 cells

To further support the role of the Sp1 site in mediating the BRL-induced up-regulation of CIC, we performed electrophoretic mobility shift assay (EMSA) using as a probe the Sp1 sequence present in the minimal CIC regulatory region.

We observed the formation of a protein complex in nuclear extracts from fibroblast cells (Fig. 9A, lane 1), which was abrogated by a 100-fold molar excess of unlabeled probe, demonstrating the specificity of the DNA binding complex (Fig. 9A, lane 2). This inhibition was no longer observed using a mutated oligodeoxyribonucleotide as competitor (Fig. 9A, lane 3). In cells treated with BRL, we observed an increase in the specific band compared with control samples (Fig. 9A, lane 4). Of note, in the presence of anti-PPARγ and anti-Sp1 antibodies, the specific bandwas immunodepleted (Fig. 9A, lane 5) and supershifted (Fig. 9A, lane 6), respectively, suggesting the presence of both proteins in the complex. Non-specific IgG used as a control did not generate either an immunodepleted or a supershifted band (Fig. 9A, lane 7). The functional interaction of PPARγ and Sp1 with the CIC promoter region was further elucidated by ChIP and Re-ChIP assays (Fig. 9B). Using anti-PPARγ, anti-Sp1, or anti-RNA polymerase II (PolII) antibodies, protein-chromatin complexeswere immunoprecipitated fromfibroblasts treated for 1h with vehicle or BRL. The PPARγ immunoprecipitated chromatin was re-immunoprecipitated with anti-Sp1 antibody. PCR was used to determine the occupancy of PPARγ, Sp1 and PolII to the CIC promoter region containing the Sp1 site. We showed that both PPARγ and Sp1 transcription factors were constitutively bound to the CIC promoter in untreated cells and that this recruitment was increased upon BRL exposure (Fig. 9B, left panel). Similar results were also obtained by PPARγ/Sp1 Re-ChIP assay (Fig. 9B, left panel). In addition, the positive regulation of the CIC transcriptional activity induced by BRL was demonstrated by an increased recruitment of RNA PolII (Fig. 9B, left panel). Although protein–chromatin complexes from adipocytes treated with BRL showed an enhanced recruitment of PPARγ and Sp1 to the CIC regulatory region, no changes in the association of RNA PolII to the Sp1 site were detected (Fig. 9B, right panel). To assess whether the divergent effects exerted by BRL on CIC expression during adipocyte differentiation might be caused by the cooperative interaction between PPARγ and positive (PCG1α and ARA-70) or negative (SMRT and NCoR) transcriptional regulators, we performed Re-ChIP assays in both cell lines. We found, after BRL exposure, an enhanced recruitment of PCG1α and ARA-70 coactivators in the Sp1-containing region of the CIC promoter in fibroblast cells (Fig. 9B, left panel),while an increased SMRT occupancywas observed in adipocyte cells (Fig. 9B, right panel). Finally, to better define the role of SMRT in the PPARγ-dependent modulation of the CIC mRNA and protein levels, RNA silencing technologieswere used to knockdown the expression of endogenous SMRT in both fibroblast and adipocyte cells. SMRT expressionwas effectively silenced as revealed by immunoblot analysis after 24 h of siRNA transfection in both cell lines (Fig. 9C). As expected, silencing of the SMRT gene had no effects on the up-regulation of CIC protein content and mRNA levels (Fig. 9C and D, left panels) induced by the specific PPARγ ligand

in fibroblast cells. In contrast, BRL was able to increase CIC expression in SMRT silenced adipocyte cells (Fig. 9C and D, right panels) highlighting a crucial role of SMRT corepressor in regulating CIC activity under adipocyte differentiation.

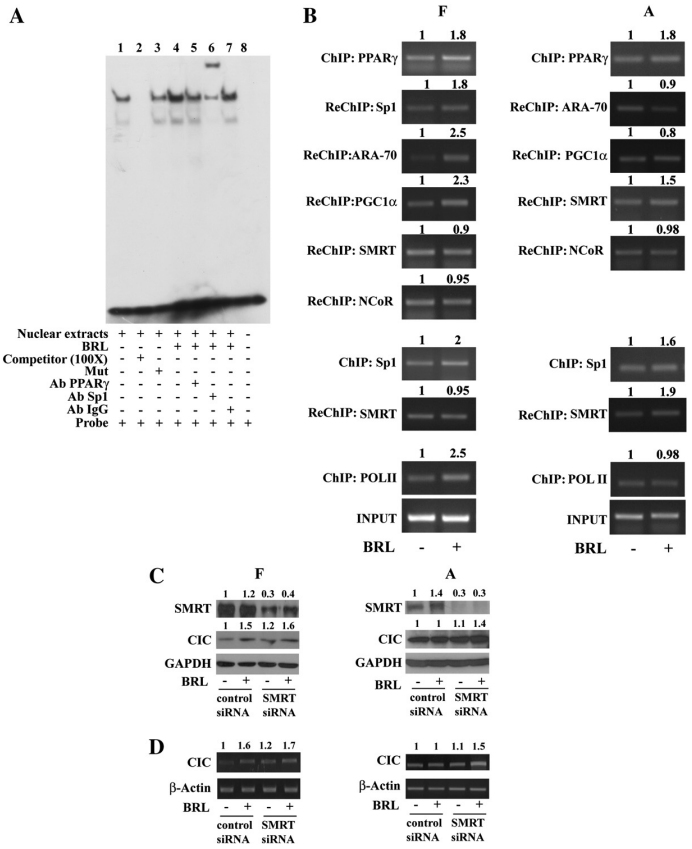

*Figure 9: PPAR**γ**/Sp1 complex binds to the Sp1 site in the CIC promoter in 3T3-L1 cells. A: Nuclear extracts from fibroblasts (lane 1) were incubated with a double-stranded Sp1 sequence probe labeled with [^{32}P] and subjected to electrophoresis in a 6% polyacrylamide gel. Competition experimentswere performed adding as competitor a 100-foldmolar excess of unlabeled (lane 2) ormutated (Mut) Sp1 probe (lane 3). In lane 4, nuclear extracts fromcells treatedwith 10**μ**M BRL for 6h. Anti-PPAR**γ** (lane 5), anti-Sp1 (lane 6) or IgG (lane 7) antibodies were incubated with nuclear extracts treated with BRL. Lane 8 contains probe alone. B: 3T3L1 fibroblasts (F) and adipocytes (A) were untreated (−) or treated with 10**μ**M BRL for 1h. The soluble chromatin was immunoprecipitated with the anti-PPAR**γ**, anti-Sp1, anti-RNA Pol II antibodies. Chromatin immunoprecipitated with the anti-PPAR**γ** antibody was re-immunoprecipitated with the anti-Sp1, anti-ARA-70, anti-PCG1**α**, anti-SMRT and anti-NCoR antibodies (ReChiP). Chromatin immunoprecipitated with the anti-Sp1 antibody was re-immunoprecipitated with the anti-SMRT antibody (ReChiP). The CIC promoter sequence containing the Sp1 site was detected by PCR with specific primers (see Materials and methods). For control input DNA, the CIC promoter was amplified from 30**μ**l initial preparations of soluble chromatin (before immunoprecipitations). C: Immunoblots for SMRT and CIC experiments in fibroblasts (F) and adipocytes (A) transfected and untreated or treated with 10**μ**M BRL for 24h as indicated. GAPDH was used as loading control. Numbers represent the average fold change of SMRT/GAPDH and CIC/GAPDH levels. D: CIC mRNA expression in fibroblasts (F) and adipocytes (A) transfected and untreated or treated with 10**μ**M BRL for 24h as indicated. **β**-Actin was used as loading control. Numbers represent the average fold change of CIC/**β**-Actin levels.*

2. Role of PPARγ in carcinogenesis

2.1 Effects of combined low doses of PPARγ and RXR ligands in breast cancer cells.

Our previous study in human cultured MCF-7 breast cancer cells, focusing on the antineoplastic role of PPARγ, showed that the synthetic PPARγ ligand BRL and RXRα ligand 9RA promote antiproliferative effects and activates different molecular pathways leading to p53-mediated apoptotic process (Bonofiglio D et al., 2009). On the basis of these observations we aim to extend the ability of nanomolar concentrations of BRL and 9RA to modulate the oncosuppressor p53 and its natural target gene p21WAF1/Cip1 not only in MCF-7 cells which express p53 wild type but also in SKBR-3 and T-47D breast cancer cells, which harbor endogenous mutant p53. We revealed that only the combination of both ligands enhanced p53 expression in all breast cancer cells tested in terms of mRNA and protein content, while the increased expression of $p21^{WAF1/Cip1}$ was highlighted only in MCF-7 cells (Fig. 10A–E), suggesting that p53 mutated form in the other two cell lines tested does not exhibit any transactivation properties. Moreover, as expected we did not observe in SKBR-3 and T-47D cells any modulation of the human wild-type p21WAF1/Cip1 promoter luciferase activity upon nanomolar concentrations of BRL and 9RA alone or in combination (data not shown), even though PPARγ can mediate the upregulation of p21WAF1/Cip1 independently of p53 (Chung SH. et al. 2002; Hong J. et al. 2004; Bonofiglio D. et al. 2008).

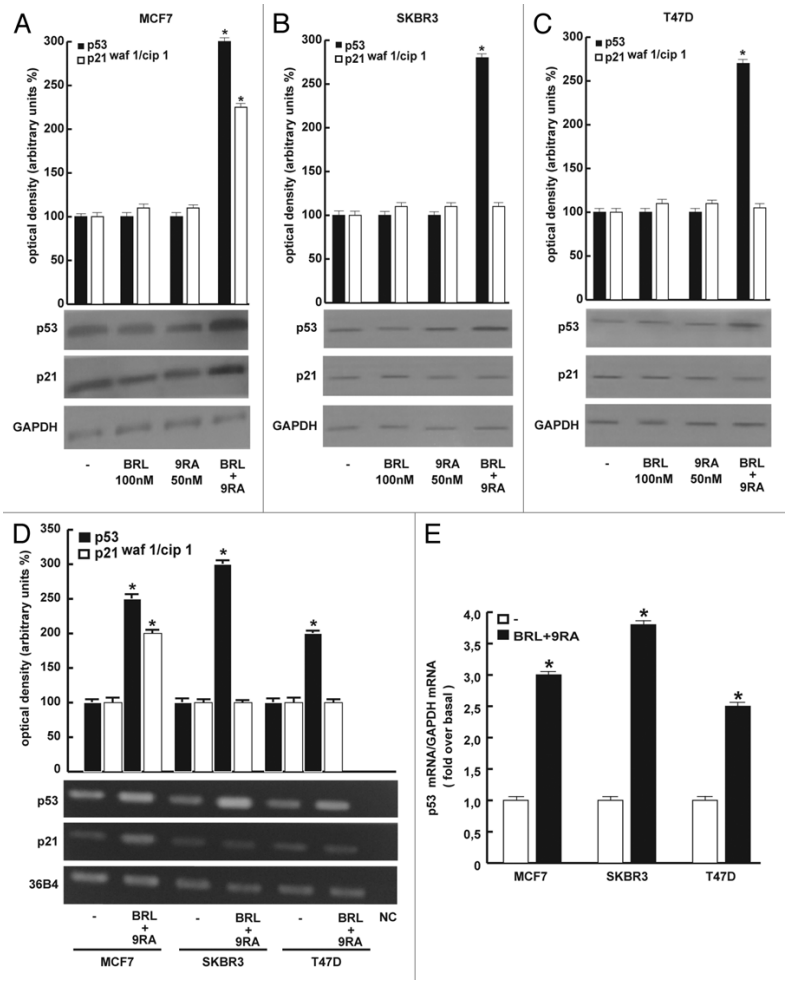

*Figure 10: Combined low doses of BRL and 9RA upregulate p53 expression in MCF-7, SKBR-3 and T-47D breast cancer cells. (A–C) Immunoblots of p53 and p21 from extracts of MCF-7, SKBR-3 and T-47D cells untreated (-) or treated with 100nM BRL and/or 50nM 9RA for 24h. GAPDH was used as loading control. The histograms show the quantitative representation of data (mean ± SD) of three independent experiments in which band intensities were evaluated in terms of optical density arbitrary units and expressed as percentages of the control which was assumed to be 100%. (D) p53 and p21 mRNA expression in MCF-7, SKBR-3 and T-47D cells untreated (-) or treated with 100nM BRL plus 50nM 9RA for 12h. The histograms show the quantitative representation of data (mean ± SD) of three independent experiments after densitometry and correction for 36B4 expression and expressed as percentages of the control which was assumed to be 100%. (E) Quantitative real-time PCR analysis of p53 mRNA expression in MCF-7, SKBR-3 and T-47D cells treated as in (D). The histograms show the quantitative representation of data (mean ± SD) of three ndependent experiments after correction for GAPDH expression. NC: RNA samples without the addition of reverse transcriptase (negative control). *p<0.05 combinedtreated vs. untreated cells.*

2.2 BRL plus 9RA treatment improves the association between p53 and bid in breast cancer cells.

p53 participates in apoptosis, even by acting directly on multiple mitochondrial targets (Murphy ME. et al. 2004). Therefore, we evaluated the involvement of Bcl-2 proteins family in regulating apoptosis. After 48 h BRL plus 9RA treatment, we determined the protein levels of Bid, Bad, Bcl-xL in both cytosolic and mitochondrial fractions of breast cancer cells. The separate treatment with low doses of either BRL or 9RA did not elicit any noticeable effect on Bid expression (data not shown), in contrast an upregulation of Bid protein content upon the combined treatment was observed in both cytosolic and mitochondrial extracts, while unchanged levels of Bad and Bcl-xL were detected in all the fractions tested (Fig. 11A). To examine whether wt and/or mutant p53 protein could associate with Bid in the cytoplasm and colocalize to the mitochondria, we performed co-immunoprecipitation experiments using cytosolic and either whole mitochondria or mitochondrial matrix extracts from breast cancer cells treated for 48 h with BRL plus 9RA. Equal amounts of protein extracts were immunoprecipitated with an anti-p53 antibody and then subjected to immunoblot with anti-Bid antibody. As seen in Figure 11B, in cytosolic immunoprecipitates we detected under physiological conditions the association between p53 and Bid that slightly increased upon BRL plus 9RA treatment, while in whole mitochondria we revealed that p53 was able to interact with the more active truncated Bid, tBid particularly in the presence of the combined treatment (Fig. 11C). In the matrix of mitochondria no association between the two proteins was observed, suggesting that this physical interaction occurs in mitochondrial membrane likely initiating this organelle dysfunction (Fig. 11D). Since it has been reported the interaction of tBid with other pro-apoptotic proteins resulting in a more global permeabilization of the outer mitochondrial membrane (Korsmeyer SJ. et al. 2000), we also explored the involvement of Bak and Bax. We detected the presence of Bak (Fig. 11B and C), but not of Bax (data not shown) as component of this multiprotein complex. Stemming from our previous findings demonstrating that p53 binds to PPARγ in breast cancer cells (Bonofiglio D. et al. 2006), we investigated in our cellular context a possible association of PPARγ to this protein complex together with its heterodimer RXRα. We observed the presence of both receptors in this complex in cytosol as well as in whole mitochondria, but not in mitochondrial matrix (Fig. 11B-D). The p53/Bid association still occured after knocking down PPARγ and RXRα (data not shown). To better define the mitochondrial colocalization of p53 and Bid, we used a red-fluorescent dye that passively diffuses across the plasma membrane and accumulates in active mitochondria. In MCF-7 cells the coexpression of both

proteins gave rise to a merged image which appears further enhanced in cells treated with BRL plus 9RA (Fig. 11E).

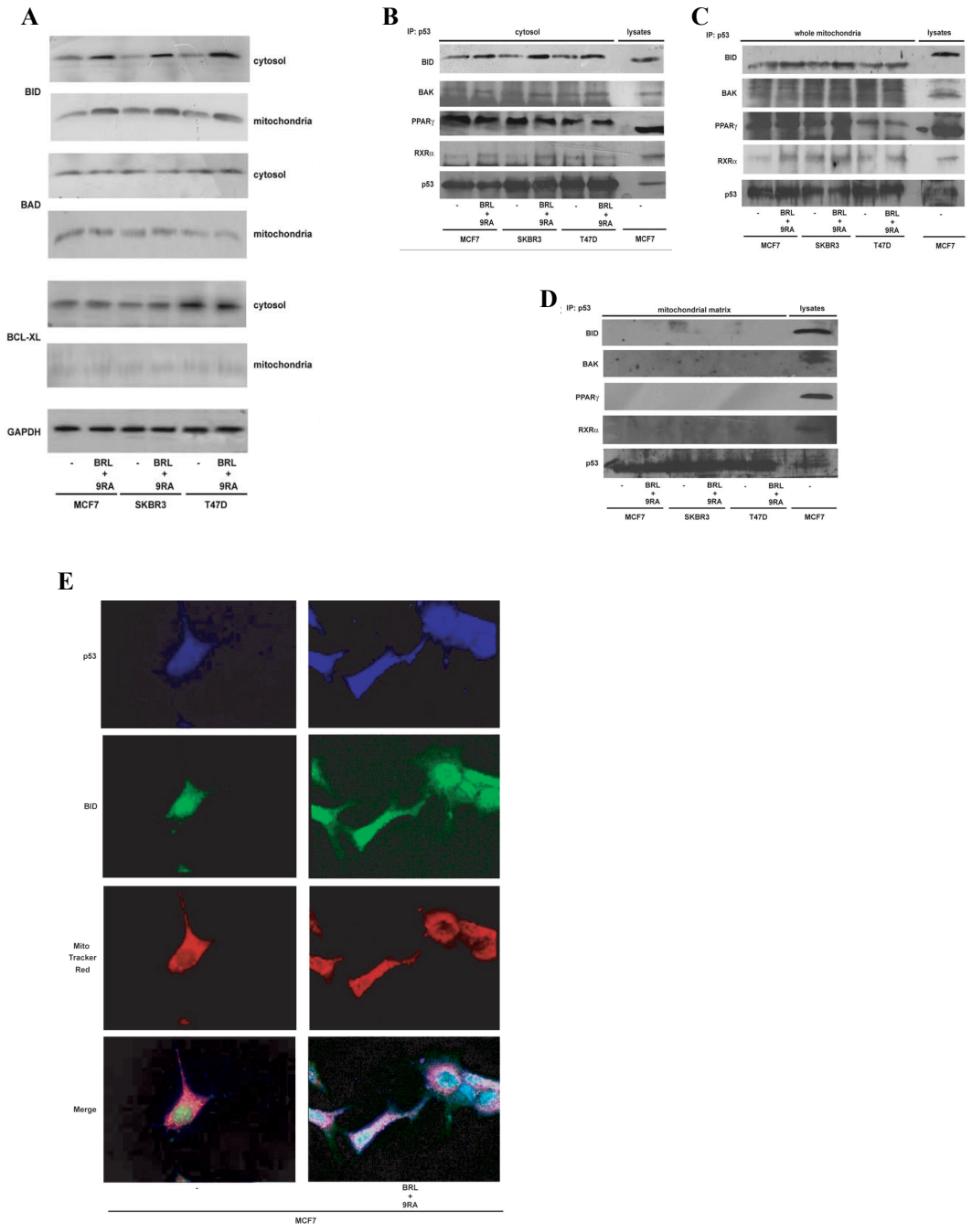

Figure 11: Upregulation of BID expression by BRL and 9RA in breast cancer cells. (A) Cytosolic and mitochondrial expression of Bid, Bad and Bcl-xL proteins in MCF-7, SKBR-3 and T-47D breast cancer cells untreated (-) or treated for 48h with 100nM BRL plus 50nM 9RA. GAPDH was used as loading control. One of three similar experiments is presented. MCF-7, SKBR-3 and T-47D cells were untreated (-) or treated for

48h with BRL plus 9RA. Cytosolic (B), whole mitochondrial (C) and mitochondrial matrix (D) extracts were immunoprecipitated with an anti-serum against p53 (IP:p53) and then the immunocomplexes were resolved in SDS-PAGE. The membrane was probed with anti-BID, anti-BAK, anti-PPARγ and anti-RXRα antibodies. To verify equal loading, the membrane was probed with an antibody against p53. One of three similar experiments is presented. MCF-7 lysates were used as positive control. (E) MCF-7 cells untreated (-) or treated with BRL plus 9RA for 48 hours were incubated in MitoTracker Red dye. Cells were immunostained with p53 and BID and then examined by fluorescent microscopy. Blue, p53; green, BID; red, MitoTracker; merge of blue, green and red as expression of colocalization in mitochondria.

2.3 Bid is involved in apoptotic events triggered by BRL plus 9RA treatment in breast cancer cells.

In order to validate the key role of Bid in the apoptotic process we used different experimental approaches after silencing Bid expression. We analyzed mitochondrial membrane potential using a fluorescent dye JC-1 in all cell lines tested after BRL plus 9RA treatment. Cells transfected with control RNAi allowed the accumulation of lipophilic dye in aggregated form in mitochondria, displaying red fluorescence as shown in Figure 13A, demonstrating the integrity of the mitochondrial membrane potential. Cells treated with both ligands exhibited green fluorescence, indicating the disruption of mitochondrial integrity, because JC-1 cannot accumulate within the mitochondria, but instead remained as a monomer in the cytoplasm. After silencing Bid expression, red fluorescence was evident in treated cells (Fig. 12A), suggesting that the integrity of the mitochondrial membrane potential is maintained in MCF-7, SKBR-3 and T-47D cells. This result well fits with a significant decrease of PARP cleavage in cells transfected with Bid RNAi and treated with ligands respect to treated cells transfected with control RNAi (Fig. 12B). Indeed in transfected cells with Bid-RNAi TUNEL assay showed after 72h treatment a strong reduction of the percentage of apoptotic cells respect to treated cells trasfected with control RNAi (Fig. 12C). All these data indicate that Bid plays an important role in the death pathway induced by low doses of PPARγ and RXR ligands in breast cancer cells.

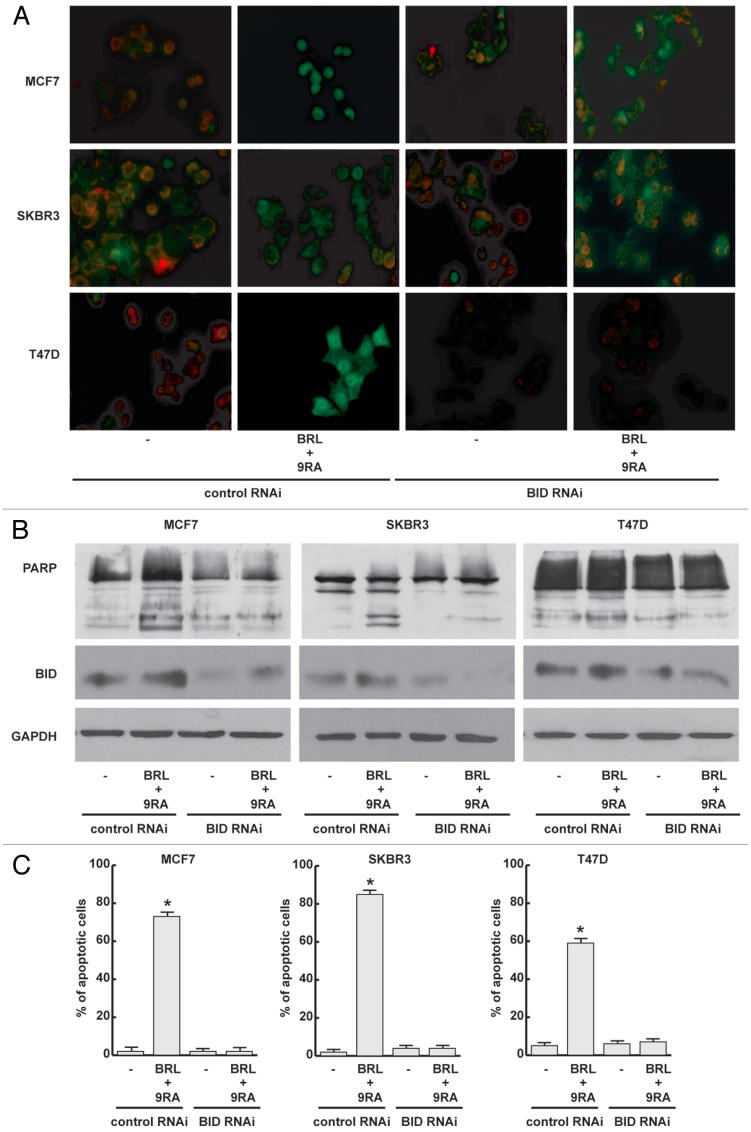

*Figure 12: Knocking down BID abrogates apoptotic events in breast cancer cells. (A) MCF-7, SKBR-3 and T-47D cells were transfected with control RNAi or with BID RNAi and treated for 48h as indicated. The results of JC-1 kit were examined by fluorescent microscopy. (B) Immunoblots of PARP and BID from total extracts of MCF-7, SKBR-3 and T47-D cells transfected and treated as in (A). GAPDH was used as loading control. One of three similar experiments is presented. (C) Cells were transfected as in (A) and treated for 72h as indicated. The histograms show the quantitative representation of data (mean ± SD) of three independent experiments performed in triplicates. *p < 0.05 combined-treated vs. untreated cells.*

2.4 The PPARγ ligands DHEA and EPEA inhibit breast cancer cell growth

Diet and particularly dietary lipids have long been studied in association with

breast cancer risk, survival, and recurrence (Glade, 1999; Rock and Demark-Wahnefried, 2002; Bougnoux et al., 2010). Increasing dietary consumption of the long chain n-3 PUFA, DHA, and EPA have been demonstrated to inhibit breast carcinogenesis by decreasing cell viability, proliferation, invasion, and increasing chemosensitivity (Evans and Hardy, 2010). In breast cancer cells DHA and EPA can be directly converted to N-acylethanolamines, DHEA, and EPEA, respectively (Brown et al., 2011); however, today their biological activities remain unexplored. On this basis, first, we aimed to evaluate the effects of increasing concentrations of DHEA and EPEA on proliferation of MCF-7 breast cancer cells by using MTT assays.We observed that both treatments strongly reduced cell viability in a dose- and timedependent manner (Fig. 13A,B). In contrast, 10μM DHEA or EPEA did not elicit any significant growth inhibitory effects on MCF-10A non-tumorigenic breast epithelial cells (Fig. 13C). The prolonged treatments up to 96h in MCF-7 cells showed greater anti-proliferative responses, with IC50 values of 0.8μM DHEA and 1.5μM EPEA (Table 2). A second approach we employed was to evaluate the anti-proliferative effects induced by DHEA and EPEA using anchorage-independent soft agar growth assays. Consistently with MTT assays, both treatments at 10μM significantly reduced colony formation in MCF-7cells (Fig. 13D). Taken together, these results show that both compounds induced a growth inhibition in MCF-7 breast cancer cells, while no effects were observed in MCF-10A breast epithelial cells.

TABLE 2. IC50 values of DHEAand EPEA in MCF-7 cells from MTT growth assay

Compounds	IC50 (μM)	95% confidence interval
DHEA	0.8	0.5–1.2
EPEA	1.5	0.9–2.5

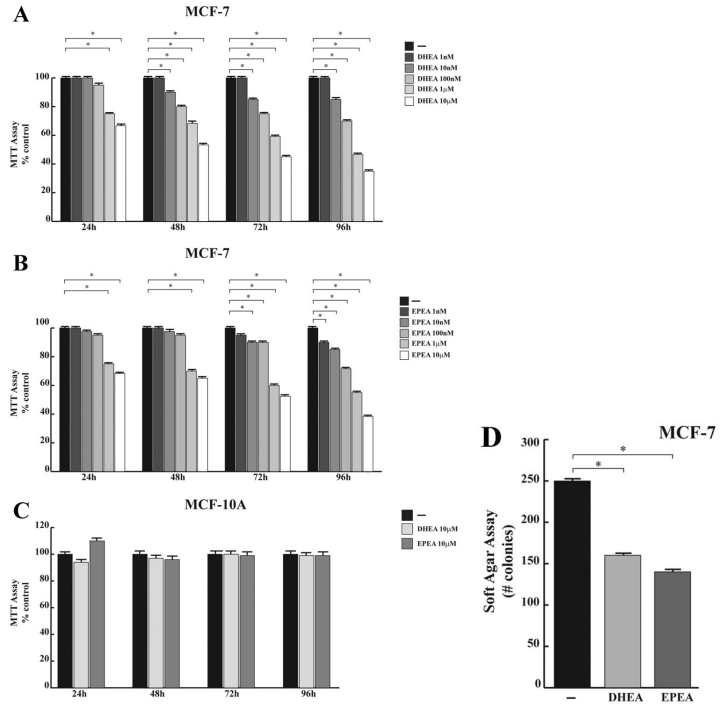

Figure 13: Effects of DHEA and EPEA on breast cancer cell growth.MTT assays in MCF-7 cells were untreated (-) or treated with increasing concentrations (1, 10, 100 nM, 1, 10μM) of DHEA (A) or EPEA(B) and in MCF-10A (C) treated with vehicle (-), DHEA or EPEA 10μM as indicated. Cell proliferation is expressed as % of control (untreated cells). The values represent the means ±SD of three different experiments, each performed with triplicate samples. D: MCF-7 cells were plated in soft agar and then untreated (-) or treated with DHEA or EPEA 10μM. Cells were allowed to grow for 14 days and the number of colonies >50mm diameter were counted and the results were graphed. Data are the mean colony number ±SD of three plates of three independent experiments. P<0.05.

Next, we investigated the ability of DHEA and EPEA to modulate PPARγ expression and activity in MCF-7 cells. Using real-time RT-PCR and immunoblotting analysis, we found an enhanced expression of PPARγ at both mRNA and protein levels in cells treated with 1mM DHEA or EPEA (Fig. 14A,B). Moreover, transiently transfected cells with a PPAR response element (PPRE) reporter plasmid, we demostrated that both compounds transactivate endogenous PPARγ. Particularly, as reported in Figure 14C, DHEA and EPEA-induced a significant enhancement in the transcriptional activation of the reporter plasmid although in a lesser extent respect to the PPARγ ligand rosiglitazone (BRL). The PPARγ antagonist GW9662 (GW) abolished the PPRE reporter activity induced by BRL and by both compounds (Fig. 14C), addressing the direct activation of PPARγ. Previous studies have shown that PPARγ regulates the transcription of phosphatase and tensin homolog on chromosome ten (PTEN) (Patel et al., 2001), a unique phosphatase that has the ability to decrease the levels

of p-AKT and consequently AKTmediated pathways. Thus, we investigated whether DHEA and EPEA were able to modulate PTEN expression and its downstream pathway in MCF-7 cells. Our results demonstrated that both compounds enhanced PTEN protein levels which were associated with the decrease of AKT-mTOR signaling pathway (Fig. 14D), suggesting a potential involvement of either apoptotic or autophagic processes.

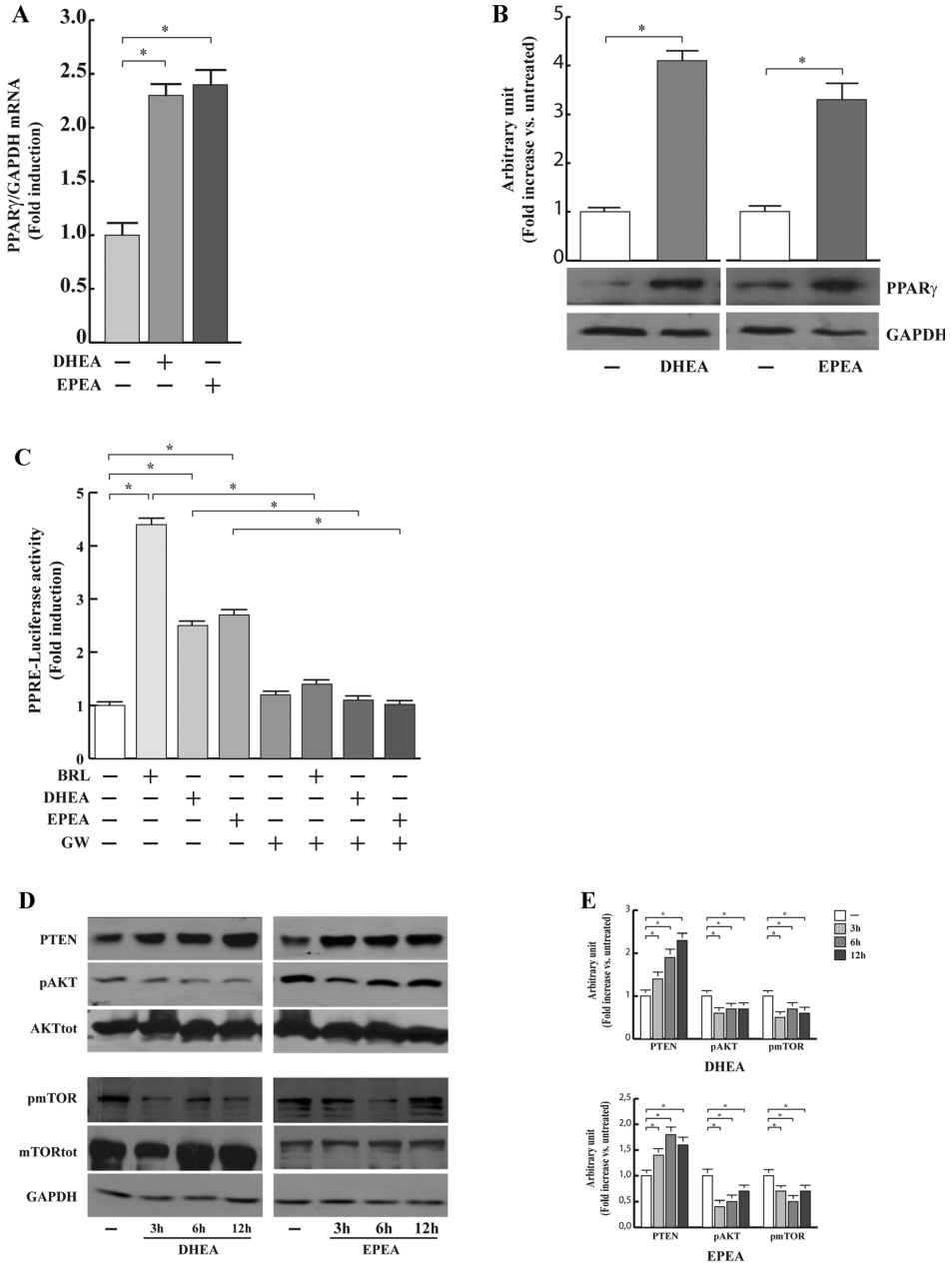

Figure 14: Activation of PPARγ by DHEA and EPEA in MCF-7 cells. A: mRNA PPARγ content, evaluated by

real-time RT-PCR, in MCF-7 cells after treatment with vehicle (-), DHEA or EPEA 1mM for 12 h. Each sample was normalized to its GAPDH mRNA content. P<0.05. B: Immunoblots of PPARγ expression from total extracts of MCF-7 cells treated as in A for 24h. GAPDH was used as loading control. The histograms represent the means ±SD of three separate experiments in which band intensities were evaluated in terms of optical density arbitrary units and expressed as fold change versus untreated (-) cells normalized for GAPDH levels. P<0.05. C: MCF-7 cells were transiently transfected with a PPARγ-response element (PPRE) reporter plasmid and untreated (-) or treated for 24h with BRL10μM, DHEA1μM, EPEA1μM, and/or GW9662 (GW) 10μM and then luciferase activity was measured. Results represent the mean ±SD of three different experiments each performed in triplicate. P<0.05. D: Cells were untreated (-) or treated with DHEA or EPEA 1μM as indicated. Equal amounts of total cellular extracts were analyzed for PTEN, phosphorylated AKT (pAKT) and mTOR (pmTOR), total AKT (AKTtot) and total mTOR (mTORtot) levels by western blotting. GAPDH was used as loading control. E: The histograms represent the means ±SD of three separate experiments in which band intensities were evaluated in terms of optical density arbitrary units and expressed as fold change between pospho-, total, and GAPDH levels.

2.5 PPARγ mediates the up-regulation of beclin-1 expression induced by DHEA and EPEA in MCF-7 cells

Autophagy is a complicated regulatory process regulated by the activation of beclin-1, a novel Bcl-2-homology (BH)-3 domain only protein (Levine and Deretic, 2007). Thus we evaluated whether DHEA and EPEA through PPARγ are able to regulate beclin-1 expression in MCF-7 cells. We found, after knocking down PPARγ expression (Fig. 15A,B), that the enhancement of beclin-1 dependent on DHEA and EPEA exposure was completely abrogated (Fig. 15C,D), addressing that this effect is specifically PPARγ-mediated.

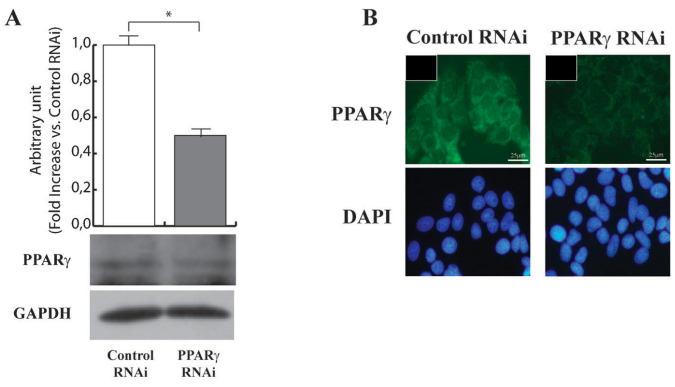

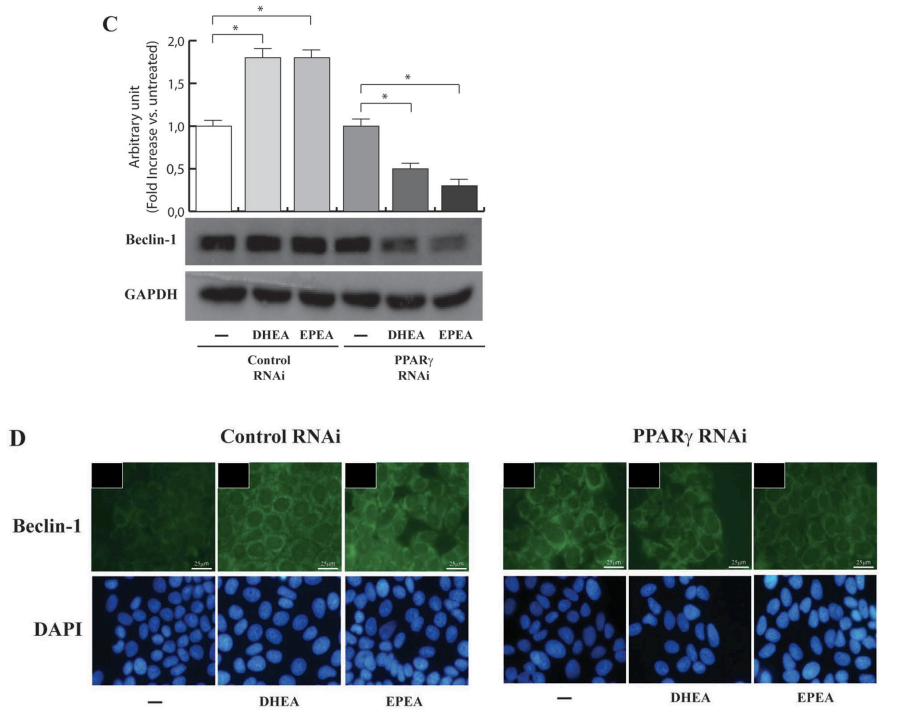

Figure 15: DHEA and EPEA reduce beclin-1/Bcl-2 complex and trigger autophagy inMCF-7cells. A: Protein extracts from MCF-7 cells untreated (-) or treated with DHEA or EPEA 1μM as indicated, were immunoprecipitated with an anti-serum against beclin-1 and then blotted with anti-Bcl-2 and anti-beclin-1 antibodies. B: Cells were untreated (-) or treated with DHEA or EPEA1mM as indicated. Equal amounts of total cellular extracts were analyzed for phosphorylated Bcl-2 (pBcl-2) and total Bcl-2 (Bcl-2) levels by western blotting. GAPDH was used as loading control. The histograms represent the means ±SD of three separate experiments in which band intensities were evaluated in terms of optical density arbitrary units and expressed as fold change between phospho-, total, and GAPDH levels. P<0.05. C: DNA laddering was performed in MCF-7 cells untreated (-) or treated with DHEA or EPEA 1mM for 12h. One of three similar experiments is presented. D: Cells were untreated (-) or treated with DHEA or EPEA 1μM as indicated. Equal amounts of total cellular extracts were analyzed for phosphorylated P38 (pP38) and total P38 (P38tot) levels by western blotting. GAPDH was used as loading control. The histograms represent the means ±SD of three separate experiments in which band intensities were evaluated in terms of optical density arbitrary units and expressed as fold change between phospho-,total, and GAPDH levels. P<0.05. E: Immunofluorescence of microtubule-associated protein 1 light-chain 3 (LC3) (upper parts) and DAPI (lower parts) in cells untreated (-) or treated with DHEA or EPEA 1mM for 6h. Small squares, negative controls. F: Mono-dansyl-cadaverine staining of MCF-7 cells untreated (-) or treated with DHEA and EPEA 1μM, and/or GW9662 (GW) 10μM for 12h. One of three similar experiments is presented.

2.6 DHEA and EPEA reduce the interaction between beclin-1 and Bcl-2 and induce autophagy in MCF-7 cells

It has been reported that beclin-1 physically interacts with the anti-apoptotic protein Bcl-2 inhibiting autophagy (Pattingre et al., 2005) and that once Bcl-2 is

phosphorylated it dissociates from beclin-1 and autophagy can occur (Wei et al., 2008). Thus, we performed coimmunoprecipitation assay in order to evaluate the effects of DHEA and EPEA on beclin-1/Bcl-2 complex formation. As shown in Figure 16A, beclin-1 was constitutively associated with Bcl-2 and treatment with both compounds reduced this association. In the same experimental conditions, we observed an increased Bcl-2 phosphorylation of serine70 (Fig. 16B). To ascertain if the treatment with DHEA or EPEA may trigger apoptotic cell death in our cell system, we evaluated changes in the internucleosomal fragmentation profile of genomic DNA, which is a diagnostic hallmark of cells undergoing apoptosis. DNA laddering revealed, after exposure to DHEA and EPEA, the absence of DNA fragmentation (Fig. 16C). Moreover, we analyzed the phosphorylation levels of p38, which negatively regulates autophagy (Comes et al., 2007; Chiacchiera and Simone, 2008), along with the expression of microtubule-associated protein 1 light-chain 3 (LC3) a specific membrane marker for the detection of early autophagosome formation in cells treated with both compounds. As shown in Figure 16D, upon DHEA or EPEA administration a reduction in the phosphorylation state of p38 associated with a significant increase in LC3 immunofluorescence could be observed in MCF-7 cells (Fig. 16E). Moreover, cells treated with DHEA or EPEA exhibited normal nuclei and did not display typical apoptotic changes with chromatin condensation and nuclear fragmentation, as evidenced by DAPI staining (Fig. 16E). Next, in order to corroborate the autophagic process induced by DHEA or EPEA in MCF-7 cells, mono-dansylcadaverine (MDC) staining was performed. As expected, the formation of autophagosomes was clearly enhanced in treatedcells (Fig. 16F). The involvement of PPARγ in DHEA- and EPEA induced autophagy was evidenced by the ability of the PPARγ antagonist GW to prevent the accumulation of MDC-labeled vacuoles (Fig. 16F). All these data indicate that DHEA and EPEA treatments induce cell death by autophagy in a PPARγ-dependent manner in MCF-7 cells.

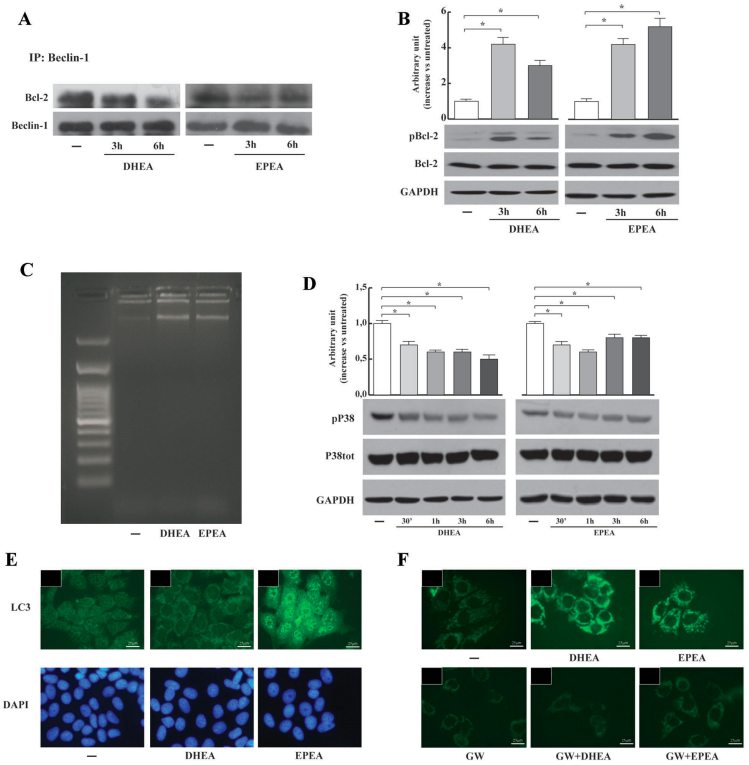

Figure 16: DHEA and EPEA reduce beclin-1/Bcl-2 complex and trigger autophagy in MCF-7cells. A: Protein extracts from MCF-7 cells untreated (-) or treated with DHEA or EPEA 1mM as indicated, were immunoprecipitated with an anti-serum against beclin-1 and then blotted with anti-Bcl-2 and anti-beclin-1 antibodies. B: Cells were untreated (-) or treated with DHEA or EPEA 1μM as indicated. Equal amounts of total cellular extracts were analyzed for phosphorylated Bcl-2 (pBcl-2) and total Bcl-2 (Bcl-2) levels by western blotting. GAPDH was used as loading control. The histograms represent the means ±SD of three separate experiments in which band intensities were evaluated in terms of optical density arbitrary units and expressed as fold change between phospho-, total, and GAPDH levels. P<0.05. C: DNA laddering was performed in MCF-7 cells untreated (-) or treated with DHEA or EPEA 1mM for 12h. One of three similar experiments is presented. D: Cells were untreated (-) or treated with DHEA or EPEA 1μM as indicated. Equal amounts of total cellular extracts were analyzed for phosphorylated P38 (pP38) and total P38 (P38tot) levels by western blotting. GAPDH was used as loading control. The histograms represent the means ±SD of three separate experiments in which band intensities were evaluated in terms of optical density arbitrary units and expressed as fold change between phospho-, total, and GAPDH levels. P<0.05. E: Immunofluorescence of microtubule-associated protein 1 light-chain 3 (LC3) (upper parts) and DAPI (lower parts) in cells untreated (-) or treated with DHEA or EPEA 1mM for 6h. Small squares, negative controls. F: Mono-dansyl-cadaverine staining of MCF-7 cells untreated (-) or treated with DHEA 1μM, EPEA 1μM, and/or GW9662 (GW) 10μM for 12h. One of three similar experiments is presented.

2.7 Combined treatment of BRL and DHEA or EPEA reduce cell death in MCF-7 cells

Having demonstrated the crucial role played by PPARγ in the growth inhibition

triggered by omega-3 ethanolamides in MCF-7 cells, we evaluated the effects of the PPARγ ligand BRL in combination with DHEA or EPEA on breast cancer cell proliferation using anchorage-independent soft agar growth assays. Our results showed that the DHEA- and EPEA-reduced cell growth was potentiated in the presence of BRL, and prevented using the PPARγ-antagonist GW, further supporting a direct involvement of this nuclear receptor (Fig. 17).

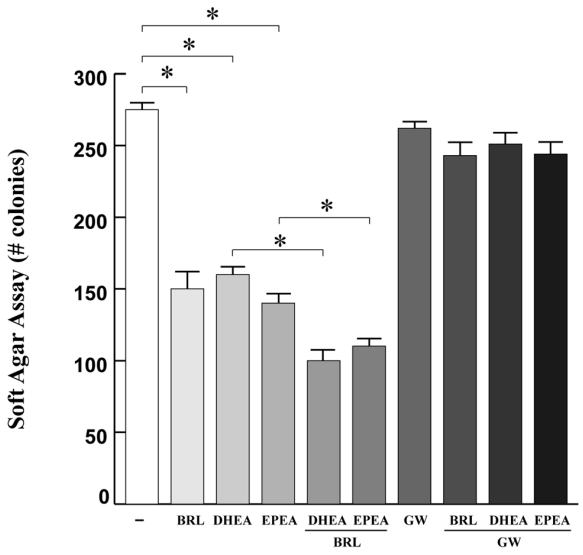

Figure 17: Effects of combined treatment of BRL and DHEA or EPEA on MCF-7 cell growth. Cells were plated in soft agar and then untreated (-) or treated with BRL 10μM, DHEA 10μM, EPEA 10μM, and/or GW9662 (GW) 10μM. Cells were allowed to grow for 14 days and the number of colonies >50mm diameter were counted and the results were graphed. Data are the mean colony number ±SD of three plates of three independent experiments. P<0.05.

Discussion

In the present study we have elucidated the dual role of PPARγ as master regulator of adipogenesis and as inhibiting factor of carcinogenesis.

In the first part of this work, we have demonstrated that activated PPARγ modulates the expression and the activity of the mitochondrial citrate carrier CIC during the differentiation stages of fibroblasts into adipocytes. Using the cultured 3T3-L1 cell system, we have shown that BRL up-regulated CIC expression and its activity in fibroblasts through PPARγ activation, while BRL was not able to modulate CIC levels in mature adipocytes. These data contradict previous findings indicating that PPARγ ligands increased CIC expression in adipocytes (Damiano F et al. 2012), although the latter measurements were performed at 7 days after differentiation induction. From our study, the specific involvement of PPARγ in up-regulating CIC expression in fibroblasts was proved by the observation that the PPARγ effect was completely abrogated in the presence of GW, a potent and selective antagonist of PPARγ. The molecular events responsible for CIC induction by the PPARγ ligand BRL were consistent with the enhanced transcriptional activation of this gene as it raised by the capability of BRL to activate CIC promoter. Although it has been recently demonstrated that CIC expression is regulated by PPARγ ligands through a PPRE site, identified at -625 bp of the CIC promoter (Damiano F et al. 2012), our functional studies using different CIC-promoter-deleted constructs identified the region of CIC promoter, spanning from -115/82, as the minimal region responsible for BRL induction, demostrating that CIC transactivation occurs independently of the PPRE site. Indeed, analysis of the minimal CIC promoter region reveals the presence of a GC-box sequence, and deletion as well as mutation of this site results in the abrogation of PPARγ transactivating activity. Furthermore, when Sp1-DNA binding activity was blocked by a selective inhibitor, both PPARγ-mediated transactivation and induction of CIC expression were subsequently abolished. In line with our results, an interesting observation is that in the presence of the Sp1mutation at -92 bp the basal activity of CIC promoter is reduced when compared with the transcriptional activity of the wild-type CIC promoter (Damiano F et al 2009). Sp1 has been considered traditionally as a ubiquitous factor associated closely with core promoter activities; it has recently been observed that it participates in the regulation of gene transcription triggered by multiple signaling pathways and metabolic or differentiation conditions. Moreover, Sp1 interacts physically and cooperates functionally with several sequence-specific activators including NF-kB, GATA, YY1, E2F1, Rb, SREBP-1 and PPARγ (Noe V et al. 1998; Rotheneder H et al. 1999; Sugawara A et al. 2002; Flück CE et al. 2004; Teferedegne B et al. 2006; Bonofiglio D et al. 2008) to modulate gene expression. In addition, it has been shown that the activation of

CIC gene expression by Sp1 is virtually abolished by methylation of the Sp1-binding elements which are present in the promoters of all CIC genes sequenced in mammals within the CpG island located immediately upstream the translocation start codon (Iacobazzi V et al. 2008). We demostrated in fibroblast cells that PPARγ/Sp1 occupancy of the Sp1-containing promoter region induced by BRL treatment was concomitant with an increase in RNA-PolII, addressing a positive CIC transcriptional regulation mediated by PPARγ. It is known that members of the nuclear hormone receptor superfamily, including PPARγ, once activated, can interact physically and modulate target gene transcription. PPARγ can regulate transcription by several distinct mechanisms, and its function seems to depend not only on ligand binding, which is known to regulate receptor conformation, but also on the context of the gene and associated promoter factors that contribute to create a gene-specific topography, achieving specific profiles of gene expression. Several studies have examined the role of coregulators in adipogenesis and demonstrated that coactivators such as PGC-1α or steroid receptor coactivators (SRCs) are essential (Feige JN et al 2007); whereas NCoR, SMRT and histone deacetylases act as negative regulators of differentiation (Picard F et al 2004; Yu C et al 2005; Jing E et al 2007). The physiological relevance of their implication in metabolic regulation has been demonstrated in the context of PPARγ-mediated adipogenesis, during which they promote a target-gene specific repression of PPARγ activity (Guan HP et al 2005). A negative action of SMRT and NCoR on fat storage has been suggested by the enhanced adipogenesis and increased expression of proadipogenic PPARγ target genes after RNAi-mediated inhibition of these corepressors (Yu C et al 2005). Our results evidenced in fibroblast cells, after BRL stimulation, an enhanced recruitment of PGC-1α and ARA-70 on the Sp1 site of the CIC promoter. In contrast, we observed that mature adipocytes treated with BRL showed an increased recruitment of SMRT corepressor to the Sp1 site within the CIC promoter along with no changes in the occupancy of RNA PolII. Finally, we demonstrated a direct involvement of SMRT in the loss of CIC promoter responsiveness to the BRL in mature adipocytes using a specific SMRT siRNA.

In conclusion, our study identifies a novel molecular mechanism through which PPARγ modulates CIC expression, a crucial mitochondrial carrier for glucose and lipid metabolism and for energy homeostasis regulation. The divergent mechanisms through which PPARγ activation may switch the modulation of CIC expression during adipocyte differentiation are schematically shown in Fig.18. We propose a model in which: i) in fibroblasts treated with BRL, PPARγ/Sp1 complex along with PGC1α and ARA-70 coactivators are recruited on the Sp1-containing region of the CIC promoter, thereby increasing CIC expression; ii) in adipocytes treated with BRL, PPARγ/Sp1 complex is associated with an enhanced recruitment of SMRT corepressor on the Sp1 site of CIC

promoter resulting in an inhibition of CIC transcription.

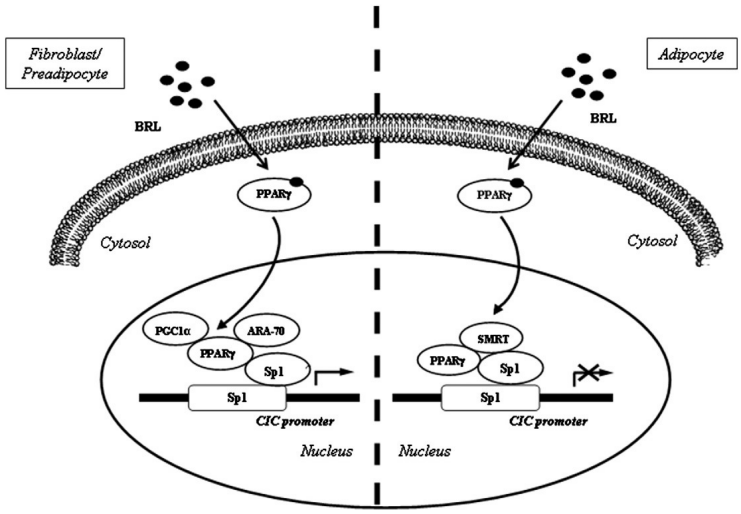

Figure 18: Proposed working model of the PPARγ-mediated regulation of CIC expression in fibroblasts and adipocytes. In fibroblasts, upon BRL treatment, PPARγ/Sp1 complex is recruited on the Sp1-containing region of CIC promoter along with PGC1-α and ARA70 coactivators, leading to an increase in CIC expression. In adipocytes, the formation of PPARγ/Sp1 complex is associated with the recruitment of SMRT corepressor, resulting in an inhibition of CIC transcription

PPARγ appears to play a role in regulating processes of proliferation and differentiation in both normal and malignant tissues (Rangwala SM. et al. 2004; Staels B. 2005). Solid tumors including breast cancers express PPARγ, and treatment with ligands leads to the development of a differentiated phenotype and inhibition of cell proliferation (Yin F et al., 2001). These studies support the role of PPARγ activators as negative regulators of cell growth and tumor progression and led us to evaluate the effects of PPARγ signaling activation in human breast cancer cells in order to expand therapeutic potential of PPARγ agonist drugs.

In the second part of the present study, we provided the first evidence that low doses of PPARγ and RXR ligands through PPARγ increasing Bid expression and its association in mitochondria induce apoptosis in different breast cancer cells. The p53 pathway is inactivated in the majority of human cancers, most likely because the pro-apoptotic function of p53 is critical to the inhibition of tumor development and progression. Although the role of p53 as a nuclear transcription factor able to activate or repress a number of p53 transcriptional targets, with the potential to promote or inhibit apoptosis, is clearly established, many evidences support a transcriptional-independent function of p53 in apoptosis. Indeed, an unexpected turn in the p53-mediated pathway to programmed cell death has emerged, with accumulating data indicating that p53 has a direct cytoplasmic role at mitochondria in activating the apoptotic machinery. Thus, a major question is to define the apoptotic function of mitochondrial p53. Increased evidence suggests

that mitochondrial p53 localization is sufficient for initiating p53-dependent apoptosis (Marchenko et al. 2000; Katsumoto et al. 1995). Furthermore, some studies reported that p53 may induce apoptosis by forming complexes with mitochondrial apoptotic proteins, such as Bcl-2/Bcl-xL (Mihara M. et al. 2003), Bad (Jiang P. et al. 2006) or Bid (Song G. et al. 2009) which are located in the outer membrane of mitochondria. We hypothesized that mechanistic insight into this process could be obtained from the identification of mitochondrial p53-interacting protein. Herein, we showed that p53 interacts with Bid in cytosol and exclusively with the truncated more active tBid in mitochondria, showing a slight increase upon BRL and 9RA treatment. Bid is a member of the "BH3 domain only" subgroup of Bcl-2 family members proposed to connect proximal death and survival signals to the core apoptotic pathway at the level of the classic family members, which bear multiple BH domains (Adams JM. et al. 1998; Gross A. et al. 1999). It has been reported that Bid is able to bind mitochondrial proteins and promote cell death, suggesting a model in which Bid serves as a "death ligand" which moves from the cytosol to the mitochondrial membrane to inactivate Bcl-2 or activate Bax and Bak and to result in cytochrome c release (Rieusset J. et al. 1999). The release of cytochrome c from mitochondria has been shown to promote the oligomerization of a cytochrome c/Apaf-1/caspase-9 complex that activates caspase-9, resulting in the cleavage of downstream effector caspases (Rieusset J. et al. 1999). We showed the involvement of Bak protein as a component of a p53/Bid protein-protein interaction in breast cancer cells, hypothesizing that it contributes to form a large pore responsible for triggering apoptotic events. The involvement of Bid in apoptosis triggered by BRL plus 9RA in breast cancer cells emerged in many different approaches after silencing Bid expression. In cells treated with both ligands in presence of Bid RNAi, the disruption of mithocondrial integrity, PARP cleavage and the number of apoptotic cells were reversed. The data described above providing new insight into the role of p53/Bid complex at the mitochondria in promoting breast cancer cell apoptosis upon low doses of PPARγ and RXR ligands (Fig.19).

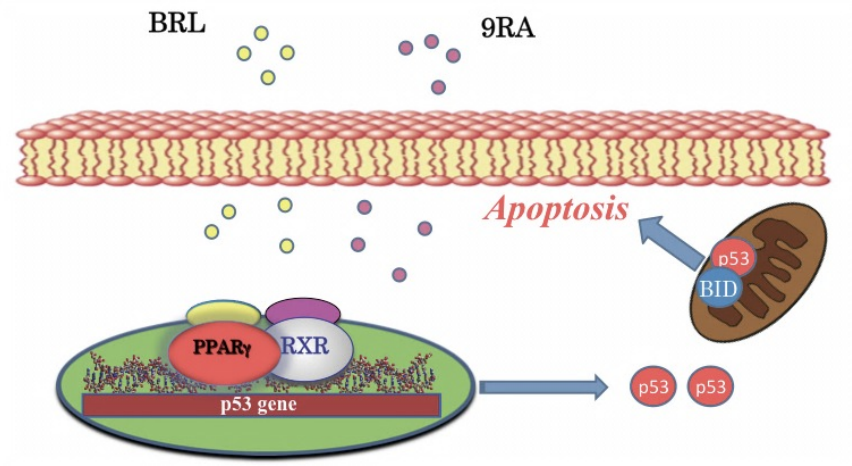

Figure 19: Molecular mechanism through which PPARγ and RXR ligands induce apoptotic events in breast cancer cells through a direct interaction between Bid and p53 on the mitochondrial membrane.

Finally, we have demostrated that omega-3 PUFA derivates, DHEA and EPEA, act as natural PPARγ ligands inducing autophagy in breast cancer cells. Our results showed that both compounds inhibit anchorage-dependent and -independent cell growth in MCF-7 breast cancer cells, whereas they don't affect growth of nontumorigenic breast epithelial cells. We evidenced that DHEA and EPEA are able to activate the endogenous PPARγ, to up-regulate its mRNA and protein levels and to enhance the expression of PTEN, a PPARγ target gene (Patel et al. 2001). PTEN's protein is a unique phosphatase that has the ability to dephosphorylate both proteins and lipids (Waite and Eng, 2002). Active PTEN leads to a decrease in the levels of p-AKT and, as a consequence, in AKT-mediated proliferation pathways. Particularly, by suppressing the phosphoinositide 3-kinase (PI3K)-AKT-mammalian target of rapamycin (mTOR) pathway, PTEN governs a plethora of cellular processes including survival, proliferation, energy metabolism, and cellular architecture. We found that the increased PTEN protein levels induced by DHEA and EPEA were associated with the suppression of AKT-mTOR signaling pathway in MCF-7 cells. As a central element of the transduction signaling involved in cell growth, mTOR when inhibited, induces autophagy. Moreover, as a critical feedback mechanism, reactivation of mTOR terminates autophagy and initiates lysosome reformation (Yu et al., 2010). Autophagy is an essential process that consists of selective degradation of cellular components. The initial step of autophagy is regulated not only by class I PI3Ks but also by activation of class III PI3K in a complex with autophagy associated protein beclin-1 (Levine and Deretic, 2007). Beclin-1 was originally discovered in a yeast two-hybrid screen as a Bcl-2-interacting protein and was the first human protein shown to be indispensable for autophagy (Liang et al., 1999). We found that DHEA and EPEA exposure enhanced beclin-1 protein levels and induced phosphorylation of Bcl-2 on ser70 promoting its dissociation

from beclin-1. Conflicting data are reported on the role of phosphorylated Bcl-2. It has been suggested that the phosphorylation of ser70 inactivates the anti-apoptotic function of Bcl-2 (Yamamoto et al. 1999), while other studies reported that phosphorylation of ser70 Bcl-2 site would enhance its anti-apoptotic functions (Ito et al. 1997). In our experimental model, DHEA and EPEA treatments did not induce any changes in the internucleosomal fragmentation profile of genomic DNA, which is a diagnostic hallmark of cells undergoing apoptosis, suggesting that the DHEA- or EPEA-induced growth inhibition does not occur through an apoptotic process, but may involve autophagic pathway. It is well known that autophagy is characterized by multiple steps which lead to final event of the autophagolysosome formation. In this biological process, we demonstrated the involvement of proteins with a pivotal role in the autophagic cell death, such as beclin-1, as mentioned above, which participates in the formation of autophagosomes and LC-3 protein, which is a specific membrane marker for the detection of early autophagosome formation. Concomitantly, as emerged by MDC fluorescence, we observed a marked increase of autophagic vacuoles formation. Notably, our results clearly demonstrated a direct involvement of PPARγ in DHEA- and EPEA-induced autophagy in MCF-7 breast cancer cells using a specific PPARγ RNAi and a selective inhibitor, providing a distinct role of PPARγ in inhibiting tumorgenesis.

Our data emphasize the importance of the two omega-3 polyunsaturated fatty acid ethanolamides DHEA and EPEA as new pharmacological tools to be perspectively implemented in the adjuvant therapy for breast cancer treatment.

References

Adams JM, Cory S: *The Bcl-2 protein family: arbiters of cell survival, Science 1998 281(5381):1322-6.*

Allred CD, Talbert DR, Southard RC, Wang X, Kilgore MW*: PPARgamma1 as a molecular target of eicosapentaenoic acid in human colon cancer (HT-29) cells, J Nutr 2008 38(2):250-6.*

Arakawa K, Ishihara T, Aoto M, Inamasu M, Kitamura K, Saito A*: An antidiabetic thiazolidinedione induces eccentric cardiac hypertrophy by cardiac volume overload in rats, Clin Exp Pharmacol Physiol 2004 31(1-2):8-13.*

Bisaccia F, De Palma A, Palmieri F: *Identification and purification of the tricarboxylate carrier from rat liver mitochondria, Biochim. Biophys. Acta, 1989 23;977(2):171-6 .*

Bisaccia F, De Palma A, Prezioso G, Palmieri F: *Kinetic characterization of the reconstituted tricarboxylate carrier from rat liver mitochondria, Biochim. Biophys. Acta, 1990 19;1019(3):250-6.*

Bischoff ED, Gottardis MM, Moon TE, Heyman RA, Lamph WW*: Beyond tamoxifen: the retinoid X receptor-selective ligand LGD1069 (TARGRETIN) causes complete regression of mammary carcinoma, Cancer Res 1998 1;58(3):479-84.*

Blume SW, Snyder RC, Ray R, Thomas S, Koller CA, Miller DM*: Mithramycin inhibits Sp1 binding and selectively inhibits transcriptional activity of the dihydrofolate reductase gene in vitro and in vivo, J Clin Invest 1991 88(5):1613-21.*

Bonofiglio D, Gabriele S, Aquila S, Catalano S, Gentile M, Middea E, Giordano F, Andò S*: Estrogen receptor alpha binds to peroxisome proliferator-activated receptor response element and negatively interferes with peroxisome proliferator-activated receptor gamma signaling in breast cancer cells, Clin Cancer Res 2005 11(17):6139-47.*

Bonofiglio D, Aquila S, Catalano S, Gabriele S, Belmonte M, Middea E, Qi H, Morelli C, Gentile M, Maggiolini M, Ando` S: *Peroxisome proliferatoractivated receptor-gamma activates p53 gene promoter binding to the nuclear factor-kappaB sequence in human MCF7 breast cancer cells Mol Endocrinol 2006 20(12):3083-92.*

Bonofiglio D, Qi H, Gabriele S, Catalano S, Aquila S, Belmonte M, Andò S*: Peroxisome proliferator-activated receptor gamma inhibits follicular and*

anaplastic thyroid carcinoma cells growth by upregulating p21Cip1/WAF1 gene in a Sp1-dependent manner, Endocr Relat Cancer 2008 113(3):423-34.

Bonofiglio D, Gabriele S, Aquila S, Qi H, Belmonte M, Catalano S, Andò S.: *Peroxisome proliferator-activated receptor gamma activates fas ligand gene promoter inducing apoptosis in human breast cancer cells. Breast Cancer Res Treat. 2009a Feb;113(3):423-34.*

Bonofiglio D, Cione E, Qi H, Pingitore A, Perri M, Catalano S, Vizza D, Panno ML, Genchi G, Fuqua SA, Andò S*: Combined low doses of PPARgamma and RXR ligands trigger an intrinsic apoptotic pathway in human breast cancer cells, Am J Pathol 2009b 175(3):1270-80.*

Bougnoux P, Hajjaji N, Maheo K, Couet C, Chevalier S*: Fatty acids and breast cancer: Sensitization to treatments and prevention ofmetastatic re-growth, Prog Lipid Res 2010 49(1):76-86.*

Brown I, Wahle KW, Cascio MG, Smoum-Jaouni R, Mechoulam R, Pertwee RG, Heys SD*: Omega-3 N-acylethanolamines are endogenously synthesised from omega-3 fatty acids in different human prostate and breast cancer cell lines, Prostaglandins Leukot Essent Fatty Acids 2011 85(6):305-10.*

Capobianco L, Bisaccia F, Michel A, Sluse FS, Palmieri F*: The N and C-termini of the tricarboxylate carrier are exposed to the cytoplasmic side of the inner mitochondrial membrane, FEBS 1995 9;357(3):297-300.*

Chapkin RS, McMurray DN, Lupton JR*: Colon cancer, fatty acids and anti-inflammatory compounds, Curr Opin. Gastroenterol 2007 778(2):466-71.*

Chapkin RS, Wang N, Fan YY, Lupton JR and Prior IA*: Docosahexaenoic acid alters the size and distribution of cell surface microdomains, Biochim Biophys Acta 2008 100(6):1152-7.*

Chiacchiera F, Simone C*: Signal-dependent regulation of gene expression as a target for cancer treatment: Inhibiting p38alpha in colorectal tumors, Cancer Lett 2008 28;265(1):16-26.*

Chung SH, Onoda N, Ishikawa T, Ogisawa K, Takenaka C, Yano Y: *Peroxisome proliferatoractivated receptor gamma activition induce cell cycle arrest via p53-independent pathway in human anaplastic thyroid cancer cells Jap J Cancer Res 2002 93(12):1358-65.*

Cohen RN*: Nuclear receptor corepressors and PPARγ, Nucl Recept Signal 2006 4:e003.*

Cohen SD, Pumford NR, Khairallah EA, Boekelheide K, Pohl LR, Amouzadeh HR, and Hinson JA: *Selective protein covalent binding and target organ toxicity, Toxicol Appl Pharmacol 1997 143(1):1-12.*

Comes F, Matrone A, Lastella P,Nico B, Susca FC, Bagnulo R, Ingravallo G, Modica S, Lo Sasso G, Moschetta A, Guanti G, Simone C*: A novel cell type-specific role of p38alpha in the control of autophagy and cell death in colorectal cancer cells, Cell Death Differ 2007 14(4):693-702.*

Damiano F, Gnoni GV, Siculella L*: Functional analysis of rat liver citrate carrier promoter: differential responsiveness to polyunsaturated fatty acids, Biochem J 2009 5;417(2):561-71.*

Damiano F, Gnoni GV, Siculella L*: Citrate carrier promoter is target of peroxisome proliferator-activated receptor alpha and gamma in hepatocytes and adipocytes, Int J Biochem Cell Biol 2012 44(4):659-68.*

De Graffenried LA, Friedrichs WE, Fulcher L, Fernandes G, Silva JM, Peralba JM, Hidalgo M: *Eicosapentaenoic acid restores tamoxifen sensitivity in breast cancer cells with high Akt activity. Authors, Journal Ann Oncol, 2003 4(7):1051-6.*

Demetri GD, Fletcher CD, Mueller E, Sarraf P, Naujoks R, Campbell N, Spiegelman BM, Singer S: *Induction of solid tumor differentiation by the peroxisome proliferator-activated receptor-gamma ligand troglitazone in patients with liposarcoma, Proc Natl Acad Sci USA 1999 30;96(7):3951-6.*

Elstner E, Müller C, Koshizuka K, Williamson EA, Park D, Asou H, Shintaku P, Said JW, Heber D, Koeffler HP*: Ligands for peroxisome proliferator-activated receptorgamma and retinoic acid receptor inhibit growth and induce apoptosis of human breast cancer cells in vitro and in BNX mice, Proc Natl Acad Sci USA 1998 95(15):8806-11.*

Elstner E, Williamson EA, Zang C, Fritz J, Heber D, Fenner M, Possinger K, Koeffler HP*: Novel therapeutic approach: ligands for PPARgamma and retinoid receptors induce apoptosis in bcl-2-positive human breast cancer cells, Breast Cancer Res Treat 2002 74(2):155-65.*

Evans LM, Hardy RW*: Optimizing dietary fat to reduce breast cancer risk: Are we there yet? Open Breast Cancer J 2010 2, 108-122.*

Fajas L, Auboeuf D, Raspé E, Schoonjans K, Lefebvre AM, Saladin R, Najib J, Laville M, Fruchart JC, Deeb S, Vidal-Puig A, Flier J, Briggs MR, Staels B, Vidal H, Auwerx J*: The organization, promoter analysis, and expression of*

the human PPARgamma gene, J Biol Chem. 1997 272(30):18779-89.

Fajas L, Fruchart JC, Auwerx J*: Transcriptional control of adipogenesis, Curr Opin Cell Biol 1998 (2):165-73.*

Feige JN, Gelman L, Michalik L, Desvergne B, Wahli W*: From molecular action to physiological outputs: peroxisome proliferator-activated receptors are nuclear receptors at the crossroads of key cellular functions, Prog Lipid Res 2006 45(2):120-59.*

Flück CE, Miller WL*: GATA-4 and GATA-6 modulate tissue-specific transcription of the human gene for P450c17 by direct interaction with Sp1, Mol Endocrinol 2004 18(5):1144-57.*

Forman B, Tontonoz P, Chen J, Brun R, Spiegelman B, Evans R*: 15-Deoxy-delta 12, 14-prostaglandin J2 is a ligand for the adipocyte determination factor PPAR gamma, Cell 1995 83(5):803-12.*

Gani OA*: Are fish oil omega-3 long-chain fatty acids and their derivatives peroxisome proliferator-activated receptor agonists? Cardiovasc Diabetol 2008 72(1):50-7.*

Gee MF, Tsuchida R, Eichler-Jonsson C, Das B, Baruchel S, Malkin D*: Vascular endothelial growth factor acts in an autocrine manner in rhabdomyosarcoma cell lines and can be inhibited with all-trans-retinoic acid, Oncogene 2005 24(54):8025-37.*

Glade MJ*: Food, nutrition, and the prevention of cancer: A global perspective, Nutrition 1999 5(6):523-6.*

Gleissman H, Segerstro L, Hamberg M, Ponthan F, Lindskog M, Johnsen JI and Kogner P: *Omega-3 fatty acid supplementation delays the progression of neuroblastoma in vivo, Int Jou of Cancer, 2010 28(7):1703-11.*

Grommes C, Landreth GE, Heneka MT*: Antineoplastic effects of peroxisome proliferator-activated receptor gamma agonists, Lancet Oncol 2004 5(7):419-29.*

Gross A, McDonnell JM, Korsmeyer SJ: *BCL-2 family members and the mitochondria in apoptosis, Genes Dev 1999 64:343-50.*

Guan HP, Ishizuka T, Chui PC, Lehrke M, Lazar MA*: Corepressors selectively control the transcriptional activity of PPARgamma in adipocytes, Genes Dev 2005 9(4):453-61.*

Hanson RW, Reshef L: *Glyceroneogenesis revisited, Biochimie 2003 85(12):1199-205.*

Hammamieh R, Chakraborty N, Miller SA, Waddy E, Barmada M, Das R, Peel SA, Day AA, Jett M: *Differential effects of omega-3 and omega-6 Fatty acids on gene expression in breast cancer cells, Journal Breast Cancer Res Treat, 2007 25;7:138.*

Hihi AK, Michalik L, Wahli W*: PPARs, Transcriptional effectors of fatty acids and their derivatives, Cell Mol Life Sci 2002 59(5):790-8.*

Hyde CA, Missailidis S: *Inhibition of arachidonic acid metabolism and its implication on cell proliferation and tumour-angiogenesis, Int Immunopharmacol 2009 9(6):701-15.*

Hong J, Samudio I, Liu S, Abdelrahim M, Safe S: *Peroxisome proliferatoractivited receptor γ-dependent activation of p21 in panc-28 pancreatic cancer cells involves Sp1 and Sp4 proteins. Endocrinology 2004 45(12):5774-85.*

Iacobazzi V, Infantino V, Palmieri F*: Epigenetic mechanisms and Sp1 regulate mitochondrial citrate carrier gene expression, Biochem Biophys Res Commun 2008 376(1):15-20.*

Ikezoe T, Miller CW, Kawano S, Heaney A, Williamson EA, Hisatake J, Green E, Hofmann W, Taguchi H, Koeffler HP*: Mutational analysis of the peroxisome proliferator-activated receptor gamma gene in human malignancies, Cancer Res 2001 ;61(13):5307-10.*

Ito T, Deng X, Carr B, May WS*: Bcl-2 phosphorylation required for anti-apoptosis function, J Biol Chem 1997 273(51):34157-63.*

Jiang P, Du WJ, Heese K, Wu M*: The Bad Guy Cooperates with Good Cop p53: Bad is transcriptionally upregulated by p53 and forms a Bad/p53 complex at the mitochondria to induce apoptosis, Mol Cell Biol 2006 26(23):9071-82.*

Jing E, Gesta S, Kahn CR*: SIRT2 regulates adipocyte differentiation through FoxO1 acetylation/deacetylation, Cell Metab 2007 6(2):105-14.*

Kang KS, Wang P, Yamabe N, Fukui M, Jay T, Zhu BT: *Docosahexaenoic acid induces apoptosis in MCF-7 cells in vitro and in vivo via reactive oxygen species formation and caspase 8 activation, PLoS ONE 2010 5(4):e10296.*

Kaplan RS, Mayor JA, Wood DO*: The mitochondrial tricarboxylate transport protein, J Biol Chem 1993 268(18):13682-90.*

Kaplan RS*: Structure and function of mitochondrial anion transport proteins, J Membr Biol 2001 179(3):165-83.*

Katsumoto T, Higaki K, Ohno K, Onodera K, *Cell cycle dependent biosynthesis and localization of p53 protein in untransformed human cells, Biol Cell 1995 84(3):167-73.*

Kitamura S, Miyazaki Y, Shinomura Y, Kondo S, Kanayama S, Matsuzawa Y: *Peroxisome proliferator-activated receptor gamma induces growth arrest and differentiation markers of human colon cancer cells, Jpn J Cancer Res 1999 90(1):75-80.*

Kondo Y, Kanzawa T, Sawaya R and Kondo, S: *The role of autophagy in cancer development and re- sponse to therapy, Nature Reviews Cancer 2005 5(9):726-34.*

Koutnikova H, Cock TA, Watanabe M, Houten SM, Champy MF, Dierich A, Auwerx J: *Compensation by the muscle limits the metabolic consequences of lipodystrophy in PPAR gamma hypomorphic mice, Proc Natl Acad Sci USA 2003 100(24):14457-62.*

Kubota T, Koshizuka K, Williamson EA, Asou H, Said JW, Holden S, Miyoshi I, Koeffler HP: *Ligand for peroxisome proliferator-activated receptor gamma (troglitazone) has potent antitumor effect against human prostate cancer both in vitro and in vivo, Cancer Res 1998 58(15):3344-52.*

Kubota N, Terauchi Y, Miki H, Tamemoto H, Yamauchi T, Komeda K, Satoh S, Nakano R, Ishii C, Sugiyama T, Eto K, Tsubamoto Y, Okuno A, Murakami K, Sekihara H, Hasegawa G, Naito M, Toyoshima Y, Tanaka S, Shiota K, Kitamura T, Fujita T, Ezaki O, Aizawa S, Kadowaki T, et al: *PPAR gamma mediates high-fat diet-induced adipocyte hypertrophy and insulin resistance, Mol Cell 1999 15(5):1027-31.*

Lanson M, Bougnoux P, Besson P, Lansac J, Hubert B, Couet C and Le Floch O: *N-6 polyunsaturated fatty acids in human breast carcinoma phosphatidylethanolamine and early relapse, Br J Cancer 1990 61(5):776-8.*

Levine B, Deretic V: *Unveiling the roles of autophagy in innate and adaptive immunity, Nat Rev Immunol 2007 7(10):767-77.*

Liang XH, Jackson S, Seaman M, Brown K, Kempkes B, Hibshoosh H, Levine B: *Induction of autophagy and inhibition of tumorigenesis by beclin 1, Nature 1999 402(6762):672-6.*

Marchenko ND, Zaika A, Moll UM: *Death signalinduced localization of p53 protein to mitochondria, a potential role in apoptotic signaling, J Biol Chem 2000 26;275(21):16202-12.*

Martin H: *Role of PPAR-gamma in inflammation. Prospects for therapeutic intervention by food components, Mutat Res 2009 669(1-2):1-7.*

Meirhaeghe A, Fajas L, Gouilleux F, Cottel D, Helbecque N, Auwerx J, Amouyel P: *A functional polymorphism in a STAT5B site of the human PPAR gamma 3 gene promoter affects height and lipid metabolism in a French population, Arterioscler Thromb Vasc Biol 2003 23(2):289-94.*

Mihara M, Erster S, Zaika A, Petrenko O, Chittenden T, Pancoska P: *p53 has a direct apoptogenic role at the mitochondria, Mol Cell 2003 1(3):577-90.*

Miles PD, Barak Y, He W, Evans RM, Olefsky JM: *Improved insulin-sensitivity in mice heterozygous for PPAR-gamma deficiency, J Clin Invest 2000 05(3):287-92.*

Mizuguchi Y, Wada A, Nakagawa K, Ito M, Okano T: *Antitumoral activity of 13-demethyl or 13-substituted analogues of all-trans retinoic acid and 9-cis retinoic acid in the human myeloid leukemia cell line HL-60, Biol Pharm Bull 2006 29(9):1803-9.*

Mueller E, Sarraf P, Tontonoz P, Evans RM, Martin KJ, Zhang M, Fletcher C, Singer S, Spiegelman BM: *Terminal differentiation of human breast cancer through PPAR gamma, Mol Cell 1998 1(3):465-70.*

Mueller E, Drori S, Aiyer A: *Genetic analysis of adipogenesis through peroxisome proliferator-activated receptor γ isoforms, Journal of Biological Chemistry, 2002 277(44):41925-30.*

Mueller E, Smith M, Sarraf P, Kroll T, Aiyer A, Kaufman DS, Oh W, Demetri G, Figg WD, Zhou XP, Eng C, Spiegelman BM, Kantoff PW: *Effects of ligand activation of peroxisome proliferator-activated receptor gamma in human prostate cancer, Proc Natl Acad Sci USA 2000 97(20):10990-5.*

Nagy L, Tontonoz P, Alvarez JG, Chen H, Evans RM: *Oxidized LDL regulates macrophage gene expression through ligand activation of PPARgamma, Cell 1998 93(2):229-40.*

Noé V, Alemany C, Chasin LA, Ciudad CJ: *Retinoblastoma protein associates with Sp1 and activates the hamster dihydrofolate reductase promoter, Oncogene 1998 16(15):1931-8.*

Palmieri F, Pierri CL, De Grassi A, Nunes-Nesi A, Fernie AR: *Evolution, structure and function of mitochondrial carriers: a review with new insights, Plant J 2011 66(1):161-81.*

Palmieri F*: The mitochondrial transporter family SLC25: identification, properties and physiopathology, Mol Aspects Med 2012 34(2-3):465-84.*

Patel L, Pass I, Coxon P, Downes CP, Smith SA, Macphee CH*: Tumor suppressor and anti-inflammatory actions of PPARgamma agonist are mediated via up-regulation of PTEN, Curr Biol 2001 15;11(10):764-8.*

Pattingre S, Tassa A, QuX, Garuti R, Liang XH, MizushimaN, Packer M, Schneider MD, Levine B: *Bcl-2 antiapoptotic proteins inhibit Beclin 1-dependent autophagy, Cell 2005 122(6):927-39.*

Picard F, Kurtev M, Chung N, Topark-Ngarm A, Senawong T, Machado De Oliveira R, Leid M, McBurney MW, Guarente L*: Sirt1 promotes fat mobilization in white adipocytes by repressing PPAR-gamma, Nature 2004 19;430(7002):921.*

Pinaire JA, Reifel-Miller A*: Therapeutic potential of retinoid x receptor modulators for the treatment of the metabolic syndrome, PPAR Res 2007 2007:94156.*

Plastina P, Meijerink J, Vincken JP, Gruppen H, Witkamp R, Gabriele B*: Selective synthesis of unsaturated N-acylethanolamines by lipase-catalyzed N-acylation of ethanolamine with unsaturated fatty acids, Lett Org Chem 2009 444-447(4).*

Raji A, Plutzky J*: Insulin resistance, diabetes, and atherosclerosis: thiazolidinediones as therapeutic interventions, Curr Cardiol Rep 2002 4(6):514-21.*

Rangwala SM and Lazar MA: *Peroxisome proliferator-activated receptor g in diabetes and metabolism, Trends Pharmacol Sci 2004 25(6):331-6.*

Ricote M, Glass CK: *PPARs and molecular mechanisms of transrepression, Biochim Biophys Acta 2007 771(8):926-35.*

Rieusset J, Auwerx J, Vidal H: *Regulation of gene expression by activation of the peroxisome proliferator-activated receptor γ with rosiglitazone (BRL 49653) in human adipocytes, Biochem Biophys Res Commun 1999 265(1):265-71.*

Roberts-Thomson SJ*: Peroxisome proliferator-activated receptors in tumorigenesis: targets of tumour promotion and treatment, Immunol Cell Biol 2000 78(4):436-41.*

Rock CL, Demark-Wahnefried W*: Nutrition and survival after the diagnosis of breast cancer: A review of the evidence, J Clin Oncol 2002 15;20(18):3939.*

Rotheneder H, Geymayer S, Haidweger E*: Transcription factors of the Sp1 family, interaction with E2F and regulation of the murine thymidine kinase promoter, J Mol Biol 1999 12;293(5):1005-15.*

Saez E, Rosenfeld J, Livolsi A, Olson P, Lombardo E, Nelson M, Banayo E, Cardiff RD, Izpisua-Belmonte JC, Evans RM*: PPAR gamma signaling exacerbates mammary gland tumor development, Genes Dev 2004 18(5):528-40.*

Sarraf P, Mueller E, Jones D, King FJ, DeAngelo DJ, Partridge JB, Holden SA, Chen LB, Singer S, Fletcher C, Spiegelman BM*: Differentiation and reversal of malignant changes in colon cancer through PPARgamma, Nat Med 1998 4(9):1046-52.*

Sarraf P, Mueller E, Smith WM, Wright HM, Kum JB, Aaltonen LA, de la Chapelle A, Spiegelman BM, Eng C*: Loss-of-function mutations in PPAR gamma associated with human colon cancer, Mol Cell 1999 3(6):799-804.*

Sax JK, Fei P, Murphy ME, Bernhard E, Korsmeyer SJ, El-Deiry WS: *BID regulation by p53 contributes to chemosensitivity, Nat Cell Biol, 2002 4(11):842-9.*

Serini S, Fasano E, Piccioni E, Cittadini AR, and Calviello G: *Dietary n-3 polyunsaturated fatty acids and the paradox of their health benefits and potential harmful effects, Chemical research in toxicology 2011 9;24(12):2093-105.*

Simeone AM, Tari AM*: How retinoids regulate breast cancer cell proliferation and apoptosis Cell Mol Life Sci 2004 61(12):1475-84.*

Song G, Chen GG, Yun JP, Lai PB: *Association of p53 with Bid induces cell death in response to etoposide treatment in hepatocellular carcinoma, Curr Cancer Drug Targets 2009 9(7):871-80.*

Spiegelman BM, Flier JS*: Adipogenesis and obesity: rounding out the big picture, Cell 1996 1;87(3):377-89.*

Spiegelman BM, Flier JS*: Obesity and the regulation of energy balance, Cell 2001 104(4):531-43.*

Sporn MB, Suh N, Mangelsdorf DJ*: Prospects for prevention and treatment of cancer with selective PPARgamma modulators (SPARMs), Trends Mol Med 2001 7(9):395-400.*

Staels B and Fruchart JC: *Therapeutic Roles of Peroxisome Proliferator–Activated Receptor Agonists, Diabetes 2005 54(8):2460-70.*

Sugawara A, Uruno A, Kudo M, Ikeda Y, Sato K, Taniyama Y, Ito S,

Takeuchi K: *Transcription suppression of thromboxane receptor gene by peroxisome proliferator-activated receptor-g via an interaction with Sp1 in vascular smooth muscle cells, J Biol Chem 2002 277(12):9676-83.*

Takamura T, Nohara E, Nagai Y, Kobayashi K: *Stage-specific effects of a thiazolidinedione on proliferation, differentiation and PPARgamma mRNA expression in 3T3-L1 adipocytes, Eur J Pharmacol 2001 422(1-3):23-9.*

Tan NS, Shaw NS, Vinckenbosch N, Liu P, Yasmin R, Desvergne B,Wahli W, Noy N: *Selective cooperation between fatty acid binding proteins and peroxisome proliferatoractivated receptors in regulating transcription, Mol Cell Biol 2002 22(14):5114-27.*

Teferedegne B, Green MR, Guo Z, Boss JM: *Mechanism of action of a distal NF-kB-dependent enhancer, Mol Cell Biol 2006 26(15):5759-70.*

Thiebaut ACM, Chaje` V, Gerber M, Boutron-Ruault MC, Joulin V, Lenoir G, Berrino F, Riboli E, Benichou J and Clavel-Chapelon F: *Dietary intakes of ω-6 and ω-3 polyunsaturated fatty acids and the risk of breast cancer, Int J Cancer 2009 124(4):924-31.*

Tontonoz P, Graves RA, Budavari AI, Erdjument-Bromage H, Lui M, Hu E, Tempst P, Spiegelman BM: *Adipocyte-specific transcription factor ARF6 is a heterodimeric complex of two nuclear hormone receptors, PPAR gamma and RXR alpha, Nucleic Acids Res 1994.*

Tontonoz P, Hu E, Graves RA, Budavari AI, Spiegelman BM: *mPPAR gamma 2: tissue-specific regulator of an adipocyte enhancer, Genes Dev 1994 8(10):1224-34.*

Tontonoz P, Hu E, Spiegelman BM: *Stimulation of adipogenesis in fibroblasts by PPAR gamma 2, a lipid-activated transcription factor, Cell. 1994 79(7):1147-56.*

Tontonoz P, Singer S, Forman BM, Sarraf P, Fletcher JA, Fletcher CD, Brun RP, Mueller E, Altiok S, Oppenheim H, Evans RM, Spiegelman BM: *Terminal differentiation of human liposarcoma cells induced by ligands for peroxisome proliferator-activated receptor gamma and the retinoid X receptor, Proc Natl Acad Sci USA 1997 94(1):237-41.*

Tontonoz P, Spiegelman BM: *Fat and beyond: the diverse biology of PPARγ, Annu Rev Biochem 2008 77:289-312.*

Tsubouchi Y, Sano H, Kawahito Y, Mukai S, Yamada R, Kohno M, Inoue K, Hla T, Kondo M: *Inhibition of human lung cancer cell growth by the peroxisome*

proliferator-activated receptor-gamma agonists through induction of apoptosis, Biochem Biophys Res Commun 2000 270(2):400-5.

Van der Laan S, Meijer OC: *Pharmacology of glucocorticoids: beyond receptors, Eur J Pharmacol 2008 585(2-3):483-91.*

Waite KA, Eng C*: Protean PTEN: Form and function, Am J Hum Genet 2002 70(4):829-44.*

Wan H, Hong WK, Lotan R*: Increased retinoic acid responsiveness in lung carcinoma cells that are nonresponsive despite the presence of endogenous retinoic acid receptor (RAR) beta by expression of exogenous retinoid receptors retinoid X receptor alpha, RAR alpha, and RAR gamma, Cancer Res 2001 61(2):556-64.*

Wang X, Southard RC, Kilgore MW*: The increased expression of peroxisome proliferator-activated receptor-gamma1 in human breast cancer is mediated by selective promoter usage, Cancer Res 2004 64(16):5592-6.*

Wei Y, Pattingre S, Sinha S, Bassik M, Levine B*: JNK1-mediated phosphorylation of Bcl-2 regulates starvation-induced autophagy, Mol Cell 2008 30(6):678-88.*

Williams CM, & Burdge G: *Long-chain n -3 PUFA: plant v. marine sources, Proceedings of the Nutrition Societ 2006 65(1):42-50.*

Willson TM, Brown PJ, Sternbach DD, Henke BR*: The PPARs: from orphan receptors to drug discovery, J Med Chem 2000 43(4):527-50.*

Wolfrum C, Borrmann CM, Borchers T, Spener F*: Fatty acids and hypolipidemic drugs regulate peroxisome proliferator-activated receptors alpha- and gamma-mediated gene expression via liver fatty acid binding protein: A signaling path to the nucleus, Proc Natl Acad Sci USA 2001 98(5):2323-8.*

Wu K, DuPré E, Kim H, Tin-U CK, Bissonnette RP, Lamph WW, Brown PH*: Receptor-selective retinoids inhibit the growth of normal and malignant breast cells by inducing G1 cell cycle blockade, Breast Cancer Res Treat 2006 96(2):147-57.*

Yamamoto K, Ichijo H, Korsmeyer SJ*: BCL-2 is phosphorylated and inactivated by an ASK1/Jun N-terminal protein kinase pathway normally activated at G2/M, Mol Cell Biol 1999 19(12):8469-78.*

Yee LD, Williams N, Wen P, Young DC, Lester J, Johnson MV, Farrar WB, Walker MJ, Povoski SP, Suster S, Eng C*: Pilot study of rosiglitazone therapy*

in women with breast cancer: effects of short-term therapy on tumor tissue and serum markers, Clin Cancer Res 2007 13(1):246-52.

Yin F, Wakino S, Liu Z: *Troglitazone inhibits growth of MCF-7 breast carcinoma cells by targeting G1 cell cycle regulators," Biochemical and Biophysical Research Communications, 2001 286(5):916-22.*

Yu C, Markan K, Temple KA, Deplewski D, Brady MJ, Cohen RN*: The nuclear receptor corepressors NCoR and SMRT decrease peroxisome proliferator-activated receptor gamma transcriptional activity and repress 3T3-L1 adipogenesis, J Biol Chem 2005 280(14):13600-5.*

Yu L, McPhee CK, Zheng L, Mardones GA, Rong Y, Peng J, Mi N, Zhao Y, Liu Z, Wan F,Hailey DW, Oorschot V, Klumperman J, Baehrecke EH, Lenardo MJ: *Termination of autophagy and reformation of lysosomes regulated by mTOR, Nature 2010 465(7300):942-6.*

Scientific publications

Perri A, Catalano S, Bonofiglio D, Vizza D, Rovito D, Qi H, Aquila S, Panza S, Rizza P, Lanzino M, Andò S.:*T3 enhances thyroid cancer cell proliferation through TRβ1/Oct-1-mediated cyclin D1 activation, Mol Cell Endocrinol. 2014 Jan 25;382(1):205-17.*

Bonofiglio D, Santoro A, Martello E, Vizza D, Rovito D, Cappello AR, Barone I, Giordano C, Panza S, Catalano S, Iacobazzi V, Dolce V, Andò S.: *Mechanisms of divergent effects of activated peroxisome proliferator-activated receptor-γ on mitochondrial citrate carrier expression in 3T3-L1 fibroblasts and mature adipocytes, Biochim Biophys Acta. 2013 Jun;1831(6):1027-36.*

Rovito D, Giordano C, Vizza D, Plastina P, Barone I, Casaburi I, Lanzino M, De Amicis F, Sisci D, Mauro L, Aquila S, Catalano S, Bonofiglio D, Andò S.: *Omega-3 PUFA ethanolamides DHEA and EPEA induce autophagy through PPARγ activation in MCF-7 breast cancer cells, J Cell Physiol. 2013 Jun;228(6):1314-22.*

Plastina P, Bonofiglio D, Vizza D, Fazio A, Rovito D, Giordano C, Barone I, Catalano S, Gabriele B.: *Identification of bioactive constituents of Ziziphus jujube fruit extracts exerting antiproliferative and apoptotic effects in human breast cancer cells, J Ethnopharmacol. 2012 Mar 27;140(2):325-32.*

Bonofiglio D., Cione E., Vizza D., Perri M., Pingitore A., Qi H., Catalano S., Rovito D., Genchi G. and Andò S.: *Bid as a potential target of apoptotic effects exerted by low doses of PPARγ and RXR ligands in breast cancer cells. Cell Cycle 2011; 10: 2344-2354.*

Abstracts and oral communications

Rovito D., Rechoum Y., Iacopetta D., Barone I., Andò S., Weigel NL., and Fuqua SAW: *Functional interaction between testicular receptors 2/4 and Era, From general pathology to molecular and translational medicine" - SIPMET Meeting, Roma, 23/24 ottobre 2013*

Rovito D., Rechoum Y., Iacopetta D., Barone I., Andò S., Weigel NL., and Fuqua SAW: *Functional interaction between testicular receptors 2/4 and Era, 9th annual Breast Cancer Research and Education Program August 2013, Houston TX.*

Rovito D., Vizza D., Barone I., Giordano C., Casaburi I., Lanzino M.,

Catalano S., Bonofiglio D., Andò S.: *Omega-3 Ethanolamides Induce Autophagy through PPARgamma Activation in Breast Cancer Cells. 1st Joint Meeting of Pathology and Laboratory Diagnostics September 12-15, 2012 Udine.*

Bonofiglio D., Santoro A., Vizza D., Rovito D., Martello E., Cappello A.R., Barone I., Giordano C., Catalano S., Dolce V., Andò S.: *Modulatory role of Peroxisome Proliferator-Activated Receptor γ on Citrate Carrier activity and expression. Experimental Biology ASIP, San Diego 21-25 April 2012.*

Giordano C., Vizza D., Rovito D., Barone I., Bonofiglio D., Panza S.,Lanzino M., Fuqua S., Catalano S. and Andò S.: *Leptin Increases HER2 Stability through HSP90 in Breast Cancer Cells. Experimental Biology ASIP, San Diego 21-25 April 2012.*

Rovito D, Vizza D, Bonofiglio D.: *Omega-3 ethanolamides induce autophagy through PPARg activation in breast cancer cells. VIII Convegno della Fondazione "Lilli Funaro", Cosenza 23-24 Febbraio 2012.*

Rovito D., Bonofiglio D.,Plastina P., Vizza D. and Andò S.: *Ziziphus jujube fruits as a source of bioactive compounds exerting antiproliferative and apoptotic effects in human breast cancer cells. VII Convegno della Fondazione "Lilli Funaro", Cosenza 1-2 Aprile 2011.*

Vizza D., Bonofiglio D., Cione E., Perri M., Pingitore A., Qi H., Catalano S., Rovito D., Panno ML., Genchi G., and Andò S.: *Bid as a potential target of apoptotic effects exerted by low doses of PPARγ and RXR ligands in breast cancer cells. VII Convegno della Fondazione "Lilli Funaro", Cosenza 1-2 Aprile 2011.*

Molecular and Cellular Endocrinology 382 (2014) 205–217

Contents lists available at ScienceDirect

Molecular and Cellular Endocrinology

journal homepage: www.elsevier.com/locate/mce

T3 enhances thyroid cancer cell proliferation through TRβ1/Oct-1-mediated cyclin D1 activation

Anna Perri [b,1], Stefania Catalano [a,1], Daniela Bonofiglio [a], Donatella Vizza [b], Daniela Rovito [a], Hongyan Qi [b], Saveria Aquila [a], Salvatore Panza [a], Pietro Rizza [a], Marilena Lanzino [a], Sebastiano Andò [a,b,*]

[a] Dept. Pharmacy, Health and Nutritional Sciences, University of Calabria, Rende, Italy
[b] Centro Sanitario, University of Calabria, Rende, Italy

ARTICLE INFO

Article history:
Received 9 June 2013
Received in revised form 30 September 2013
Accepted 1 October 2013
Available online 9 October 2013

Keywords:
T3
Thyroid cancer
Thyroid hormone receptor β1
Oct-1

ABSTRACT

Several studies have demonstrated that thyroid hormone T3 promotes cancer cell growth, even though the molecular mechanism involved in such processes still needs to be elucidated. In this study we demonstrated that T3 induced proliferation in papillary thyroid carcinoma cell lines concomitantly with an up-regulation of cyclin D1 expression, that is a critical mitogen-regulated cell-cycle control element. Our data revealed that T3 enhanced the recruitment of the TRβ1/Oct-1 complex on Octamer-transcription factor-1 site within cyclin D1 promoter, leading to its transactivation. In addition, silencing of TRβ1 or Oct-1 expression by RNA interference reversed both increased cell proliferation and up-regulation of cyclin D1, underlying the important role of both transcriptional factors in mediating these effects. Finally, T3-induced increase in cell growth was abrogated after knocking down cyclin D1 expression. All these findings highlight a new molecular mechanism by which T3 promotes thyroid cancer cell growth.

1. Introduction

The thyroid hormone (TH) T3 is an important regulator of growth, metabolism and differentiation. The classical mechanism of action of T3 has been assumed to begin in the cell nucleus and to require participation of receptor protein for TH in the nuclear compartment. The thyroid hormone receptors (TRs), members of the nuclear receptors superfamily, derived from two genes alpha and beta, located on two different chromosomes. Alternate splicing of primary transcripts gives rise to six TR isoforms: α1, β1, α2, β2, α3 and β3. The expression of these TR isoforms is developmentally regulated and tissue-dependent. The two major isoforms of TRs, TRα1 and TRβ1, that bind T3 with high affinity, in the nuclear compartment heterodimerize with retinoid X receptor or, in some cases, homodimerize, binding to the thyroid responsive elements (TREs), typically located on the promoters of target genes (Bassett et al., 2003; Davis et al., 2007; Lazar and Chin, 1990; Oetting and Yen, 2007; Weiss and Ramos, 2004). The classical genomic mechanism has been complemented in the past decade by description of TH actions that are now understood to involve novel extranuclear (non-genomic) mechanisms in a variety of cells. Such non-genomic mechanisms, involving nuclear receptors residing in the cytosol of unstimulated or stimulated cells through activation of several intracellular signaling pathways appear to be relevant to proliferation and motility of several tumor cells (Davis et al., 2007).

Many authors reported that THs induce proliferative effects in normal cell types including human fibroblasts (Cao et al., 2005), pituitary cells (Storey et al., 2006), cardiomyocytes (Kenessey and Ojamma, 2006), pancreatic B cells (Verga Falzacappa et al., 2007) and ovarian granulose cells (Verga Falzacappa et al., 2009a,b). Moreover, THs play a permissive role in breast, glial, renal, prostate, papillary and follicular thyroid cancer tumor cell proliferation (Davis et al., 2008; Hall et al., 2008; Hsieh and Juang, 2005; Lin et al., 2006; Poplawski and Nauman, 2008; Verga Falzacappa et al., 2009a,b).

In the last years, a large body of evidence has shown that disruption of cell cycle control mechanism is a common pathway in human cancer; in particular, overexpression of cyclin D1 is one of most commonly observed alterations in some forms of breast cancer, hepatocellular carcinoma, esophagus cancer, heads-neck squamous cancer, colon and urinary bladder cancer (Wang et al., 2000). In addition, recently Balta et al., reported that cyclin D1 expression is significantly increased in papillary thyroid cancer (PTC) respect to control, addressing to cyclin D1 level

Abbreviations: TH, thyroid hormone; TRs, thyroid hormone receptors; TRβ1, thyroid hormone receptor β1; Oct-1, Octamer-transcription factor-1; CycD1, cyclin D1.

* Corresponding author. Address: Dept. Pharmacy, Health and Nutritional Sciences, University of Calabria, 87036 Arcavacata di Rende (CS), Italy. Tel.: +39 0984 496201; fax: +39 0984 496203.
E-mail address: sebastiano.ando@unical.it (S. Andò).
[1] These authors contributed equally to this work.

0303-7207/$ - see front matter © 2013 Elsevier Ireland Ltd. All rights reserved.
http://dx.doi.org/10.1016/j.mce.2013.10.001

expression a potential prognostic role in patients with PTC (Balta et al., 2012). For instance, cyclin D1 induction is one of the earlier events in cell proliferation induced by T3 through TRβ1, suggesting that this cyclin might be a common target responsible for the mitogenic activity of ligands of nuclear receptors (Kowalik et al., 2010; Pibiri et al., 2001).

The human cyclin D1 promoter contains multiple transcription factor binding sites such as AP1, NFkB, E2F, Oct-1 and so on (Eric et al., 2008). Octamer Transcription factor-1 (Oct-1), a member of the POU (Pit1, Oct-1, unc86) family of transcription factors, is involved in the transcriptional regulation of a variety of genes expression related to cell cycle, development and hormonal signals. It has been shown that Oct-1 acts not only as a transcriptional activator but also as a transcriptional repressor for certain genes (Boulon et al., 2002; Brockman and Shuler, 2005; Kakizawa et al., 1999, 2001; Magné et al., 2003; Prefontaine et al., 1998); however, the mechanism of the bifunctional transcriptional activity of Oct-1 is not fully understood.

In the present study we explored the molecular mechanism eliciting the proliferative effects of T3 in a well-differentiated papillary thyroid cancer cell line, FB-2 (Basolo et al., 2002). We showed that T3 enhances cyclin D1 expression and induces proliferative effects in a TRβ1 dependent manner by binding of TRβ1/Oct-1 complex to Oct-1 site within cyclin D1 promoter gene.

2. Materials and methods

2.1. Reagents

3,5,3′-Tri-iodothyronine (T3) and LY294002 were purchased by Sigma–Aldrich (St. Louis, MO, USA).

2.2. Plasmids

The plasmids containing the human cyclin D1 promoter or its deletions (p−2966/+142, p−848/+142, p−254/+142 and p−136/+142) were kindly provided by Prof A. Weisz (University of Naples, Italy). These fragments were inserted into the luciferase vector pXP2. The human cyclin promoter plasmid-bearing OCT-1-responsive element-mutated site (Oct-1 mut) was generated by PCR using as template the cyclin D1 promoter plasmid p−254/+142 with the following primers: (mutation is shown as lowercase letters): forward 5′-ATATGTCGACGGCTGCAGCGGGGCGATcgtaATTTCTATGAAAACC-3′ and reverse 5′-TATAAGATCTTCCTGGGCAGCTGGAGGGCT-3′. The amplified DNA fragment was digested with SalI and BglII and ligated into pX2-basic vector. Mutation was confirmed by DNA sequencing. The TRB1 expression vector plasmid was kindly provided by M. Mathis (University Health Sciences Center Shreveport, Louisiana).

2.3. Cell cultures

Human well-differentiated thyroid papillary carcinoma cells (FB-2 and TPC1) and human follicular thyroid carcinoma cell line (WRO) (a gift respectively from Prof. Basolo, University of Pisa, Italy and Dr. Arturi, University of Magna Grecia, Catanzaro, Italy) were cultured in Dulbecco's Modified Eagle's medium (DMEM) plus glutamax, (GIBCO-BRL, Gaithersburg, MD) supplemented with 10% fetal bovine serum (FBS; Invitrogen) and 1 mg/ml penicillin–streptomycin (P/S). Cells were maintained at 37 °C under humidified conditions of 95% air and 5% CO_2. FRTL-5 cells, a thyroid follicular cell line derived from normal rat thyroid (a gift from Prof. Tonacchera, University of Pisa, Italy) was cultured in Coon's modification of Ham' F12 medium supplemented with 2 mM L-glutamine, 0.01 UI/ml TSH, 10 μg/ml insulin, 10 nM hydrocortisone, 5 μg/ml transferrin, 10 ng/ml somatostatin, 10 ng/ml glycyl-L-histidyl-L-lysine acetate, 5% fetal bovine serum and 1 mg/ml penicillin–streptomycin (P/S) (Sigma–Aldrich – St. Louis, MO, USA). Prior to treatments, FB-2, TPC1 and WRO cells were harvested with serum free medium (SFM) and FRTL-5 were starved from TSH (Degrassi et al., 1998), for 24 h.

2.4. Free-3,5,3′-tri-iodothyronine measurement by RIA

A competitive in-house immunoassay was applied to measure free triiodothyronine (FT3) concentration in cell surnatants (RIA IMMUNOTECH – Backman Coulture Company). Briefly, FB-2 cells were treated in SFM with T3 100 nM, and after 20 min surnatant from cells was collected. 100 μl of surnatant were mixed with 400 μl of ^{125}I-labeled anti T3 mouse monoclonal antibody for 2 h at room temperature (RT) following the manufacturer's protocol. FT3 results were presented as the original concentrations of the supernatants and were given as pM.

2.5. RT-PCR and real-time RT-PCR assays

Cells were grown in 60 mm^2 dishes to 60–70% confluence and exposed to treatments in SFM. The total cellular RNA was extracted using TRIZOL reagent (Invitrogen) as suggested by the manufacturer. The purity and integrity were checked spectroscopically and by gel electrophoresis before carrying out the analytical procedures. The evaluation of gene expression was performed by the RT-PCR method. For TRβ1, TRα1 and the internal control gene 36B4, the primers were: TRβ1 forward: 5′-CTC TGT GTA GTG TGT GGT GA-3′; TRβ1reverse: 5′-TCA TCC AGC ACC AAA TCT GT-3′; TRα1forward: 5′-GCC AAA AAA CTG CCC ATG TTC TCC GAG-3′; TRα1reverse: 5′-GGC AGG CCC CGA TCA TGC GGA GGT CAG-3′; 36B4 forward: 5′-CTC AAC ATC TCC CCC TTC TC-3′; 36B4 reverse: 5′-CAA ATC CCA TAT CCT CGT CC-3′ to yield respectively the products of 229 bp, 445 bp and 408 bp. The PCR was performed for 35 cycles for TRβ1 (94 °C for 1 min, 55 °C for 1 min, and 72 °C for 2 min), 35 cycles for TRα1 (94 °C for 1 min, 55 °C for 1 min, and 72 °C for 2 min) and 15 cycles (94 °C for 1 min, 58 °C for 1 min, and 72° C for 2 min) to amplify 36B4 in the presence of 1 μl of first strand cDNA, 1 μM each of the primers mentioned above, 0.5 μM dNTP, Taq DNA polymerase (2 units/tube), and 2.2 μM magnesium chloride in a final volume of 25 μl. To check for the presence of DNA contamination, a reverse transcription-PCR was performed on 1 μg of total RNA without Moloney murine leukemia virus reverse transcriptase (the negative control). Cyclin D1 gene expression in FB-2 cells untreated (−) or treated with 100 nM T3 for 6, 12 and 24 h, was evaluated by real-time RT-PCR. Total RNA was reverse transcribed with the RETROscript kit; 5 μl of diluted (1:3) cDNA was analyzed in triplicates by real-time PCR in an iCycler iQ Detection System (Bio-Rad) using SYBR Green Universal PCR Master Mix, following the manufacturer's recommendations. Each sample was normalized on its GAPDH mRNA content. Primers used for the amplification were: forward 5′-GATGCCAACCTCCTCAACGAC-3′ and reverse 5′-CTCCTCGCACTTCTGTTCCTC-3′ (cyclin D1); forward 5′-CCCACTCCTCCACCTTTGAC-3′ and reverse 5′-TGTTGCTGTAGCCAAATTCGTT-3′(GAPDH). The relative gene expression levels were calculated as described (Sirianni et al., 2007).

2.6. Transient transfection assay

FB-2 cells were transfected in SFM using the FUGENE 6 reagent with the mixture containing 0.1 μg of human cyclin D1 promoter constructs. In another sets of experiments FB-2 cells were co-transfected with p−254/−136 cyclin D1 promoter and TRβ1expression vector plasmids. 24 h after transfection, the cells were untreated or treated with 100 nM T3 for 12 h. TK Renilla luciferase plasmid

(10 ng per each well) was used. Firefly and Renilla luciferase activities were measured by Dual Luciferase kit. The firefly luciferase data for each sample were normalized based on the transfection efficiency measured by Renilla luciferase activity.

2.7. Electrophoretic mobility shift assay (EMSA)

Nuclear extracts from FB-2 cells were prepared as previously described for EMSA (Andrews and Faller, 1991). Briefly, cells plated into 10 cm dishes were grown to 60–70% confluence, shifted to SFM for 24 h, and then treated with 100 nM T3 for 6 h. Thereafter, the cells were scraped into 1.5 ml cold PBS. They were pelleted for 10 s and resuspended in 400 μl cold buffer A (10 mM HEPES–KOH (pH 7.9) at 4 °C, 1.5 mM MgCl2, 10 mM KCl, 0.5 mM dithiothreitol, 0.2 mM PMSF, 1 mM leupeptin) by flicking the tube. The cells were then allowed to swell on ice for 10 min and then vortexed for 10 s. The samples were then centrifuged for 10 s and the supernatant fraction discarded. The pellet was resuspended in 50 μl cold Buffer B (20 mM HEPES–KOH (pH 7.9), 25% glycerol, 1.5 mM $MgCl_2$, 420 mM NaCl, 0.2 mM EDTA, 0.5 mM dithiothreitol, 0.2 mM PMSF, 1 mM leupeptin) and incubated in ice for 20 min for high-salt extraction. Cellular debris was removed by centrifugation for 2 min at 4 °C and the supernatant fraction (containing DNA-binding proteins) was stored at −80 °C. The probe was generated by annealing single-stranded oligonucleotides, labeled with [l32P] ATP (Perkin Elmer) and T4 polynucleotide kinase, and purified using Sephadex G50 spin columns (Amersham Pharmacia). The DNA sequences used as probe or as cold competitors are the following (the nucleotide motifs of interest are underlined, and mutations are shown as lowercase letters): forward 5′GGC GATTTGCATTTCTATGA-3′; reverse 5′-TCATAGAAATGCAAATCGCC-3′; forward 5′GGCGATcgtaATTTCTATGA-3′; reverse 5′-TAGAAATtacgATCGCCCCGC-3′ (Oct-1 mut). The protein-binding reactions were carried out in 20 μl of buffer [20 mmol/L HEPES (pH 8), 1 mmol/L EDTA, 50 mmol/L KCl, 10 mmol/L DTT, 10% glycerol, 1 mg/ml BSA, 50 μg/ml poly(dI/dC)] with 50,000 cpm of labeled probe, 20 μg of FB-2 nuclear proteins or an appropriate amount of TRβ1 protein, and 5 μg of poly (dI-dC). The mixtures were incubated at RT for 20 min in the presence or absence of unlabeled competitor oligonucleotides. For experiments involving anti-TRβ1 and anti-Oct-1 antibodies, the reaction mixture was incubated with these antibodies at 4 °C for 12 h before addition of labeled probe. The entire reaction mixture was electrophoresed through a 6% polyacrylamide gel in 0.25 × Tris borate–EDTA for 3 h at 150 V. The gel was dried and subjected to autoradiography at −70 °C.

2.8. Chromatin immunoprecipitation assay (ChIP)

For ChIP assay FB-2 cells were grown in 10 cm dishes to 60–70% confluence, shifted to SFM for 24 h, and then treated with 100 nM T3 for 30 min, 1 and 2 h. Thereafter, the cells were washed twice with PBS and cross-linked with 1% formaldehyde at 37 °C for 10 min. Next, the cells were washed twice with PBS at 4 °C, collected, resuspended in 200 μl of lysis buffer (1% SDS, 10 mM EDTA, 50 mM Tris–HCl (pH 8.1)) and left on ice for 10 min. Then, the cells were sonicated four times for 10 s at 30% of maximal power (Sonics and Materials Inc., Vibra Cell 500 W) and collected by centrifugation at 14,000 rpm for 10 min, at 4 °C. The supernatants were diluted in 1.3 ml IP buffer (0.01% SDS, 1.1% Triton X-100, 1.2 mM EDTA, 16.7 mM Tris–HCl (pH 8.1), 16.7 mM NaCl) followed by immunoclearing with 80 μl sonicated salmon sperm DNA/protein A agarose (UBI, DBA Srl, Milan, Italy) for 1 h at 4 °C. The precleared chromatin was immunoprecipitated with anti-TRβ1and anti-RNA Pol II antibodies or a normal mouse serum IgG as negative control (Santa Cruz Biotechnology). Pellets were washed and eluted with elution buffer (1% SDS, 0.1 M $NaHCO_3$) and digested with proteinase K. DNA was obtained by phenol/chloroform/ isoamyl alcohol extractions and precipitated with ethanol and resuspended with 20 μl of TE buffer pH 8.0. 2 μl of each sample were used for PCR amplification with: (i) primers flanking the Oct-1 sequence present in the cyclin D1 promoter region (forward 5′-GATTCTTTGGCCGTCT GTCC-3′; reverse 5′-GCCCCTGTAGTCCGGTTTTCATAG-3′); (ii) primers upstream the Oct-1 site (forward 5′-GCGCATGCTAAGTAGTAAC C-3′; reverse 5′-GGGAAGAGGGGTGCAGGGGC-3′). The PCR conditions were 1 min at 94 °C, 1 min at 65 °C, and 2 min at 72 °C. The amplification products obtained in 35 cycles were analyzed in a 2% agarose gel and visualized by Ethidium bromide staining.

2.9. Immunoblotting

The cells were grown in 10 cm dishes to 60–70% confluence and exposed to treatments in SFM, as indicated. Cells were then harvested in cold PBS and resuspended in a lysis buffer. Total proteins were obtained using a RIPA-buffer containing 50 mM Tris-HCl, (pH 7.5), 150 mM NaCl, 1% Nonidet P-40 (NP-40), 0.5% sodium deoxycholate, 1% Sodium–Dodecyl–Sulfate (SDS) and protease inhibitors (0.1 mM Na_3VO_4, 1% phenylmethylsulphonyl fluoride (PMSF), 20 mg/ml aprotinin). Cytoplasmatic proteins were obtained using a lysing buffer containing: 50 mM HEPES pH 7.5, 150 mM NaCl, 1% Triton X-100, 1.5 mM $MgCl_2$, 1 mM EGTA pH 7.5, glycerol 10%, protease inhibitors as above reported. Following the collection of cytoplasmic proteins, the nuclei were lysed with the buffer containing 20 mM HEPES pH 8, 0.1 mM EDTA, 5 mM $MgCl_2$, 0.5 M NaCl, 20% glycerol, 1% NP-40 and protease inhibitors as above reported. The protein concentration was determinated using Bio-Rad Assay (Bio-Rad Laboratories). A 30 μg portion of protein lysates was used for western blotting (WB), resolved on a 10% SDS-polycrylamide gel and transferred to a nitrocellulose membrane (Bio-Rad). Filters were blocked for non-specific reactivity by incubation for 1 h at RT in 5% non-fat dry milk dissolved in TBST 1X and then incubated for 16 h at 4 °C with: TRβ1, Total Akt, Total ERK, Total c-Src, Total GSK3Bβ, PI3K-p85α, phospho Akt 1/2/3-Ser 473, Cyclin D1, Oct-1 and pGSK3βSer 9 (Santa Cruz Biotecnology), phospho ERK 1/2 and phosphoSrc Ser 419 (Cell Signaling). As loading, all membranes were subsequently stripped of the first antibody and reprobed with anti-GAPDH or anti-Lamin B antibodies (Santa Cruz Biotecnology). The antigen-antibody complex was detected by incubation of the membranes for 1 h at RT with peroxidase-coupled goat anti-mouse or anti-rabbit IgG and revealed using the enhanced chemiluminescence system (ECL system, Amersham Pharmacia). The blots were then exposed to Kodak films (Sigma).

2.10. Immunoprecipitation

Whole-cell lysates (500 μg), obtained as above reported, were incubated for 2 h with 20 μL protein A/G-agarose beads at 4 °C and then centrifuged at 12,000 rpm for 5 min. The supernatants were then incubated overnight with 10 μl of mouse anti- TRβ1, or mouse anti-Oct-1 or rabbit anti-PI3K p85α antibodies and 20 μL of protein A/G. Immunoprecipitates were collected by centrifugation at 12,000 rpm for 10 min, followed by washing three times with HNTG (immunoprecipitation IP) buffer (50 mM HEPES, pH 7.4; 50 mM NaCl; 0.1% Triton X-100; 10% glycerol; 1 mM phenylmethylsulfonylfluoride; 10 μg/ml leupeptin; 10 μg/ml aprotinin; 2 μg/ml pepstatin). Following the final wash, supernatant was removed. Samples were resuspended in the Laemmli sample buffer, subjected to SDS-polyacrylammide gel electrophoresis (10% gel) and then transferred onto a nitrocellulose membrane. The immunoprecipitated proteins were detected by Western Blot using a rabbit anti-PI3K p85α or mouse anti-Oct-1 or mouse anti-TRβ1

antibodies. Immunoprecipitation with protein A/G alone was used as negative control. Membranes were stripped of bound antibodies by incubation in glycine (0.2 m, pH 2.6) for 30 min at RT. Before reprobing with different primary antibodies, stripped membranes were washed extensively in TBST and placed in blocking buffer (TBST containing 5% milk).

2.11. PI3K kinase assay

Cells were grown in 10 cm dishes to 60–70% confluence and exposed to treatments for 20 min in SFM and then lysates with 500 μL of RIPA-buffer plus protease inhibitors as above reported. Cell lysates were centrifuged at 12,000 rpm for 5 min; 500 μg of total protein were incubated overnight with the anti-p85A antibody and 500 μL of HNTG (IP) buffer. Immunocomplexes were recovered by incubation with protein A/G-agarose. The immunoprecipitates were washed once with cold PBS, twice with 0.5 M LiCl, 0.1 M Tris (pH = 7.4) and finally with 10 mM Tris, 100 mM NaCl and 1 mM EDTA. The presence of PI3K activity in immunoprecipitates was determined by incubating the beads with reaction buffer containing 10 mm HEPES (pH 7.4), 10 mm $MgCl_2$, 50 μm ATP, 20 μCi [γ-32P] ATP and 10 μg L-α-phosphatidylinositol-4,5-bis phosphate (PI-4, 5-P2) for 20 min at 37 °C. The reactions were stopped by adding 100 μl of HCl 1 mM. Phospholipids were extracted with 200 μl $CHCl_3$/methanol. For extraction of lipids, 200 μl chloroform:methanol (1:1, vol/vol) were added to the samples and vortexed for 20 s. Phase separation was facilitated by centrifugation at 5000 rpm for 2 min in a tabletop centrifuge. The upper phase was removed, and the lower chloroform phase was washed once more with clear upper phase. The washed chloroform phase was dried under a stream of nitrogen gas and redissolved in 30 μl of chloroform. The labeled products of the kinase reaction, the PI phosphates, were spotted onto trans-1,2-diaminocyclohexane-N,N,N_,N_-tetraacetic acid–treated silica gel 60 thin-layer chromatography plates state running solvent used for TLC. Radioactive spots were visualized by autoradiography.

2.12. RNA interference (RNAi)

Cells were plated in 10 cm dishes in the regular growth medium the day before transfection to 60–70% confluence. On the second day, the medium was changed with SFM without P/S and the cells were transfected with stealth RNA interference (siRNA) targeted human TRβ1, human Oct-1, human CycD1 or with a scrambled siRNA to a final concentration of 100 nM, as recommended by the manufacturer (Invitrogen). After 5 h, the transfection medium was changed with SFM with P/S in order to avoid Lipofectamine 2000 (Invitrogen) toxicity the cells were exposed to T3, 100 nM and then treated for WB analysis and proliferation assay.

2.13. Cell proliferation assays

FB-2, TPC1, WRO and FRTL-5 cells were seeded in 6-well plates in a regular growth medium. On the second day, the cells were incubated in SFM for 24 h and then cultured with treatments or with vehicle. The medium was renewed every 2 days together with the appropriate treatments. [3H] thymidine (1 μCi/ml; New England Nuclear, Newton, MA, USA) was added to the medium for last 6 h before lysis. After rinsing with PBS, the cells were washed once with 10% and thrice with 5% trichloroacetic acid. The cells were lysed by adding 0.1 M NaOH and then incubated for 30 min at 37 °C. [3H] thymidine incorporation was determinated by scintillation counting. The effects of T3 on cell proliferation were measured 0, 24, 48 and 72 h following initial exposure to treatment by counting TPC1, FB-2,WRO and FRTL-5 cells using a Burker's chamber, with cell viability determined by trypan blue dye exclusion.

2.14. Statistical analysis

Optical densities were measured using the Scion Image software (Scion Corporation). Statistical analysis was performed using ANOVA followed by Newman–Keuls testing to determine differences in means. $p < 0.05$ was considered as statistically significant; ns was considered not statistically significant.

3. Results

3.1. Thyroid hormone T3 induces proliferative effects in FB-2 cells

We first aimed to examine, in a human well-differentiated thyroid cancer cells, designated FB-2, and in their ancestor cell line, TPC1 (Meireles et al., 2007) the expression levels of the two major TR isoforms, TRα1 and TRβ1. As shown in Fig. 1A and B, the expression of TRβ1in terms of mRNA and protein level was well detectable in FB-2 and TPC1 cells; follicular thyroid cancer cell line, WRO, was used as a positive control (Chen et al., 2000). Thyroid hormone receptor α1 was only scantly present (data not shown), suggesting that TRβ1 is the predominant TR isoform in FB-2 and TPC1 cells.

Since previous studies have demonstrated the ability of T3 to exert proliferative effects in several tumor cell lines (Davis et al., 2008; Hall et al., 2008; Hsieh and Juang, 2005; Lin et al., 2006; Poplawski and Nauman, 2008; Verga Falzacappa et al., 2009a,b), we investigated if T3 was able to stimulate FB-2 cell growth. Our data showed that T3 significantly increased thymidine incorporation in a dose-dependent manner. These effects were more evident after longer treatment as evidenced by a 2.2-fold increase upon 100 nM for 48 h compared to the untreated cells (Fig. 1C). Taken together, these results showed that T3 induced stimulatory effects on FB-2 cell proliferation. Similar biological growth effects, induced by T3, were also observed in TPC1 cells (Fig. S.1A). Moreover, we showed that T3 was able to induce cell growth effect also in WRO cells (data not shown), while any effect was observed in rat normal thyroid cell line, FRTL-5 (Fig. 1D). Notably, the proliferative effect was significant at 1 nM T3 concentration and maximally evident upon 100 nM T3 exposure. We confirm the cell growth effect exerted by thyroid hormone in FB-2, TPC1, WRO and FRTL-5 cells by counting with trypan blue exclusion (data not shown). It's important to underline that RIA measurement in surnatant from FB-2 cells treated with T3 100 nM showed a free T3 concentration of 89.2 ± 0.2 pM. This is probably due to the bovine serum protein-binding and Mg-complexing of T3 that occurs in medium. Next, we investigated the effects of short-term stimulation with T3 100 nM on phosphorylation levels of ERK, Akt, and Src that represent the main downstream effectors of proliferation and pro-survival signaling. As reported in Fig. 1E T3 treatment increased phosphorylation of ERK, Akt and Src.

3.2. TRβ1 is involved in the rapid activation of AKT induced by T3

The involvement of TRβ1 in T3-activation of the above explored signaling transduction pathways was investigated after TRβ1siRNA. In preliminary experiment we evaluated, after 24, 48 and 72 h of siRNA transfection, that TRβ1 protein expression was effectively silenced as revealed by Western Blotting (Fig. 2A). It was extremely interesting to reveal how, in the presence of TRβ1knocked down, the T3 activation of pERK1/2 and pSrc still persisted, while a reduction of Akt phosphorylation was observed. These findings address a specific role of T3/TRβ1 complex in the rapid activation of the Akt transduction pathway (Fig. 2B). Thus, to elucidate the involvement of TRβ1in mediating Akt activation, we evaluated, by co-immunoprecipitation studies, whether TR interacts with

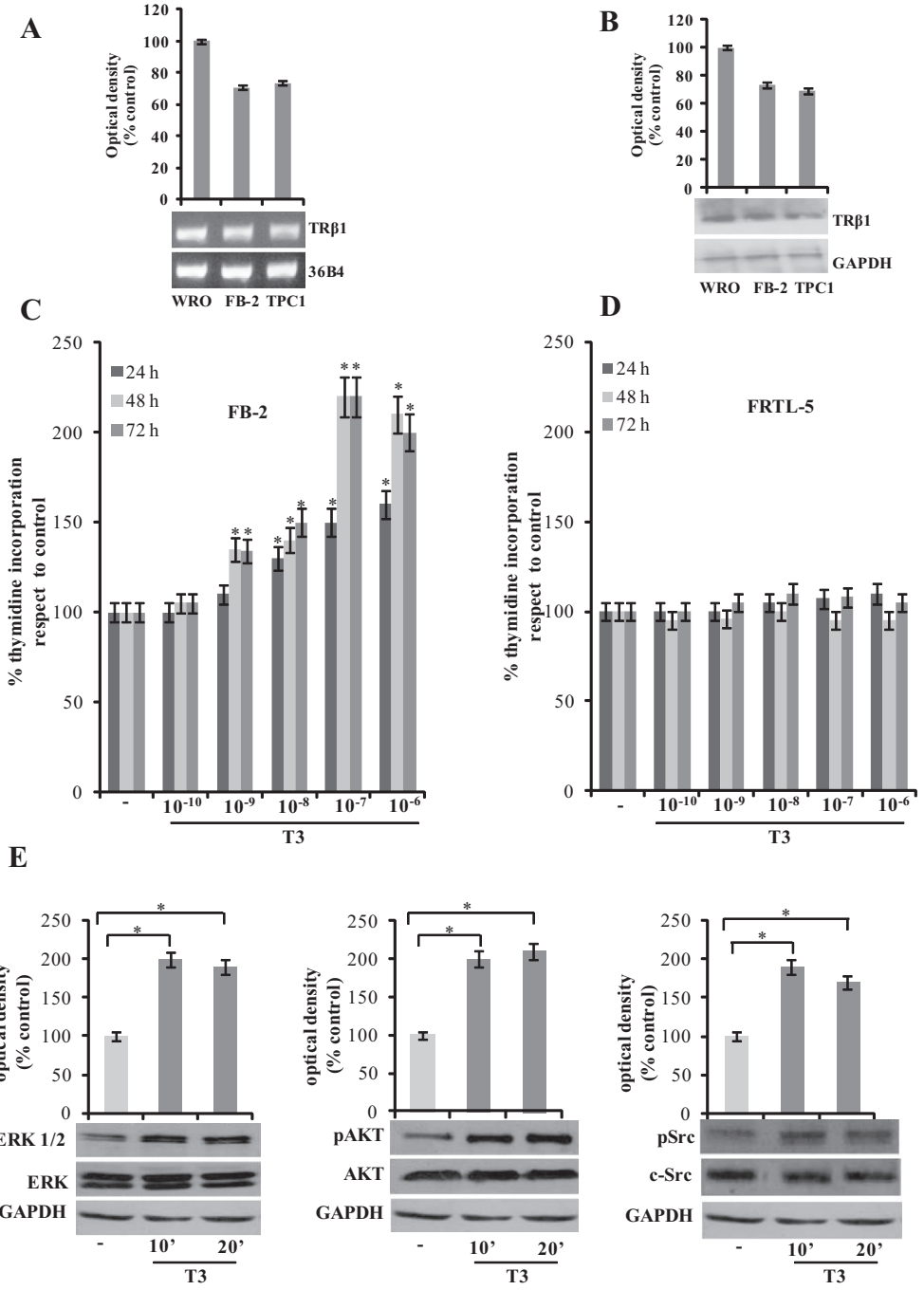

Fig. 1. Effects of T3 on thyroid cancer cell growth (A) TRβ1 mRNA expression evaluated by RT-PCR in WRO, FB-2 and TPC1 cells; 36B4 mRNA levels were determined as internal control. (B) Immunoblots of TRβ1 from WRO, FB-2 and TPC1 cells. GAPDH expression was used as loading. (C) FB-2 and (D) FRTL-5 cells were untreated (−) or treated with increasing T3 concentrations for 24, 48 and 72 h. Six hours before lysis, [3H] thymidine was added. [3H] thymidine incorporation was determined by scintillation counting. The results represent the means ± SD of three independent experiments, each performed in triplicate and expressed as percentage of growth *vs* control which was assumed to be 100%. (E) Immunoblots of pERK1/2, pAKT, pSrc from total protein extracts of FB-2 cells untreated (−) or treated with T3 100 nM for 10 and 20 min. Total ERK, AKT and c-Src were used to normalize respectively pERK1/2, pAKT and pSrc expression. GAPDH expression was used as internal loading. Immunoblots show a single representative of three separate experiments. The histograms represent the means ± SD of three separate experiments between phospho/total/GAPDH levels in which band intensities were evaluated in terms of optical density arbitrary units and expressed as percentages of the control which was assumed to be 100%. $^{*}p < 0.05$.

the regulatory subunit of PI3-kinase, p85α. As shown in Fig. 2C, using total cell lysates by FB-2 cells immunoprecipitated with the anti-TRβ1 antibody, we evidenced that TRβ1 is constitutively associated with p85A. The short treatment with T3 did not modify this physical association. We confirmed the formation of this protein–protein complex, by immunoprecipitation with the anti-p85 α antibody and then detection of TRβ1on western blot analysis (data not shown). To assess the influence of TRβ1/p85α complex on the PI3K/Akt transduction cascade, we evaluated the short effect of T3 on PI3K activity and on GSK3βSer9. Our results showed an enhanced PI3K activity after T3 treatment, concomitantly with a strong increase in GSK3B phosphorylation at serine 9, inducing

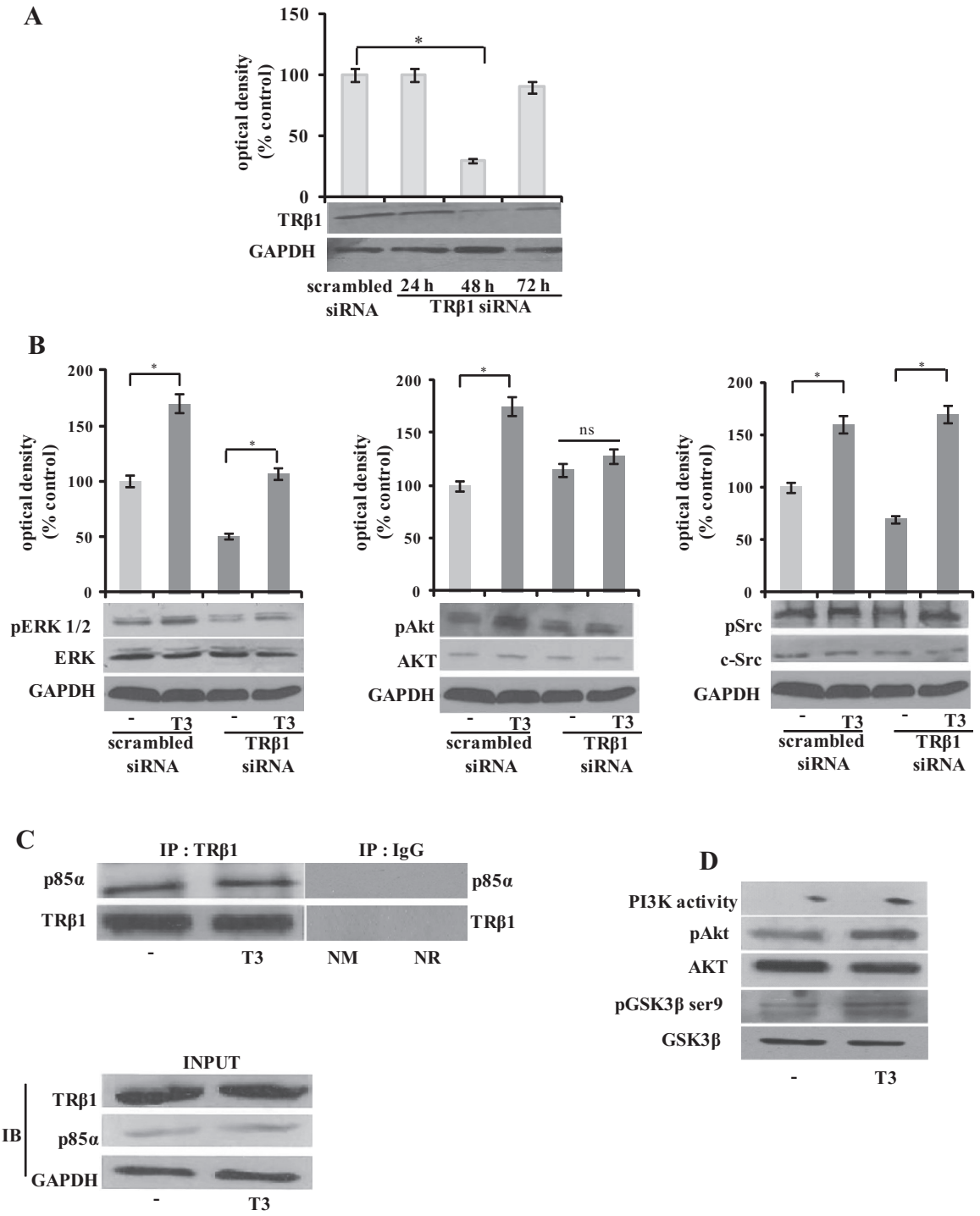

Fig. 2. TRβ1 mediates the rapid activation of AKT induced by T3. (A) TRβ1 protein expression (evaluated by WB) in FB-2 cells transfected with scrambled siRNA or with targeted human TRβ1 mRNA sequence (TRβ1 siRNA) as reported in Materials and Methods. GAPDH expression was used as loading control. The histograms show the means ± SD of three independent experiments, each performed in triplicate and expressed as percentages of the control which was assumed to be 100%. $^{*}p < 0.05$. (B) Immunoblots of pERK1/2, pAKT and pSrc of FB-2 cells transfected using scrambled siRNA or TRβ1 siRNA untreated (−) or treated with T3 100 nM for 20 min. Total ERK, AKT and c-Src were used to normalize respectively pERK1/2, pAKT and pSrc expression. GAPDH expression was used as internal loading. Immunoblots show a single representative of three separate experiments. The histograms represent the means ± SD of three separate experiments between phospho/total/GAPDH levels in which band intensities were evaluated in terms of optical density arbitrary units and expressed as percentages of the control which was assumed to be 100%. $^{*}p < 0.05$; ns, nonsignificant. (C) FB-2 cells were untreated (−) or treated with T3 100 nM for 20 min. Total cell lysates were immunoprecipitated with anti-TRβ1 antibody and then subjected to immunoblot analyses with anti-p85α and and anti-TRβ1 antibodies. Negative control was performed by incubation of cell lysates with protein A/G agarose and normal mouse (NM) or rabbit (NR) antisera. The samples without immunoprecipitation (INPUT) were used to confirm the expression of each protein. One of three similar experiments is presented. (D) FB-2 cells were untreated (−) or treated with T3 100 nM for 20 min. 500 μg of cell lysates were used for PI3K activity as described in Materials and Methods. The autoradiograph presented is representative of one of experiments that were performed at least three times. Immunoblots of pAKT and pGSK3β(Ser9) from FB-2 untreated (−) or treated with T3 100 nM for 20 min. Total AKT and GSK3β were used to normalize respectively pAKT and pGSK3β expression. One of three similar experiments is presented.

its inactivation (Fig. 2D). GSK3β, a well-known main target of pAkt, normally phosphorylates and promotes the degradation of cyclin D1 (Takahashi-Yanaga and Sasaguri, 2008).

3.3. T3 increases cyclin D1 expression and its promoter activity

Cyclin D1 is a critical mitogen-regulated cell-cycle control element whose transcriptional modulation plays a crucial role in cancer growth and progression. Thus, we evaluated the ability of T3 to modulate cyclin D1 expression in FB-2 cells. Our results revealed that T3 100 nM induced an up-regulation of cyclin D1 protein content together with an increase of its mRNA both in FB-2 cells (Fig. 3A and B) as well as in TPC1 cells (Fig. S. 1B and C). To test whether TH might modulate cyclin D1 promoter activity, FB-2 cells were transiently transfected with a cyclin D1 promoter reporter plasmid (p2966/+142) and left treated with 100 nM T3 for 12 h. As reported in Fig. 3C, TH administration increased cyclin D1 promoter activity by 2.5 fold induction respect to untreated cells.

To define the T3 responsive region of the cyclin D1 promoter, a series of 5′-promoter-deleted constructs expressing different binding sites, such as TRE, GAS, CRE, Oct-1 and Sp1, were used and tested for promoter activity in FB-2 cells. The plasmids p−848/+142 and p−254/+142 of the cyclin D1 promoter showed an increased transcriptional activity upon T3 stimulation with respect to untreated cells. On the contrary, we observed that, in the presence of the p−136/+142 construct, T3 was unable to transactivate cyclin D1 promoter activity (Fig. 3C). These results suggested that the region from −254 to −136 was required for the transactivation of cyclin D1 promoter by T3. The nucleotide analysis of this region revealed a Oct-1 site as a putative effector of T3/TR activity. Thus, we performed site-directed mutagenesis on the Oct-1 domain (Oct-1 Mut) within the cyclin D1 promoter. Mutation of this domain abrogated T3 effects (Fig. 3D). These latter results demonstrate that the integrity of Oct-1-binding site is necessary for T3 modulation of cyclin D1promoter activity in thyroid cancer cells. The crucial role of T3 is further strengthened by the observation that the overexpression of TRβ1 (Fig. 3E) in FB-2 cells enhanced the up-regulatory effect of T3 on the activity of the cyclin D1 promoter (Fig. 3F) as well as on cyclin D1 protein expression (Fig. 3G).

3.4. T3 enhances recruitment of TRβ1/Oct-1 on Oct-1 site containing region of the cyclin D1 promoter

To investigate whether Oct-1 site mediates the T3 up-regulation of cyclin D1, we performed electrophoretic mobility shift assay (EMSA) using synthetic oligodeoxyribonucleotidies corresponding to the Oct-1 site located in the human cyclin D1 gene promoter, as probe. In nuclear extracts from FB-2 cells (Fig. 4A) we observed the formation of a complex (lane 1), which was abrogated by 100-fold molar excess of unlabeled probe (lane 2) as well as by the use of a mutated probe (lane 4), demonstrating the specificity of the DNA-binding complex. T3 administration induced an increase in the DNA binding activity compared with untreated sample (lane 3). The inclusion of anti-TRβ1or anti-Oct-1 antibodies in the reactions attenuated the specific bands (lanes 5 and 6 respectively). This effect was more evident in the presence of both antibodies (lane 7), indicating the coexistence of both proteins in DNA binding complex. Normal mouse IgG addition did not affect protein-DNA complex formation (lane 8).

To assess whether TRβ1 and Oct-1 may physically interact we performed coimmunoprecipitation studies using protein fractions from FB-2 cells treated with T3. As shown in Fig. 4B (upper panel), the formation of an TRβ1 and Oct-1 complex was detected in untreated cells, and this association was enhanced upon T3 treatment in nuclear extracts. This result well correlated with a rapid nuclear translocation of Oct-1 upon T3 treatment (Fig. 4B lower panel). Next, to better determine the physiological relevance of the Oct-1 site containing region of cyclin D1 promoter, we investigated whether TRβ1 interacts with this region as it exists in native chromatin, performing ChIP assay in FB-2 cells. As shown in Fig. 4C, the results indicated that TRβ1 was constitutively bound to Oct-1 site in untreated cells and that this recruitment was increased upon T3 treatment. The up-regulatory role of TRβ1 on cyclin D1 promoter was further evidenced by the TRβ1 and RNA Pol II occupancy onto the cyclin D1 promoter, that both appeared to be enhanced after T3 exposure (Fig. 4C). Finally, using as negative control primers that amplify a region of cyclin D1 upstream the Oct-1 site the TRβ1 immunoprecipitated chromatin analyzed by PCR did not show any recruitment onto cyclin D1 promoter region (data not shown).

3.5. Cyclin D1 expression and cell proliferation T3-induced are mediated by both TRβ1 and Oct-1

To better define the contribution of TRβ1and Oct-1 on TH-mediated cyclin D1 expression and FB-2 cellular proliferation, we silenced these two transcription factors. First we evaluated, by Western Blotting analysis, after 24, 48 and 72 h of siRNA transfection that Oct-1 protein expression was effectively silenced (Fig. 5A). As shown in Fig. 5B and C, silencing of TRβ1or Oct-1 expression significantly reversed cyclin D1 up-regulation induced by T3. Moreover, we observed that growth stimulatory effects of T3 were abrogated in cells expressing TRβ1or Oct-1 knocked down (Fig. 5D and E). These data further support that both TRβ1and Oct-1 mediate the proliferative effects induced by T3 in papillary thyroid cancer cell line cells. Finally to demonstrate that T3-induced cell proliferation is mediated through cyclin D1 we transfected FB-2 cells with a specific siRNA targeting human CycD1. As shown in Fig. 5F after knocking down CycD1 the upregulatory effects of T3 on cell proliferation was completely reversed.

4. Discussion

The controversial role of TH in carcinogenesis has been reported, although the precise mechanisms responsible for differential effects remain incompletely clarified. Some studies have reported that T3 suppresses cell proliferation in neuroblastoma and fibroblasts cells (Perez-Juste and Aranda, 1999; Porlan et al., 2008). However, most published studies have described proliferative effects of TH on breast, glial, renal, prostate and thyroid cancer cells (Davis et al., 2006, 2008; Hall et al., 2008; Hernandez et al., 1999; Hsieh and Juang, 2005; Lin et al., 2009; Tang et al., 2004; Verga Falzacappa et al., 2009a,b).

In this study we demonstrated that in papillary thyroid cancer cells supra-physiological doses of T3 are able to induce proliferative effects in a dose-dependent manner, while no growth effects were observed in rat normal thyroid cell line, FRTL-5 at all doses tested. These findings are consistent with the described coexistence of thyroid cancer and hyperthyroidism, although with an incidence highly variable (ranging between 0.2% and 21.0%) (Yeh et al., 2013) and with the observation that the estimated prevalence of malignancy within hot nodules is about of 3.1% (Mirfakhraee et al., 2013). Particularly, hyperthyroidism should be carefully considered in patients with papillary thyroid cancer exhibiting $BRAF^{V600E}$ mutation, the most common genetic alteration, that has been significantly associated with extra-thyroidal extension, metastases, recurrence, and mortality (Nucera et al., 2010). On the other hand, in our study low doses of T3 do not elicit growth effects in thyroid cancer cells. This observation appears to be important when related to the semi-suppressive therapy with THs, L-T4 alone or plus T3, that is commonly used after thyroidec-

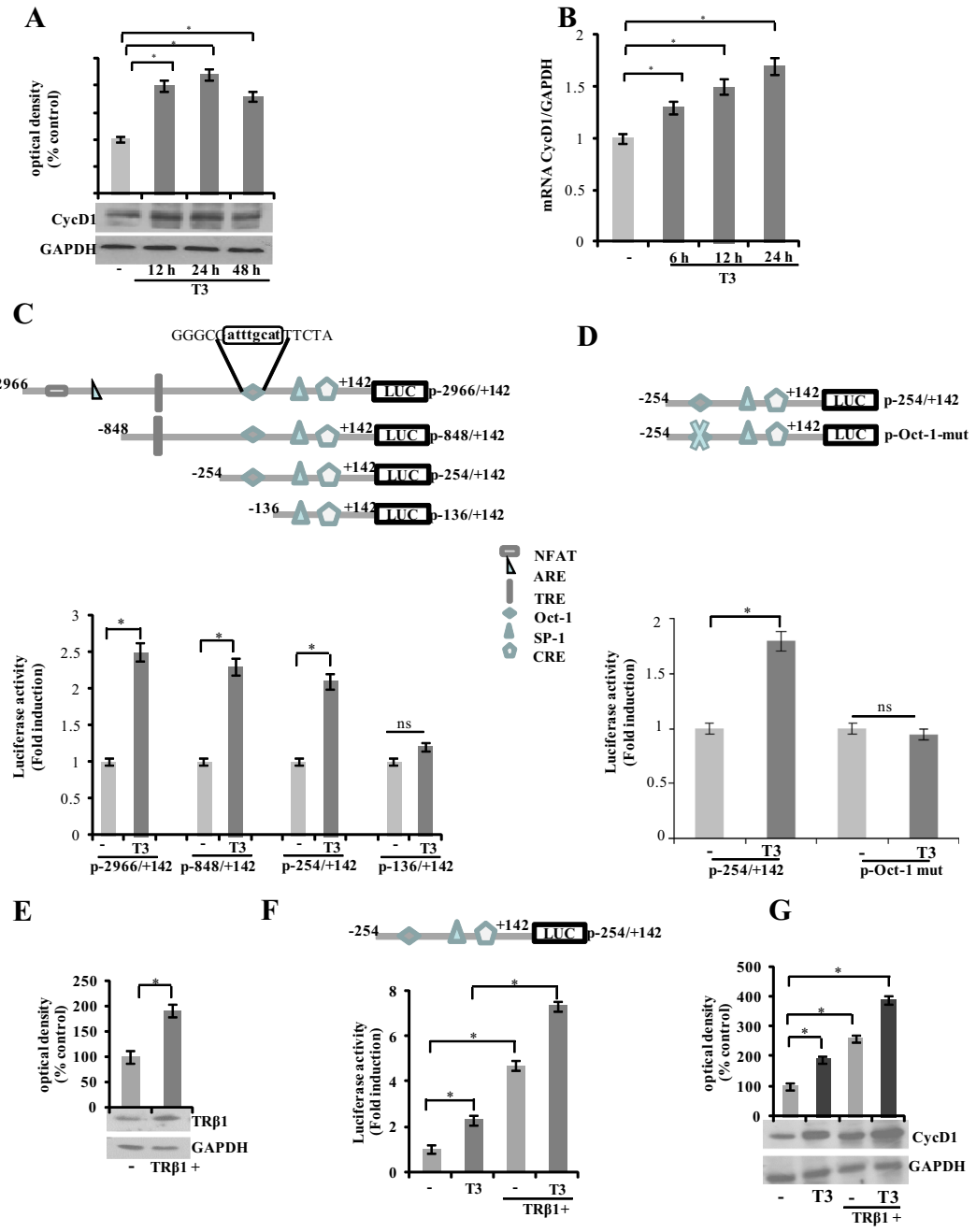

Fig. 3. T3 up-regulates cyclin D1 expression and its promoter activity. (A) Total protein extracts of FB-2 cells untreated (−) or treated with T3 100 nM for 12, 24 and 48 h were subjected to immunoblots analysis with human cyclin D1 (CycD1) antibody. GAPDH served as loading control. Immunoblots show a single representative of three separate experiments. The histograms represent the means ± SD of three separate experiments in which band intensities were evaluated in terms of optical density arbitrary units and expressed as percentages of the control which was assumed to be 100%. $^{*}p < 0.05$. (B) Total RNA extracts from cells untreated (−) or treated with T3 100 nM for 6, 12 and 24 h was subjected to RT-real time PCR assay using specific primers for cyclin D1 or GAPDH as reported in Materials and Methods. $^{*}p < 0.05$. (C) Schematic representation of human cyclin D1 promoter fragments used in this study. Transcriptional activity of FB-2 cells with promoter constructs is shown. FB-2 cells were transfected for 24 h and left untreated (−) or treated with T3 100 nM for 12 h. The luciferase activities were normalized to the internal transfection control and values of untreated cells (−) were set as 1 fold induction upon which the activity induced by treatment was calculated. The values represent the mean ± SD of three separate experiments. $^{*}p < 0.05$; ns, nonsignificant. (D) Site-direcetd mutagenesis of the putative Oct-1 site was performed as described in Materials and Methods section. FB-2 cells transfected with p−254/+142 or p-Oct-1-mut constructs were untreated (−) or treated with T3 100 nM for 12 h. The luciferase activities were normalized to the internal transfection control and values of untreated cells (−) were set as 1 fold induction upon which the activity induced by treatment was calculated. The values represent the mean ± SD of three separate experiments. $^{*}p < 0.05$; ns, nonsignificant. (E) FB-2 cells were transfected with TRβ1 expression vector (TRβ1 +), and TRβ1 protein expression was detected by immunoblot analysis. GAPDH served as loading control. Immunoblot show single representative of three separate experiments. The histograms represent the means ± SD of three separate experiments in which band intensities were evaluated in terms of optical density arbitrary units and expressed as percentages of the control which was assumed to be 100%. $^{*}p < 0.05$. (F) FB-2 cells were co-transfected with TRβ1+ and p−254/+142 constructs and then untreated (−) or treated with T3 100 nM for 12 h. The luciferase activities were normalized to the internal transfection control and values of untreated cells (−) were set as 1 fold induction upon which the activity induced by treatment was calculated. The values represent the mean ± SD of three separate experiments. $^{*}p < 0.05$. (G) In the same experimental conditions, total protein extracts of FB-2 cells untreated (−) or treated with T3 100 nM for 24 h were subjected to immunoblots analysis with human CycD1 antibody. GAPDH served as loading control. Immunoblots show a single representative of three separate experiments. The histograms represent the means ± SD of three separate experiments in which band intensities were evaluated in terms of optical density arbitrary units and expressed as percentages of the control which was assumed to be 100%. $^{*}p < 0.05$.

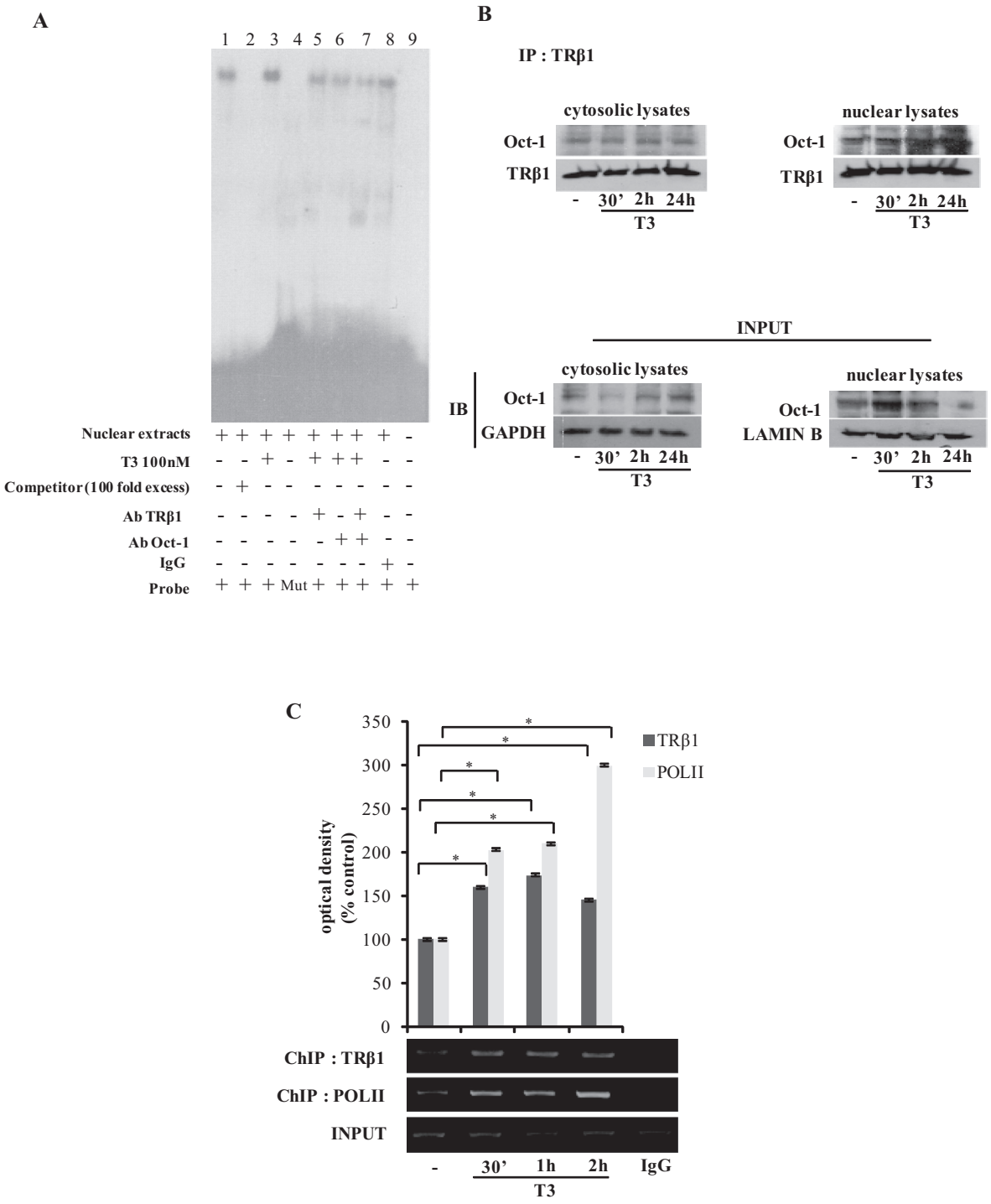

Fig. 4. T3 enhances Oct-1/TRβ1 recruitment on cyclin D1 promoter. (A) Nuclear extracts from FB-2 cells were incubated with a double-stranded Oct-1 specific consensus sequence labeled with [32P]ATP and subjected to electrophoresis in a 6% polyacrylamide gel (lane 1). Competition experiments were done by adding as competitor a 100-fold molar excess of unlabeled probe (lane 2) and with a labeled oligonucleotide containing a mutated Oct-1 (lane 4). FB-2 nuclear extracts treated with T3 100 nM for 6 h incubated with probe (lane 3). The specificity of the binding was tested by adding to the reaction mixture anti-TRβ1 (lane 5) or anti-Oct-1 (lane 6) antibodies or both antibodies (lane 7). IgG did not affect Oct-1 complex formation (lane 8). Lane 9 contains probe alone. (B) FB-2 cells were untreated (−) or treated with T3 100 nM for 30 min, 2 and 24 h. Cytosolic and nuclear proteins were immunoprecipitated with anti-TRβ1 antibody and then subjected to immunoblot analyses with anti-Oct-1 and anti-TRβ1 antibodies (upper panel). The cytosol and nuclear extracts without immunoprecipitation (INPUT) were used to confirm the expression of each protein. GAPDH (cytosol) and Lamin B (nuclear) expression were used as a control for gel loading and to exclude the contamination of the cytosol with the nuclear components and *vice versa*. One of three similar experiments is presented (lower panel). (C) Cells were untreated (−) or treated with T3 100 nM for 30 min, 1 and 2 h. The preacleared chromatin was immunoprecipitated with specific anti-TRβ1 and anti-RNA polymerase II (POL II) antibodies. IgG, control samples. Cyclin D1 promoter sequences containing Oct-1 site was detected by PCR with specific primers as detailed in Materials and Methods. To determine input DNA, the cyclin D1 promoter fragment was amplified from 30 μl purified soluble chromatin before immunoprecipitation. Immunoblots show a single representative of three separate experiments. The histograms represent the means ± SD of three separate experiments in which band intensities were evaluated in terms of optical density arbitrary units and expressed as percentages of the control, which was assumed to be 100%. $^{*}p < 0.05$.

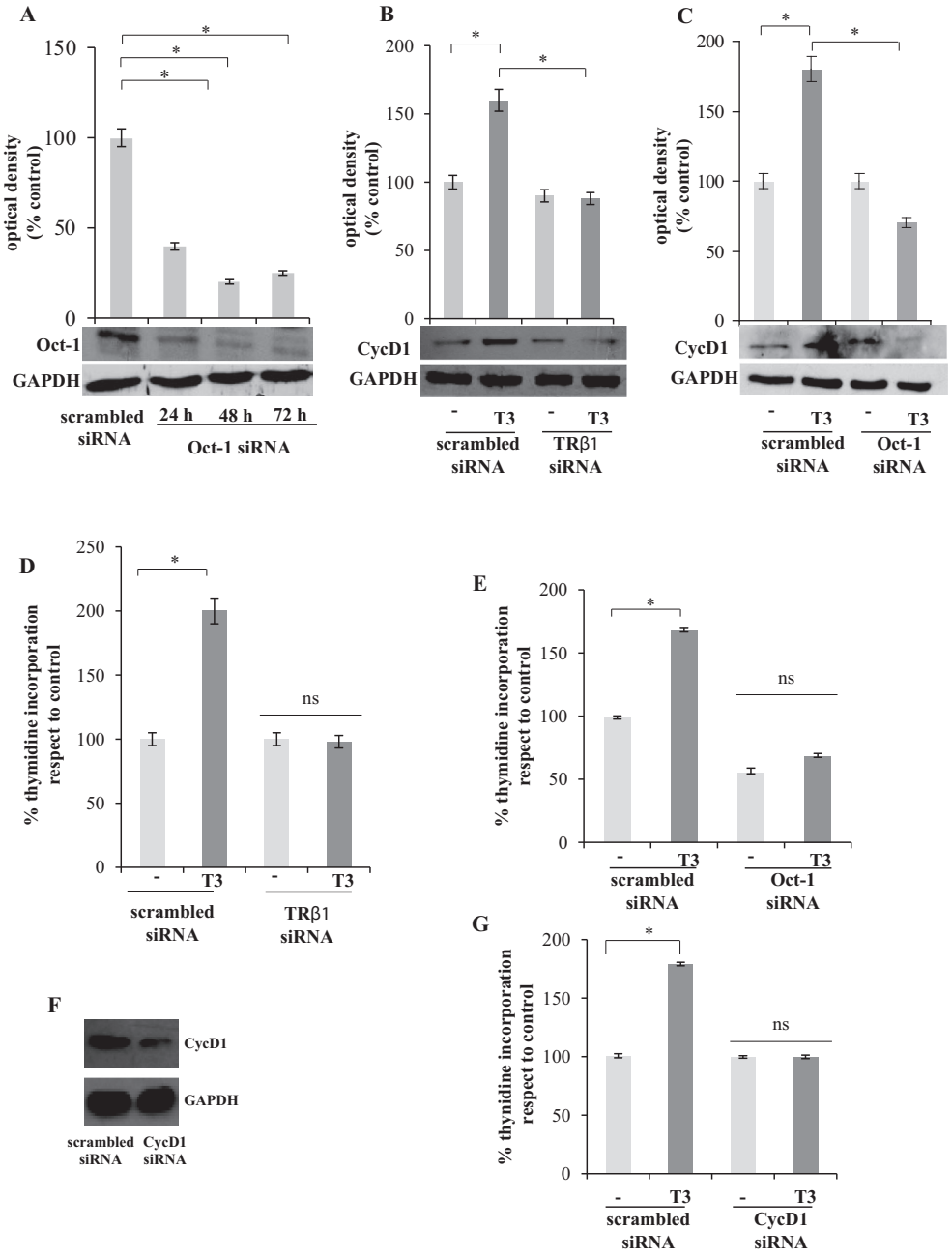

Fig. 5. TRβ1 and Oct-1 mediate the up-regulation of cyclin D1 and the proliferative effects induced by T3 in FB-2 cells. (A) Oct-1 protein expression (evaluated by WB) in FB-2 cells transfected with scrambled siRNA or with targeted human Oct-1 mRNA sequence (Oct-1siRNA) as reported in Materials and Methods. GAPDH expression was used as loading control. Immunoblots show a single representative of three separate experiments. The histograms show the means ± SD of three independent experiments, each performed in triplicate and expressed as percentages of the control which was assumed to be 100%. $^{*}p < 0.05$. (B and C) Immunoblot of cyclin D1. Cells were transfected with scrambled siRNA or TRβ1 siRNA (B) or Oct-1 siRNA (C) and untreated (−) or treated with T3 100 nM for 48 h. GAPDH expression was used as loading control. Immunoblots show a single representative of three separate experiments. The histograms show the means ± SD of three independent experiments performed in triplicate and express as percentages of the control which was assumed to be 100%. $^{*}p < 0.05$. (D and E) Cells were transfected with scrambled siRNA or TRβ1 siRNA (D) or Oct-1 siRNA (E) and untreated (−) or treated with T3 100 nM for 48 h. Cell proliferation was evaluated by [3H] thymidine incorporation. The results represent the means ± SD of three independent experiments, each performed in triplicate and expressed as percentage of growth *vs* control which was assumed to be 100%. $^{*}p < 0.05$; ns, non significant. (F) Cyc D1 protein expression (evaluated by WB) in FB-2 cells transfected with scrambled siRNA or with targeted human CycD1 mRNA sequence (CycD1siRNA) for 48 h. GAPDH expression was used as loading control. (G) Cells were transfected with scrambled siRNA or CycD1siRNA and untreated (−) or treated with T3 100 nM for 48 h. Cell proliferation was evaluated by [3H] thymidine incorporation. The results represent the means ± SD of three independent experiments, each performed in triplicate and expressed as percentage of growth vs control which was assumed to be 100%. $^{*}p < 0.05$; ns, nonsignificant.

tomy in patients affected by differentiated thyroid cancer, in which the concentration of free T3 is in the normal range.

Our data revealed that in a well differentiated papillary cancer cell FB2 short term exposure of T3 exerts a significant activation of ERK, AKT and Src that represent the main downstream effectors of proliferation and pro-survival signaling. We showed the involvement of TRβ1 in the T3-rapid AKT phosphorylation, since knocking down of gene encoding TRβ1 led to an abolishment of T3-induced AKT activation. These observations are in agreement with previous studies that have been focused their research on the so-called "non-genomic" action of T3 (Cao et al., 2005; Davis et al., 2007; Storey et al., 2006), which is often related to activation

of rapid signaling pathways involved in cellular process as proliferation and survival. Interestingly, it has been reported that some of these effects involve TRs located outside the nucleus, since up to 10% of TRs are located in the cytoplasm (Davis et al., 2008). Moreover, data obtained in different cell models evidenced that liganded or unliganded cytoplasmatic TRs bind to the p85α subunit of PI3K and activate the PI3K signaling pathway, including the phosphorylation of AKT, a mammalian target of rapamycin (mTOR) and its substrate p70S6K (Cao et al., 2005; Hiroi et al., 2006; Moeller et al., 2006; Verga Falzacappa et al., 2007). According to above reported findings, we showed that in FB-2 cells, TRβ1 interacts with the subunit p85α of PI3K, although this interaction is not influenced by the rapid hormone treatment; of interest, T3 enhances the PI3K activity, suggesting that T3 binding to TR activates the kinase. On the other hand, we observed that T3 triggers a cascade of events that are PI3K-dependent, since we demonstrated that pAKT induces a phosphorylation of glycogen synthase Kinase-3β, GSK3β, a main target of PI3K pathway. The GSK3β is an important regulator of several cellular processes, including cell cycle progression, proliferation and apoptosis (Takahashi-Yanaga et al., 2008).

Of interest, we observed that T3-exposure up-regulates both cyclin D1 mRNA and protein levels in FB-2 cells. Functional experiments using cyclin D1 promoter deleted constructs, showed that TH induces cyclin D1 promoter activity and that the region spanning from −254 to −136, which contains Oct-1 site, was required for the responsiveness to T3. It has been reported that unliganded TR induces a transcriptional activation of Oct-1 by decreasing the amount of silencing mediator for retinoic and thyroid hormone receptors (SMRT) that interacts with Oct1 POU domain. In addition, the authors demonstrated that liganded-TR, increasing the amounts of SMRT that can be recruit by Oct-1, represses the transcriptional activity of Oct-1 (Kakizawa et al., 2001). Besides, transcriptional regulation by THs requires synergistic action of the TR with others trans-acting factors, including Oct-1 (Voz et al., 1992). Our data showed a constitutive TRβ1/Oct-1 association which increases upon T3 administration in nuclear compartment. Besides, we evidenced that T3, through Oct-1, induces an activation of cyclin D1 promoter activity. Oct-1 can function both as a cyclin D1 transcriptional repressor and inducer (Boulon et al., 2002; Kakizawa et al., 1999; Magné et al., 2003). Oct-1 is thought to repress cyclin D1 transcription because stimulation of mammary epithelial cells with prolactin induces cyclin D1 promoter activity by removing Oct-1 from the cyclin D1 promoter (Brockman Shuler, 2005). Conversely, Oct-1 can form a complex with CREB to activate CRE-mediated cyclin D1 gene transcription, acting as a transcriptional co-activator for CREB (Boulon et al., 2002). Magné et al, reported that thrombopoietin (TPO)-activated Stat5 directly binds Oct-1 in a hemapoietic cell line and that this complex binds to the Oct-1-GAS2 site in the cyclin D1 promoter, leading to enhanced promoter activity (Magné et al., 2003).

We demonstrated, by EMSA and ChIP studies, that T3 enhances the binding of TRβ1/Oct-1 complex to Oct-1 site containing cyclin D1 promoter gene. The latter results are concomitant with an enhanced RNA Polymerase II occupancy, consistent with the increased cyclin D1 transcriptional activity. The crucial role of TRβ1 and Oct-1 on the proliferative effects and the up-regulation of cyclin D1 induced by T3 strongly emerges from our data showing that silencing TRβ1 or Oct-1 expression reverses both observed events. Finally, T3-induced increase in cell growth was abrogated after knocking down cyclin D1 expression.

4.1. Conclusions

A hypothetical model of the investigated genomic and non-genomic mechanism through which T3/TRβ1 activation may modulate thyroid cancer cell growth is shown in Fig. 6. In FB-2 cells, T3 stimulation enhances the recruitment of TRβ1/Oct-1 on Oct-1 site

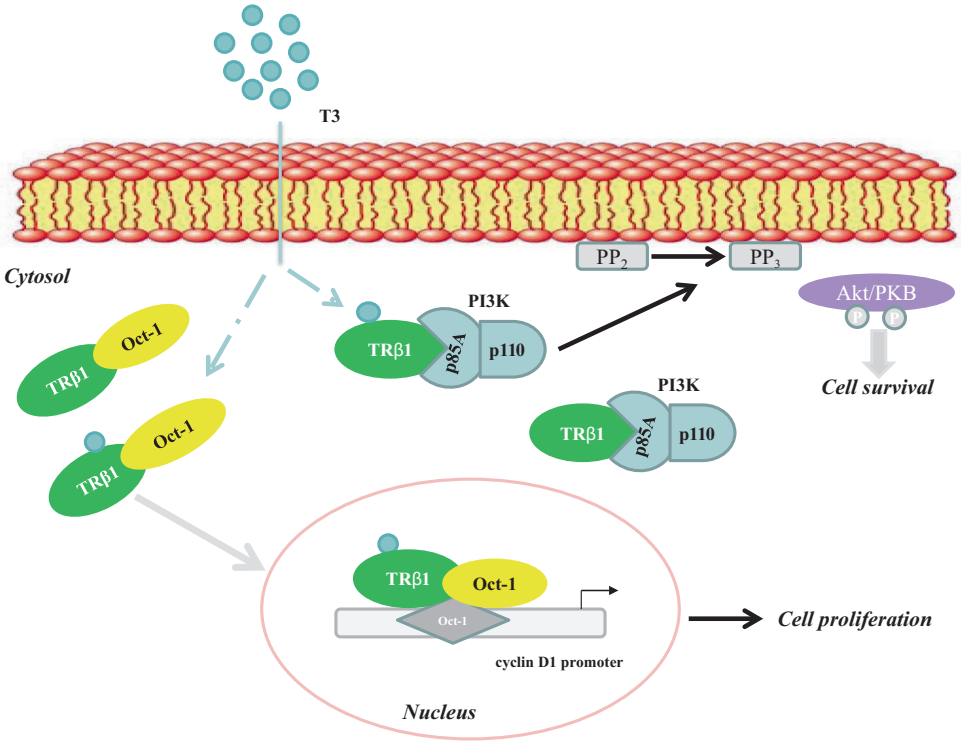

Fig. 6. Proposed working model of T3/TRβ1 in modulating cyclin D1 expression and cell proliferation in papillary thyroid cancer cells. T3 enhances the recruitment of TRβ1/Oct-1 complex on the Oct-1 site containing region of the cyclin D1 promoter with consequent increased cyclin D1 expression. In addition, T3, binding to cytoplasmatic TRβ1/p85α complex, leads to activation of PI3K and its downstream signaling cascade involved in cell survival.

located onto cyclin D1 promoter, activating cyclin D1 transcription. In addition, T3/TRβ1, interacts with the regulatory subunit of PI3K (p85α) in the cytosol, leading to activation of PI3K and its downstream signaling cascade, including AKT phosphorylation, a main key regulator of cell survival.

Acknowledgements

This work was supported by 'Epidemiologic Observatory Endemic Goiter and Iodine prophylaxis', Calabria Region, Centro Sanitario, AIRC and MURST and Ex 60% 2011.

Appendix A. Supplementary material

Supplementary data associated with this article can be found, in the online version, at http://dx.doi.org/10.1016/j.mce.2013.10.001.

References

Andrews, N.C., Faller, D.V., 1991. A rapid micropreparation technique for extraction of DNA-binding proteins from limiting numbers of mammalian cells. Nucleic Acids Research 19, 2499.

Balta, A.Z., Filiz, A.I., Kurt, Y., Sucullu, I., Yucel, E., Akin, M.L., 2012. Prognostic value of oncoprotein expressions in thyroid papillary carcinoma. Medical Oncology 29, 734–741.

Basolo, F., Giannini, R., Toniolo, A., Casalone, R., Nikiforova, M., Pacini, F., Elisei, R., Miccoli, P., Berti, P., Faviana, P., Fiore, L., Monaco, C., Pierantoni, M.G., Fedele, M., Nikiforov, Y.E., Santoro, M., Fusco, A., 2002. Establishment of a non-tumorigenic papillary thyroid cell line (FB-2) carrying the RET/PTC1 rearrangement. International Journal of Cancer 97, 608–614.

Bassett, J.H., Harvey, C.B., William, G.R., 2003. Mechanisms of thyroid hormone receptor-special nuclear and extra nuclear actions. Molecular and Cellular Endocrinology 213, 1–11.

Boulon, S., Dantonel, J.C., Binet, V., Vié, A., Blanchard, J.M., Hipskind, R.A., Philips, A., 2002. Oct-1 potentiates CREB.driven cyclin D1 promoter activation via a phosphor-CREB and CREB binding protein-independent mechanism. Molecular and Cellular Biology 22, 7769–7779.

Brockman, J.L., Shuler, L.A., 2005. Prolactin signals via Stat5 and Oct-1 to the proximal cyclin D1 promoter. Molecular and Cellular Endocrinology 239, 45–53.

Cao, X., Kambe, F., Moeller, L.C., Refetoff, S., Seo, H., 2005. Thyroid hormone induces rapid activation of Akt/protein Kinase B-mammalian target of rapamycin-p70S6K cascade trough phosphatidylinositol 3-Kinase in human fibroblast. Molecular Endocrinology 19, 102–112.

Chen, S.T., Shieh, H.Y., Lin, J.D., Chang, K.S., Lin, K.H., 2000. Overexpression of thyroid hormone receptor beta1 is associated with thyrotropin receptor gene expression and proliferation in a human thyroid carcinoma cell line. The Journal of Endocrinology 165, 379–389.

Davis, F.B., Tang, H.Y., Shih, A., Keating, T., Lansing, L., Hercbergs, A., Fenstermaker, R.A., Mousa, A., Mousa, S.A., Davis, P.J., Lin, H.Y., 2006. Acting via a cell surface receptor, thyroid hormone is a growth factor for glioma cells. Cancer Research 66, 7270–7275.

Davis, P.J., Leonard, J., Davis, F.B., 2007. Mechanisms of non-genomic actions of thyroid hormone. Frontiers in Neuroendocrinology 29, 211–218.

Davis, P.J., Davis, F.B., Lin, H.Y., 2008. Promotion by thyroid hormone of cytoplasm-to-nucleus shuttling of thyroid hormone receptors. Steroids 73, 1013–1017.

Degrassi, A., Monaco, M.C., Lisignoli, G., Belvedere, O., Oneguzzi, S., Malangone, W., Bonora, M.L., Piacentini, A., Lavaroni, S., Scarbolo, M., Ambesi-Impiombato, F.S., Facchini, A., 1998. Cell cycle synchronization of FRTL5 cells. A physiological model system. Journal of Experimental and Clinical Cancer Research 17, 527–532.

Eric, A., Klein, E.A., Assoian, R.K., 2008. Transcriptional regulation of the cyclin D1 gene at a glance. Journal of Cell Science 121, 3853–3857.

Hall, L.C., Salazar, E.P., Staci, R., Liu, N., 2008. Effects of thyroid hormones on human breast cancer cell proliferation. Journal of Steroid Biochemistry and Molecular Biology 109, 57–66.

Hernandez, G.B., Park, K.S., Zhan, Q., Cheng, S.Y., 1999. Thyroid hormone-induced cell proliferation in GC cells is mediated by changes in G1 cyclin/cyclin-dependent kinase levels and activity. Endocrinology 140, 5267–5274.

Hiroi, Y., Kim, H.H., Ying, H., Furuya, F., Huang, Z.H., Simoncini, T., Noma, K., Ueki, K., Nguyen, N.H., Scanlan, T.S., Moskowitz, M.A., Cheng, S.Y., Liao, J.K., 2006. Rapid non-genomic actions of thyroid hormone. Proceeding of the National Academy of Sciences 103, 14104–14109.

Hsieh, M.L., Juang, H.H., 2005. Cell growth effects of triiodothyronine and expression of thyroid hormone receptor in prostate carcinoma cells. Journal of Andrology 26, 422–428.

Kakizawa, T., Miyamoto, T., Ichikawa, K., Kanedo, A., Suzuki, S., Hara, M., Nagasawa, T., Takeda, T., Mori, J., Kumagai, M., Hashizume, K., 1999. Functional interaction between Oct-1 and Retinoid X receptor. The Journal of Biological Chemistry 27, 19103–19108.

Kakizawa, T., Miyamoto, T., Ichikawa, K., Takeda, T., Susuki, S., Mori, J., Kumagai, M., Yamashita, K., Hashizume, K., 2001. Silencing mediator for retinoid and thyroid hormone receptors interacts with octamer transcription factor-1 and acts as a transcriptional repressor. Journal of Biological Chemistry 30, 9720–9725.

Kenessey, A., Ojamaa, K., 2006. Thyroid hormone stimulates protein synthesis in the cardiomyocyte by activating the Akt-mTOR and p70S6K pathways. The Journal of Biological Chemistry 281, 20666–20672.

Kowalik, M.A., Perra, A., Pibiri, M., Cocco, M.T., Samarut, J., Plateroti, M., Ledda-Columbano, G.M., Columbano, A., 2010. TRB is the critical thyroid hormone receptor isoform in T3-induced proliferation of hepatocytes and pancreatic acinar cells. Journal of Hepatology 53, 686–692.

Lazar, M.A., Chin, W.W., 1990. Nuclear thyroid hormone receptors. Journal Clinical Investigation 86, 1777–1782.

Lin, H.Y., Sun, M., Tang, H.Y., Lin, C., Luidens, M.K., Mousa, S.A., Incerpi, S., Drusano, G.L., Davis, F.B., Davis, P.J., 2009. L-thyroxine *vs* 3,5,3′-triiodo-L-thyroxne and cell proliferation: activation of mitogen-activated protein kinase and phosphatidylinositol3-kinase. American Journal of Physiology Cell Physiology 295, 980–991.

Lin, H.Y., Tang, H.Y., Shih, A., Keating, T., Cao, G., Davis, P.J., Davis, F.B., 2006. Thyroid hormone is a MAPK-dependent growth factor for thyroid cancer cells and is anti-apoptotic. Steroids 72, 180–187.

Magné, S., Caron, S., Charon, M., Rouyez, M.C., Dusanter-Fourt, I., 2003. STAT5 and Oct-1 form a stable complex that modulates cyclin D1 expression. Molecular and Cellular Biology 24, 8934–8945.

Meireles, A.M., Preto, A., Rocha, A.S., Rebocho, A.P., Máximo, V., Pereira-Castro, I., Moreira, S., Feijão, T., Botelho, T., Marques, R., Trovisco, V., Cirnes, L., Alves, C., Velho, S., Soares, P., Sobrinho-Simões, M., 2007. Molecular and genotypic characterization of human thyroid follicular cell carcinoma-derived cell lines. Thyroid 17, 707–715.

Mirfakhraee, S., Mathews, D., Peng, L., Woodruff, S., Zigman, J.M., 2013. A solitary hyperfunctioning thyroid nodule harboring thyroid carcinoma: review of the literature. Thyroid Res., 4;6(1):7.

Moeller, L.C., Cao, X., Dumitrescu, A.M., Seo, H., Refetoff, S., 2006. Thyroid hormone mediated changes in gene expression can be initiated by cytosolic action of the thyroid hormone receptor B through the phosphatidylinositol 3-kinase pathway. Nuclear Receptor Signaling 4, 1–4.

Nucera, C., Lawler, J., Hodin, R., Parangi, S., 2010. The BRAFV600E mutation: what is it really orchestrating in thyroid cancer? Oncotarget 1, 751–756.

Oetting, A., Yen, P.M., 2007. New insights into thyroid hormone action. Best Practice and Research Clinical Endocrinology and Metabolism 21, 193–208.

Perez-Juste, G., Aranda, A., 1999. The cyclin-dependent kinase inhibitor p27(Kip1) is involved in thyroid hormone-mediated neuronal differentiation. Journal of Biological Chemistry 274, 5026–5031.

Pibiri, M., Ledda-Columbano, G.M., Cossu, C., Simbula, G., Menegazzi, M., Columbano, A., 2001. Cyclin D1 is an early target in hepatocyte proliferation induced by thyroid hormone (T3). Federation of American Societies for Experimental Biology 15, 1006–1013.

Poplawski, P., Nauman, A., 2008. Thyroid hormone -triiodothyronine- has contrary effect on proliferation of human proximal tubules cell line (HK2) and renal cancer cell lines (caki2, Caki1) – role of E2F4, E2F5 and p107, p130. Thyroid Research 13, 1–5.

Porlan, E., Vidaurre, O.G., Rodríguez-Peña, A., 2008. Thyroid hormone receptor-beta (TR beta1) impairs cell proliferation by the transcriptional inhibition of cyclins D1, E and A2. Oncogene 27, 2795–2800.

Prefontaine, G.G., Lemieux, M.E., Giffin, W., Shild-Poulter, C., Pope, L., LaCasse, E., Walker, P., Hache, R., 1998. Recruitment of octamer transcription factors to DNA by glucocorticoid receptor. Molecular and Cellular Biology 18, 3416–3430.

Sirianni, R., Chimento, A., Malivindi, R., Mazzitelli, I., Andò, S., Pezzi, V., 2007. Insulin-like growth factor-I, regulating aromatase expression through steroidogenic factor 1, supports estrogen-dependent tumor Leydig cell proliferation. Cancer Research 67, 8368–8377.

Storey, N.M., Gentile, S., Ullah, H., Russo, A., Muessel, M., Erxleben, C., Armstrong, D.L., 2006. Rapid signaling at the plasma membrane by a nuclear receptor for thyroid hormone. Proceedings of the National Academy Sciences 103, 5197–5201.

Takahashi-Yanaga, F., Sasaguri, T., 2008. GSK-3β regulates cyclin D1 expression: a new target for chemiotherapy. Cell Signaling 20, 581–589.

Tang, H.Y., Lin, H.Y., Zhang, J., Davis, P.J., Davis, F.B., 2004. Thyroid hormone causes mitogen-activated protein kinase-dependent phosphorylation of the nuclear estrogen receptor. Endocrinology 145, 3265–3272.

Verga Falzacappa, C., Mangialardo, C., Patriarca, V., Bucci, B., Amendola, D., Raffa, S., Torrisi, M.R., Silvestrini, G., Ballanti, P., Moriggi, G., Stigliano, A., Brunetti, E., Toscano, V., Misiti, S., 2009a. Thyroid hormone induce cell proliferation and survival in ovarian granulosa cells COV434. Journal of Cellular Physiology 221, 242–253.

Verga Falzacappa, C., Patriarca, V., Bucci, B., Mangialardo, C., Michienzi, S., Moriggi, G., Stigliano, A., Brunetti, E., Toscano, V., Misiti, S., 2009b. The TRB1 is essential in mediating T3 action on Akt pathway in human pancreatic insulinoma cells. Journal of Cellular Biochemistry 106, 835–848.

Verga Falzacappa, C., Petrucci, E., Patriarca, V., Michienzi, S., Stigliano, A., Brunetti, E., Toscano, V., Misiti, S., 2007. Thyroid hormone receptor TRB1 mediates Akt activation by T3 in pancreatic B cells. Journal of Molecular Endocrinology 38, 221–233.

Voz, M.L., Peers, B., Wiedig, M.J., Jacquemin, P., Belayew, A., Martial, J.A., 1992. Transcriptional regulation by triiodothyronine requires synergistic action of the thyroid receptor with another trans-acting factor. Molecular Cell Biology 12, 3991–3997.

Wang, S., Lloyd, R.V., Hutzler, M.J., Safran, M.S., Patwardhan, N.A., Khan, A., 2000. The role of cell cycle regulatory protein, cyclin D1, in the progression of thyroid cancer. Modern Pathology 13, 882–887.

Weiss, R.E., Ramos, H.E., 2004. Thyroid hormone receptor subtypes and their interaction with steroid receptor coactivators. Vitamins and Hormones 68, 185–207.

Yeh, N.C., Chou, C.W., Weng, S.F., Yang, C.Y., Yen, F.C., Lee, S.Y., Wang, J.J., Tien, K.J., 2013. Hyperthyroidism and thyroid cancer risk: a population-based cohort study. Expert Clinical Endocrinology Diabetes 121, 402–406.

Biochimica et Biophysica Acta 1831 (2013) 1027–1036

Contents lists available at SciVerse ScienceDirect

Biochimica et Biophysica Acta

journal homepage: www.elsevier.com/locate/bbalip

Mechanisms of divergent effects of activated peroxisome proliferator-activated receptor-γ on mitochondrial citrate carrier expression in 3T3-L1 fibroblasts and mature adipocytes ☆

Daniela Bonofiglio [a,1], Antonella Santoro [a,1], Emanuela Martello [a], Donatella Vizza [a], Daniela Rovito [a], Anna Rita Cappello [a], Ines Barone [a,b], Cinzia Giordano [b], Salvatore Panza [b], Stefania Catalano [a], Vito Iacobazzi [c], Vincenza Dolce [a,*,2], Sebastiano Andò [a,b,**,2]

[a] Dept. Pharmacy, Health Sciences and Nutritional, University of Calabria 87036 Arcavacata di Rende (Cosenza), Italy
[b] Centro Sanitario, University of Calabria 87036 Arcavacata di Rende (Cosenza), Italy
[c] Dept of Biosciences, Biotechnology and Farmacological Sciences, and Center of Excellence in Comparative Genomics, University of Bari, 70125 Bari, Italy

ARTICLE INFO

Article history:
Received 9 July 2012
Received in revised form 16 January 2013
Accepted 18 January 2013
Available online 28 January 2013

Keywords:
Citrate carrier
Mitochondrion
PPARgamma
Adipocyte
Sp1

ABSTRACT

The citrate carrier (CIC), a nuclear-encoded protein located in the mitochondrial inner membrane, plays an important metabolic role in the transport of acetyl-CoA from the mitochondrion to the cytosol in the form of citrate for fatty acid and cholesterol synthesis. Citrate has been reported to be essential for fibroblast differentiation into fat cells. Because peroxisome proliferator-activated receptor-gamma (PPARγ) is known to be one of the master regulators of adipogenesis, we aimed to study the regulation of CIC by the PPARγ ligand rosiglitazone (BRL) in 3T3-L1 fibroblasts and in adipocytes. We demonstrated that BRL up-regulated CIC mRNA and protein levels in fibroblasts, while it did not elicit any effects in mature adipocytes. The enhancement of CIC levels upon BRL treatment was reversed using the PPARγ antagonist GW9662, addressing how this effect was mediated by PPARγ. Functional experiments using a reporter gene containing rat CIC promoter showed that BRL enhanced CIC promoter activity. Mutagenesis studies, electrophoretic-mobility-shift assay and chromatin-immunoprecipitation analysis revealed that upon BRL treatment, PPARγ and Sp1 are recruited on the Sp1-containing region within the CIC promoter, leading to an increase in CIC expression. In addition, mithramycin, a specific inhibitor for Sp1-DNA binding activity, abolished the PPARγ-mediated up-regulation of CIC in fibroblasts. The stimulatory effects of BRL disappeared in mature adipocytes in which PPARγ/Sp1 complex recruited SMRT corepressor to the Sp1 site of the CIC promoter. Taken together, our results contribute to clarify the molecular mechanisms by which PPARγ regulates CIC expression during the differentiation stages of fibroblasts into mature adipocytes.

1. Introduction

The mitochondrial citrate carrier (CIC), a nuclear-encoded protein which belongs to the mitochondrial carrier family is located in the inner membrane of mitochondria [1–3] and consists of three tandemly related domains of approximately 100 amino acids in length that span the membrane six times with both the N- and C-termini protruding toward the cytosol [4,5]. CIC exports citrate from the mitochondria to the cytosol where citrate is cleaved by ATP-citrate lyase to acetyl-CoA and oxaloacetate. Acetyl-CoA is used for fatty acid and sterol biosynthesis; whereas oxaloacetate is reduced to malate, which in turn is converted to pyruvate via malic enzyme with production of NADPH plus H^+. In addition to its role in fatty acid synthesis, CIC is involved in other processes such as gluconeogenesis, insulin secretion, histone acetylation and inflammation [6–10].

In rat, CIC activity was found to be decreased in diabetic and hypothyroid animals [11,12]. Later, it has been shown that CIC gene promoter contains an active FOXA site and that FOXA1 controls glucose-stimulated insulin secretion in INS-1 cells by transcriptional regulation of the CIC gene [13]. As for other lipogenic enzymes, CIC activity and expression are controlled by various nutritional states [14–17]. For instance, dietary polyunsaturated fatty acids (PUFA) inhibited CIC expression at both transcriptional and post-transcriptional levels, while saturated and monounsaturated fatty acid-enriched diet administration to rats did not have any effects [7,17,18]. Indeed, a PUFA response region containing the binding sites for some transcription factors such as SREBP-1 (sterol regulatory element binding protein-1), Sp1 (Specificity protein1) and

☆ Footnotes: This work was supported by MURST and Ex 60% and Reintegration AIRC/Marie Curie International Fellowship in Cancer Research to IB.
* Corresponding author. Tel.: +39 0984 493177; fax: +39 0984 493271.
** Corresponding author. Tel.: +39 0984 496201; fax: +39 0984 496203.
E-mail addresses: vdolce@unical.it (V. Dolce), sebastiano.ando@unical.it (S. Andò).
[1] Equally contributed to the work.
[2] Joint Senior Authors.

1388-1981/$ – see front matter © 2013 Elsevier B.V. All rights reserved.
http://dx.doi.org/10.1016/j.bbalip.2013.01.014

NF-Y (Nuclear Factor-Y) has been identified in the CIC gene promoter [7,19,20]. SREBP-1 activates the expression of CIC in HepG2 cells [7], hepatocytes [20] and mammary epithelium [21]. Recently, Damiano et al. have demonstrated that CIC expression, in hepatocytes and adipocytes, is regulated by ligands of peroxisome proliferator-activated receptor (PPAR) α and γ, identifying a peroxisome proliferator-activated receptor responsive element (PPRE) motif at −625 bp of CIC promoter [22].

PPARs are members of nuclear hormone receptors superfamily that function as ligand-dependent transcription factors [23]. Three PPAR isoforms, α, β/δ, and γ, are expressed in multiple species in a tissue-specific manner [24,25]. Among them, PPARγ integrates the control of energy, lipid and glucose homeostasis participating in the transcriptional activation of several genes important for adipocyte maturation, lipid accumulation, and insulin-sensitive glucose transport, as adipocyte fatty acid binding protein aP2, CCAAT/enhancer-binding protein-α (C/EBPα), Perilipin, and GLUT4 [26–29], phosphoenolpyruvate carboxykinase [30,31] and glycerol kinase [32]. Moreover, it has been demonstrated a role for PPARγ in cell differentiation, growth arrest and apoptosis in a large variety of cells [33–36]. Natural ligands of PPARγ include fatty acids and prostaglandin derivatives, while synthetic ligands of PPARγ are the insulin-sensitizing thiazolidinediones, as rosiglitazone (BRL).

Due to this knowledge, aim of our study was to define whether PPARγ may differently regulate CIC expression during the differentiation of 3T3-L1 fibroblasts into mature adipocyte cells. We have provided evidence, for the first time, that activated PPARγ up-regulates CIC expression in fibroblasts through Sp1 site present within CIC promoter region. The stimulatory effects of BRL disappear in mature adipocytes in which PPARγ/Sp1 complex recruits SMRT corepressor to the Sp1 site of the CIC promoter. Our results contribute to clarify the molecular mechanisms by which PPARγ during adipogenesis regulates CIC expression, which represents a crucial cross-point for several metabolic pathways.

2. Materials and methods

2.1. Reagents

BRL49653 (BRL) was purchased from Alexis (San Diego, CA, USA), the irreversible PPARγ antagonist GW9662 (GW) and mithramycin (M) were purchased from Sigma (Milan, Italy).

2.2. Cell culture and differentiation

The 3T3-L1 fibroblasts were maintained in Dulbecco's modified Eagle's medium (DMEM) supplemented with 10% (v/v) fetal bovine serum, 2 mM L-glutamine, 100 U penicillin and 100 μg/ml streptomycin (Sigma) in an atmosphere of 5% CO_2 at 37 °C. The cells were cultured until confluence had been reached, and then differentiation was induced 2 days thereafter (designated as "day 0") by adding 3-isobutyl-1-methylxanthine, dexamethasone and insulin (Sigma) to make their final concentrations of 0.5 mM, 1 μM and 1 μg/ml, respectively. After 72 h, the medium was changed to maturation medium supplemented with 1 μM dexamethasone and 1 μg/ml insulin. Cells were fed with maturation medium every 48 h, obtaining adipocytes at an early stage of differentiation (preadipocytes) after 7 days and mature adipocytes after 14 days from day 0. Cell differentiation was monitored by evaluating cell morphology under phase-contrast microscopy. Cells were considered to be adipocytes when numerous lipid droplets were observed in the cytoplasm. More than 90% of cells expressed the adipocyte phenotype. Cells were switched to serum-free medium the day before each experiment and then treated as indicated.

2.3. Mitochondrial isolation

3T3-L1 fibroblasts and mature adipocytes were grown in 10-cm dishes and exposed to treatments in serum-free medium as indicated before fractionation. Mitochondria were isolated as described previously [37]. Briefly, cells were washed with ice cold PBS, collected by scrapping in cold PBS and, after centrifugation (600 ×*g*, 4 °C, 10 min), resuspended in 200 mM sucrose, 10 mM Tris–MOPS and 1 mM EDTA/Tris, pH 7.4 (STE buffer). Cells were homogenized by glass Potter homogenization and mitochondria were then isolated by serial centrifugations. The mitochondrial pellet was resuspended in lysis buffer for immunoblotting analysis and in STE buffer for transport measurements.

2.4. Immunoblot analysis

Cells were grown in 10-cm dishes to 70% to 80% confluence and exposed to treatments in serum-free medium as indicated. Cells were then harvested in cold PBS and resuspended in lysis buffer containing 50 mM Tris–HCl (pH 8), 150 mM NaCl, 2 mM EDTA, 20% glycerol, 1% NP-40, and inhibitors (0.1 mM sodium orthovanadate, 1% phenylmethylsulfonylfluoride, and 20 mg/ml aprotinin). Equal amounts of total protein lysates or mitochondrial extracts, isolated as described above, were resolved on 10% SDS-polyacrylamide gel, transferred onto a nitrocellulose membrane (Amersham Biosciences, Milan, Italy), and probed with the antibody directed against human C terminal-CIC [5] or PPARγ (Santa Cruz Biotechnology, Inc., Santa Cruz, CA, USA). A mouse monoclonal antibody against the β-subunit of human F1-ATPase (β-ATPase) (BD Biosciences, San Josè, CA, USA) was used as a loading control to ensure that any differences in protein expression between pre- and post-differentiation cells were not due to the increase in number of mitochondria, typically occurring to mature adipocytes during differentiation. Antigen–antibody complexes were detected using anti-rabbit or anti-mouse IgG-coupled horseradish peroxidase (Pierce, Rockford, IL, USA) and revealed using the ECL Western Blotting Analysis System (Amersham). The bands of interest were quantified by the Scion Image laser densitometry scanning program.

2.5. Mitochondria reconstitution and transport measurements

Isolated mitochondria from 3T3-L1 fibroblasts and mature adipocytes were solubilized in a buffer containing 3% Triton X-114, 4 mg/ml cardiolipin, 10 mM Na_2SO_4, 0.5 mM EDTA, and 5 mM PIPES, pH 7 using modifications of the method described previously by Jordens et al. [38]. After incubation for 20 min at 4 °C, the mixture was centrifuged at 138,000 ×*g* for 10 min. The supernatant was incorporated into phospholipid vesicles by cyclic removal of the detergent [39]. The reconstitution mixture consisted of 0.04 mg protein solution, 10% Triton X-114, 10% phospholipids (egg lecithin from Fluka, Milan, Italy) as sonicated liposomes, 10 mM citrate, 0.85 mg/ml cardiolipin (Sigma) and 20 mM PIPES; pH 7.0. The mixture was recycled 13 times through an Amberlite column. All phases were performed at 4 °C, except for the passages through Amberlite, which were carried out at room temperature. To measure citrate transport, external substrate was removed from the proteoliposomes on Sephadex G-75 columns pre-equilibrated with buffer A (50 mM NaCl and 10 mM PIPES, pH 7.0). Transport at 25 °C was started by the addition of 0.5 mM [^{14}C]citrate (Amersham) to the eluted proteoliposomes and terminated by the 'inhibitor-stop' method with the addition of 20 mM 1,2,3-benzene-tricarboxylate [40,41]. In control samples, the inhibitor was added simultaneously to the labeled substrate. Finally, the external radioactivity was removed from the Sephadex G-75 columns and radioactivity in the liposomes was measured [39]. Transport activity was calculated by subtracting the control values from the experimental values.

2.6. RT-PCR assay

Total RNA was extracted from 3T3-L1 fibroblasts, pre-adipocytes and mature adipocytes using a Trizol reagent (Invitrogen, Milan, Italy) according to the manufacturer's protocol. RNA was quantified spectrophotometrically and its quality was checked by electrophoresis through agarose gels stained with ethidium bromide. CIC and PPARγ expression were analyzed by the real-time polymerase chain reaction (RT-PCR) method as described previously [42], using the following primers: CIC forward 5′-CTGTCAGGTTTGGGATGTTC-3′ and reverse 5′-GTGGGTTCATAGGTTTGTTG-3′; PPARγ forward 5′ GGTGA AACTCTGGGAGATTC-3′ and reverse 5′-CAACCATTGGGTCAGCTCTT-3′; β-actin forward 5′-AGGCATCCTGACCCTGAAGTAC-3′ and reverse 5′-TC TTCATGAGGTAGTCTGTCAG-3′. PCR was performed for 34 cycles for CIC (94 °C 1 min, 66 °C 1 min, 72 °C 1 min), 32 cycles for PPARγ (94 °C 1 min, 67 °C 1 min, 72 °C 1 min) and 24 cycles for β-actin (94 °C 1 min, 60 °C 1 min, 72 °C 1 min).

2.7. Plasmid and reporter vector construction

The plasmid pCIC1437 containing the rat CIC gene promoter region spanning from −1473 to +35 bp was amplified from Rat Genomic DNA (Novagen, Merck Bioscience, Germany) by nested PCR as previously described [42] using the following primers: sense 5′-AGAGCTCCAGAC CATGTGC-3′ and antisense 5′-AGTTTGGCTTTCCCGGACC-3′; nested-sense (pCIC1473for) 5′-TGAGGTACCAACAAGCCCCTCAGAGGCTG-3′ and nested-antisense (pCICrev) 5′-TGAAAGCTTTCGACCTCGGGTCCGAGCC-3′. The amplified DNA fragment was digested with *KpnI* and *HindIII* and then cloned into the pGL3 basic vector (Promega, Milan, Italy). The pCIC1473 plasmid was used as template to generate the different deleted constructs: pCIC284 (−284 to +35 bp), pCIC145 (−145 to +35 bp), pCIC115 (−115 to +35 bp) and pCIC82 (−82 to +35 bp).

Forward primers are listed in Table 1; the reverse primer was pCICrev for all the constructs.

The mutation of Sp1 site included from −115 to −82 region was obtained by site-directed mutagenesis using QuickChange kit (Stratagene, La Jolla, CA) performed on pCIC115 plasmid. The mutagenic primers to construct the pCIC115-Sp1mut are listed in Table 1. The plasmid pCIC-3xSp1, containing a threefold repeat of wild type responsive Sp1 site, was constructed by annealing between the following forward and reverse primers: forward: 5′-CATGGTACCTAATGCGGGGCGGATG CGGGGCGGAAGCGGGGCGGATCCAAGCTTTAG-3′; reverse: 5′-CTAAAG CTTGGATCCGCCCCGCTTCCGCCCCGCATCCGCCCCGCATTAGGTACCATG-3′. The fragment obtained by annealing was used as template in a PCR reaction conducted with the following forward and reverse primers 5′-CATGGTACCTAATGCGGG-3′ and 5′-CTAAAGCTTGGATCCGCC-3′, respectively. The DNA fragment was digested with *KpnI* and *HindIII* and then cloned into the pGL3 basic vector (Promega, Milan, Italy).

The sequence of the different constructs was verified by nucleotide sequence analysis.

2.8. Transient transfection assays

3T3-L1 fibroblasts were transiently transfected using the Lipofectamine 2000 reagent (Invitrogen, Milan, Italy) with the described rat CIC promoter constructs for 18 h. After transfection, cells were treated as described for 12 h. Thymidine kinase–Renilla luciferase plasmid was used to normalize the efficiency of the transfection. Firefly and Renilla luciferase activities were measured with the Dual Luciferase Kit (Promega) according to the manufacturer's recommendations.

Table 1
Oligonucleotides used for CIC promoter constructs.

Construct	Oligonucleotide sequence
pCIC1473	5′-TGAGGTACCAACAAGCCCCTCAGAGGCTG-3′
pCIC284	5′-TGAGGTACCTACCCGCTTTGGCAAAGAGTTGC-3′
pCIC145	5′-TAGGGTACCAGTTTCCCGGCTGGCAC-3′
pCIC115	5′-TAGGGTACCGGCGGGGCTCAGCTCAG-3′
pCIC82	5′-TAGGGTACCCCGGGGAGCTGACGTGA-3′
pCIC115Sp1mut For	5′-GCTCAGGCCACGCGGATCCGAGCCGGGGAGCTGAC-3′
pCIC115Sp1mut Rev	5′-GTCAGCTCCCCGGCTCGGATCCGCGTGGCCTGAGC-3′

2.9. Electrophoretic mobility shift assays (EMSA)

Nuclear extracts from 3T3-L1 fibroblasts were prepared as previously described [43]. The probe was generated by annealing single-stranded oligonucleotides labeled with [^{32}P]ATP and tyrosine polynucleotide kinase and then purified using Sephadex G-50 spin columns (Sigma). The DNA sequence used as probe or as cold competitor was as follows (the nucleotide motif of interest is underlined and mutations are shown as lowercase letters): Sp1 5′-AGGCCA CGCGGGGCGGAGCCCGGGA-3′, mutated Sp1 5′-AGGCCACGCGattaGG AGCCCGGGA-3′.

The protein-binding reactions were carried out in 20 μl of buffer [20 mM HEPES (pH 8), 1 mM EDTA, 50 mM KCl, 10 mM dithiothreitol, 10% glycerol, 1 mg/ml BSA, 50 μg/ml poly(dI/dC)] with 50,000 cpm of labeled probe, and 5 μg of fibroblast nuclear protein. The mixtures were incubated at room temperature for 20 min in the presence or absence of unlabeled competitor oligonucleotides. For the experiments involving anti-PPARγ and anti-Sp1 antibodies (Santa Cruz Biotechnology), the reaction mixture was incubated with these antibodies at 4 °C for 30 min before addition of the labeled probe. The entire reaction mixture was electrophoresed through a 6% polyacrylamide gel in 0.25× Tris-borate-EDTA for 3 h at 150 V. Gel was dried and subjected to autoradiography at −80 °C.

2.10. Chromatin immunoprecipitation (ChIP) and re–ChIP assays

3T3-L1 fibroblasts and mature adipocytes were grown in 10-cm dishes to 50%–60% confluence, starved with serum-free medium for 24 h and then treated with BRL. Thereafter, cells were washed twice with PBS and cross-linked with 1% formaldehyde and sonicated. Supernatants were immunocleared with salmon sperm DNA/protein A agarose for 1 h at 4 °C. The precleared chromatin was immunoprecipitated with specific anti-PPARγ, anti-Sp1, or anti-polymerase II (POLII) antibodies (Santa Cruz Biotechnology). The anti-PPARγ samples were reimmunoprecipitated with anti-Sp1, anti-ARA70, anti-PCG1α (Santa Cruz Biotechnology), anti-SMRT or anti-NCoR (Novus Biologicals, Milan, Italy) antibodies. The anti-Sp1 samples were reimmunoprecipitated with anti-SMRT antibody. A normal mouse serum IgG was used as negative control. Pellets were washed, eluted with elution buffer (1% SDS, 0.1 mol/l $NaHCO_3$), and digested with proteinase K. DNA was obtained by phenol/chloroform/isoamyl alcohol extractions and was precipitated with ethanol. Five microliters of each sample and input were used for PCR with the primers flanking the Sp1 sequence present in the CIC promoter region: 5′-TAGCGTTGCTGTCCGGAGACCA-3′ and 5′-GAGACCAC GACCAATTCTGGT-3′. The amplification products obtained were analyzed in 2% agarose gel and visualized by ethidium bromide staining.

2.11. RNA silencing

3T3-L1 fibroblasts and mature adipocytes were transfected with RNA duplex of stealth siRNA targeted for the mouse SMRT mRNA sequence (Ambion, ID:s74031) or with a control siRNA used as a control for non-sequence-specific effects to a final concentration of 100 nM using Lipofectamine 2000 as recommended by the manufacturer. After 5 h the transfection medium was changed with serum-free medium and then the cells were exposed to treatments.

2.12. Statistical analysis

Statistical analysis was performed using ANOVA followed by Newman–Keuls' testing to determine differences in means. $P<0.05$ was considered as statistically significant.

3. Results

3.1. Functional characterization of CIC in 3T3-L1 cells

We first aimed to investigate the expression and activity of CIC in mitochondrial extracts from 3T3-L1 fibroblasts (F) and mature adipocytes (A, 14 days after differentiation induction). Immunoblot analysis, using an antibody raised against the carboxy-terminus of the mature CIC protein, revealed a weak immunoreactive band in fibroblasts at 34 kDa, corresponding to the mitochondrial CIC, while a 4.5-fold increase in band intensity was observed in mature adipocytes (Fig. 1A). A similar pattern of CIC expression was also found in total extracts of both fibroblasts and adipocytes (Fig. 1B). The activity of CIC in mitochondrial extracts from 3T3-L1 fibroblasts and mature adipocyte cells was tested by assaying the rate of the [^{14}C]citrate/citrate exchange in reconstituted liposomes [40,41]. As shown in Fig. 1C, the uptake of radioactive L-citrate in liposomes reconstituted with mitochondrial extracts from fibroblasts was approximately 45% lower compared to liposomes reconstituted with the mitochondrial extracts from mature adipocyte cells (132 ± 14.4 versus 238 ± 25.0 nmol citrate/mg protein, respectively).

3.2. The PPARγ ligand BRL up-regulates CIC expression in 3T3-L1 fibroblasts

Since PPARγ is considered to be one of the master regulators of adipocyte differentiation, we evaluated the involvement of this nuclear receptor in the modulation of CIC expression during adipocyte differentiation. We tested the effects of BRL49653 (BRL), a synthetic and specific ligand of PPARγ, in 3T3-L1 fibroblasts (F), in pre-adipocytes (P), which are adipocytes at an early stage of differentiation, and in mature adipocytes (A). The results obtained demonstrated that BRL treatment up-regulated CIC mRNA expression in fibroblasts and to a lesser extent in pre-adipocytes, while it did not elicit any effects on mature adipocytes (Fig. 2A). As previously reported [44], the expression level of PPARγ mRNA was enhanced in BRL-treated fibroblasts and pre-adipocytes and reduced in BRL-treated mature adipocytes (Fig. 2A). Moreover, CIC protein content in fibroblasts increased 4-fold after treatment with BRL for 24 h compared to untreated fibroblasts (Fig. 2B). This up-regulation was abrogated by GW9662 (GW), an irreversible PPARγ antagonist, demonstrating a direct involvement of PPARγ (Fig. 2B). As expected, in mature adipocytes BRL treatment did not modulate CIC protein levels, while it down-regulated PPARγ protein expression, which was reversed in the presence of GW (Fig. 2C).

Finally, we investigated the effects of the PPARγ ligand BRL on CIC activity in mitochondrial extracts from fibroblasts and adipocytes. We found that the uptake of [^{14}C]citrate in BRL-treated fibroblasts was enhanced as compared to untreated cells (192 ± 21.2 versus 130 ± 15 nmol citrate/mg protein, respectively), reaching the CIC activity levels measured in mature adipocytes (235 ± 24 nmol citrate/mg protein), while BRL did not exert any effects in mature adipocytes (Fig. 2D). Taken together, these data suggest that activated PPARγ is able to induce CIC expression and increase CIC activity only in fibroblasts.

3.3. BRL transactivates CIC gene promoter in 3T3-L1 fibroblasts

The aforementioned observations prompted us to investigate whether BRL is able to modulate CIC transcriptional activity. Thus, we performed functional assays by transiently transfecting 3T3-L1

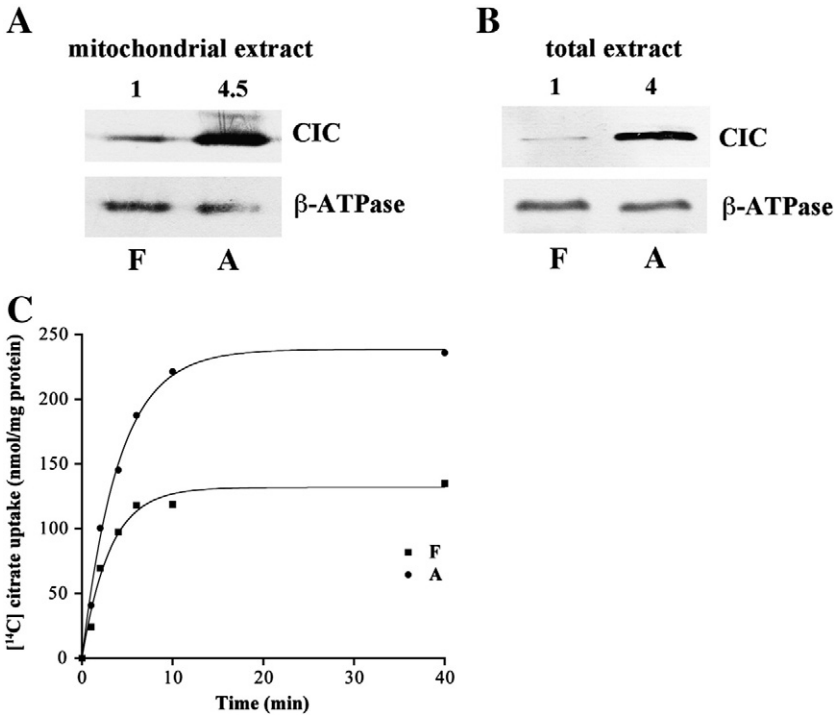

Fig. 1. CIC expression and activity in 3T3-L1 cells. Immunoblots for CIC expression from mitochondria (A) and total extracts (B) of fibroblasts (F) and mature adipocytes (A). Beta subunit of mitochondrial ATPase (β-ATPase) was used as loading control. Numbers represent the average fold change of CIC/β-ATPase levels. C: Rate of [^{14}C]citrate/citrate exchange in fibroblast and adipocyte mitochondria. Transport was initiated by adding 0.5 mM [^{14}C]citrate to proteoliposomes containing 10 mM citrate and reconstituted with mitochondria isolated from either fibroblasts (square) or mature adipocytes (circle). The transport reaction was stopped at the indicated times. The data represent means of three independent experiments.

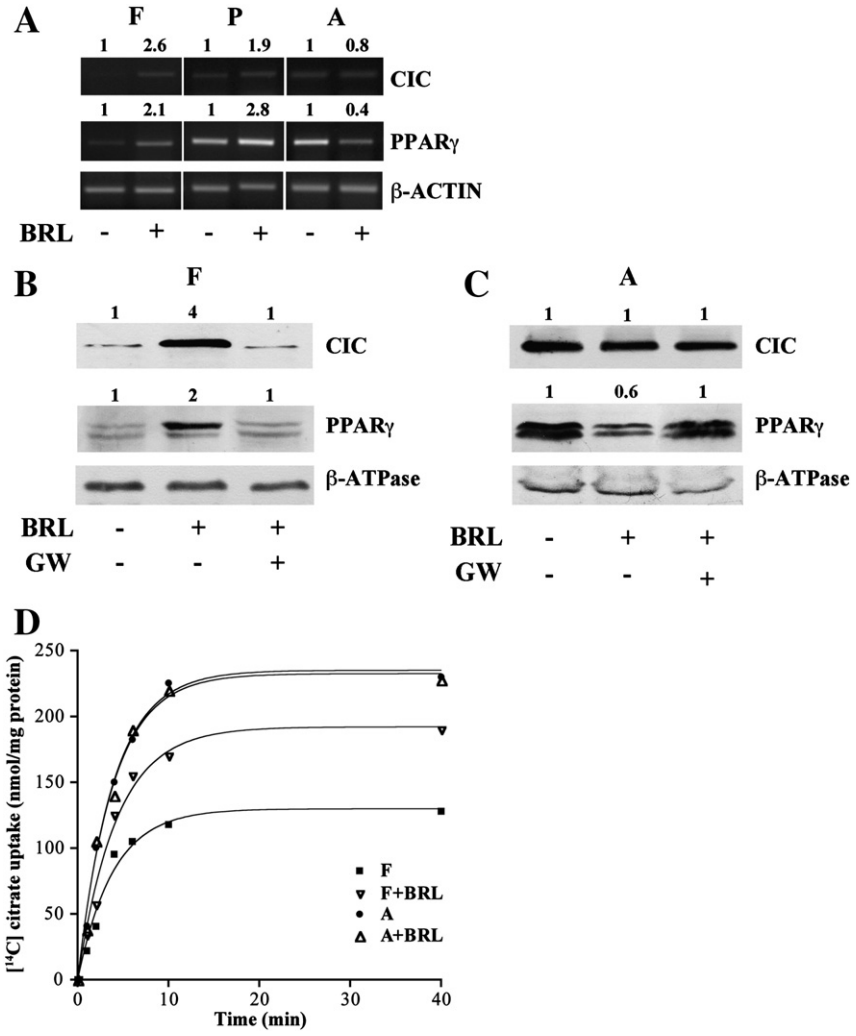

Fig. 2. Activated PPARγ up-regulates CIC expression and activity in fibroblasts. A: CIC and PPARγ mRNA expression in 3T3-L1 fibroblasts (F), preadipocytes (P) and mature adipocytes (A) untreated (−) or treated with 10 μM BRL for 24 h. β-ACTIN was used as loading control. Numbers represent the average fold change of CIC or PPARγ/β-ACTIN levels. Immunoblots for CIC and PPARγ expression from total extracts of fibroblast (B) and mature adipocyte cells (C) untreated (−) or treated with 10 μM BRL in the presence or not of 10 μM GW for 24 h. β-ATPase was used as loading control. Numbers represent the average fold change of CIC or PPARγ/β-ATPase levels. D: [^{14}C]citrate/citrate exchange in fibroblast and adipocyte mitochondria untreated or treated with BRL. Transport was initiated by adding 0.5 mM [^{14}C]citrate to proteoliposomes containing 10 mM citrate and reconstituted with mitochondria isolated from untreated fibroblasts (square), BRL-treated fibroblasts (down-pointing triangle), adipocytes (circle) and BRL-treated adipocytes (up-pointing triangle). The transport reaction was stopped at the indicated times. The data represent means of three independent experiments.

fibroblasts with a plasmid containing rat CIC regulatory sequence pCIC1473 (−1473/+35) and found that BRL significantly induced luciferase activity (Fig. 3A). This effect was no longer noticeable in the presence of GW, confirming that the transactivation of CIC by BRL occurred in a PPARγ-dependent manner (data not shown). The rat CIC promoter contains multiple responsive elements for different transcription factors, including glucocorticoid receptor (GR), estrogen receptor alpha (ERα), PPARγ and α, c/EBPα and Sp1 (Fig. 3A). To identify the region within the CIC promoter responsible for the BRL-induced transactivation, the activity of the different CIC promoter–deleted constructs pCIC284 (−284/+35), pCIC145 (−145/+35), pCIC115 (−115/+35) and pCIC82 (−82/+35) was tested. In transfection experiments performed using the aforementioned plasmids pCIC284, pCIC145 and pCIC115, responsiveness to BRL was still observed (Fig. 3A). Of note, BRL was able to transactivate all tested constructs independently of the PPRE site, which was recently identified at −625 bp [22]. In contrast, in cells transfected with the promoter–deleted construct pCIC82 we did not detect any increase in luciferase activity (Fig. 3A). Consequently, the region from −115 to −82, which contains the Sp1 motif, was the minimal region of CIC promoter responsible for BRL induction.

Thus, we performed site-directed mutagenesis on the minimal responsive Sp1 domain (pCIC115-Sp1mut) within the CIC promoter (Fig. 3A). Mutation of this domain abrogated BRL effects (Fig. 3A) demonstrating that the integrity of Sp1-binding site is necessary for PPARγ modulation of CIC promoter activity. To strengthen the importance of the Sp1 site in CIC promoter modulation by BRL, we performed transfection experiments using a construct (pCIC-3xSp1) bearing threefold repeat of wild type responsive Sp1 site located in the minimal region of CIC promoter. BRL treatment induced a 1.7 fold increase in luciferase activity respect to untreated cells (Fig. 3B).

In addition, functional experiments and RT-PCR analysis were performed using mithramycin that binds to GC boxes and prevents sequential Sp1 binding to its consensus sequence [45]. Our results showed that mithramycin was able to abrogate the BRL-induced CIC transcriptional activity as well as its mRNA expression in fibroblast cells (Fig. 3C and D).

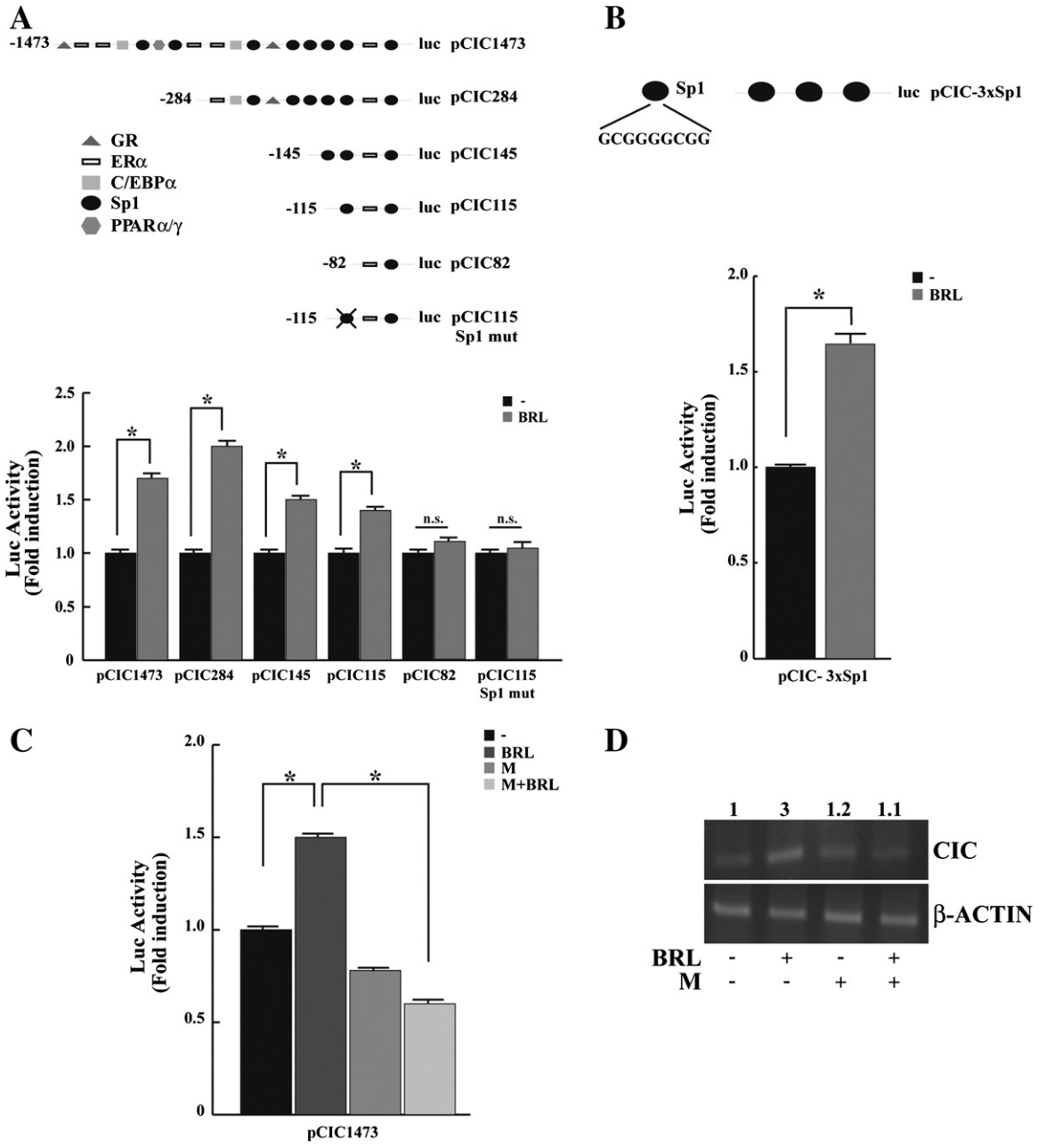

Fig. 3. BRL transactivates CIC transcriptional activity in fibroblasts. A:*Upper panel*, schematic representation of the CIC promoter constructs used in this study. *Lower panel*, 3T3-L1 fibroblasts were transiently transfected with luciferase plasmids containing the CIC promoter (pCIC1473), its deletions (pCIC284, pCIC145, pCIC115 and pCIC82) or pCIC115-Sp1mut mutated in Sp1 site and then untreated (−) or treated with 10 μM BRL for 12 h. B: *Upper panel*, schematic representation of the pCIC-3xSp1 construct used in this study. *Lower panel*, cells transiently transfected with pCIC-3xSp1were untreated (−) or treated with 10 μM BRL for 12 h. C: Cells transiently transfected with pCIC1473 were untreated (−) or treated with 10 μM BRL and/or 100 nM mithramycin (M) for 12 h. Luciferase activity of untreated cells was set as 1-fold induction, upon which treatments were calculated. Columns are the means ± S.D. of three independent experiments performed in triplicate.*P<0.05, n.s. = non significant. D: CIC mRNA expression in 3T3-L1 fibroblasts untreated (−) or treated with 10 μM BRL and/or 100 nM mithramycin (M) for 24 h. Numbers represent the average fold change of CIC/β-ACTIN levels.

3.4. BRL enhances recruitment of PPARγ and Sp1 to the CIC promoter in 3T3-L1 cells

To further support the role of the Sp1 site in mediating the BRL-induced up-regulation of CIC, we performed electrophoretic mobility shift assay (EMSA) using as a probe the Sp1 sequence present in the minimal CIC regulatory region. We observed the formation of a protein complex in nuclear extracts from fibroblast cells (Fig. 4A, lane 1), which was abrogated by a 100-fold molar excess of unlabeled probe, demonstrating the specificity of the DNA binding complex (Fig. 4A, lane 2). This inhibition was no longer observed using a mutated oligodeoxyribonucleotide as competitor (Fig. 4A, lane 3). In cells treated with BRL, we observed an increase in the specific band compared with control samples (Fig. 4A, lane 4). Of note, in the presence of anti-PPARγ and anti-Sp1 antibodies, the specific band was immunodepleted (Fig. 4A, lane 5) and supershifted (Fig. 4A, lane 6), respectively, suggesting the presence of both proteins in the complex. Non-specific IgG used as a control did not generate either an immunodepleted or a supershifted band (Fig. 4A, lane 7). The functional interaction of PPARγ and Sp1 with the CIC promoter region was further elucidated by ChIP and Re-ChIP assays (Fig. 4B). Using anti-PPARγ, anti-Sp1, or anti-RNA polymerase II (POLII) antibodies,

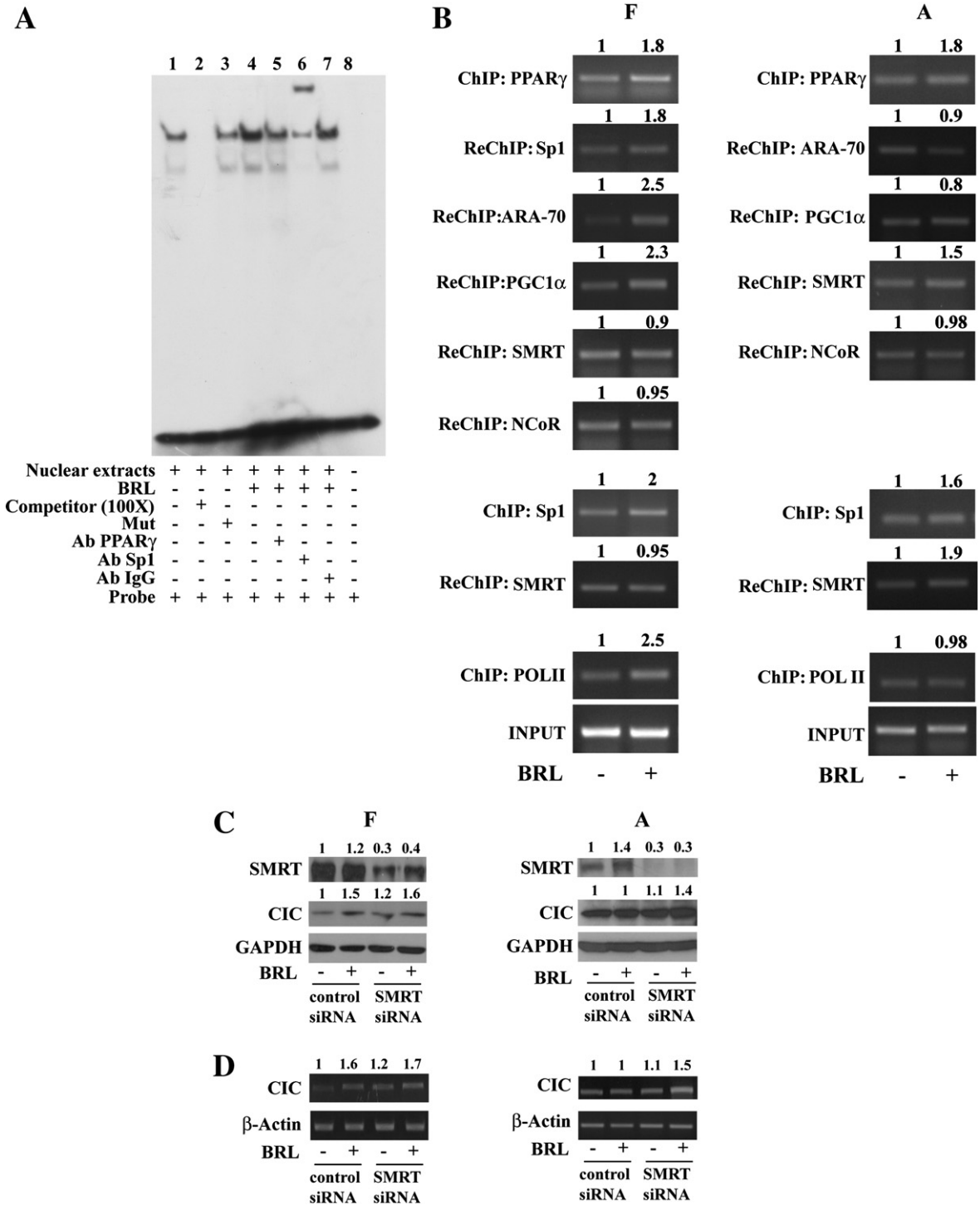

Fig. 4. PPARγ/Sp1 complex binds to the Sp1 site in the CIC promoter in 3T3-L1 cells. A: Nuclear extracts from fibroblasts (lane 1) were incubated with a double-stranded Sp1 sequence probe labeled with [^{32}P] and subjected to electrophoresis in a 6% polyacrylamide gel. Competition experiments were performed adding as competitor a 100-fold molar excess of unlabeled (lane 2) or mutated (Mut) Sp1 probe (lane 3). In lane 4, nuclear extracts from cells treated with 10 μM BRL for 6 h. Anti-PPARγ (lane 5), anti-Sp1 (lane 6) or IgG (lane 7) antibodies were incubated with nuclear extracts treated with BRL. Lane 8 contains probe alone. B: 3T3L1 fibroblasts (F) and adipocytes (A) were untreated (−) or treated with 10 μM BRL for 1 h. The soluble chromatin was immunoprecipitated with the anti-PPARγ, anti-Sp1, anti-RNA Pol II antibodies. Chromatin immunoprecipitated with the anti-PPARγ antibody was re-immunoprecipitated with the anti-Sp1, anti-ARA-70, anti-PCG1α, anti-SMRT and anti-NCoR antibodies (ReChiP). Chromatin immunoprecipitated with the anti-Sp1 antibody was re-immunoprecipitated with the anti-SMRT antibody (ReChiP). The CIC promoter sequence containing the Sp1 site was detected by PCR with specific primers (see Materials and methods). For control input DNA, the CIC promoter was amplified from 30 μl initial preparations of soluble chromatin (before immunoprecipitations). C: Immunoblots for SMRT and CIC experiments in fibroblasts (F) and adipocytes (A) transfected and untreated or treated with 10 μM BRL for 24 h as indicated. GAPDH was used as loading control. Numbers represent the average fold change of SMRT/GAPDH and CIC/GAPDH levels. D: CIC mRNA expression in fibroblasts (F) and adipocytes (A) transfected and untreated or treated with 10 μM BRL for 24 h as indicated. β-Actin was used as loading control. Numbers represent the average fold change of CIC/β-Actin levels.

protein-chromatin complexes were immunoprecipitated from fibroblasts treated for 1 h with vehicle or BRL. The PPARγ immunoprecipitated chromatin was re-immunoprecipitated with anti-Sp1 antibody. PCR was used to determine the occupancy of PPARγ, Sp1 and POLII to the CIC promoter region containing the Sp1 site. We showed that both PPARγ and Sp1 transcription factors were constitutively bound to

the CIC promoter in untreated cells and that this recruitment was increased upon BRL exposure (Fig. 4B, left panel). Similar results were also obtained by PPARγ/Sp1 Re-ChIP assay (Fig. 4B, left panel). In addition, the positive regulation of the CIC transcriptional activity induced by BRL was demonstrated by an increased recruitment of RNA POLII (Fig. 4B, left panel). Although protein–chromatin complexes from adipocytes treated with BRL showed an enhanced recruitment of PPARγ and Sp1 to the CIC regulatory region, no changes in the association of RNA POLII to the Sp1 site were detected (Fig. 4B, right panel).

To assess whether the divergent effects exerted by BRL on CIC expression during adipocyte differentiation might be caused by the cooperative interaction between PPARγ and positive (PCG1α and ARA-70) or negative (SMRT and NCoR) transcriptional regulators, we performed Re-ChIP assays in both cell lines. We found, after BRL exposure, an enhanced recruitment of PCG1α and ARA-70 coactivators in the Sp1-containing region of the CIC promoter in fibroblast cells (Fig. 4B, left panel), while an increased SMRT occupancy was observed in adipocyte cells (Fig. 4B, right panel). Finally, to better define the role of SMRT in the PPARγ-dependent modulation of the CIC mRNA and protein levels, RNA silencing technologies were used to knockdown the expression of endogenous SMRT in both fibroblast and adipocyte cells. SMRT expression was effectively silenced as revealed by immunoblot analysis after 24 h of siRNA transfection in both cell lines (Fig. 4C). As expected, silencing of the SMRT gene had no effects on the up-regulation of CIC protein content and mRNA levels (Fig. 4C and D, left panels) induced by the specific PPARγ ligand in fibroblast cells. In contrast, BRL was able to increase CIC expression in SMRT silenced adipocyte cells (Fig. 4 C and D, right panels) highlighting a crucial role of SMRT corepressor in regulating CIC activity under adipocyte differentiation.

4. Discussion

In this study, we have demonstrated that activated PPARγ modulates the expression and the activity of the mitochondrial CIC during the differentiation stages of fibroblasts into adipocytes.

PPARγ, a ligand-activated transcription factor, plays a key role in adipocyte biology by regulating their differentiation, maintenance, and lipid metabolism [46–48]. Actually, PPARγ is considered the master regulator of adipogenesis participating in the transcriptional activation of several adipogenic and lipogenic genes [49,50]. It is known that cellular fat synthesis is regulated at various steps [51,52]. Particularly, the regulation of fatty acid synthesis via CIC or dicarboxylate carriers is essential for adipocyte differentiation from the early differentiation stage of 3T3-L1 fibroblasts into mature fat cells [53].

Using the cultured 3T3-L1 cell system, we have shown that BRL up-regulated CIC expression and activity in fibroblasts through PPARγ activation, while BRL was not able to modulate CIC levels in mature adipocytes. These data contradict previous findings indicating that PPARγ ligands increased CIC expression in adipocytes [22], although the latter measurements were performed at 7 days after differentiation induction.

From our study, the specific involvement of PPARγ in up-regulating CIC expression in fibroblasts was proved by the observation that the PPARγ effect was completely abrogated in the presence of GW, a potent and selective antagonist of PPARγ. The molecular events responsible for CIC induction by the PPARγ ligand BRL were consistent with the enhanced transcriptional activation of this gene as it raised by the capability of BRL to activate CIC promoter. Multiple transcription factor binding sites within the rat and human CIC promoter have been described, including FOXA, SRE, GR, C/EBP, ER and Sp1 binding sequences. Functional studies using different CIC-promoter-deleted constructs identified the region of CIC promoter, spanning from −115/−82, as the minimal region responsible for BRL induction. Of note, this region of rat CIC promoter shows a very high degree of sequence similarity with the corresponding portion of the mouse CIC gene**s** (approximately 94% identity). Although it has been recently demonstrated that CIC expression is regulated by PPARγ ligands through a PPRE site, identified at −625 bp of the CIC promoter [22], our results showed that CIC transactivation occurs independently of the PPRE site, suggesting that other transcription factors are involved in PPARγ-mediated CIC induction. Indeed, analysis of the minimal CIC promoter region reveals the presence of a GC-box sequence, and deletion as well as mutation of this site results in the abrogation of PPARγ transactivating activity. The ability of activated PPARγ to transactivate CIC promoter through Sp1 was confirmed in functional assays using a construct carrying threefold repeat of the cognate Sp1 motif within the minimal region of CIC gene promoter. It could be clearly seen that luciferase expression was significantly increased upon BRL treatment.

Furthermore, when Sp1-DNA binding activity was blocked by a selective inhibitor, both PPARγ-mediated transactivation and induction of CIC expression were subsequently abolished. In line with our results, an interesting observation is that in the presence of the Sp1 mutation at −92 bp the basal activity of CIC promoter is reduced when compared with the transcriptional activity of the wild-type CIC promoter [20].

Sp1 has been considered traditionally as a ubiquitous factor associated closely with core promoter activities; it has recently been observed that it participates in the regulation of gene transcription triggered by multiple signaling pathways and metabolic or differentiation conditions. Moreover, Sp1 interacts physically and cooperates functionally with several sequence-specific activators including NF-kB, GATA, YY1, E2F1, Rb, SREBP-1 and PPARγ [54–59] to modulate gene expression. In addition, it has been shown that the activation of CIC gene expression by Sp1 is virtually abolished by methylation of the Sp1-binding elements which are present in the promoters of all CIC genes sequenced in mammals within the CpG island located immediately upstream the translocation start codon [19]. For the first time, our results have revealed a novel important regulatory role of Sp1 in regulating CIC promoter activity. In nuclear extracts from fibroblast cells treated with BRL, EMSA showed a strong increase in the Sp1-DNA binding that was immunodepleted by anti-Sp1 and anti-PPARγ antibodies, suggesting the presence of both proteins in the complex. In addition, ChIP and Re-ChIP assays demonstrated that PPARγ/Sp1 occupancy of the Sp1-containing promoter region induced by BRL treatment was concomitant with an increase in RNA-Pol II, addressing a positive CIC transcriptional regulation mediated by PPARγ.

It is known that members of the nuclear hormone receptor superfamily, including PPARγ, once activated, can interact physically and modulate target gene transcription. PPARγ can regulate transcription by several distinct mechanisms, and its function seems to depend not only on ligand binding, which is known to regulate receptor conformation, but also on the context of the gene and associated promoter factors that contribute to create a gene-specific topography, achieving specific profiles of gene expression. Several studies have examined the role of coregulators in adipogenesis and demonstrated that coactivators such as PGC-1α or steroid receptor coactivators (SRCs) are essential [60]; whereas NCoR, SMRT and histone deacetylases act as negative regulators of differentiation [61–63]. The physiological relevance of their implication in metabolic regulation has been demonstrated in the context of PPARγ-mediated adipogenesis, during which they promote a target-gene specific repression of PPARγ activity [64]. A negative action of SMRT and NCoR on fat storage has been suggested by the enhanced adipogenesis and increased expression of proadipogenic PPARγ target genes after RNAi-mediated inhibition of these corepressors [62].

Our results evidenced in fibroblast cells, after BRL stimulation, an enhanced recruitment of PGC-1α and ARA-70 on the Sp1 site of the CIC promoter. In contrast, we observed that mature adipocytes treated with BRL showed an increased recruitment of SMRT corepressor to the Sp1 site within the CIC promoter along with no changes in the occupancy of RNA POLII. Finally, we demonstrated a direct involvement of SMRT in the loss of CIC promoter responsiveness to the BRL in mature adipocytes using a specific SMRT siRNA.

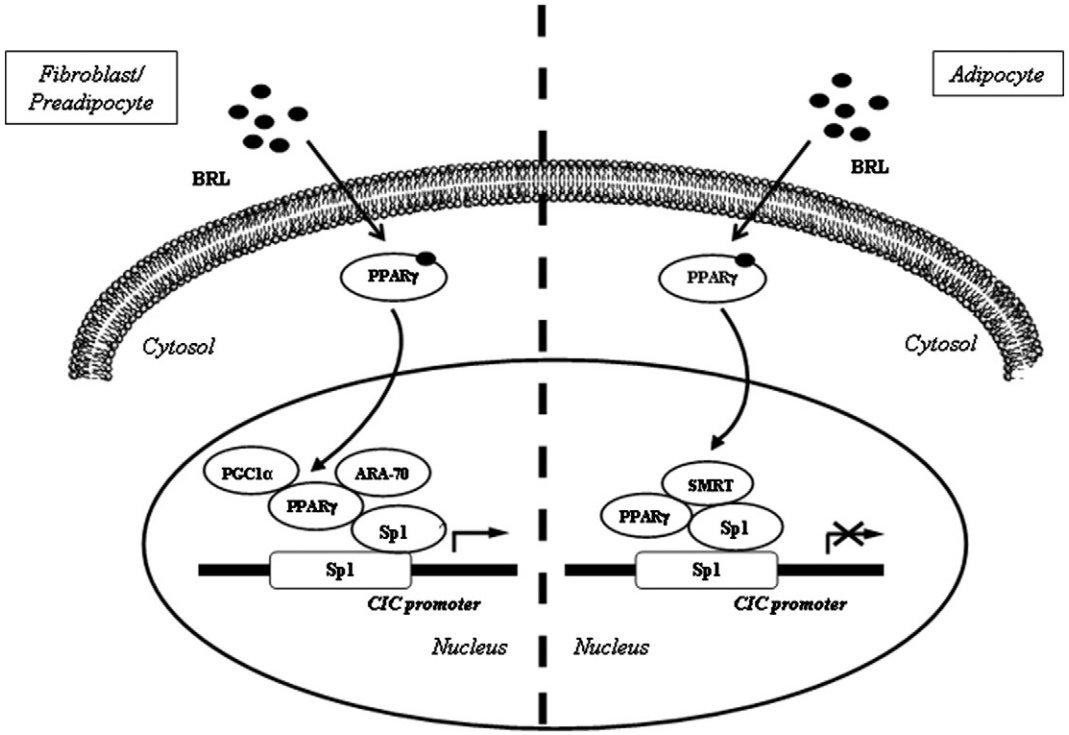

Fig. 5. Proposed working model of the PPARγ-mediated regulation of CIC expression in fibroblasts and adipocytes. In fibroblasts, upon BRL treatment, PPARγ/Sp1 complex is recruited on the Sp1-containing region of CIC promoter along with PGC1-α and ARA70 coactivators, leading to an increase in CIC expression. In adipocytes, the formation of PPARγ/Sp1 complex is associated with the recruitment of SMRT corepressor, resulting in an inhibition of CIC transcription.

In conclusion, our study identifies a novel molecular mechanism through which PPARγ modulates CIC expression, a crucial mitochondrial carrier for glucose and lipid metabolism and for energy homeostasis regulation. The divergent mechanisms through which PPARγ activation may switch the modulation of CIC expression during adipocyte differentiation are schematically shown in Fig. 5. We propose a model in which: i) in fibroblasts treated with BRL, PPARγ/Sp1 complex along with PGC1α and ARA-70 coactivators are recruited on the Sp1-containing region of the CIC promoter, thereby increasing CIC expression; ii) in adipocytes treated with BRL, PPARγ/Sp1 complex is associated with an enhanced recruitment of SMRT corepressor on the Sp1 site of CIC promoter resulting in an inhibition of CIC transcription.

References

[1] R.S. Kaplan, Structure and function of mitochondrial anion transport proteins, J. Membr. Biol. 179 (2001) 165–183.
[2] F. Palmieri, The mitochondrial transporter family SLC25: identification, properties and physiopathology, Mol. Aspects Med. (2012), http://dx.doi.org/10.1016/j.mam.2012.05.005 (in press).
[3] F. Palmieri, C.L. Pierri, A. De Grassi, A. Nunes-Nesi, A.R. Fernie, Evolution, structure and function of mitochondrial carriers: a review with new insights, Plant J. 66 (2011) 161–181.
[4] R.S. Kaplan, J.A. Mayor, D.O. Wood, The mitochondrial tricarboxylate transport protein, J. Biol. Chem. 268 (1993) 13682–13690.
[5] L. Capobianco, F. Bisaccia, A. Michel, F.S. Sluse, F. Palmieri, The N and C-termini of the tricarboxylate carrier are exposed to the cytoplasmic side of the inner mitochondrial membrane, FEBS Lett. 357 (1995) 297–300.
[6] J.W. Joseph, M.V. Jensen, O. Ilkayeva, F. Palmieri, C. Alárcon, C.J. Rhodes, C.B. Newgard, The mitochondrial citrate/isocitrate carrier plays a regulatory role in glucose-stimulated insulin secretion, J. Biol. Chem. 281 (2006) 35624–35632.
[7] V. Infantino, V. Iacobazzi, F. De Santis, M. Mastrapasqua, F. Palmieri, Transcription of the mitochondrial citrate carrier gene: role of SREBP-1, upregulation by insulin and downregulation by PUFA, Biochem. Biophys. Res. Commun. 356 (2007) 249–254.
[8] P. Morciano, C. Carrisi, L. Capobianco, L. Mannini, G. Burgio, G. Cestra, G.E. De Benedetto, D.F. Corona, A. Musio, G. Cenci, A conserved role for the mitochondrial citrate transporter Sea/SLC25A1 in the maintenance of chromosome integrity, Hum. Mol. Genet. 18 (2009) 4180–4188.
[9] V. Infantino, P. Convertini, L. Cucci, M.A. Panaro, M.A. Di Noia, R. Calvello, F. Palmieri, V. Iacobazzi, The mitochondrial citrate carrier: a new player in inflammation, Biochem. J. 438 (2011) 433–436.
[10] A.R. Cappello, C. Guido, A. Santoro, M. Santoro, L. Capobianco, D. Montanaro, M. Madeo, S. Andò, V. Dolce, S. Aquila, The mitochondrial citrate carrier (CIC) is present and regulates insulin secretion by human male gamete, Endocrinology 153 (2012) 1743–1754.
[11] V.G. Gnoni, P. Priore, J.H.M. Geelen, L. Siculella, The mitochondrial citrate carrier: metabolic role and regulation of its activity and expression, IUBMB Life 61 (2009) 987–994.
[12] F. Damiano, E. Mercuri, E. Stanca, G.V. Gnoni, L. Siculella, Streptozotocin-induced diabetes affects in rat liver citrate carrier gene expression by transcriptional and posttranscriptional mechanisms, Int. J. Biochem. Cell Biol. 43 (2011) 1621–1629.
[13] V. Iacobazzi, V. Infantino, F. Bisaccia, A. Castegna, F. Palmieri, Role of FOXA in mitochondrial citrate carrier gene expression and insulin secretion, Biochem. Biophys. Res. Commun. 385 (2009) 220–224.
[14] V. Zara, G.V. Gnoni, Effect of starvation on the activity of the mitochondrial tricarboxylate carrier, Biochim. Biophys. Acta 1239 (1995) 33–38.
[15] L. Siculella, S. Sabetta, R. di Summa, M. Leo, A.M. Giudetti, F. Palmieri, G.V. Gnoni, Starvation induced posttranscriptional control of rat liver mitochondrial citrate carrier expression, Biochem. Biophys. Res. Commun. 299 (2002) 418–423.
[16] A.M. Giudetti, S. Sabetta, R. di Summa, M. Leo, F. Damiano, L. Siculella, G.V. Gnoni, Differential effects of coconut oil- and fish oil-enriched diets on tricarboxylate carrier in rat liver mitochondria, J. Lipid Res. 44 (2003) 2135–2141.
[17] L. Siculella, S. Sabetta, F. Damiano, A.M. Giudetti, G.V. Gnoni, Different dietary fatty acids have dissimilar effects on activity and gene expression of mitochondrial tricarboxylate carrier in rat liver, FEBS Lett. 578 (2004) 280–284.
[18] L. Siculella, F. Damiano, S. Sabetta, G.V. Gnoni, n-6 PUFAs downregulate expression of the tricarboxylate carrier in rat liver by transcriptional and posttranscriptional mechanisms, J. Lipid Res. 45 (2004) 1333–1340.
[19] V. Iacobazzi, V. Infantino, F. Palmieri, Epigenetic mechanisms and Sp1 regulate mitochondrial citrate carrier gene expression, Biochem. Biophys. Res. Commun. 376 (2008) 15–20.
[20] F. Damiano, G.V. Gnoni, L. Siculella, Functional analysis of rat liver citrate carrier promoter: differential responsiveness to polyunsaturated fatty acids, Biochem. J. 417 (2009) 561–571.
[21] M.C. Rudolph, J. Monks, V. Burns, M. Phistry, R. Marians, M.R. Foote, D.E. Bauman, S.M. Anderson, M.C. Neville, Sterol regulatory element binding protein and dietary lipid regulation of fatty acid synthesis in the mammary epithelium, Am. J. Physiol. Endocrinol. Metab. 299 (2010) E918–E927.
[22] F. Damiano, G.V. Gnoni, L. Siculella, Citrate carrier promoter is target of peroxisome proliferator-activated receptor alpha and gamma in hepatocytes and adipocytes, Int. J. Biochem. Cell Biol. 44 (2012) 659–668.
[23] B. Desvergne, W. Wahli, Peroxisome proliferator-activated receptors: nuclear control of metabolism, Endocr. Rev. 20 (1999) 649–688.

[24] S.A. Kliewer, B.M. Forman, B. Blumberg, E.S. Ong, U. Borgmeyer, D.J. Mangelsdorf, K. Umesono, R.M. Evans, Differential expression and activation of a family of murine peroxisome proliferator-activated receptors, Proc. Natl. Acad. Sci. 91 (1994) 7355–7359.
[25] O. Braissant, F. Foufelle, C. Scotto, M. Dauca, W. Wahli, Differential expression of peroxisome proliferator activated receptor (PPARs): tissue distribution of PPAR-α, -β, and -γ in the adult rat, Endocrinology 137 (1996) 354–366.
[26] P. Tontonoz, E. Hu, R.A. Graves, A.I. Budavari, B.M. Spiegelman, mPPAR gamma 2: tissue-specific regulator of an adipocyte enhancer, Genes Dev. 8 (1994) 1224–1234.
[27] A. Chawla, J.J. Repa, R.M. Evans, D.J. Mangelsdorf, Nuclear receptors and lipid physiology: opening the X-files, Science 294 (2001) 1866–1870.
[28] G.A. Francis, E. Fayard, F. Picard, J. Auwerx, Nuclear receptors and the control of metabolism, Annu. Rev. Physiol. 65 (2003) 261–311.
[29] B.G. Shearer, W.J. Hoekstra, Recent advances in peroxisome proliferator-activated receptor science, Curr. Med. Chem. 10 (2003) 267–280.
[30] J.M. Way, W.W. Harrington, K.K. Brown, W.K. Gottschalk, S.S. Sundseth, T.A. Mansfield, R.K. Ramachandran, T.M. Willson, S.A. Kliewer, Comprehensive messenger ribonucleic acid profiling reveals that PPARγ activation has coordinate effects on gene expression in multiple insulin-sensitive tissues, Endocrinology 142 (2001) 1269–1277.
[31] J. Huang, S.H. Hsia, T. Imamura, I. Usui, J.M. Olefsky, Annexin II is a thiazolidinedione responsive gene involved in insulin-induced glucose transporter isoform 4 translocation in 3T3-L1 adipocytes, Endocrinology 145 (2004) 1579–1586.
[32] V. Ribon, J.H. Johnson, H.S. Camp, A.R. Saltiel, Thiazolidinediones and insulin resistance: PPARγ activation stimulates expression of the CAP gene, Proc. Natl. Acad. Sci. 95 (1998) 14751–14756.
[33] C. Grommes, G.E. Landreth, M.T. Heneka, Antineoplastic effects of peroxisome proliferator-activated receptor gamma agonists, Lancet Oncol. 5 (2004) 419–429.
[34] D. Bonofiglio, S. Aquila, S. Catalano, S. Gabriele, M. Belmonte, E. Middea, H. Qi, C. Morelli, M. Gentile, M. Maggiolini, S. Andò, Peroxisome proliferator-activated receptor-gamma activates p53 gene promoter binding to the nuclear factor-kappaB sequence in human MCF7 breast cancer cells, Mol. Endocrinol. 20 (2006) 3083–3092.
[35] D. Bonofiglio, S. Gabriele, S. Aquila, H. Qi, M. Belmonte, S. Catalano, S. Andò, Peroxisome proliferator-activated receptor gamma activates fas ligand gene promoter inducing apoptosis in human breast cancer cells, Breast Cancer Res. Treat. 113 (2009) 423–434.
[36] D. Bonofiglio, E. Cione, D. Vizza, M. Perri, A. Pingitore, H. Qi, S. Catalano, D. Rovito, G. Genchi, S. Andò, Bid as a potential target of apoptotic effects exerted by low doses of PPARγ and RXR ligands in breast cancer cells, Cell Cycle 10 (2011) 2344–2354.
[37] C. Frezza, S. Cipolat, L. Scorrano, Organelle isolation: functional mitochondria from mouse liver, muscle and cultured fibroblasts, Nat. Protoc. 2 (2007) 287–295.
[38] E.Z. Jordens, L. Palmieri, M. Huizing, L.P. van den Heuvel, R.C. Sengers, A. Dörner, W. Ruitenbeek, F.J. Trijbels, J. Valsson, G. Sigfusson, F. Palmieri, J.A. Smeitink, Adenine nucleotide translocator 1 deficiency associated with Sengers syndrome, Ann. Neurol. 52 (2002) 95–99.
[39] F. Palmieri, C. Indiveri, F. Bisaccia, V. Iacobazzi, Mitochondrial metabolite carrier proteins: purification, reconstitution, and transport studies, Methods Enzymol. 260 (1995) 349–369.
[40] F. Bisaccia, A. De Palma, F. Palmieri, Identification and purification of the tricarboxylate carrier from rat liver mitochondria, Biochim. Biophys. Acta 977 (1989) 171–176.
[41] F. Bisaccia, A. De Palma, G. Prezioso, F. Palmieri, Kinetic characterization of the reconstituted tricarboxylate carrier from rat liver mitochondria, Biochim. Biophys. Acta 1019 (1990) 250–256.
[42] D. Iacopetta, R. Lappano, A.R. Cappello, M. Madeo, E.M. De Francesco, A. Santoro, R. Curcio, L. Capobianco, V. Pezzi, M. Maggiolini, V. Dolce, SLC37A1 gene expression is up-regulated by epidermal growth factor in breast cancer cells, Breast Cancer Res. Treat. 122 (2010) 755–764.
[43] N.C. Andrews, D.V. Faller, A rapid micropreparation technique for extraction of DNA-binding proteins from limiting numbers of mammalian cells, Nucleic Acids Res. 19 (1991) 2499.
[44] T. Takamura, E. Nohara, Y. Nagai, K. Kobayashi, Stage-specific effects of a thiazolidinedione on proliferation, differentiation and PPARgamma mRNA expression in 3T3-L1 adipocytes, Eur. J. Pharmacol. 422 (2001) 23–29.
[45] S.W. Blume, R.C. Snyder, R. Ray, S. Thomas, C.A. Koller, D.M. Miller, Mithramycin inhibits Sp1 binding and selectively inhibits transcriptional activity of the dihydrofolate reductase gene in vitro and in vivo, J. Clin. Invest. 88 (1991) 1613–1621.
[46] F. Picard, J. Auwerx, PPARγ and glucose homeostasis, Annu. Rev. Nutr. 22 (2002) 167–197.
[47] J.N. Feige, L. Gelman, L. Michalik, B. Desvergne, W. Wahli, From molecular action to physiological outputs: peroxisome proliferator-activated receptors are nuclear receptors at the crossroads of key cellular functions, Prog. Lipid Res. 45 (2006) 120–159.
[48] P. Tontonoz, B.M. Spiegelman, Fat and beyond: the diverse biology of PPARγ, Annu. Rev. Biochem. 77 (2008) 289–312.
[49] W. He, Y. Barak, A. Hevener, P. Olson, D. Liao, J. Le, M. Nelson, E. Ong, J.M. Olefsky, R.M. Evans, Adipose-specific peroxisome proliferator-activated receptor γ knockout causes insulin resistance in fat and liver but not in muscle, Proc. Natl. Acad. Sci. 100 (2003) 15712–15717.
[50] J.B. Seo, H.M. Moon, W.S. Kim, Y.S. Lee, H.W. Jeong, E.J. Yoo, J. Ham, H. Kang, M. Park, K.R. Steffensen, T.M. Stulnig, J. Gustafsson, S.D. Park, J.B. Kim, Activated liver X receptors stimulate adipocyte differentiation through induction of peroxisome proliferator-activated receptor γ expression, Mol. Cell. Biol. 24 (2004) 3430–3444.
[51] R.A. Coleman, T.M. Lewin, D.M. Muoio, Physiological and nutritional regulation of enzymes of triacylglycerol synthesis, Annu. Rev. Nutr. 20 (2000) 77–103.
[52] R.W. Hanson, L. Reshef, Glyceroneogenesis revisited, Biochimie 85 (2003) 1199–1205.
[53] K. Kajimoto, H. Terada, Y. Baba, Y. Shinohara, Essential role of citrate export from mitochondria at early differentiation stage of 3T3-L1 cells for their effective differentiation into fat cells, as revealed by studies using specific inhibitors of mitochondrial di- and tricarboxylate carriers, Mol. Genet. Metab. 85 (2005) 46–53.
[54] V. Noé, C. Alemany, L.A. Chasin, C.J. Ciudad, Retinoblastoma protein associates with Sp1 and activates the hamster dihydrofolate reductase promoter, Oncogene 16 (1998) 1931–1938.
[55] H. Rotheneder, S. Geymayer, E. Haidweger, Transcription factors of the Sp1 family: interaction with E2F and regulation of the murine thymidine kinase promoter, J. Mol. Biol. 293 (1999) 1005–1015.
[56] A. Sugawara, A. Uruno, M. Kudo, Y. Ikeda, K. Sato, Y. Taniyama, S. Ito, K. Takeuchi, Transcription suppression of thromboxane receptor gene by peroxisome proliferator-activated receptor-c via an interaction with Sp1 in vascular smooth muscle cells, J. Biol. Chem. 277 (2002) 9676–9683.
[57] C.E. Flück, W.L. Miller, GATA-4 and GATA-6 modulate tissue-specific transcription of the human gene for P450c17 by direct interaction with Sp1, Mol. Endocrinol. 18 (2004) 1144–1157.
[58] B. Teferedegne, M.R. Green, Z. Guo, J.M. Boss, Mechanism of action of a distal NF-kB-dependent enhancer, Mol. Cell. Biol. 26 (2006) 5759–5770.
[59] D. Bonofiglio, H. Qi, S. Gabriele, S. Catalano, S. Aquila, M. Belmonte, S. Andò, Peroxisome proliferator-activated receptor gamma inhibits follicular and anaplastic thyroid carcinoma cells growth by upregulating p21Cip1/WAF1 gene in a Sp1-dependent manner, Endocr. Relat. Cancer 15 (2008) 545–557.
[60] J.N. Feige, J. Auwerx, Transcriptional coregulators in the control of energy homeostasis, Trends Cell Biol. 6 (2007) 292–301.
[61] F. Picard, M. Kurtev, N. Chung, A. Topark-Ngarm, T. Senawong, R. Machado De Oliveira, M. Leid, M.W. McBurney, L. Guarente, Sirt1 promotes fat mobilization in white adipocytes by repressing PPAR-gamma, Nature 429 (2004) 771–776.
[62] C. Yu, K. Markan, K.A. Temple, D. Deplewski, M.J. Brady, R.N. Cohen, The nuclear receptor corepressors NCoR and SMRT decrease peroxisome proliferator-activated receptor gamma transcriptional activity and repress 3T3-L1 adipogenesis, J. Biol. Chem. 280 (2005) 13600–13605.
[63] E. Jing, S. Gesta, C.R. Kahn, SIRT2 regulates adipocyte differentiation through FoxO1 acetylation/deacetylation, Cell Metab. 6 (2007) 105–114.
[64] H.P. Guan, T. Ishizuka, P.C. Chui, M. Lehrke, M.A. Lazar, Corepressors selectively control the transcriptional activity of PPARgamma in adipocytes, Genes Dev. 19 (2005) 453–461.

Journal of Cellular Physiology

Omega-3 PUFA Ethanolamides DHEA and EPEA Induce Autophagy Through PPARγ Activation in MCF-7 Breast Cancer Cells

DANIELA ROVITO,[1] CINZIA GIORDANO,[2] DONATELLA VIZZA,[1] PIERLUIGI PLASTINA,[3] INES BARONE,[2,4] IVAN CASABURI,[1] MARILENA LANZINO,[1] FRANCESCA DE AMICIS,[1] DIEGO SISCI,[1] LOREDANA MAURO,[4] SAVERIA AQUILA,[1] STEFANIA CATALANO,[1] DANIELA BONOFIGLIO,[1]** AND SEBASTIANO ANDÒ[2,4]*

[1]*Department of Pharmaco-Biology, University of Calabria, Arcavacata di Rende (CS), Italy*

[2]*Centro Sanitario, University of Calabria, Arcavacata di Rende (CS), Italy*

[3]*Department of Pharmaceutical Sciences, University of Calabria, Arcavacata di Rende (CS), Italy*

[4]*Cell Biology, University of Calabria, Arcavacata di Rende (CS), Italy*

The omega-3 long chain polyunsaturated fatty acids, docosahexaenoic acid (DHA), and eicosapentaenoic acid (EPA), elicit anti-proliferative effects in cancer cell lines and in animal models. Dietary DHA and EPA can be converted to their ethanolamide derivatives, docosahexaenoyl ethanolamine (DHEA), and eicosapentaenoyl ethanolamine (EPEA), respectively; however, few studies are reported on their anti-cancer activities. Here, we demonstrated that DHEA and EPEA were able to reduce cell viability in MCF-7 breast cancer cells whereas they did not elicit any effects in MCF-10A non-tumorigenic breast epithelial cells. Since DHA and EPA are ligands of Peroxisome Proliferator-Activated Receptor gamma (PPARγ), we sought to determine whether PPARγ may also mediate DHEA and EPEA actions. In MCF-7 cells, both compounds enhanced PPARγ expression, stimulated a PPAR response element-dependent transcription as confirmed by the increased expression of its target gene PTEN, resulting in the inhibition of AKT-mTOR pathways. Besides, DHEA and EPEA treatment induced phosphorylation of Bcl-2 promoting its dissociation from beclin-1 which resulted in autophagy induction. We also observed an increase of beclin-1 and microtubule-associated protein 1 light chain 3 expression along with an enhanced autophagosomes formation as revealed by mono-dansyl-cadaverine staining. Finally, we demonstrated the involvement of PPARγ in DHEA- and EPEA-induced autophagy by using siRNA technology and a selective inhibitor. In summary, our data show that the two omega-3 ethanolamides exert anti-proliferative effects by inducing autophagy in breast cancer cells highlighting their potential use as breast cancer preventive and/or therapeutic agents.

J. Cell. Physiol. 228: 1314–1322, 2013.

Breast cancer is the most frequently diagnosed cancer and the leading cause of cancer death in females worldwide, accounting for 23% of the total new cancer cases and 14% of the total cancer deaths in 2008 (Jemal et al., 2011). The development of breast cancer has been associated with genetic, environmental, hormonal, and nutritional factors. Among dietary factors, long

Daniela Rovito and Cinzia Giordano contributed equally to this work.

Daniela Bonofiglio and Sebastiano Andò Joint Senior Authors.

The authors declare they have no conflict of interest.

Contract grant sponsor: Associazione Italiana Ricerca sul Cancro (AIRC) IG 11595.
Contract grant sponsor: Reintegration AIRC/Marie Curie International Fellowship.
Contract grant sponsor: AIRC MFAG 6180.
Contract grant sponsor: MURST and Ex 60%.
Contract grant sponsor: Lilli Funaro Foundation.
Contract grant sponsor: FSE (Fondo Sociale Europeo) and Calabria Region.

*Correspondence to: Sebastiano Andò, Department of Cell Biology, University of Calabria, Arcavacata di Rende (CS), Arcavacata, Cosenza 87036, Italy. E-mail: sebastiano.ando@unical.it

**Correspondence to: Daniela Bonofiglio, Department of Pharmaco-Biology, University of Calabria, Arcavacata di Rende (CS), Arcavacata, Cosenza 87036, Italy. E-mail: daniela.bonofiglio@tin.it

Manuscript Received: 18 October 2012
Manuscript Accepted: 8 November 2012

Accepted manuscript online in Wiley Online Library (wileyonlinelibrary.com): 20 November 2012.
DOI: 10.1002/jcp.24288

chain fatty acids have been implicated in breast cancer risk, although their role in the promotion or prevention of breast cancer development and progression is not properly understood and remains still controversial.

Polyunsatured fatty acids (PUFAs), for long time solely considered of as an energy source in our bodies, have been proven to be highly active molecules. They can act as transcription factors modulating protein synthesis, as ligands in signal transduction, and as membrane components able to regulate the fluidity, permeability, and dynamics of cell membranes (Chapkin et al., 2008). Most fatty acids can be synthesized in the human body, but not all. In particular, essential fatty acids which are those required for biological processes, must be obtained from dietary sources (Williams and Burdge, 2006). The two major families of essential fatty acids are the omega-3 and omega-6 PUFAs, whose ratio in the body is believed to be of higher importance than the absolute levels of a certain fatty acid (Gleissman et al., 2010). Existing reports suggest that omega-6 essential fatty acids are tipically proinflammatory and are linked with initiation and progression of carcinogenesis (Lanson et al., 1990; Cohen, 1997; Chapkin et al., 2007; Hyde and Missailidis, 2009); whereas omega-3 essential fatty acids have broad health benefits, including anti-cancer properties (Serini et al., 2011 and references therein). Indeed, consumption of the two main omega-3 fatty acids, eicosapentaenoic acid (EPA), and docosahexaenoic acid (DHA), naturally present in fish, is associated with decreased cancer risk of the breast, prostate, colon, and kidney (Smith-Warner et al., 2006; Wolk et al., 2006; Courtney et al., 2007; Fradet et al., 2009; Thiebaut et al., 2009; West et al., 2010). Three main anti-neoplastic activities of omega-3 fatty acids have been proposed: (i) alteration of membrane fluidity and cell surface receptor function; (ii) modulation of COX activity; and (iii) increased cellular oxidative stress. Besides, in breast cancer cells DHA strongly reduces cell viability and DNA synthesis promoting cell death via apoptosis (Kang et al., 2010); while EPA has been shown to inhibit mitogen activation of AKT enhancing the growth inhibitory response to the anti-estrogen tamoxifen (DeGraffenried et al., 2003). These findings are consistent with microarray studies revealing that both fatty acids are able to modulate the expression of genes involved in the regulation of apoptosis, defense immunity, and cell growth in several breast cancer cell lines (Hammamieh et al., 2007). The anti-cancer activities exerted by EPA and DHA are also due to their ability to bind Peroxisome Proliferator-Activated Receptor gamma (PPARγ) (Gani, 2008).

PPARγ is a member of the nuclear receptor family of ligand-dependent transcription factors, which is well known for its metabolic functions (Desvergne and Wahli, 1999), but it is also involved in cell-cycle control, inflammation, atherosclerosis, apoptosis, and carcinogenesis (Rocchi and Auwerx, 1999). In the past few years, we have investigated different molecular mechanisms through which activated PPARγ induces anti-proliferative effects, cell-cycle arrest, and apoptosis in human breast cancer cells (Bonofiglio et al., 2005, 2006, 2009a).

In the present study we demonstrate, for the first time, that the two ethanolamide derivatives of DHA and EPA, Docosahexaenoylethanolamine (DHEA) and Eicosapentaenoylethanolamine (EPEA), respectively, through PPARγ activation induce cell growth inhibition triggering autophagy in breast cancer cells.

Materials and Methods

Reagents

BRL49653 (BRL) was purchased from Alexis (San Diego, CA), the irreversible PPARγ antagonist GW9662 (GW) and mithramycin (M) were purchased from Sigma–Aldrich (Milan, Italy).

Synthesis of DHEA and EPEA

N-Docosahexaenoylethanolamine (DHEA) and *N*-Eicosapentaenoylethanolamine (EPEA) were prepared from ethanolamine and their corresponding fatty acids, DHA, and EPA, respectively (Sigma–Aldrich) using an enzymatic procedure as described earlier (Plastina et al., 2009). Briefly, the method is based on a direct condensation reaction between ethanolamine and the fatty acid (molar ratio 1:1), carried out at 40°C in hexane, for 15 h, using Novozym®435 (consisting of immobilized *Candida antarctica* Lipase B) as the catalyst. Compounds were purified by column chromatography on silica gel. Authenticity of the products was verified by electrospray ionization-MS, ^{1}H NMR, ^{13}C NMR, and IR.

Cell culture

Human breast cancer MCF-7 cells were grown in Dulbecco's modified Eagle's medium-F12 plus glutamax containing 5% newborn calf serum (Invitrogen, Carlsbad, CA), and 1 mg/ml penicillin–streptomycin. MCF-10A normal breast epithelial cells were grown in Dulbecco's modified Eagle's medium-F12 plus glutamax containing 5% horse serum (Invitrogen), 1 mg/ml penicillin–streptomycin, 0.5 μg/ml hydrocortisone, and 10 μg/ml insulin. Before each experiment, cells were grown in phenol red-free media, containing 1% charcoal-stripped foetal bovine serum (cs-FBS) for 24 h and then treated as described.

Cell viability assay

Cell viability was determined with the 3-(4,5-dimethylthiazol- 2-yl)-2,5-diphenyltetrazolium (MTT) assay. MCF-7 cells (3×10^6 cells/ml) were grown in 24-well plates and exposed to treatments as indicated, in 1% cs-FBS. Hundred microliter of MTT (2 mg/ml, Sigma, Milan, Italy) were added to each well, and the plates were incubated for 2 h at 37°C followed by medium removal and solubilization in 500 μl DMSO. The absorbance was measured at a test wavelength of 570 nm in Beckman Coulter. The IC50 values were calculated using GraphPad Prism 4 (GraphPad Software, Inc., San Diego, CA) as described (Gu et al., 2012).

Anchorage-independent soft agar growth assays

Cells (50,000/well) were plated in 2 ml of 0.35% agarose with 5% cs-FBS in phenol red-free media, in a 1% agarose base in 24-well plates. Two days after plating, media containing control vehicle, or treatments was added to the top layer, and the media was replaced every 2 days. After 14 days, 200 μl of MTT was added to each well and allowed to incubate at 37°C for 4 h. Plates were then placed in 4°C overnight and colonies >50 μm diameter from triplicate assays were counted.

Data are the mean colony number of three plates and representative of two independent experiments, each performed in triplicate, analyzed for statistical significance ($P < 0.05$) using a two-tailed Student's *t*-test, performed by Graph Pad Prism 4.

Immunoblot analysis

MCF-7 cells were grown in 6 cm dishes to 70–80% confluence and exposed to treatments as indicated in 1% cs-FBS as indicated. Cells were harvested in cold phosphate-buffered saline (PBS) and resuspended in total ripa buffer containing 1% NP40, 0.5% Na-deoxycholate, 0.1% SDS, and inhibitors (0.1 mM sodium orthovanadate, 1% phenylmethylsulfonylfluoride or PMSF, 20 mg/ml aprotinin). Protein concentration was determined by Bio-Rad Protein Assay (Bio-Rad Laboratories, Hercules, CA). Equal amounts of cell extract proteins (40 μg) were resolved under denaturing conditions by electrophoresis in 8–11% polyacrylamide gels containing SDS (SDS–PAGE), and transferred to nitrocellulose membranes by electro-blotting. After blocking the transferred nitrocellulose membranes were incubated using anti-PPARγ, anti-beclin-1, anti-PTEN, anti-phospho-AKT (ser473), anti-AKT (AKTtot), anti-phospho-Bcl-2 (ser70), anti-Bcl-2, anti-GAPDH

(Santa Cruz Biotechnology, Santa Cruz, CA), anti-phospho-mTOR (Ser2448), anti-mTOR (mTORtot), anti-phospho-P38 MAPK (Thr180/Tyr182), anti-P38 (P38tot) (Cell Signaling, Denvers, MA) antibodies overnight at 4°C. Immunoblotting was performed as previously described (Bonofiglio et al., 2009b). Blots shown are representative of two or three individual experiments and the intensity of bands representing relevant proteins was measured by Scion Image laser densitometry scanning program.

Immunoprecipitation

Five hundred microgram of total proteins were incubated overnight with 1 μg of anti-beclin-1 antibody and 500 μl of HNTG (immunoprecipitation) buffer [50 mmol/L HEPES (pH 7.4), 50 mmol/L NaCl, 0.1% Triton X-100, 10% glycerol, 1 mmol/L phenylmethylsulfonyl fluoride, 10 μg/ml leupeptin, 10 μg/ml aprotinin, 2 μg/ml pepstatin]. Immunocomplexes were recovered by incubation with protein A/G-agarose. The immunoprecipitates were centrifuged, washed twice with HNTG buffer and then used for immunoblott analysis. Membranes were probed with anti-Bcl2 and anti-beclin-1 antibodies.

RT-PCR/real-time PCR

MCF7 cells were grown in 6 cm dishes to 70–80% confluence, and exposed to treatments in 1% CT-FBS as indicated. Total cellular RNA was extracted using TRIZOL reagent (Invitrogen) as suggested by the manufacturer. The RNA sample was treated with DNase I (Ambion, Austin, TX), and purity and integrity of the RNA was confirmed both spectroscopically and electrophoretically. RNA was then reversed transcribed with High Capacity cDNA Reverse Transcription Kit (Applied Biosystems, Monza, Italy). Analysis of PPARγ gene expression was performed using real-time reverse transcription PCR. cDNA was diluted 1:3 in nuclease-free water and 5 μl were analyzed in triplicates by real-time PCR in an iCycler iQ Detection System (Bio-Rad, Milan, Italy) using SYBR Green Universal PCR Master Mix with 0.1 mmol/L of each primer in a total volume of 30 μl reaction mixture following the manufacturer's recommendations. Each sample was normalized on its GAPDH mRNA content. Relative gene expression levels were normalized to the basal, untreated sample chosen as calibrator. Final results are expressed as folds of difference in gene expression relative to GAPDH mRNA and calibrator, calculated following the ΔC_t method, as follows:

Relative expression (folds) $= 2 - (\Delta C_{tsample} - \Delta C_{tcalibrator})$ where ΔC_t values of the sample and calibrator were determined by subtracting the average C_t value of the GAPDH mRNA reference gene from the average C_t value of the analyzed gene. For PPARγ and GAPDH the primers were: 5′-GAG CCC AAG TTT GAG TTT GC-3′ (PPARγ forward) and 5-CTG TGA GGA CTC AGG GTG GT-3 (PPARγ), 5′-CCC ACT CCT CCA CCT TTG AC-3′ (GAPDH forward), 5′-TGT TGC TGT AGC CAA ATT CGT-3′ (GAPDH reverse). Negative controls contained water instead of first strand cDNA.

Transient transfection assay

MCF7 cells were plated into 24-well plates with 500 ml regular growth medium the day before transfection. The medium was replaced with phenol red-free media, containing 1% cs-FBS the day of transfection, which was performed using Fugene 6 (Roche, Indianapolis, IN) reagent, as recommended by the manufacturer, with a mixture containing 0.5 μg of 3XPPRE-TK ligated to a luciferase reporter gene (PPRE) into the pGL3 vector and 20 ng of TK Renilla luciferase plasmid. After 6 h of transfection, the medium was changed and the cells were treated as described for 12 h and then lysed them in 50 μl passive lysis buffer. Firefly and Renilla luciferase activities were measured by Dual Luciferase kit (Promega, Madison, WI). The firefly luciferase data for each sample were normalized based on the transfection efficiency measured by Renilla luciferase activity and data were reported as fold induction.

RNA interference (RNAi)

Cells were plated in 6 cm dishes with regular growth medium the day before the transfection to 60–70% confluence. On the second day the medium was changed with 1% cs-FBS and cells were transfected with a stealth RNAi targeted human PPARγ mRNA sequence 5′-AGA AUA AUA AGG UGG AGA UGC AGG C-3′ (Invitrogen), or with a stealth RNAi-negative control (Invitrogen) to a final concentration of 100 nM using Lipofectamine 2000 (Invitrogen) as recommended by the manufacturer. After 5 h the transfection medium was changed with complete 1% cs-FBS in order to avoid Lipofectamine 2000 toxicity, cells were exposed to treatments as indicated and subjected to different experiments.

Immunofluorescence

MCF7 cells were seeded on glass coverslips in complete growth medium. On the second day, the medium was changed with 1% cs-FBS and cells were treated for 6 h, washed with PBS, and then fixed with 4% paraformaldehyde in PBS for 20 min at room temperature. Next, cells were permeabilized with 0.2% Triton X-100 in PBS for 5 min, blocked with 5% bovine serum albumin for 30 min, and incubated with anti-beclin-1, anti-LC3 (Santa Cruz), anti-PPARγ primary antibodies (1:100) in PBS overnight at 4°C. The day after the cells were washed three times with PBS and incubated with anti-mouse or anti-rabbit secondary antibodies conjugated with FITC (fluorescein isothiocyanate; green; 1:200) for 1 h at room temperature. 4′,6-Diamidino-2-phenylindole (DAPI; Sigma) was used for the determination of the nuclei. To check the specificity of immunolabeling the primary antibody was replaced by normal mouse serum (negative control). The images were acquired using fluorescent microscopy (Leica Microsystems, Milan, Italy, AF6000).

DNA fragmentation

DNA fragmentation was determined by gel electrophoresis. MCF-7 cells were grown in 10 cm dishes to 70% confluence and exposed to treatments as indicated. After 6 h cells were collected and washed with PBS and pelleted at 1,800 rpm for 5 min. The samples were resuspended in 0.5 ml of extraction buffer (50 mmol/L Tris–HCl, pH 8; 10 mmol/L EDTA, 0.5% SDS) for 20 min in rotation at 4°C. DNA was extracted three times with phenol–chloroform and one time with chloroform. The aqueous phase was used to precipitate nucleic acids with 0.1 volumes of 3 M sodium acetate and 2.5 volumes cold ethanol overnight at −20°C. The DNA pellet was resuspended in 15 μl of H_2O treated with RNase A for 30 min at 37°C. The absorbance of the DNA solution at 260 and 280 nm was determined by spectrophotometry. The extracted DNA (40 μg/lane) was subjected to electrophoresis on 1.5% agarose gels. The gels were stained with ethidium bromide and then photographed.

Mono-dansyl-cadaverine (MDC) staining

Mono-dansyl-cadaverine (MDC; Sigma–Aldrich; Biederbick et al., 1995) was used to visualize autophagic vacuoles. MCF-7 cells were plated six-well plates on coverslips in phenol-red DMEM-F12. Media was replaced the following day with DMEM-F12 containing 1% cs-FBS. After 12 h of treatment, cells were stained using 0.05 mM MDC in PBS at 37°C for 10 min. After incubation, cells were washed four times with PBS and immediately analyzed by fluorescence microscopy.

Statistical analysis

Data were analyzed for statistical significance ($P < 0.05$) using a two-tailed Student's *t*-test, performed by Graph Pad Prism 4. Standard deviations (SD) are shown.

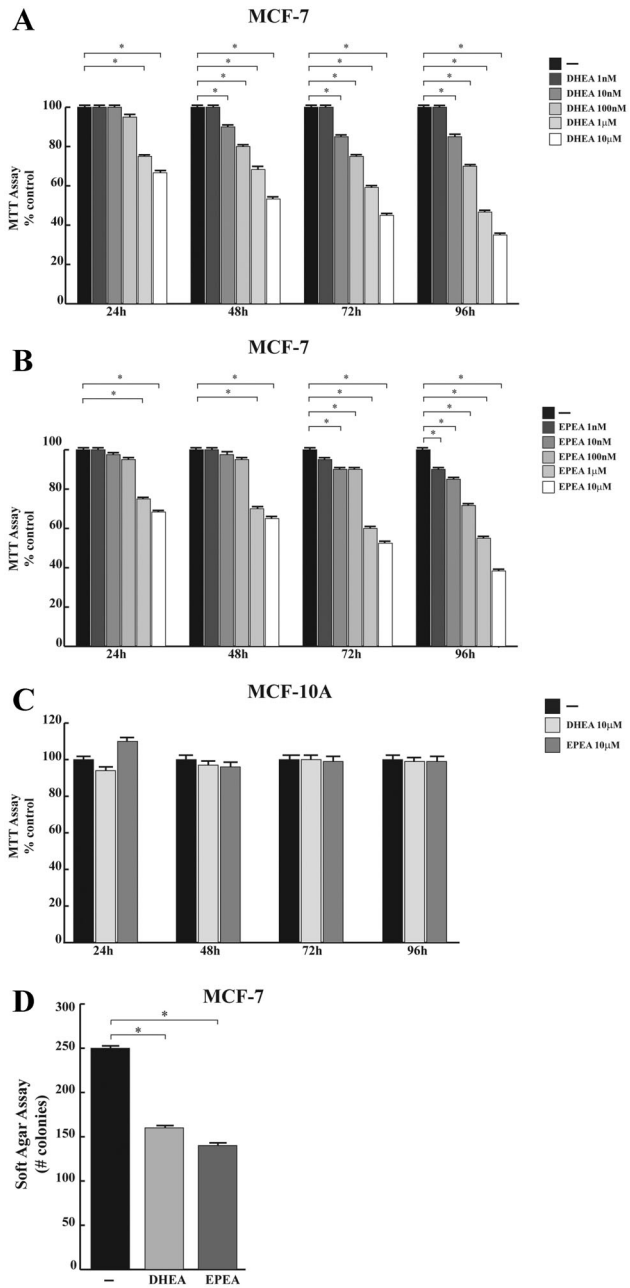

Fig. 1. Effects of DHEA and EPEA on breast cancer cell growth. MTT assays in MCF-7 cells were untreated (−) or treated with increasing concentrations (1, 10, 100 nM, 1, 10 μM) of DHEA (A) or EPEA (B) and in MCF-10A (C) treated with vehicle (−), DHEA or EPEA 10 μM as indicated. Cell proliferation is expressed as % of control (untreated cells). The values represent the means ± SD of three different experiments, each performed with triplicate samples. D: MCF-7 cells were plated in soft agar and then untreated (−) or treated with DHEA or EPEA 10 μM. Cells were allowed to grow for 14 days and the number of colonies >50 μm diameter were counted and the results were graphed. Data are the mean colony number ± SD of three plates of three independent experiments. *$P < 0.05$.

Results

Omega-3 polyunsaturated fatty acids ethanolamides DHEA and EPEA inhibit breast cancer cell growth

First, we aimed to evaluate the effects of increasing concentrations of DHEA and EPEA on proliferation of MCF-7 breast cancer cells by using MTT assays. We observed that both treatments strongly reduced cell viability in a dose- and time-dependent manner (Fig. 1A,B). In contrast, 10 μM DHEA or EPEA did not elicit any significant growth inhibitory effects on MCF-10A non-tumorigenic breast epithelial cells (Fig. 1C). The prolonged treatments up to 96 h in MCF-7 cells showed greater anti-proliferative responses, with IC50 values of 0.8 μM DHEA and 1.5 μM EPEA (Table 1). A second approach we employed was to evaluate the anti-proliferative effects induced by DHEA and EPEA using anchorage-independent soft agar growth assays. Consistently with MTT assays, both treatments at 10 μM significantly reduced colony formation in MCF-7cells (Fig. 1D).

TABLE 1. IC_{50} values of DHEA and EPEA in MCF-7 cells from MTT growth assay

Compounds	IC_{50} (μM)	95% confidence interval
DHEA	0.8	0.5–1.2
EPEA	1.5	0.9–2.5

Taken together, these results show that both compounds induced a growth inhibition in MCF-7 breast cancer cells, while no effects were observed in MCF-10A breast epithelial cells.

DHEA and EPEA transactivate PPARγ in MCF-7 cells

Starting from previous findings showing that DHA and EPA act as PPARγ activators (Gani, 2008; Martin, 2009), we investigated whether their ethanolamide derivatives DHEA and EPEA may also modulate PPARγ expression and activity in MCF-7 cells. Using real-time RT-PCR and immunoblotting analysis, we found an enhanced expression of PPARγ at both mRNA and protein levels in cells treated with 1 μM DHEA or EPEA (Fig. 2A,B). To assess the ability of both compounds to transactivate endogenous PPARγ, we transiently transfected cells with a PPAR response element (PPRE) reporter plasmid. As reported in Figure 2C, DHEA and EPEA-induced a significant enhancement in the transcriptional activation of the reporter plasmid although in a lesser extent respect to the PPARγ ligand rosiglitazone (BRL). The PPARγ antagonist GW9662 (GW) abolished the PPRE reporter activity induced by BRL and by both compounds (Fig. 2C), addressing the direct activation of PPARγ.

Previous studies have shown that PPARγ regulates the transcription of *phosphatase and tensin homolog on chromosome ten* (*PTEN*) (Patel et al., 2001), a unique phosphatase that has the ability to decrease the levels of p-AKT and consequently AKT-mediated pathways. Thus, we investigated whether DHEA and EPEA were able to modulate PTEN expression and its downstream pathway in MCF-7 cells. Our results demonstrated that both compounds enhanced PTEN protein levels which were associated with the decrease of AKT-mTOR signaling pathway (Fig. 2D), suggesting a potential involvement of either apoptotic or autophagic processes.

PPARγ mediates the up-regulation of beclin-1 expression induced by DHEA and EPEA in MCF-7 cells

Autophagy is a complicated regulatory process regulated by the activation of beclin-1, a novel Bcl-2-homology (BH)-3 domain only protein (Levine and Deretic, 2007). Thus we evaluated whether DHEA and EPEA through PPARγ are able to regulate beclin-1 expression in MCF-7 cells.

We found, after knocking down PPARγ expression (Fig. 3A,B), that the enhancement of beclin-1 dependent on DHEA and EPEA exposure was completely abrogated (Fig. 3C,D), addressing that this effect is specifically PPARγ-mediated.

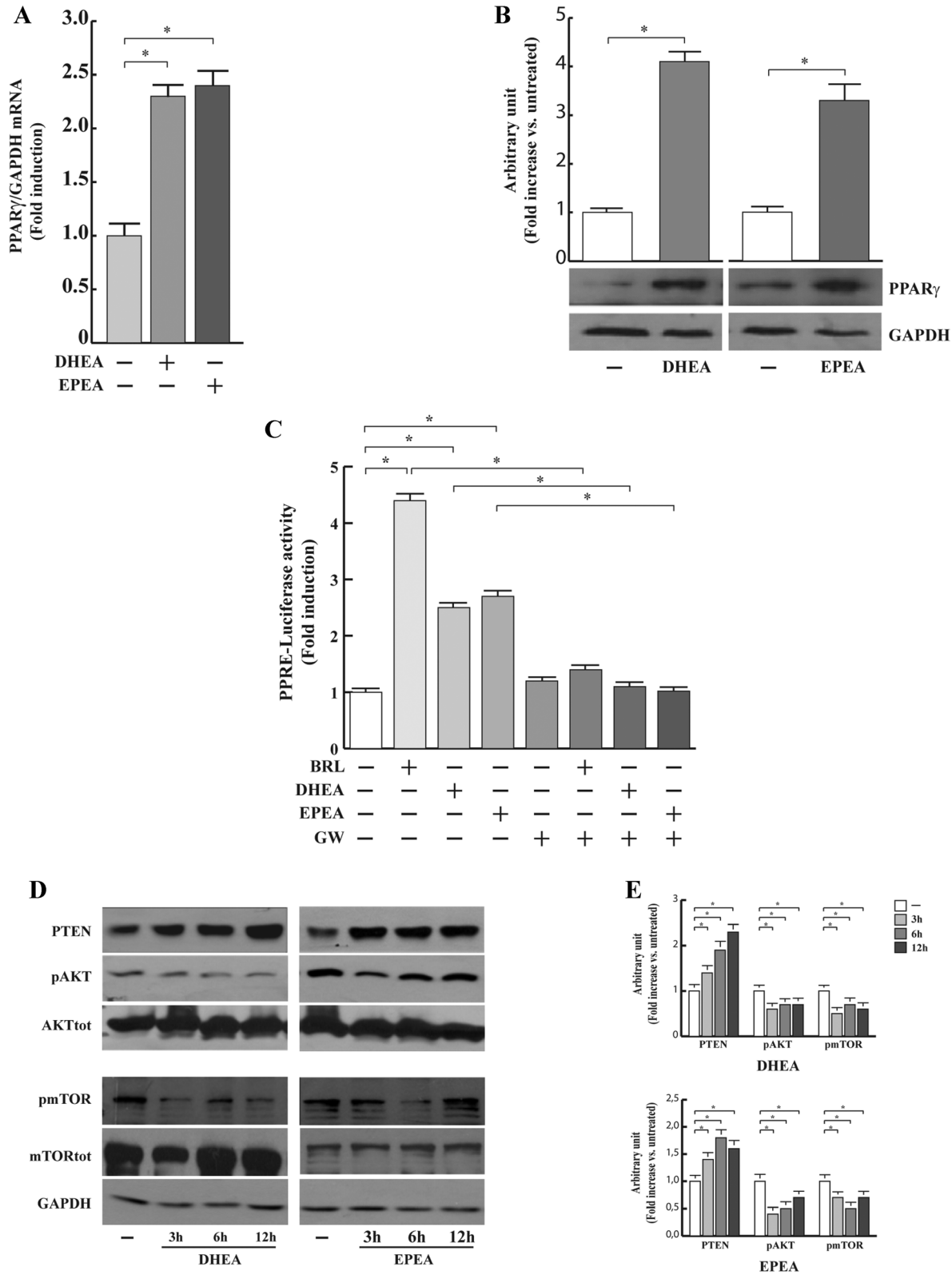

Fig. 2. Activation of PPARγ by DHEA and EPEA in MCF-7 cells. A: mRNA PPARγ content, evaluated by real-time RT-PCR, in MCF-7 cells after treatment with vehicle (−), DHEA or EPEA 1 μM for 12 h. Each sample was normalized to its GAPDH mRNA content. *$P < 0.05$. B: Immunoblots of PPARγ expression from total extracts of MCF-7 cells treated as in A for 24 h. GAPDH was used as loading control. The histograms represent the means ± SD of three separate experiments in which band intensities were evaluated in terms of optical density arbitrary units and expressed as fold change versus untreated (−) cells normalized for GAPDH levels. *$P < 0.05$. C: MCF-7 cells were transiently transfected with a PPARγ-response element (PPRE) reporter plasmid and untreated (−) or treated for 24 h with BRL 10 μM, DHEA 1 μM, EPEA 1 μM, and/or GW9662 (GW) 10 μM and then luciferase activity was measured. Results represent the mean ± SD of three different experiments each performed in triplicate. *$P < 0.05$. D: Cells were untreated (−) or treated with DHEA or EPEA 1 μM as indicated. Equal amounts of total cellular extracts were analyzed for PTEN, phosphorylated AKT (pAKT) and mTOR (pmTOR), total AKT (AKTtot) and total mTOR (mTORtot) levels by western blotting. GAPDH was used as loading control. E: The histograms represent the means ± SD of three separate experiments in which band intensities were evaluated in terms of optical density arbitrary units and expressed as fold change between phospho-, total, and GAPDH levels.

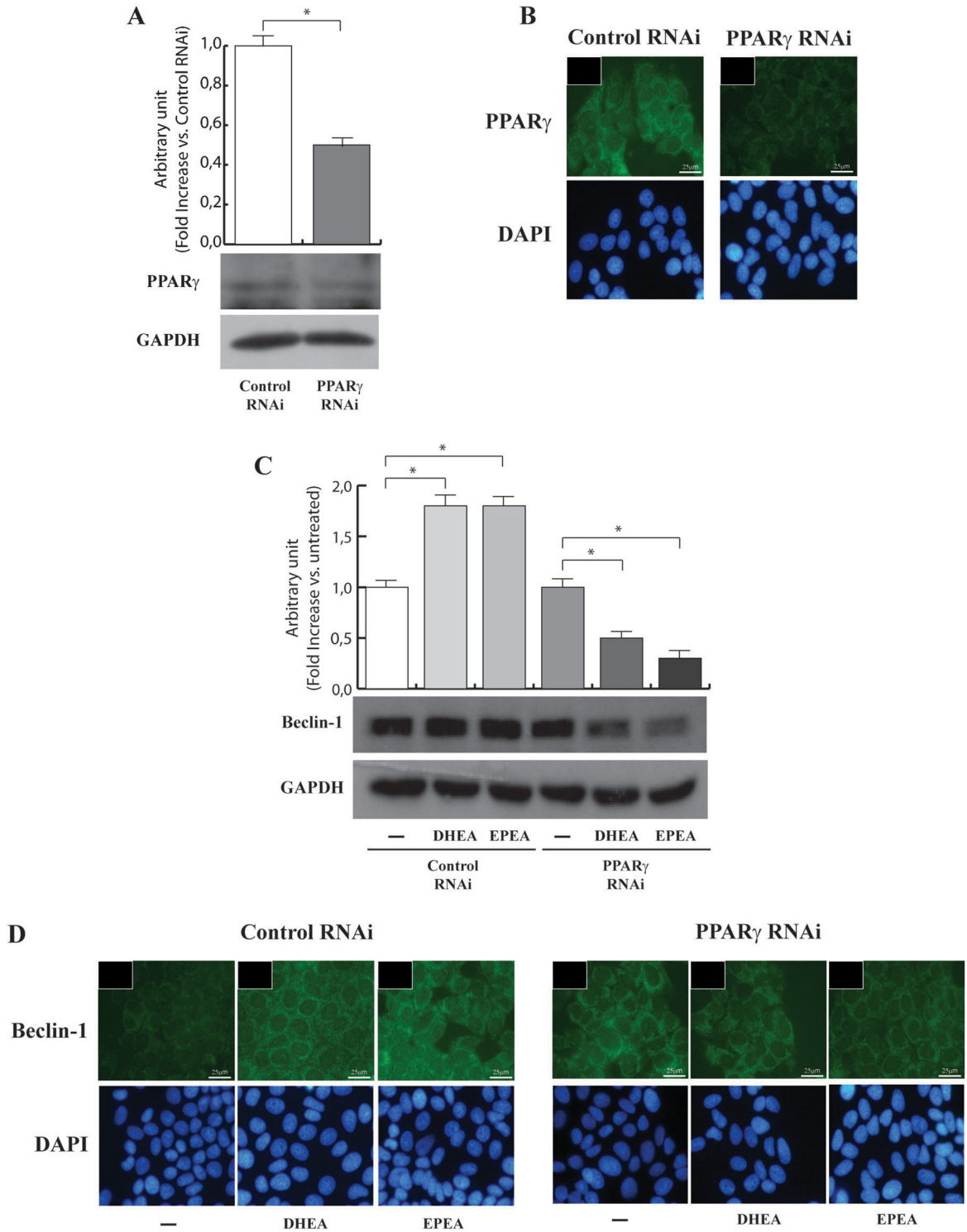

Fig. 3. PPARγ-mediated up-regulation of beclin-1 protein expression by DHEA and EPEA in MCF-7 cells. A: PPARγ expression in cells transfected with control RNA interference (RNAi) or with PPARγ RNAi as reported in Materials and Methods Section. GAPDH was used as loading control. The histograms represent the means ± SD of three separate experiments in which band intensities were evaluated in terms of optical density arbitrary units and expressed as fold change versus untreated cells (—) normalized for GAPDH levels. *$P < 0.05$. B: Immunofluorescence of PPARγ and DAPI in cells transfected as in A. Small squares, negative controls. C: Immunoblots of beclin-1 protein expression in MCF-7 cells transfected with control RNA interference (RNAi) or with PPARγ RNAi as reported in Materials and Methods Section and untreated (—) or treated with DHEA or EPEA 1 μM for 6 h. GAPDH was used as loading control. The histograms represent the means ± SD of three separate experiments in which band intensities were evaluated in terms of optical density arbitrary units and expressed as fold change versus untreated cells (—) normalized for GAPDH levels. *$P < 0.05$. D: Immunofluorescence of beclin-1 (upper parts) and DAPI (lower parts) in cells transfected and treated as in A. Small squares, negative controls.

DHEA and EPEA reduce the interaction between beclin-1 and Bcl-2 and induce autophagy in MCF-7 cells

It has been reported that beclin-1 physically interacts with the anti-apoptotic protein Bcl-2 inhibiting autophagy (Pattingre et al., 2005) and that once Bcl-2 is phosphorylated it dissociates from beclin-1 and autophagy can occur (Wei et al., 2008). Thus, we performed coimmunoprecipitation assay in order to evaluate the effects of DHEA and EPEA on beclin-1/Bcl-2 complex formation. As shown in Figure 4A, beclin-1 was constitutively associated with Bcl-2 and treatment with both

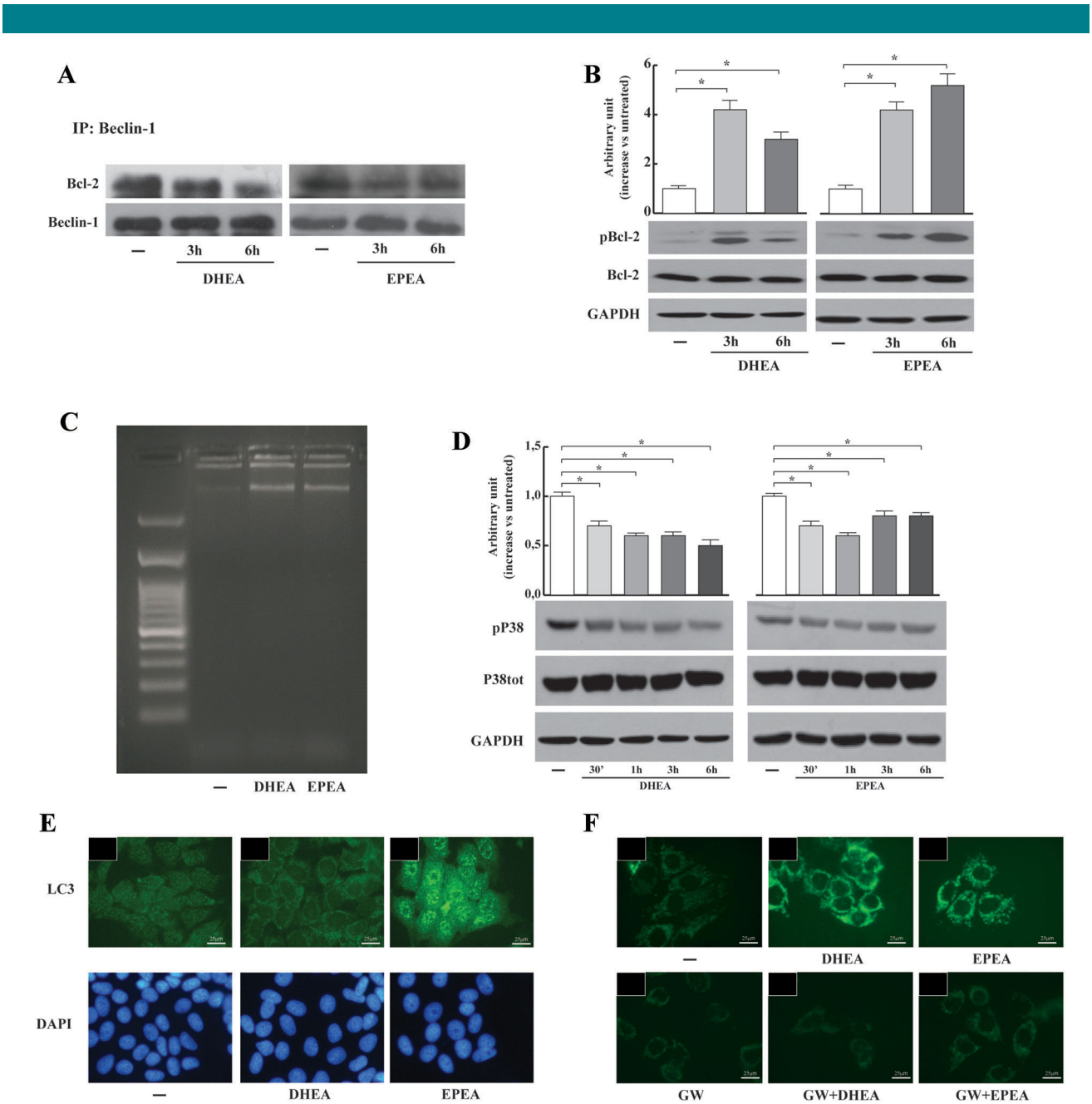

Fig. 4. DHEA and EPEA reduce beclin-1/Bcl-2 complex and trigger autophagy in MCF-7 cells. A: Protein extracts from MCF-7 cells untreated (−) or treated with DHEA or EPEA 1 μM as indicated, were immunoprecipitated with an anti-serum against beclin-1 and then blotted with anti-Bcl-2 and anti-beclin-1 antibodies. B: Cells were untreated (−) or treated with DHEA or EPEA 1 μM as indicated. Equal amounts of total cellular extracts were analyzed for phosphorylated Bcl-2 (pBcl-2) and total Bcl-2 (Bcl-2) levels by western blotting. GAPDH was used as loading control. The histograms represent the means ± SD of three separate experiments in which band intensities were evaluated in terms of optical density arbitrary units and expressed as fold change between phospho-, total, and GAPDH levels. *$P < 0.05$. C: DNA laddering was performed in MCF-7 cells untreated (−) or treated with DHEA or EPEA 1 μM for 12 h. One of three similar experiments is presented. D: Cells were untreated (−) or treated with DHEA or EPEA 1 μM as indicated. Equal amounts of total cellular extracts were analyzed for phosphorylated P38 (pP38) and total P38 (P38tot) levels by western blotting. GAPDH was used as loading control. The histograms represent the means ± SD of three separate experiments in which band intensities were evaluated in terms of optical density arbitrary units and expressed as fold change between phospho-, total, and GAPDH levels. *$P < 0.05$. E: Immunofluorescence of microtubule-associated protein 1 light-chain 3 (LC3) (upper parts) and DAPI (lower parts) in cells untreated (−) or treated with DHEA or EPEA 1 μM for 6 h. Small squares, negative controls. F: Mono-dansyl-cadaverine staining of MCF-7 cells untreated (−) or treated with DHEA 1 μM, EPEA 1 μM, and/or GW9662 (GW) 10 μM for 12 h. One of three similar experiments is presented.

compounds reduced this association. In the same experimental conditions, we observed an increased Bcl-2 phosphorylation of serine70 (Fig. 4B).

To ascertain if the treatment with DHEA or EPEA may trigger apoptotic cell death in our cell system, we evaluated changes in the internucleosomal fragmentation profile of genomic DNA, which is a diagnostic hallmark of cells undergoing apoptosis. DNA laddering revealed, after exposure to DHEA and EPEA, the absence of DNA fragmentation (Fig. 4C).

Moreover, we analyzed the phosphorylation levels of p38, which negatively regulates autophagy (Comes et al., 2007; Chiacchiera and Simone, 2008), along with the expression of microtubule-associated protein 1 light-chain 3 (LC3) a specific membrane marker for the detection of early autophagosome formation in cells treated with both compounds. As shown in Figure 4D, upon DHEA or EPEA administration a reduction in the phosphorylation state of p38 associated with a significant increase in LC3 immunofluorescence could be observed in MCF-7 cells (Fig. 4E). Moreover, cells treated with DHEA or EPEA exhibited normal nuclei and did not display typical apoptotic changes with chromatin condensation and nuclear fragmentation, as evidenced by DAPI staining (Fig. 4E).

Next, in order to corroborate the autophagic process induced by DHEA or EPEA in MCF-7 cells, mono-dansyl-cadaverine (MDC) staining was performed. As expected, the formation of autophagosomes was clearly enhanced in treated-cells (Fig. 4F). The involvement of PPARγ in DHEA- and EPEA-induced autophagy was evidenced by the ability of the PPARγ antagonist GW to prevent the accumulation of MDC-labeled vacuoles (Fig. 4F).

All these data indicate that DHEA and EPEA treatments induce cell death by autophagy in a PPARγ-dependent manner in MCF-7 cells.

Combined treatment of BRL and DHEA or EPEA reduce cell death in MCF-7 cells

Having demonstrated the crucial role played by PPARγ in the growth inhibition triggered by omega-3 ethanolamides in MCF-7 cells, we evaluated the effects of the PPARγ ligand BRL in combination with DHEA or EPEA on breast cancer cell proliferation using anchorage-independent soft agar growth assays. Our results showed that the DHEA- and EPEA-reduced cell growth was potentiated in the presence of BRL, and prevented using the PPARγ-antagonist GW, further supporting a direct involvement of this nuclear receptor (Fig. 5).

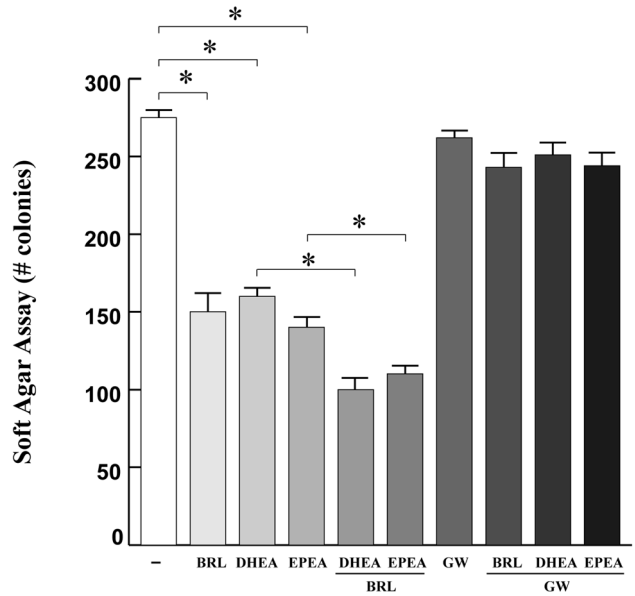

Fig. 5. Effects of combined treatment of BRL and DHEA or EPEA on MCF-7 cell growth. Cells were plated in soft agar and then untreated (–) or treated with BRL 10 μM, DHEA 10 μM, EPEA 10 μM, and/or GW9662 (GW) 10 μM. Cells were allowed to grow for 14 days and the number of colonies >50 μm diameter were counted and the results were graphed. Data are the mean colony number ± SD of three plates of three independent experiments. *$P < 0.05$.

Discussion

Diet and particularly dietary lipids have long been studied in association with breast cancer risk, survival, and recurrence (Glade, 1999; Rock and Demark-Wahnefried, 2002; Bougnoux et al., 2010). Increasing dietary consumption of the long chain n-3 PUFA, DHA, and EPA have been demonstrated to inhibit breast carcinogenesis by decreasing cell viability, proliferation, invasion, and increasing chemosensitivity (Evans and Hardy, 2010). In breast cancer cells DHA and EPA can be directly converted to *N*-acylethanolamines, DHEA, and EPEA, respectively (Brown et al., 2011); however, to date their biological activities remain unexplored.

Herein, we have shown, for the first time, that DHEA or EPEA treatment inhibits anchorage-dependent and -independent cell growth in MCF-7 breast cancer cells through PPARγ activation, whereas it does not affect growth of non-tumorigenic breast epithelial cells. In agreement with our findings, it has been demonstrated that n-3 PUFAs and their derivatives act as natural ligands of PPARγ which mediates their effects on cell function (Wolfrum et al., 2001; Tan et al., 2002; Hihi et al., 2002; Allred et al., 2008). Our results evidenced that both compounds are able to activate the endogenous PPARγ, up-regulate its mRNA and protein levels and enhance the expression of PTEN, a PPARγ target gene (Patel et al., 2001).

PTEN's protein is a unique phosphatase that has the ability to dephosphorylate both proteins and lipids (Waite and Eng, 2002). Active PTEN leads to a decrease in the levels of p-AKT and, as a consequence, in AKT-mediated proliferation pathways. Particularly, by suppressing the phosphoinositide 3-kinase (PI3K)-AKT-mammalian target of rapamycin (mTOR) pathway, PTEN governs a plethora of cellular processes including survival, proliferation, energy metabolism, and cellular architecture. We found that the increased PTEN protein levels induced by DHEA and EPEA was associated with the suppression of AKT-mTOR signaling pathway in MCF-7 cells. As a central element of the transduction signaling involved in cell growth, mTOR when inhibited, induces autophagy. Moreover, as a critical feedback mechanism, reactivation of mTOR terminates autophagy and initiates lysosome reformation (Yu et al., 2010).

Autophagy is an essential process that consists of selective degradation of cellular components. The initial step of autophagy is regulated not only by class I PI3Ks but also by activation of class III PI3K in a complex with autophagy-associated protein beclin-1 (Levine and Deretic, 2007). Beclin-1 was originally discovered in a yeast two-hybrid screen as a Bcl-2-interacting protein and was the first human protein shown to be indispensable for autophagy (Liang et al., 1999).

We found that DHEA and EPEA exposure enhanced beclin-1 protein levels and induced phosphorylation of Bcl-2 on ser70 promoting its dissociation from beclin-1. Conflicting data are reported on the role of phosphorylated Bcl-2. It has been suggested that the phosphorylation of ser70 inactivates the anti-apoptotic function of Bcl-2 (Yamamoto et al., 1999), while other studies reported that phosphorylation of ser70 Bcl-2 site

would enhance its anti-apoptotic functions (Ito et al., 1997). In our experimental model, DHEA and EPEA treatments did not induce any changes in the internucleosomal fragmentation profile of genomic DNA, which is a diagnostic hallmark of cells undergoing apoptosis, suggesting that the DHEA- or EPEA-induced growth inhibition does not occur through an apoptotic process, but may involve autophagic pathway.

It is well known that autophagy is characterized by multiple steps which lead to final event of the autophagolysosome formation. In this biological process, we demonstrated the involvement of proteins with a pivotal role in the autophagic cell death, such as beclin-1, as mentioned above, which participates in the formation of autophagosomes and LC-3 protein, which is a specific membrane marker for the detection of early autophagosome formation. Concomitantly, as emerged by MDC fluorescence, we observed a marked increase of autophagic vacuoles formation. Notably, our results clearly demonstrated a direct involvement of PPARγ in DHEA- and EPEA-induced autophagy in MCF-7 breast cancer cells using a specific PPARγ RNAi and a selective inhibitor, providing a distinct role of PPARγ in inhibiting tumorigenesis. Moreover, the PPARγ ligand BRL strongly potentiates the growth inhibition exerted by DHEA and EPEA giving emphasis to the potential of their combined treatment in breast cancer.

In conclusion, the present findings demonstrated that treatment with DHEA or EPEA, switching into the autophagic cell death, is effective in inhibiting the growth of MCF-7 breast cancer cell line. Understanding the mechanism of action of dietary components having preventive and therapeutic effects on cancer is one of the main challenges for modern science. Our data emphasize the importance of the two omega-3 polyunsaturated fatty acid ethanolamides DHEA and EPEA as new pharmacological tools to be perspectively implemented in the adjuvant therapy for breast cancer treatment.

Acknowledgments

We are grateful to Dr. R. Evans (The Salk Institute, San Diego, CA) for providing tk-PPREx3-luc.

Literature Cited

Allred CD, Talbert DR, Southard RC, Wang X, Kilgore MW. 2008. PPARgamma1 as a molecular target of eicosapentaenoic acid in human colon cancer (HT-29) cells. J Nutr 138:250–256.

Biederbick A, Kern HF, Elsässer HP. 1995. Monodansylcadaverine (MDC) is a specific in vivo marker for autophagic vacuoles. Eur J Cell Biol 66:3–14.

Bonofiglio D, Gabriele S, Aquila S, Catalano S, Gentile M, Middea E, Giordano F, Andò S. 2005. Estrogen receptor alpha binds to peroxisome proliferator-activated receptor (PPAR) response element and negatively interferes with PPARgamma signalling in breast cancer cells. Clin Cancer Res 11:6139–6147.

Bonofiglio D, Aquila S, Catalano S, Gabriele S, Belmonte M, Middea E, Qi H, Morelli C, Gentile M, Maggiolini M, Andò S. 2006. Peroxisome proliferator-activated receptoractivates p53 gene promoter binding to the nuclear factor-kappa B sequence in human MCF7 breast cancer cells. Mol Endocrinol 20:3083–3092.

Bonofiglio D, Gabriele S, Aquila S, Qi H, Belmonte M, Catalano S, Andò S. 2009a. Peroxisome proliferator-activated receptoractivates fas ligand gene promoter inducing apoptosis in human breast cancer cells. Breast Cancer Res Treat 113:423–434.

Bonofiglio D, Cione E, Qi H, Pingitore A, Perri M, Catalano S, Vizza D, Panno ML, Genchi G, Fuqua SA, Andò S. 2009b. Combined low doses of PPARgamma and RXR ligands trigger an intrinsic apoptotic pathway in human breast cancer cells. Am J Pathol 175:1270–1280.

Bougnoux P, Hajjaji N, Maheo K, Couet C, Chevalier S. 2010. Fatty acids and breast cancer: Sensitization to treatments and prevention of metastatic re-growth. Prog Lipid Res 49:76–86.

Brown I, Wahle KW, Cascio MG, Smoum-Jaouni R, Mechoulam R, Pertwee RG, Heys SD. 2011. Omega-3 N-acylethanolamines are endogenously synthesised from omega-3 fatty acids in different human prostate and breast cancer cell lines. Prostaglandins Leukot Essent Fatty Acids 85:305–310.

Chapkin RS, McMurray DN, Lupton JR. 2007. Colon cancer, fatty acids and anti-inflammatory compounds. Curr Opin Gastroenterol 23:48–54.

Chapkin RS, McMurray DN, Davidson LA, Patil BS, Fan YY, Lupton JR. 2008. Bioactive dietary long-chain fatty acids: Emerging mechanisms of action. Br J Nutr 100:1152–1157.

Chiacchiera F, Simone C. 2008. Signal-dependent regulation of gene expression as a target for cancer treatment: Inhibiting p38alpha in colorectal tumors. Cancer Lett 265:16–26.

Cohen LA. 1997. Breast cancer risk in rats fed a diet high in n–6 polyunsaturated fatty acids during pregnancy. J Natl Cancer Inst 89:662–663.

Comes F, Matrone A, Lastella P, Nico B, Susca FC, Bagnulo R, Ingravallo G, Modica S, Lo Sasso G, Moschetta A, Guanti G, Simone C. 2007. A novel cell type-specific role of p38alpha in the control of autophagy and cell death in colorectal cancer cells. Cell Death Differ 14:693–702.

Courtney ED, Matthews S, Finlayson C, Di Pierro D, Belluzzi A, Roda E, Kang JY, Leicester RJ. 2007. Eicosapentaenoic acid (EPA) reduces crypt cell proliferation and increases apoptosis in normal colonic mucosa in subjects with a history of colorectal adenomas. Int J Colorectal Dis 22:765–776.

DeGraffenried LA, Friedrichs WE, Fulcher L, Fernandes G, Silva JM, Peralba JM, Hidalgo M. 2003. Eicosapentaenoic acid restores tamoxifen sensitivity in breast cancer cells with high Akt activity. Ann Oncol 14:1051–1056.

Desvergne B, Wahli W. 1999. Peroxisome proliferator-activated receptors: Nuclear control of metabolism. Endocr Rev 20:649–688.

Evans LM, Hardy RW. 2010. Optimizing dietary fat to reduce breast cancer risk: Are we there yet? Open Breast Cancer J 2:108–122.

Fradet V, Cheng I, Casey G, Witte JS. 2009. Dietary omega-3 fatty acids, cyclooxygenase-2 genetic variation, and aggressive prostate cancer risk. Clin Cancer Res 15:2559–2566.

Gani OA. 2008. Are fish oil omega-3 long-chain fatty acids and their derivatives peroxisome proliferator-activated receptor agonists? Cardiovasc Diabetol 20:1–6.

Glade MJ. 1999. Food, nutrition, and the prevention of cancer: A global perspective. American Institute for Cancer Research/World Cancer Research Fund, American Institute for Cancer Research, 1997. Nutrition 15:523–526.

Gleissman H, Johnsen JI, Kogner P. 2010. Omega-3 fatty acids in cancer, the protectors of good and the killers of evil? Exp Cell Res 316:1365–1373.

Gu G, Barone I, Gelsomino L, Giordano C, Bonofiglio D, Statti G, Menichini F, Catalano S, Andò S. 2012. Oldenlandia diffusa extracts exert antiproliferative and apoptotic effects on human breast cancer cells through ERα/Sp1-mediated p53 activation. J Cell Physiol 227:3363–3372.

Hammamieh R, Chakraborty N, Miller SA, Waddy E, Barmada M, Das R, Peel SA, Day AA, Jett M. 2007. Differential effects of omega-3 and omega-6 fatty acids on gene expression in breast cancer cells. Breast Cancer Res Treat 101:7–16.

Hihi AK, Michalik L, Wahli W. 2002. PPARs: Transcriptional effectors of fatty acids and their derivatives. Cell Mol Life Sci 59:790–798.

Hyde CA, Missailidis S. 2009. Inhibition of arachidonic acid metabolism and its implication on cell proliferation and tumour-angiogenesis. Int Immunopharmacol 9:701–715.

Ito T, Deng X, Carr B, May WS. 1997. Bcl-2 phosphorylation required for anti-apoptosis function. J Biol Chem 272:11671–11673.

Jemal A, Bray F, Center MM, Ferlay J, Ward E, Forman D. 2011. Global cancer statistics. CA Cancer J Clin 61:69–90.

Kang KS, Wang P, Yamabe N, Fukui M, Jay T, Zhu BT. 2010. Docosahexaenoic acid induces apoptosis in MCF-7 cells in vitro and in vivo via reactive oxygen species formation and caspase 8 activation. PLoS ONE 5:e10296.

Lanson M, Bougnoux P, Besson P, Lansac J, Hubert B, Couet C, Le Floch O. 1990. N–6 polyunsaturated fatty acids in human breast carcinoma phosphatidylethanolamine and early relapse. Br J Cancer 61:776–778.

Levine B, Deretic V. 2007. Unveiling the roles of autophagy in innate and adaptive immunity. Nat Rev Immunol 7:767–777.

Liang XH, Jackson S, Seaman M, Brown K, Kempkes B, Hibshoosh H, Levine B. 1999. Induction of autophagy and inhibition of tumorigenesis by beclin 1. Nature 402:672–676.

Martin H. 2009. Role of PPAR-gamma in inflammation. Prospects for therapeutic intervention by food components. Mutat Res 669:1–7.

Patel L, Pass I, Coxon P, Downes CP, Smith SA, Macphee CH. 2001. Tumor suppressor and anti-inflammatory actions of PPARgamma agonist are mediated via up-regulation of PTEN. Curr Biol 11:764–768.

Pattingre S, Tassa A, Qu X, Garuti R, Liang XH, Mizushima N, Packer M, Schneider MD, Levine B. 2005. Bcl-2 antiapoptotic proteins inhibit Beclin 1-dependent autophagy. Cell 122:927–939.

Plastina P, Meijerink J, Vincken JP, Gruppen H, Witkamp R, Gabriele B. 2009. Selective synthesis of unsaturated *N*-acylethanolamines by lipase-catalyzed *N*-acylation of ethanolamine with unsaturated fatty acids. Lett Org Chem 6:444–447.

Rocchi S, Auwerx J. 1999. Peroxisome proliferator-activated receptor-gamma: A versatile metabolic regulator. Ann Med 31:342–351.

Rock CL, Demark-Wahnefried W. 2002. Nutrition and survival after the diagnosis of breast cancer: A review of the evidence. J Clin Oncol 20:3302–3316.

Serini S, Fasano E, Piccioni E, Cittadini AR, Calviello G. 2011. Dietary n−3 polyunsaturated fatty acids and the paradox of their health benefits and potential harmful effects. Chem Res Toxicol 24:2093–2105.

Smith-Warner SA, Spiegelman D, Ritz J, Albanes D, Beeson WL, Bernstein L, Berrino F, van den Brandt PA, Buring JE, Cho E, Colditz GA, Folsom AR, Freudenheim JL, Giovannucci E, Goldbohm RA, Graham S, Harnack L, Horn-Ross PL, Krogh V, Leitzmann MF, McCullough ML, Miller AB, Rodriguez C, Rohan TE, Schatzkin A, Shore R, Virtanen M, Willett WC, Wolk A, Zeleniuch-Jacquotte A, Zhang SM, Hunter DJ. 2006. Methods for pooling results of epidemiologic studies: The pooling project of prospective studies of diet and cancer. Am J Epidemiol 63:1053–1064.

Tan NS, Shaw NS, Vinckenbosch N, Liu P, Yasmin R, Desvergne B, Wahli W, Noy N. 2002. Selective cooperation between fatty acid binding proteins and peroxisome proliferator-activated receptors in regulating transcription. Mol Cell Biol 22:5114–5127.

Thiebaut AC, Chajes V, Gerber M, Boutron-Ruault MC, Joulin V, Lenoir G, Berrino F, Riboli E, Benichou J, Clavel-Chapelon F. 2009. Dietary intakes of omega-6 and omega-3 polyunsaturated fatty acids and the risk of breast cancer. Int J Cancer 124:924–931.

Waite KA, Eng C. 2002. Protean PTEN: Form and function. Am J Hum Genet 70:829–844.

Wei Y, Pattingre S, Sinha S, Bassik M, Levine B. 2008. JNK1-mediated phosphorylation of Bcl-2 regulates starvation-induced autophagy. Mol Cell 30:678–688.

West NJ, Clark SK, Phillips RK, Hutchinson JM, Leicester RJ, Belluzzi A, Hull MA. 2010. Eicosapentaenoic acid reduces rectal polyp number and size in familial adenomatous polyposis. Gut 59:918–925.

Williams CM, Burdge G. 2006. Long-chain n-3 PUFA: Plant v. marine sources. Proc Nutr Soc 65:42–50.

Wolfrum C, Borrmann CM, Borchers T, Spener F. 2001. Fatty acids and hypolipidemic drugs regulate peroxisome proliferator-activated receptors alpha- and gamma-mediated gene expression via liver fatty acid binding protein: A signaling path to the nucleus. Proc Natl Acad Sci USA 98:2323–2328.

Wolk A, Larsson SC, Johansson JE, Ekman P. 2006. Long-term fatty fish consumption and renal cell carcinoma incidence in women. JAMA 296:1371–1376.

Yamamoto K, Ichijo H, Korsmeyer SJ. 1999. BCL-2 is phosphorylated and inactivated by an ASK1/Jun N-terminal protein kinase pathway normally activated at G2/M. Mol Cell Biol 19:8469–8478.

Yu L, McPhee CK, Zheng L, Mardones GA, Rong Y, Peng J, Mi N, Zhao Y, Liu Z, Wan F, Hailey DW, Oorschot V, Klumperman J, Baehrecke EH, Lenardo MJ. 2010. Termination of autophagy and reformation of lysosomes regulated by mTOR. Nature 465:942–946.

Journal of Ethnopharmacology xxx (2012) xxx–xxx

Contents lists available at SciVerse ScienceDirect

Journal of Ethnopharmacology

journal homepage: www.elsevier.com/locate/jethpharm

Identification of bioactive constituents of *Ziziphus jujube* fruit extracts exerting antiproliferative and apoptotic effects in human breast cancer cells

Pierluigi Plastina[a,*], Daniela Bonofiglio[b,c], Donatella Vizza[b,c], Alessia Fazio[a], Daniela Rovito[b,c], Cinzia Giordano[c], Ines Barone[c,d], Stefania Catalano[b,c], Bartolo Gabriele[a,*]

[a] Department of Pharmaceutical Sciences, University of Calabria, 87036 Arcavacata di Rende, Cosenza, Italy
[b] Department of Pharmaco-Biology, University of Calabria, 87036 Arcavacata di Rende, Cosenza, Italy
[c] Health Center, University of Calabria, 87036 Arcavacata di Rende, Cosenza, Italy
[d] Department of Cell Biology, University of Calabria, 87036 Arcavacata di Rende, Cosenza, Italy

ARTICLE INFO

Article history:
Received 29 July 2011
Received in revised form 3 January 2012
Accepted 13 January 2012
Available online xxx

Keywords:
Apoptosis
Breast cancer
Traditional Chinese medicine
Triterpenic acids
Ziziphus jujube

ABSTRACT

Ethnopharmacological relevance: Ziziphus extracts have been used in Traditional Chinese Medicine for the treatment of cancer.
Aim of the study: In the present study we have investigated the effects of *Ziziphus jujube* extracts (ZEs) on breast cancer.
Materials and methods: We evaluated the effects of increasing concentrations of ZEs on ERα positive MCF-7 and ERα negative SKBR3 breast cancer cell proliferation using MTT assays. Apoptosis was analyzed by evaluating the involvement of some pro-apoptotic proteins, including Bax, Bad, Bid and PARP cleavage by immunoblotting analysis. Moreover, the effects of ZEs treatment on apoptosis were tested by both DNA fragmentation and terminal deoxynucleotidyl transferase dUTP nick end-labeling (TUNEL) staining. By using chromatographic techniques, we identified the constituents of the effective extracts.
Results: ZE1, ZE2, and ZE4 exerted significant antiproliferative effects on estrogen receptor alpha (ERα) positive MCF-7 (IC_{50} values of 14.42, 7.64, 1.69 μg/mL) and ERα negative SKBR3 (IC_{50} values of 14.06, 6.21, 3.70 μg/mL) human breast cancer cells. Remarkably, ZEs did not affect cell viability of both normal human fibroblasts BJ1-hTERT and nonmalignant breast epithelial MCF-10A cells. Treatment with ZEs induced cell death by apoptosis in both malignant breast cells. We found that the most effective extracts ZE2 and ZE4 shared a number of triterpenic acids, already known for their anticancer activities.
Conclusions: Our data provide a rational base for the use of *Ziziphus* extracts in the treatment of breast cancer in Traditional Chinese Medicine.

1. Introduction

In the last decades, phytochemicals have attracted a growing attention as anti-cancer agents (Aravindaram and Yang, 2010; Tosetti et al., 2009) due to their ability to modulate apoptosis signaling pathways (Fulda, 2010). In this perspective, the study of herbal formulations from Traditional Chinese Medicine (TCM) represent a challenging research field, since TCM has been applied for the treatment of cancers in China for many years (Hsiao and Liu, 2010).

Ziziphus species (Rhamnaceae family) are mainly distributed in the subtropical and tropical regions of Asia and America, but also in the Mediterranean region. Different parts of the plant of *Ziziphus* are commonly used in TCM for curing various diseases such as digestive disorders, weakness, liver complaints, obesity, urinary troubles, diabetes, skin infections, loss of appetite, fever, pharyngitis, bronchitis, anaemia, diarrhea, insomnia, and cancer (Bown, 1995; Him-Che, 1985). Much effort has been devoted to verifying the effectiveness of *Ziziphus* against cancer. Indeed, *Ziziphus* extracts, alone or in combination with other botanical formulations, have been shown to exert anticancer activities on several tumor cell lines (Chan et al., 2005; Huang et al., 2007, 2008; Huang et al., 2009; Lee et al., 2003; Saif et al., 2010; Vahedi et al., 2008). However, to the best of our knowledge, antiproliferative effects of *Ziziphus* extracts on breast cancer cells have not been reported so far.

Abbreviations: AcOEt, ethyl acetate; *n*-BuOH, 1-buthanol; cs, charcoal-stripped; DPPH, 1,1-diphenyl-2-picryl hydrazyl; DW, dry weight; ERα, estrogen receptor alpha; FBS, fetal bovine serum; FID, flame ionization detector; GLC, gas–liquid chromatography; MTT, 3-(4,5-dimethylthiazol-2-yl)-2,5-diphenyltetrazolium; MeOH, methanol; PARP, poly (ADP–ribose) polymerase; TE, Trolox equivalent; ZEs, *Ziziphus jujube* extracts.

* Corresponding authors. Tel.: +39 984 493013; fax: +39 984 492044.
E-mail addresses: p.plastina@unical.it (P. Plastina), b.gabriele@unical.it (B. Gabriele).

0378-8741/$ – see front matter © 2012 Elsevier Ireland Ltd. All rights reserved.
doi:10.1016/j.jep.2012.01.022

In the present study we have investigated the potential antiproliferative activity of *Ziziphus jujube* fruit extracts on estrogen receptor alpha (ERα) positive MCF-7 and ERα negative SKBR3 human breast cancer cells. Moreover, we have studied their antioxidant properties by evaluating their radical scavenging activity, and analyzed their content by using chromatographic techniques to identify the principal bioactive phytochemicals.

2. Materials and methods

2.1. Plant materials and reagents

Ziziphus jujuba P. Mill. cv. Lang fruits growing in Lamezia Terme, Italy, were supplied by "Azienda agricola Bertolami SAS" of Mr. Carmelo Bertolami (pick-up period: September 2009). A voucher specimen (accession no. 21814) of the plant was deposited in the *Erbarium CLA* at the Botanical Garden of the University of Calabria (Rende, Italy).

HPLC grade solvents were from Carlo Erba Reagenti (Milan, Italy). Fatty acid methyl ester standards, DPPH, Trolox (2,5,7,8-tetramethylchroman-2-carboxylic acid), 3,4-dihydroxybenzoic acid, ursolic acid, oleanolic acid and betulinic acid were from Sigma–Aldrich (Milan, Italy).

2.2. Preparation of the extracts

Two different methods were employed for the extraction of the lyophilized fruits of *Ziziphus* (Z.) *jujube*. Method 1. Lyophilized fruits of *Ziziphus jujube* deprived of seeds (100 g, corresponding to 500 g of fresh fruits) were used. The extracts were prepared by following extraction (4 × 200 mL) with *n*-hexane (ZE1), chloroform (ZE2), 80% ethanol, followed by rotary evaporation and extraction from the remaining water mixture with AcOEt (ZE3).

Method 2. Lyophilized fruits of *Ziziphus jujube* deprived of seeds (100 g, corresponding to 500 g of fresh fruits) were defatted at room temperature with *n*-hexane (4 × 200 mL), and extracted with MeOH by exhaustive maceration (4 × 200 ml) to yield 50 g of residue, which was successively dissolved in water and partitioned with AcOEt (ZE4) and *n*-BuOH (ZE5).

All extracts were dried and then re-dissolved in ethanol to make the stocking solution for use on cells.

2.3. Cell culture

Estrogen receptor alpha (ERα) positive MCF-7 breast cancer cells were cultured in DMEM F-12 medium supplemented with 5% new-born calf serum (Invitrogen, Milan, Italy), 1 mmol/L L-glutamine (Sigma Aldrich), and 1 mg/mL penicillin/streptomycin (Sigma Aldrich).

ERα negative SKBR3 breast cancer cells and immortalized normal human foreskin fibroblasts BJ1-hTERT (kindly provided by Dr. Michael P. Lisanti, The Jefferson Stem Cell Biology and Regenerative Medicine Center; Jefferson University; Philadelphia, USA) were grown in phenol red-free RPMI 1640, containing 10% fetal bovine serum (FBS) (Invitrogen).

MCF-10A nonmalignant breast epithelial cells were cultured in DMEM F-12 medium supplemented with 5% Horse Serum (Invitrogen), 1 mmol/L L-glutamine (Sigma Aldrich), 0.5 μg/mL hydrocortisone (Sigma Aldrich), 10 μg/mL insulin and 1 mg/mL penicillin/streptomycin (Sigma Aldrich).

Before each experiment, cells were grown in phenol red-free medium containing 1% charcoal-stripped (cs) FBS for 24 h and then treated as described.

2.4. Cell viability assay

Cell viability was determined by using the 3-(4,5-dimethylthiazol-2-yl)-2,5-diphenyltetrazolium (MTT) assay. Cells (3×10^4 cells/mL) were plated in 24 well plates and serum-starved for 24 h in phenol red-free media with 1% cs-FBS before the addition of *Ziziphus jujube* extracts for 48 and 72 h as indicated. The MTT assay was performed as the following: 100 μl of MTT (2 mg/mL) (Sigma Aldrich) were added to each well, and the plates were incubated for 2 h at 37 °C. Then, 500 μl of DMSO (Sigma Aldrich) were added to solubilise the cells. The absorbance was measured with the Ultrospec 2100 Prospectrophotometer (Amersham-Biosciences, Milan, Italy) at a test wavelength of 570 nm.

A minimum of three experiments at 72 h, with 4 different doses of different *Ziziphus jujube* extracts, ZE1, ZE2 and ZE4 respectively, in triplicate, was combined for IC_{50} calculations. The absorbance readings were used to determine the IC_{50} using GraphPad Prism 4 (GraphPad Software, Inc., San Diego, CA). Briefly, values were log-transformed, normalized, and nonlinear regression analysis was used to generate a sigmoidal dose-response curve to calculate IC_{50} values for each cell line.

2.5. Immunoblotting analysis

MCF-7 and SKBR3 cells were grown to 70% confluence and then treated in 1% cs-FBS media for 48 h as indicated. Cells were then harvested in cold PBS and lysed in buffer containing 50 mmol/L Tris–HCl (pH 7.4), 150 mmol/L NaCl, 2% NP40, 0.25% deoxycholic acid, 1 mmol/L EDTA, 1 mmol/L Na_3VO_4, and 1:100 protease inhibitors cocktail (Calbiochem, Nottingham, UK). Protein concentration was determined by Bio-Rad Protein Assay (Bio-Rad Laboratories, Hercules, CA, USA). Equal amount of proteins were resolved on 11% SDS–polyacrylamide gel, transferred to a nitrocellulose membrane and probed with antibodies against Bax, Bad, Bid and Poly (ADP-ribose) polymerase (PARP) (Santa Cruz, Biotechnology, CA, USA). To ensure equal loading, all membranes were stripped (0.2 M glycine, pH 2.6, for 30 min at room temperature) of the first antibody and reprobed with a mouse monoclonal anti-β-actin antibody (Santa Cruz). The antigen–antibody complex was detected by incubation of the membranes for 1 h at room temperature with peroxidase-coupled goat anti-rabbit or anti-mouse antibodies and revealed using the enhanced chemiluminescence (ECL) system (Amersham Pharmacia, Buckinghamshire UK).

2.6. DNA fragmentation

DNA fragmentation was determined by gel electrophoresis. MCF-7 and SKBR3 cells were grown in 10 cm dishes to 70% confluence and exposed to treatments as indicated. After 56 h, cells were collected, washed with PBS and pelletted at 1800 rpm for 5 min. The samples were resuspended in 0.5 mL of extraction buffer (50 mM Tris–HCl, pH 8; 10 mM EDTA, 0.5% SDS) for 20 min in rotation at 4 °C. DNA was extracted three times with phenol–chloroform and one time with chloroform. The aqueous phase was used to precipitate nucleic acids with 0.1 volumes of 3 M sodium acetate and 2.5 volumes cold ethanol overnight at −20 °C. The DNA pellet was resuspended in 15 μL of H_2O treated with RNAse A for 30 min at 37 °C. The absorbance of the DNA solution at 260 and 280 nm was determined by spectrophotometry. The extracted DNA (10 μg/lane) was subjected to electrophoresis on 1.8% agarose gels. The gels were stained with ethidium bromide and then photographed.

Please cite this article in press as: Plastina, P., et al., Identification of bioactive constituents of *Ziziphus jujube* fruit extracts exerting antiproliferative and apoptotic effects in human breast cancer cells. J. Ethnopharmacol. (2012), doi:10.1016/j.jep.2012.01.022

2.7. TUNEL assay

Apoptosis was determined by enzymatic labeling of DNA strand breaks using terminal deoxynucleotidyl transferase-mediated deoxyuridine triphosphate nick end-labeling (TUNEL). TUNEL labeling was conducted using DeadEnd™ Fluorometric TUNEL System (Promega) and performed according to the manufacturer's instructions. Briefly, cells treated for 56 h with *Ziziphus* extracts, were fixed in freshly prepared 4% paraformaldehyde solution in PBS (pH 7.4) for 25 min at 4 °C. After fixation cells were permeabilized in 0.2% Triton® X-100 solution in PBS for 5 min. After washing twice with washing buffer for 5 min, the cells were covered with 100 μl of equilibration buffer at room temperature for 5–10 min. The labeling reaction was performed using terminal deoxynucleotidyl transferase end-labeling TdT and fluorescein-dUTP cocktail for each sample and incubated for 1 h at 37 °C where TdT catalyses the binding of fluorescein-dUTP to free 3′OH ends in the nicked DNA. After rinsing, cells were washed with 20× SSC solution buffer and subsequently incubated with 100 μl of DAPI to stain nuclei, protected from light, analyzed and photographed by using a fluorescent microscope.

2.8. Determination of the DPPH• radical scavenging activity

The scavenging activity was evaluated using the DPPH• test (Jayaprakasha and Patil, 2007). Each extract was dissolved in MeOH and tested at four different concentrations (0.1, 1, 10, and 50 μg/mL). More specifically, standard solutions of the extracts (1.5, 0.3, 0.03, and 0.003 mg/mL of MeOH) were prepared. An aliquot of each solution (100 μL) was pipetted into 2.0 ml of MeOH. A methanolic solution of DPPH (100 μL, 1 mM) was added and the volume of the samples was adjusted to 3.0 mL by adding MeOH. After shaking vigorously, the tubes were allowed to stand at 27 °C for 20 min. MeOH was used for the baseline correction. Trolox (0, 100, 200, 300, 400, and 500 μM) was used as a standard. The absorbance (A) of all the samples and standards were measured at 517 nm. Analysis was done in triplicate for each sample and each concentration of standard. The antioxidant activity was reported in μmol of Trolox equivalents per gram of dry sample weight (μmol TE/g DW).

2.9. GLC analysis

The method of Lepage was used to directly transform the fatty acids into their corresponding methyl esters (Lepage and Roy, 1986). One hundred mg of ZE1 was precisely weighed in a glass tube. 300 μg of tridecanoic acid (C13:0), dissolved in 2 ml of methanol–benzene 4:l (v/v) were precisely weighed and added to the sample, as internal standard. Acetyl chloride (200 μl) was slowly added to the magnetically stirred mixture over a period of 1 min. The tube was tightly closed with Teflon-lined cap and subjected to methanolysis at 100 °C for 1 h with stirring. After cooling the tube in water, 5 mL of 6% K_2CO_3 solution was slowly added. The tube was then shaken and centrifuged, and an aliquot of the benzene upper phase was injected into the gas-chromatograph.

GLC analyses were carried out on a Shimadzu GC-2010 system equipped with an AOC-20i autosampler, split/splitless injector, and a FID detector (Shimadzu, Milan, Italy), using the following experimental conditions: the column used was a fused-silica capillary column (Equity-5 m, Supelco, Milan, Italy), coated with 5% diphenyl–95% dimethylsiloxane (30 m × 0.25 mm id × 0.25 μm d_f); the oven temperature increased from 50 to 250 °C with a rate of 3.0 °C/min; the injection volume was 1.0 μL, in the split mode (30:1). Helium was used as carrier gas at 30.1 cm/s of linear velocity (u) with an inlet pressure of 99.8 kPa. The detector temperature was set at 280 °C. The hydrogen flow rate was 50.0 mL/min; the air flow rate was 400 mL/min; the make up flow rate (N_2/air) was 50 mL/min. Sampling rate was 80 ms. The quantitative determination of the fatty acid methyl esters (FAMEs) was obtained by the external standard method using authentic FAMEs. The response factor for each component was considered equal to 1, and three replicates of each sample were made. Experimental results are expressed as the mean values.

2.10. LC–UV and LC–MS/MS analyses

HPLC analyses were carried out using a Shimadzu LC-20AB, equipped with an autosampler SIL-20AHT and an UV/VIS detector SPD-20A; the column used was a discovery C18 (Supelco) (250 mm × 4.6 mm id, 5 μm particle size). The mobile phase consisted of 0.1% acetic acid (A) and MeOH (B), programmed as follows: 0 min, 20% B; 0–25 min, 75% B; 25–50 min, 100% B; 50–55 min, 20% B; 55–60 min, 20% B. The injected volume was 20 μL at a flow rate of 1 mL/min. Quantitative determination of 3,4-dihydroxybenzoic acid (protocatechuic acid) was carried out by means of calibration curve with authentic compound as external standard.

The LC–MS/MS analyses were acquired on an ABSciex API 2000 mass spectrometer coupled with a JASCO PU-2080*PLUS* HPLC. The column used was a discovery C18 (Supelco) (150 mm × 4.6 mm id, 5 μm particle size). The mobile phase consisted of 0.1% acetic acid (A) and MeOH (B), programmed as follows: 0 min, 70% B; 0–55 min, 90% B; 55–70 min, 100% B; 70–80 min, 100% B; 80–85 min, 70% B; 85–90 min, 70% B. The injected volume was 20 μL at a flow rate of 0.3 mL/min. A turbo ion spray ionization source was used and the spectra in the negative ion mode were obtained under the following conditions: ionspray voltage (IS) 4500 V; curtain gas 10 psi; temperature 400 °C; ion source gas (1) 35 psi; ion source gas (2) 45 psi; declustering and focusing potentials 50 and 200 V, respectively.

2.11. Statistical analysis

Each datum point represents the mean ± S.D. of three different experiments. Data were analyzed by Student's t test using the GraphPad Prism 4 software program. $P < 0.05$ was considered as statistically significant.

3. Results and discussion

3.1. Ziziphus jujube extracts inhibit breast cancer cell survival

We first evaluated the effects of increasing concentrations (100 ng/mL, 1 μg/mL, 10 μg/mL and 50 μg/mL) of ZE1, ZE2, ZE3, ZE4 and ZE5 *Ziziphus jujube* extracts on ERα positive MCF-7 and ERα negative SKBR3 breast cancer cell proliferation using MTT assays. We observed that treatment for 48 h and 72 h with ZE1, ZE2 and ZE4 extracts reduced cell viability in MCF-7 and SKBR3 cells in a time and dose dependent manner (Fig. 1A and B), while ZE3 and ZE5 extracts did not exert any antiproliferative effects (data not shown). The greatest antiproliferative response was obtained with ZE4 extract as evidenced by the lowest IC_{50} values shown in Table 1 with the following rank order of efficacy: ZE4 > ZE2 > ZE1 extracts in both MCF-7 and SKBR3 breast cancer cells. It is worth noting that treatment with ZE1, ZE2 and ZE4 extracts did not elicit any noticeable effects on cell viability in MCF-10A nonmalignant breast epithelial cells and BJ1-hTERT immortalized normal human foreskin fibroblasts cells (Fig. 1C and D). The latter results suggest that inhibitory effects exerted by ZEs are selective for breast cancer cells.

Please cite this article in press as: Plastina, P., et al., Identification of bioactive constituents of *Ziziphus jujube* fruit extracts exerting antiproliferative and apoptotic effects in human breast cancer cells. J. Ethnopharmacol. (2012), doi:10.1016/j.jep.2012.01.022

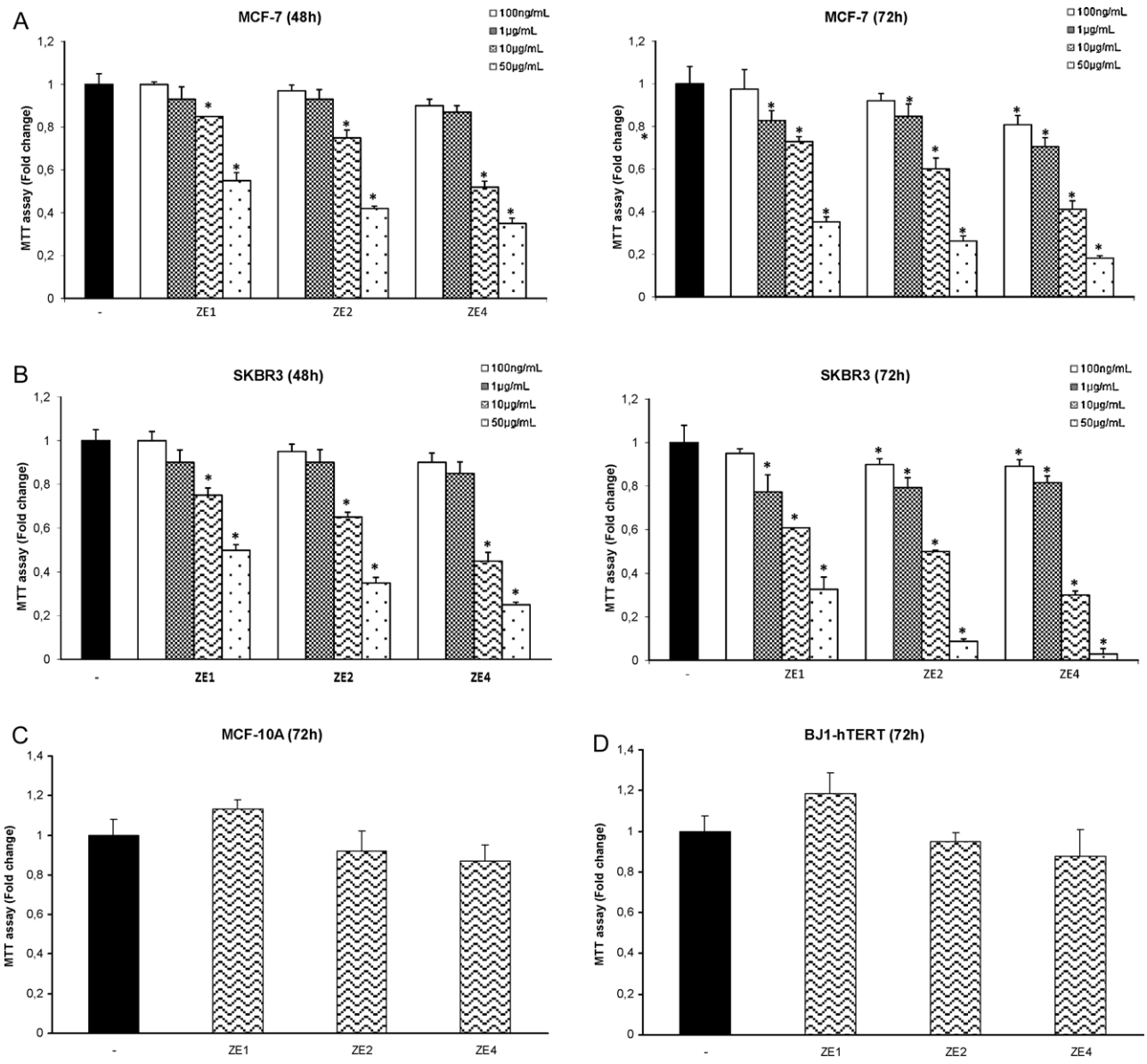

Fig. 1. Antiproliferative effects of *Ziziphus jujube* extracts in breast cancer cells. MTT proliferation assays in MCF-7 (A) and SKBR3 (B) cells treated with vehicle (−) or ZE1, ZE2 and ZE4 extracts for 48 h and 72 h as indicated. MTT proliferation assays in MCF-10A cells (C) and in BJ1-hTERT cells (D) treated with vehicle (−) or ZE1, ZE2 and ZE4 extracts (10 μg/mL) for 72 h. The results are expressed as fold change respect to control ± SD of triplicate wells and are representative of three separate experiments. $^{*}p < 0.05$ treated vs untreated cells.

3.2. Induction of apoptosis by Ziziphus jujube extracts

It has been previously demonstrated that induction of apoptosis is one of the mechanisms for the anticancer activities of *Ziziphus jujube* extracts (ZEs) in different cell lines (Huang et al., 2007; Vahedi et al., 2008). Thus, to investigate whether the treatment with ZEs may induce cell death by apoptosis in our model system, we used different approaches. First, we evaluated the involvement of some pro-apoptotic proteins such as Bax, Bad and Bid and proteolysis of poly (ADP–ribose) polymerase (PARP), a known substrate of effector caspases, by immunoblotting analysis. We found an increase in the levels of Bax, Bad and Bid expression as well as the enhancement of proteolytic form of PARP (89 kDa) in MCF-7 and SKBR3 breast cancer cells upon *Ziziphus jujube* extracts treatments compared to the control (Fig. 2A). PARP cleavage was increased after exposure with ZEs extracts, as evidenced by densitometric analysis of the bands. The second approach we employed was to determine whether *Ziziphus* jujube extracts treatment may induce changes in the internucleosomal fragmentation profile of genomic DNA, a diagnostic hallmark of cells undergoing apoptosis by both DNA laddering and TUNEL assay. Agarose-gel electrophoresis of chromosomal DNA extracted from MCF-7 and SKBR3 cells revealed,

Table 1
IC_{50} values of ZE1, ZE2 and ZE4 *Ziziphus jujube* extracts for MCF-7 and SKBR3 cells.

Cell lines	IC_{50} (μg/mL) ZE1	95% confidence interval	IC_{50} (μg/mL) ZE2	95% confidence interval	IC_{50} (μg/mL) ZE4	95% confidence interval
MCF-7	14.42	9.21–22.59	7.64	5.34–10.92	1.69	1.05–2.72
SKBR3	14.06	10.03–19.71	6.21	4.32–8.94	3.70	2.83–4.85

Please cite this article in press as: Plastina, P., et al., Identification of bioactive constituents of *Ziziphus jujube* fruit extracts exerting antiproliferative and apoptotic effects in human breast cancer cells. J. Ethnopharmacol. (2012), doi:10.1016/j.jep.2012.01.022

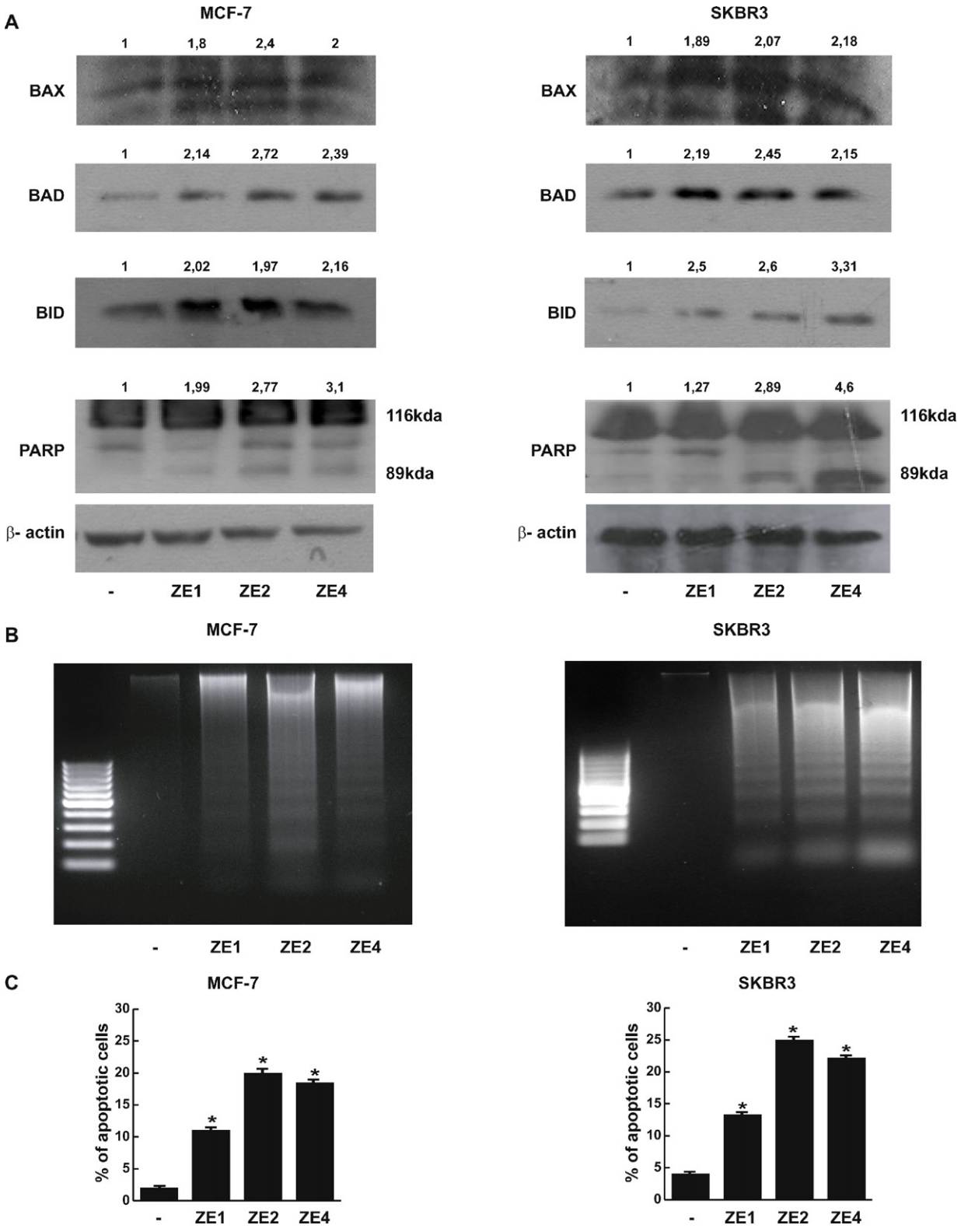

Fig. 2. Apoptosis triggered by *Ziziphus jujube* extracts in breast cancer cells. (A) Immunoblots of Bax, Bad, Bid and PARP from total extracts of MCF-7 and SKBR3 cells treated with vehicle (−) or with 10 μg/mL of ZE1, ZE2 and ZE4 jujube extracts for 48 h. β-actin was used as a loading control. Numbers on top of the blots represent the average fold change between Bax, Bad, Bid, cleaved PARP and β-actin protein expression vs vehicle-treated cells. (B) DNA laddering was performed in MCF-7 and SKBR3 cells treated with vehicle (−) or with 10 μg/mL of ZE1, ZE2 and ZE4 jujube extracts for 56 h. One of three similar experiments is presented. (C) Terminal deoxynucleotidyl transferase-mediated dUTP nick end labeling (TUNEL) staining for apoptosis was performed in MCF-7 and SKBR3 cells following ZEs treatments for 56 h. Columns represent quantitation of apoptotic cells from two independent experiments performed in triplicate; bars, ±SD. $^{*}p < 0.05$ treated vs vehicle-treated cells.

Please cite this article in press as: Plastina, P., et al., Identification of bioactive constituents of *Ziziphus jujube* fruit extracts exerting antiproliferative and apoptotic effects in human breast cancer cells. J. Ethnopharmacol. (2012), doi:10.1016/j.jep.2012.01.022

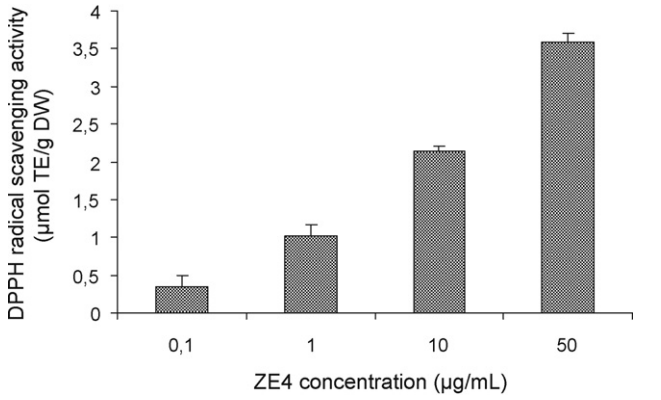

Fig. 3. DPPH• radical scavenging activity of *Ziziphus jujube* extract ZE4 at four different concentrations. The results are means (±SD) of three separate experiments. The antioxidant activity was reported by μmoles of Trolox equivalents per gram of dry sample weight (μmol TE/g DW).

after exposure with ZE1, ZE2 and ZE4 jujube extracts treatments, a marked DNA fragmentation consisting of multimers of approximately 180–200 bp (Fig. 2B). Accordingly, as shown in Fig. 2C, the percentage of TUNEL-positive cells significantly increased after ZEs treatments in both MCF-7 and SKBR3 cells compared to the control.

All these data show that *Ziziphus jujube* extracts may induce cell death by apoptosis in human breast malignant cells.

3.3. Determination of the DPPH• radical scavenging activity

In order to correlate the anticancer effects shown before with potential antioxidant properties, we used DPPH method to evaluate the ability of free radical scavenging of *Ziziphus jujube* extracts. Antioxidants react very quickly with DPPH that has a characteristic absorption at 517 nm. The decrease of the absorption values indicates a DPPH concentration decrease and thus the scavenging potentials of the extracts. As shown in Fig. 3, at the higher concentration used (50 μg/mL), ZE4 exhibited a free radical scavenging activity of 3.6 μmol TE/g DW, being still effective also at the lowest concentration (0.1 μg/mL). On the other hand, ZE1 and ZE2 did not exert any radical scavenging effect at the concentrations used (data not shown).

3.4. Analysis of Ziziphus jujube extract ZE1

We used GLC analysis to identify and quantify fatty acid methyl esters (FAMEs) produced by direct transesterification on the hexane extract ZE1. Table 2 shows the results obtained. The total amount of unsaturated fatty acids was almost three times more than that of saturated fatty acids, and, in particular, MUFAs account for about

Table 2
Amount of FAMEs after transesterification of ZE1 jujube extract.

Peak	Compound	Chain	Amount (mg/100 mg)
1	Lauric acid	12:0	3.16
2	Myristic acid	14:0	0.72
3	Myristoleic acid	14:1	3.56
4	Palmitic acid	16:0	2.16
5	Palmitoleic acid	16:1 n-7	5.25
6	Palmitoleic acid isomer	16:1 n-9	7.49
7	Stearic acid	18:0	0.56
8	Oleic acid	18:1	1.36
9	Linoleic acid	18:2	1.05
10	Linolenic acid	18:3	0.19
11	Docosanoic acid	22:0	0.25

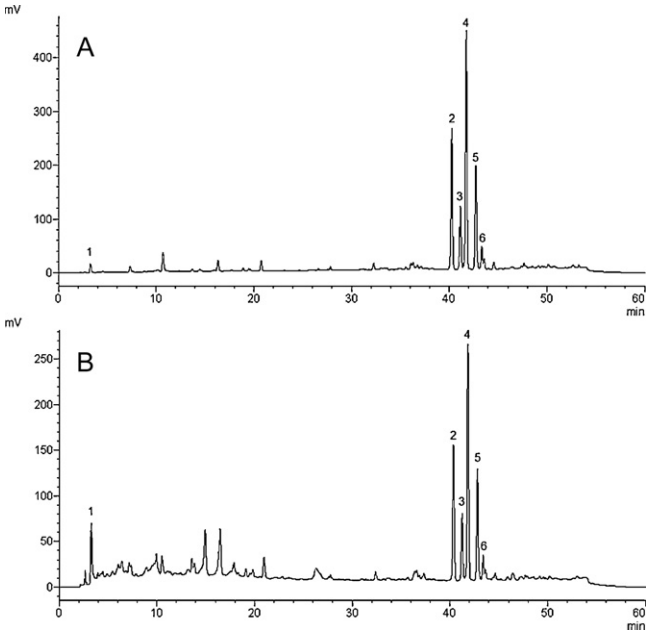

Fig. 4. Chromatographic separations of ZE2 (A) and ZE4 (B). The chromatograms were recorded at 280 nm.

68% of total fatty acids. There is increasing evidence that unsaturated free fatty acids can cause cell death by promoting apoptosis in breast cancer cells (Bocca et al., 2010; Grossmann et al., 2009; Moon et al., 2010; Yuan et al., 2009). PUFAs have been reported to be the most effective (Hawkins et al., 1999), but an increasing attention has been given the role of MUFAs in the last few years (Escrich et al., 2007). In agreement with previous data (Gusakova et al., 1999), we found that the most abundant compounds were the isomers of palmitoleic acid 16:1 n-9 and n-7, which could be, at least in part, responsible for the anti-cancer effects elicited by ZE1.

3.5. Analysis of Ziziphus jujube extracts ZE2 and ZE4

We used LC–UV and LC–MS/MS to analyze *Ziziphus jujube* extracts ZE2 and ZE4. In Fig. 4, the LC–UV chromatograms corresponding to ZE2 (A) and ZE4 (B) are shown. The two profiles are almost similar and share a series of peaks (1–6).

Peak 1 has been identified as 3,4-dihydroxybenzoic acid (protocatechuic acid). The amount of this compound was 2 mg/g of extract in the case of ZE4 and 0.28 mg/g of extract in the case of

Table 3
Spectrometric data of compounds found in ZE2 and ZE4 jujube extracts.

ESI (−)	Fragments	MW	Compound
153	109	154	Protocatechuic acid
485	439, 423	486	Ceanothic acid
469	451, 409, 407	470	Pomonic acid
471	453, 427, 393	472	Alphitolic acid
471	453, 427, 393	472	Maslinic acid
485	439, 423	486	Epiceanothic acid
617	145	618	3-*O*-(*cis*-*p*-coumaroyl)-alphitolic acid
617	145	618	2-*O*-(*cis*-*p*-Coumaroyl)-alphitolic acid
617	145	618	3-*O*-(*trans*-*p*-coumaroyl)-alphitolic acid
617	145	618	3-*O*-(*cis*-*p*-Coumaroyl)-maslinic acid
617	145	618	3-*O*-(*trans*-*p*-coumaroyl)-maslinic acid
455	–	456	Betulinic acid
455	–	456	Oleanolic acid
455	–	456	Ursolic acid
453	407	454	Betulonic acid
453	407	454	Oleanonic acid
453	407	454	Ursonic acid

Please cite this article in press as: Plastina, P., et al., Identification of bioactive constituents of *Ziziphus jujube* fruit extracts exerting antiproliferative and apoptotic effects in human breast cancer cells. J. Ethnopharmacol. (2012), doi:10.1016/j.jep.2012.01.022

ZE2. Both extracts contain several triterpenic acids, in the free or esterified form, identified by comparison with commercially available authentic standards or by comparison with literature data, on the basis of elution order and MS/MS fragmentation (Guo et al., 2010). The results are summarized in Table 3.Compounds with *m/z* 617 have been attributed to *p*-coumaroyl derivatives of maslinic acid and alphitolic acid, on the basis of literature data (Lee et al., 2004; Yagi et al., 1978a,b), and considering that the MS/MS spectrum of all these compounds showed a fragment ion at *m/z* 145 $[M\text{-}472-H]^-$. These compounds correspond to peaks 2–6 observed in Fig. 4. Triterpenic acids are an important group of substances widespread in plants (Wagner and Elmadfa, 2003), which have been shown to be beneficial to maintain and improve health, by reducing stress and carcinogenesis (He and Liu, 2007; Laszczyk, 2009; Rabi and Bishayee, 2009). Some of them, namely, alphitolic acid, betulinic acid, and ursolic acid have been shown to exert antiproliferative activity in MCF-7 human breast cancer cells (Amico et al., 2006; Ikeda et al., 2008; Rabi and Bishayee, 2009; Yeh et al., 2010), with ursolic acid being effective in breast cancer also *in vivo* (De Angel et al., 2010). Ursolic acid and oleanolic acid have been found to induce apoptosis in HuH7 human hepatocellular carcinoma cells (Shyu et al., 2010). Betulinic acid was found to effectively induce tumor cell death in a broad spectrum of cancer cells *in vitro* and *in vivo* (Mullauer et al., 2010). Maslinic acid induces apoptosis in HT29 human colon cancer cells via the mitochondrial apoptotic pathway (Reyes-Zurita et al., 2009). Moreover, the esterified derivatives of *p*-coumaroylmaslinic acid and *p*-coumaroylalphityolic acid inhibit proliferation in MCF-7 cells (He and Liu, 2007) and in various tumor cell lines (Lee et al., 2003), respectively. On the basis of our results, the antitumor effects elicited by ZE2 and ZE4 can be therefore attributed to the presence of triterpenic acids. The slightly different efficacies between the two extracts can be tentatively explained on the basis of the higher amount of protocatechuic acid found in ZE4. This compound has been found to exert radical scavenging activities (Zhang et al., 2010), cytotoxic effects in HepG2 hepatocellular carcinoma cells (Yip et al., 2006), and to induce apoptosis in several malignant cells, including human breast cancer cells (Yin et al., 2009). This is in agreement with previous findings showing that a synergistic effect between triterpenic acids from apple extracts and polyphenols is responsible for the antiproliferative activity in MCF-7 human breast cancer cells (Yang and Liu, 2009). Moreover, this difference fits well with our finding that ZE4 was effective as radical scavenger, whereas ZE2 did not exert any radical scavenging effects. It is tempting to speculate that the beneficial effects of *Ziziphus jujube* fruits on breast cancer cells derive from the additive and synergistic effects of different bioactive compounds, rather than from a single component.

4. Conclusions

In conclusion, we have found for the first time that *Ziziphus jujube* extracts are effective in inhibiting the growth and inducing apoptosis in MCF-7 and SKBR3 breast cancer cell lines. Remarkably, they elicited no effects on immortalized normal human foreskin fibroblasts cells and nonmalignant epithelial breast cells. Triterpenic acids resulted the bioactive compounds present in the most effective extracts (ZE2 and ZE4). Our data provide a strong rational base for the use in Traditional Chinese Medicine of *Ziziphus* extracts in the treatment of cancers. Moreover, our results highlight that *Ziziphus jujube* are valuable fruits rich in bioactive compounds with potential human health benefits. More experiments are in progress to understand the molecular targets and pathways affected by *Ziziphus jujube*.

Acknowledgments

This work was supported by Foundation Lilli Funaro, MIUR Ex 60% and Reintegration AIRC/Marie Curie International Fellowship in Cancer Research to IB.

We thank C. Bertolami (Azienda agricola Bertolami SAS, Lamezia Terme, Italy) for the *Ziziphus jujube* fruits supply.

References

Amico, V., Barresi, V., Condorelli, D., Spatafora, C., Tringali, C., 2006. Terpenoids from almond hulls (*Prunus dulcis*): identification and structure–activity relationships. Journal of Agricultural and Food Chemistry 54, 810–814.
Aravindaram, K., Yang, N.-S., 2010. Anti-inflammatory plant natural products for cancer therapy. Planta Medica 76, 1103–1117.
Bown, D., 1995. Encyclopaedia of Herbs and their Uses. Dorling Kindersley, London.
Bocca, C., Bozzo, F., Cannito, S., Colombatto, S., Miglietta, A., 2010. CLA reduces breast cancer cell growth and invasion through ER alpha and PI3K/Akt pathways. Chemico-Biological Interactions 183, 187–193.
Chan, A.S.L., Yip, E.C.H., Yung, L.Y., Pang, H.H., Luk, S.C.W., Pang, S.F., Wong, Y.H., 2005. Immuno-regulatory effects of CKBM on the activities of mitogen-activated protein kinases and the release of cytokines in THP-1 monocytic cells. Biological & Pharmaceutical Bulletin 28, 1645–1650.
De Angel, R.E., Smith, S.M., Glickman, R.D., Perkins, S.N., Hursting, S.D., 2010. Antitumor effects of ursolic acid in a mouse model of postmenopausal breast cancer. Nutrition and Cancer 62, 1074–1086.
Escrich, E., Moral, R., Grau, L., Costa, I., Solanas, M., 2007. Molecular mechanisms of the effects of olive oil and other dietary lipids on cancer. Molecular Nutrition & Food Research 51, 1279–1292.
Fulda, S., 2010. Modulation of apoptosis by natural products for cancer therapy. Planta Medica 76, 1075–1079.
Grossmann, M.E., Mizuno, N.K., Dammen, M.L., Schuster, T., Ray, A., Cleary, M.P., 2009. Eleostearic acid inhibits breast cancer proliferation by means of an oxidation-dependent mechanism. Cancer Prevention Research 2, 879–886.
Guo, S., Duan, J.-A., Tang, Y.-P., Yang, N.-Y., Qian, D.-W., Su, S.-L., Shang, E.-X., 2010. Characterization of triterpenic acids in fruits of *Ziziphus* species by HPLC-ELSD-MS. Journal of Agricultural and Food Chemistry 58, 6285–6289.
Gusakova, S.D., Sagdullaev, S.S., Aripov, K.N., Baser, K.H.C., Kurkcuoglu, M., Demirci, B., 1999. Isomers of palmitoleic acid in lipids and volatile substances from the fruits of *Ziziphus jujube*. Chemistry of Natural Compounds 35, 401–403.
Hawkins, R.A., Sangster, K., Arends, M.J., 1999. The apoptosis-inducing effects of polyunsaturated fatty acids (PUFAs) on benign and malignant breast cells in vitro. Breast 1, 16–20.
He, X., Liu, R.H., 2007. Triterpenoids isolated from apple peels have potent antiproliferative activity and may be partially responsible for apple's anticancer activity. Journal of Agricultural and Food Chemistry 55, 4366–4370.
Him-Che, Y., 1985. Handbook of Chinese Herbs and Formulas. Institute of Chinese Medicine, pp. S219–S224.
Hsiao, W.L.W., Liu, L., 2010. The role of traditional Chinese herbal medicines in cancer therapy – from TCM theory to mechanistic insights. Planta Medica 76, 1118–1131.
Huang, X.D., Kojima-Yuasa, A., Norikura, T., Kennedy, D.O., Hasuma, T., Matsui-Yuasa, I., 2007. Mechanism of the anti-cancer activity of *Zizyphus jujuba* in HepG2 cells. American Journal of Chinese Medicine 35, 517–532.
Huang, X.D., Kojima-Yuasa, A., Xu, S.H., Norikura, T., Kennedy, D.O., Hasuma, T., Matsui-Yuasa, I., 2008. Green tea extract enhances the selective cytotoxic activity of *Ziziphus jujuba* extracts in HepG2 cells. American Journal of Chinese Medicine 36, 729–744.
Huang, X.D., Kojima-Yuasa, A., Xu, S.H., Kennedy, D.O., Hasuma, T., Matsui-Yuasa, I., 2009. Combination of *Ziziphus jujuba* and Green Tea extracts exerts excellent cytotoxic activity in HepG2 cells via reducing the expression of APRIL. American Journal of Chinese Medicine 37, 169–179.
Ikeda, Y., Murakami, A., Ohigashi, H., 2008. Ursolic acid: an anti- and pro-inflammatory triterpenoid. Molecular Nutrition & Food Research 52, 26–42.
Jayaprakasha, G.K., Patil, B.S., 2007. In vitro evaluation of the antioxidant activities in fruit extracts from citron and blood orange. Food Chemistry 101, 410–418.
Laszczyk, M.N., 2009. Pentacyclic triterpenes of the lupane, oleanane and ursane group as tools in cancer therapy. Planta Medica 75, 1549–1560.
Lee, S.-M., Min, B.-S., Lee, C.-G., Kim, K.-S., Kho, Y.-H., 2003. Cytotoxic triterpenoids from the fruits of *Zizyphus jujube*. Planta Medica 69, 1051–1054.
Lee, S.-M., Park, J.-G., Lee, Y.-H., Lee, C.-G., Min, B.-S., Kim, J.-H., Lee, H.-K., 2004. Anti-complementary activity of triterpenoides from fruits of *Zizyphus jujube*. Biological & Pharmaceutical Bulletin 27, 1883–1886.
Lepage, G., Roy, C.C., 1986. Direct transesterification of all classes of lipids in a one-step reaction. Journal of Lipid Research 27, 114–120.
Moon, H.-S., Guo, D.-D., Lee, H.-G., Choi, Y.-J., Kang, J.-S., Jo, K., Eom, J.-M., Yun, C.-H., Cho, C.-S., 2010. Alpha-eleostearic acid suppresses proliferation of MCF-7 breast cancer cells via activation of PPAR gamma and inhibition of ERK 1/2. Cancer Science 101, 396–402.
Mullauer, F.B., Kessler, J.H., Medema, J.P., 2010. Betulinic acid, a natural compound with potent anticancer effects. Anti-Cancer Drugs 21, 215–227.
Rabi, T., Bishayee, A., 2009. Terpenoids and breast cancer chemoprevention. Breast Cancer Research and Treatment 115, 223–239.

Please cite this article in press as: Plastina, P., et al., Identification of bioactive constituents of *Ziziphus jujube* fruit extracts exerting antiproliferative and apoptotic effects in human breast cancer cells. J. Ethnopharmacol. (2012), doi:10.1016/j.jep.2012.01.022

Reyes-Zurita, F.-J., Rufino-Palomares, E.E., Lupiáñez, J.A., Cascante, M., 2009. Maslinic acid a natural triterpene from *Olea europaea* L., induces apoptosis in HT29 human colon-cancer cells via the mitochondrial apoptotic pathway. Cancer Letters 273, 44–54.

Saif, M.W., Lansigan, F., Ruta, S., Lamb, L., Mezes, M., Elligers, K., Grant, N., Jiang, Z.-L., Liu, S.H., Cheng, Y.-C., 2010. Phase I study of the botanical formulation PHY906 with capecitabine in advanced pancreatic and other gastrointestinal malignancies. Phytomedicine 17, 161–169.

Shyu, M.-H., Kao, T.-C., Yen, G.-C., 2010. Oleanolic acid and ursolic acid induce apoptosis in HuH7 human hepatocellular carcinoma cells through a mitochondrial-dependent pathway and downregulation of XIAP. Journal of Agricultural and Food Chemistry 58, 6110–6118.

Tosetti, F., Noonan, D.M., Albini, A., 2009. Metabolic regulation and redox activity as mechanisms for angioprevention by dietary phytochemicals. International Journal of Cancer 125, 1997–2003.

Vahedi, F., Najafi, M.F., Bozari, K., 2008. Evaluation of inhibitory effect and apoptosis induction of *Zyzyphus Jujube* on tumor cell lines, an in vitro preliminary study. Cytotechnology 56, 105–111.

Wagner, K.H., Elmadfa, I., 2003. Biological relevance of terpenoids. Annals of Nutrition and Metabolism 47, 95–106.

Yagi, A., Okamura, N., Haraguchi, Y., Noda, K., Nishioka, I., 1978a. Studies on the constituents of *Zizyphus Fructus* I. Structure of three new p-coumaroylates of alphitolic acid. Chemical & Pharmaceutical Bulletin 26, 1798–1802.

Yagi, A., Okamura, N., Haraguchi, Y., Noda, K., Nishioka, I., 1978b. Studies on the constituents of *Zizyphus Fructus* II. Structure of new p-coumaroylates of maslinic acid. Chemical & Pharmaceutical Bulletin 26, 3075–3079.

Yang, J., Liu, R.H., 2009. Synergistic effect of apple extracts and quercetin 3-β-D-glucoside combination on antiproliferative activity in MCF-7 human breast cancer cells in vitro. Journal of Agricultural and Food Chemistry 57, 8581–8586.

Yeh, C.-T., Wu, C.-H., Yen, G.-C., 2010. Ursolic acid, a naturally occurring triterpenoid, suppresses migration and invasion of human breast cancer cells by modulating c-Jun *N*-terminal kinase. Akt and mammalian target of rapamycin signaling. Molecular Nutrition & Food Research 54, 1285–1295.

Yin, M.C., Lin, C.C., Wu, H.C., Tsao, S.M., Hsu, C.K., 2009. Apoptotic effects of protocatechuic acid in human breast, lung, liver, cervix, and prostate cancer cells: potential mechanisms of action. Journal of Agricultural and Food Chemistry 57, 6468–6473.

Yip, E.C.H., Chan, A.S.L., Pang, H., Tam, Y.K., Wong, Y.H., 2006. Protocatechuic acid induces cell death in HepG2 hepatocellular carcinoma cells through a c-Jun N-terminal kinase-dependent mechanism. Cell Biology and Toxicology 22, 293–302.

Yuan, X.-L., He, F., Chen, Q., Yang, X.-L., Yang, D.-P., Wang, D.-M., Zhong, L., 2009. Studies on PPAR gamma signal pathway of conjugated linoleic acid isomers induce apoptosis of human breast cancer cell line SKBr3. Progress in Biochemistry and Biophysics 36, 491–499.

Zhang, H., Jiang, L., Ye, S., Ye, Y., Ren, F., 2010. Systematic evaluation of antioxidant capacities of the ethanolic extract of different tissues of jujube (*Ziziphus jujuba* Mill.) from China. Food and Chemical Toxicology 48, 1461–1465.

Please cite this article in press as: Plastina, P., et al., Identification of bioactive constituents of *Ziziphus jujube* fruit extracts exerting antiproliferative and apoptotic effects in human breast cancer cells. J. Ethnopharmacol. (2012), doi:10.1016/j.jep.2012.01.022

Cell Cycle 10:14, 2344-2354; July 15, 2011; © 2011 Landes Bioscience

Bid as a potential target of apoptotic effects exerted by low doses of PPARγ and RXR ligands in breast cancer cells

Daniela Bonofiglio,[1,†] Erika Cione,[1,†] Donatella Vizza,[1] Mariarita Perri,[1] Attilio Pingitore,[1] Hongyan Qi,[1] Stefania Catalano,[1] Daniela Rovito,[1] Giuseppe Genchi[1] and Sebastiano Andò[2-4,*]

[1]Department of Pharmaco-Biology; [2]Department of Cellular Biology; [3]Centro Sanitario; [4]Faculty of Pharmacy Nutritional and Health Sciences; University of Calabria; Cosenza, Italy

[†]These authors contributed equally to this work.

Key words: PPARγ, RXR, apoptosis, mitochondria, Bid, breast cancer

The combined treatment with nanomolar doses of the PPARγ ligand Rosiglitazone (BRL) and the RXR ligand 9-cis-retinoic acid (9RA) induces a p53-dependent apoptosis in MCF7, SKBR3 and T47D human breast cancer cells. Since MCF7 cells express a wild-type p53 protein, while SKBR3 and T47D cells harbor endogenous mutant p53, we elucidated the mechanism through which PPARγ and RXR ligands triggered apoptotic processes independently of p53 transcriptional activity. We showed an upregulation of Bid expression enhancing the association between Bid/p53 in both cytosol and mitochondria after the ligand treatment. Particularly in the mitochondria, the complex involves the truncated Bid that plays a key role in the apoptotic process induced by BRL and 9RA, since the disruption of mitochondrial membrane potential, the induction of PARP cleavage and the percentage of TUNEL-positive cells were reversed after knocking down Bid. Moreover, PPARγ and RXR ligands were able to reduce mitochondrial GST activity, which was no longer noticeable silencing Bid expression, suggesting the potential of Bid in the regulation of mitochondrial intracellular reactive oxygen species scavenger activity. Our data, providing new insight into the role of p53/Bid complex at the mitochondria in promoting breast cancer cell apoptosis upon low doses of PPARγ and RXR ligands, address Bid as a potential target in the novel therapeutical strategies for breast cancer.

Introduction

The p53 mutation is found in more than half of all human cancer patients. Cancers with loss of p53 function are often resistant to chemotherapeutic agents, mainly because of the absence of p53-dependent apoptosis.[1-3] The p53-dependent apoptosis largely relies on the capability of p53 to act as a transcription factor, although recent reports show that the transcription-independent function of p53 plays a role in this process as well. For instance, apoptosis can still occur in the presence of inhibitors of protein synthesis or when p53 mutants unable of acting as transcription factors are ectopically expressed. The mechanism through which p53 mediates apoptosis in various cancer cells includes the activation of two major execution programs downstream of the death signal: the caspase pathway and organelle dysfunction, of which mitochondrial dysfunction is best characterized.[4-9] Part of the transcription-independent mechanism may also involve a direct interaction between p53 and multiple targets in the mitochondria, such as the apoptotic member Bcl-x_L, leading to the release of both Bax and Bid from Bcl-x_L sequestration. Following a death signal, these pro-apoptotic members undergo a conformational change that enables them to target and integrate into membranes, especially the outer mitochondrial membrane, leading to an increased permeabilization.[10,11] As noted Bid might serve as a "death ligand," which translocates as truncated p15Bid (tBid) to mitochondria, where it inserts into the outer membrane to activate other resident mitochondrial "receptor" proteins to release cytochrome *c*. Alternatively, it is also conceivable that Bid would itself function as a downstream effector participating in an intramembranous pore that releases cytochrome *c*. To date, Bid is the one molecule absolutely required for the release of cytochrome *c* in loss-of-function approaches, including immunodepletion and gene knockout.[12]

In a recent work, we demonstrated that combined treatment with nanomolar levels of the PPARγ ligand Rosiglitazone (BRL) and the RXR ligand 9-cis-retinoic acid (9RA) induce a p53-dependent intrinsic apoptosis in MCF7, SKBR3 and T47D breast cancer cells.[13] Of note, MCF7 cells express the wild type p53 protein able to induce growth arrest and apoptosis, mainly through the activation of a growing plethora of p53-responsive target genes,[14-16] while SKBR3 and T47D human breast carcinoma cell lines carry endogenous mutant p53His175 and p53Phe194, respectively, which affect p53 transcriptional activity.

*Correspondence to: Sebastiano Andò; Email: sebastiano.ando@unical.it
Submitted: 04/21/11; Accepted: 05/16/11
DOI: 10.4161/cc.10.14.15917

In this report, we extend our previous study on p53-mediated apoptosis induced by low doses of BRL and 9RA in MCF7, SKBR3 and T47D breast cancer cells to elucidate the mechanism through which PPARγ and RXR ligands can trigger apoptotic processes independently of p53 transcriptional activity. Our results showed that BRL and 9RA induce the intrinsic apoptotic pathway through an upregulation of Bid expression and a formation of p53/tBid/Bak multicomplex localized on mitochondria of breast carcinoma cells.

Results

p53 and p21 expression upon combined low doses of BRL plus 9RA in breast cancer cells. We aimed to examine the potential ability of nanomolar concentrations of BRL and 9RA to modulate p53 and its natural target gene $p21^{WAF1/Cip1}$. We revealed that only the combination of both ligands enhanced p53 expression in all breast cancer cells tested in terms of mRNA and protein content, while the increased expression of $p21^{WAF1/Cip1}$ was highlighted only in MCF7 cells (**Fig. 1A–E**), suggesting that the p53 mutated form in the other two cell lines tested does not exhibit any transactivation properties. Moreover, as expected, we did not observe in SKBR3 and T47D cells any modulation of the human wild-type $p21^{WAF1/Cip1}$ promoter luciferase activity upon nanomolar concentrations of BRL and 9RA alone or in combination (data not shown), even though PPARγ can mediate the upregulation of $p21^{WAF1/Cip1}$ independently of p53.[17-19]

BRL plus 9RA treatment improves the association between p53 and bid in breast cancer cells. p53 participates in apoptosis, even by acting directly on multiple mitochondrial targets.[20] Therefore, we evaluated the involvement of the Bcl-2 protein family in regulating apoptosis. After 48 h BRL plus 9RA treatment, we determined the protein levels of Bid, Bad, Bcl-x_L in both cytosolic and mitochondrial fractions of breast cancer cells. The separate treatment with low doses of either BRL or 9RA did not elicit any noticeable effect on Bid expression (**Sup. Fig. 1**); in contrast, an upregulation of Bid protein content upon the combined treatment was observed in both cytosolic and mitochondrial extracts, while unchanged levels of Bad and Bcl-x_L were detected in all the fractions tested (**Fig. 2A**). The protein synthesis inhibitor cycloheximide (CX) prevented the enhancement of Bid expression, suggesting that Bid is ex novo synthesized (**Fig. 2B**). The transcriptional activity of Bid was confirmed by using qtPCR, which clearly showed a significant upregulation of Bid mRNA in all breast cancer cells (**Fig. 2C**). The enhancement of Bid transcript levels upon treatment was reversed after silencing PPARγ, suggesting that the effect is PPARγ-mediated (**Fig. 2D and E**).

To examine whether wt and/or mutant p53 protein could associate with Bid in the cytoplasm and colocalize to the mitochondria, we performed co-immunoprecipitation experiments using cytosolic and either whole mitochondria or mitochondrial matrix extracts from breast cancer cells treated for 48 h with BRL plus 9RA. Equal amounts of protein extracts were immunoprecipitated with an anti-p53 antibody and then subjected to immunoblot with anti-Bid antibody. As seen in **Figure 3A**, in cytosolic immunoprecipitates, we detected under physiological conditions the association between p53 and Bid that slightly increased upon BRL plus 9RA treatment, while in whole mitochondria we revealed that p53 was able to interact with the more active truncated Bid, tBid, particularly in the presence of the combined treatment (**Fig. 3B**). In the matrix of mitochondria, no association between the two proteins was observed, suggesting that this physical interaction occurs in the mitochondrial membrane, likely initiating this organelle dysfunction (**Fig. 3C**). Since it has been reported the interaction of tBid with other pro-apoptotic proteins, resulting in a more global permeabilization of the outer mitochondrial membrane,[12] we also explored the involvement of Bak and Bax. We detected the presence of Bak (**Fig. 3A and B**) but not of Bax (data not shown) as component of this multiprotein complex. Stemming from our previous findings demonstrating that p53 binds to PPARγ in breast cancer cells,[21] we investigated in our cellular context a possible association of PPARγ to this protein complex together with its heterodimer RXRα. We observed the presence of both receptors in this complex in the cytosol as well as in whole mitochondria but not in the mitochondrial matrix (**Fig. 3A–C**). The p53/Bid association still occured after knocking down PPARγ and RXRα, as shown in **Supplemental Figure 2**. To better define the mitochondrial colocalization of p53 and Bid, we used a red fluorescent dye that passively diffuses across the plasma membrane and accumulates in active mitochondria. In MCF7 cells, the coexpression of both proteins gave rise to a merged image, which appears further enhanced in cells treated with BRL plus 9RA (**Fig. 3D**).

Bid is involved in apoptotic events triggered by BRL plus 9RA treatment in breast cancer cells. In order to validate the key role of Bid in the apoptotic process, we used different experimental approaches after silencing Bid expression. We analyzed mitochondrial membrane potential using a fluorescent dye JC-1 in all cell lines tested after BRL plus 9RA treatment. Cells transfected with control RNAi allowed the accumulation of lipophilic dye in aggregated form in mitochondria, displaying red fluorescence, as shown in **Figure 4A**, demonstrating the integrity of the mitochondrial membrane potential. Cells treated with both ligands exhibited green fluorescence, indicating the disruption of mitochondrial integrity, because JC-1 cannot accumulate within the mitochondria but instead remains as a monomer in the cytoplasm. After silencing Bid expression, red fluorescence was evident in treated cells (**Fig. 4A**), suggesting that the integrity of the mitochondrial membrane potential is maintained in MCF7, SKBR3 and T47D cells. This result fits well with a significant decrease of PARP cleavage in cells transfected with Bid RNAi and treated with ligands with respect to treated cells transfected with control RNAi (**Fig. 4B**). Indeed, in transfected cells with Bid-RNAi, TUNEL assay showed after 72 h treatment a strong reduction of the percentage of apoptotic cells with respect to treated cells trasfected with control RNAi (**Fig. 4C**). All these data indicate that Bid plays an important role in the death pathway induced by low doses of PPARγ and RXR ligands in breast cancer cells.

BRL plus 9RA reduce glutathione S-transferase antioxidative enzyme activity and induce lipid peroxidation in breast cancer cells. Since an isoform of the antioxidant defense

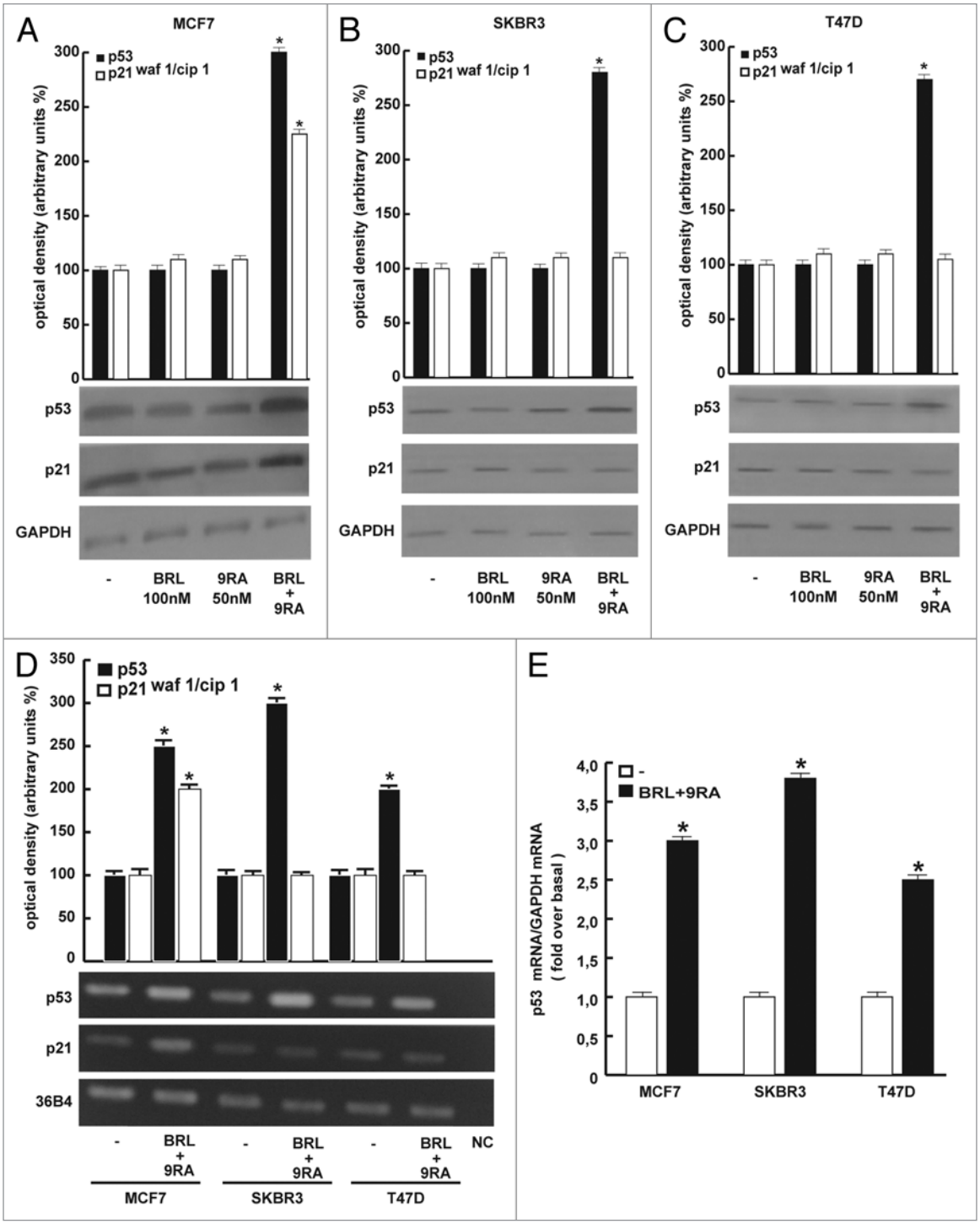

Figure 1. Combined low doses of BRL and 9RA upregulate p53 expression in MCF7, SKBR3 and T47D breast cancer cells. (A–C) Immunoblots of p53 and p21 from extracts of MCF7, SKBR3 and T47D cells untreated (-) or treated with 100 nM BRL and/or 50 nM 9RA for 24 hours. GAPDH was used as a loading control. The histograms show the quantitative representation of data (mean ± SD) of three independent experiments, in which band intensities were evaluated in terms of optical density arbitrary units and expressed as percentages of the control, which was assumed to be 100%. (D) p53 and p21 mRNA expression in MCF7, SKBR3 and T47D cells untreated (-) or treated with 100 nM BRL plus 50 nM 9RA for 12 hours. The histograms show the quantitative representation of data (mean ± SD) of three independent experiments after densitometry and correction for 36B4 expression expressed as percentages of the control, which was assumed to be 100%. (E) Quantitative real-time PCR analysis of p53 mRNA expression in MCF7, SKBR3 and T47D cells treated as in (D). The histograms show the quantitative representation of data (mean ± SD) of three independent experiments after correction for GAPDH expression. NC, RNA samples without the addition of reverse transcriptase (negative control). *$p < 0.05$ combined-treated vs. untreated cells.

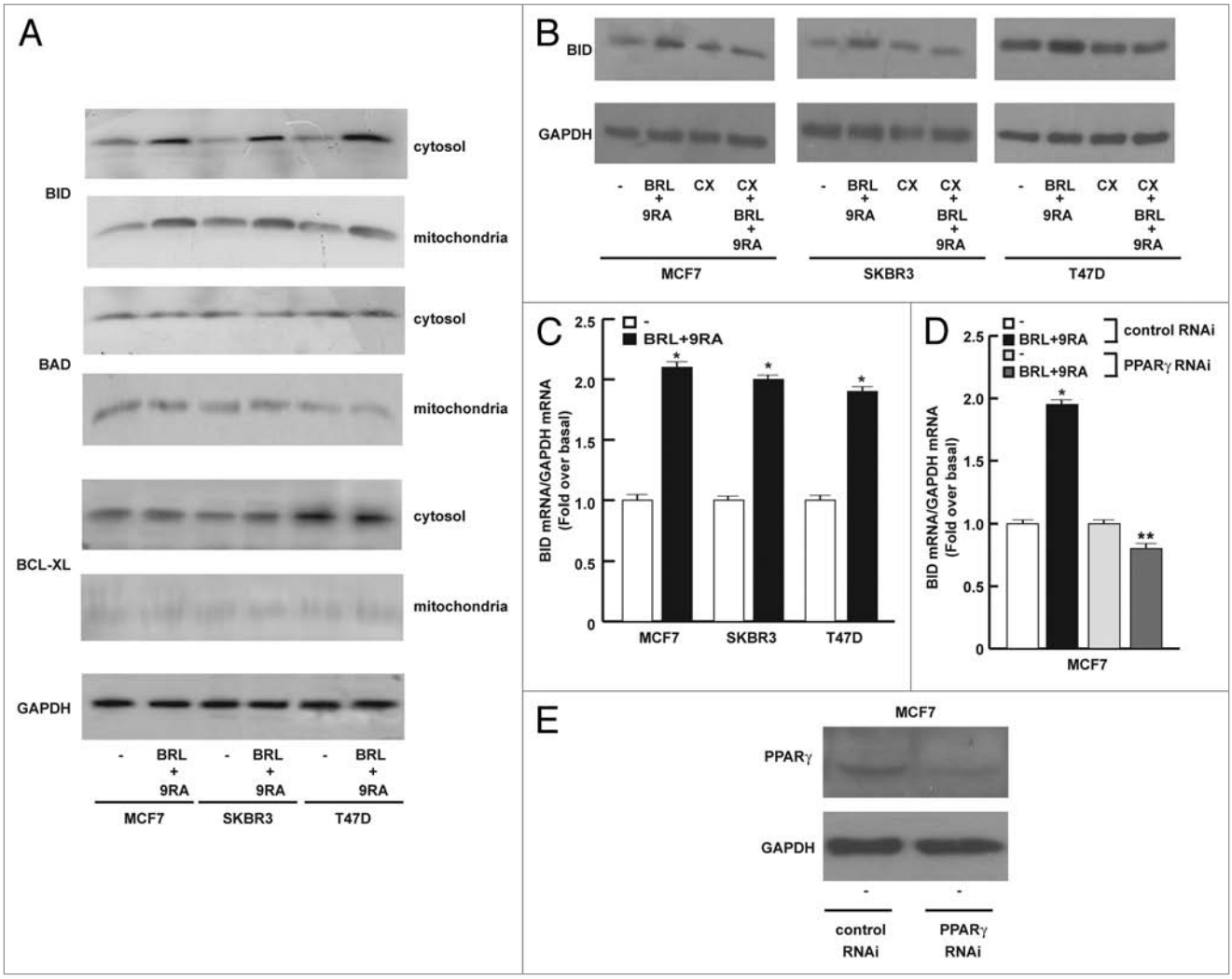

Figure 2. Upregulation of BID expression by BRL and 9RA in breast cancer cells. (A) Cytosolic and mitochondrial expression of BID, BAD and BCL-X_L proteins in MCF7, SKBR3 and T47D breast cancer cells untreated (-) or treated for 48 hours with 100 nM BRL plus 50 nM 9RA. GAPDH was used as a loading control. One of three similar experiments is presented. (B) Immunoblots of BID from total extracts of MCF7, SKBR3 and T47D cells treated as in (A) and/or with 50 μM protein synthesis inhibitor cycloheximide (CX). GAPDH was used as a loading control. One of three similar experiments is presented. (C) Quantitative real-time PCR analysis of BID mRNA expression in MCF7, SKBR3 and T47D cells treated for 24 hours as indicated. (D) Quantitative real-time PCR analysis of BID mRNA expression in MCF7 cells transfected with control RNAi or with PPARγ RNAi and treated for 24 hours as indicated. The histograms show the quantitative representation of data (mean ± SD) of three independent experiments after correction for GAPDH expression. (E) Immunoblots of PPARγ from extracts of MCF7 cells transfected with control RNAi or with PPARγ RNAi. GAPDH was used as a loading control. *$p < 0.05$ combined-treated vs. untreated cells. **$p < 0.05$ combined-treated cells transfected with PPARγ RNAi vs. combined-treated cells transfected with control RNAi.

glutathione S-transferase (GST) is located at the mitochondrial membranes, we measured its enzimatic activity in mitochondrial extracts of MCF7, SKBR3 and T47D cells after BRL plus 9RA treatment. Interestingly, GST activity was reduced with respect to untreated cells, while in the presence of Bid RNAi, this effect was no longer noticeable (**Fig. 5A**), addressing that BRL plus 9RA treatment negatively regulates mitochondrial scavenger activity via Bid. Moreover, we estimated the presence of malondialdehyde (MDA), a common end product of lipid peroxidation, as an index of oxidative stress induced by both ligands. As shown in **Figure 5B and C**, the lipid peroxidation was considerably increased by the treatment in both total cellular and mitochondrial extracts of all breast cancer cells.

Discussion

In the present study, we provided the first evidence that low doses of PPARγ and RXR ligands through PPARγ increasing Bid expression and its association with p53 in mitochondria induces apoptosis in different breast carcinoma cells.

The p53 pathway is inactivated in the majority of human cancers, most likely because the pro-apoptotic function of p53 is critical to the inhibition of tumor development and progression. Although the role of p53 as a nuclear transcription factor able to activate or repress a number of p53 transcriptional targets, with the potential to promote or inhibit apoptosis, is clearly established, many evidences support a transcriptional-independent

Figure 3A–C (For D, see following page). Physical association between p53 and BID in breast cancer cells. MCF7, SKBR3 and T47D cells were untreated (-) or treated for 48 hours with BRL plus 9RA. Cytosolic (A), whole mitochondrial (B) and mitochondrial matrix (C) extracts were immunoprecipitated with an antiserum against p53 (IP:p53), and then the immunocomplexes were resolved in SDS-PAGE. The membrane was probed with anti-BID, anti-BAK, anti-PPARγ and anti-RXRα antibodies. To verify equal loading, the membrane was probed with an antibody against p53. One of three similar experiments is presented. MCF7 lysates were used as positive control.

function of p53 in apoptosis. Indeed, an unexpected turn in the p53-mediated pathway to programmed cell death has emerged, with accumulating data indicating that p53 has a direct cytoplasmic role at mitochondria in activating the apoptotic machinery.[20] Thus, a major question is to define the apoptotic function of mitochondrial p53. Increased evidence suggests that mitochondrial p53 localization is sufficient for initiating p53-dependent apoptosis.[22,23] Furthermore, some studies reported that p53 may induce apoptosis by forming complexes with mitochondrial apoptotic proteins, such as Bcl-2/Bcl-x_L,[24] Bad[25] or Bid,[26] which are located in the outer membrane of mitochondria. We hypothesize that mechanistic insight into this process could be obtained from the identification of mitochondrial p53-interacting protein.

The novelty of the present study raises the evidence that, in response to the combined BRL and 9RA treatment in breast cancer cells, we observed a PPARγ-dependent upregulation of Bid expression. Although it has been reported that Bid is transcriptionally regulated by p53,[27] our results address an p53-independent transcriptional regulation of the Bid gene, since we also found increased Bid transcript levels in SKBR3 and T47D breast cancer cells harboring mutated p53. Having demonstrated that PPARγ activation increased both p53 and Bid expression we moved to study their enhanced association in different cellular compartments in response to BRL plus 9RA. Here we showed that p53 interacts with Bid in cytosol and exclusively with the truncated more active tBid in mitochondria, showing a slight increase upon BRL and 9RA treatment.

Bid is a member of the "BH3 domain only" subgroup of Bcl-2 family members proposed to connect proximal death and survival signals to the core apoptotic pathway at the level of the classic family members, which bear multiple BH domains.[28,29] It has been reported that Bid is able to bind mitochondrial proteins and promote cell death, suggesting a model in which Bid served as a "death ligand" which moved from the cytosol to

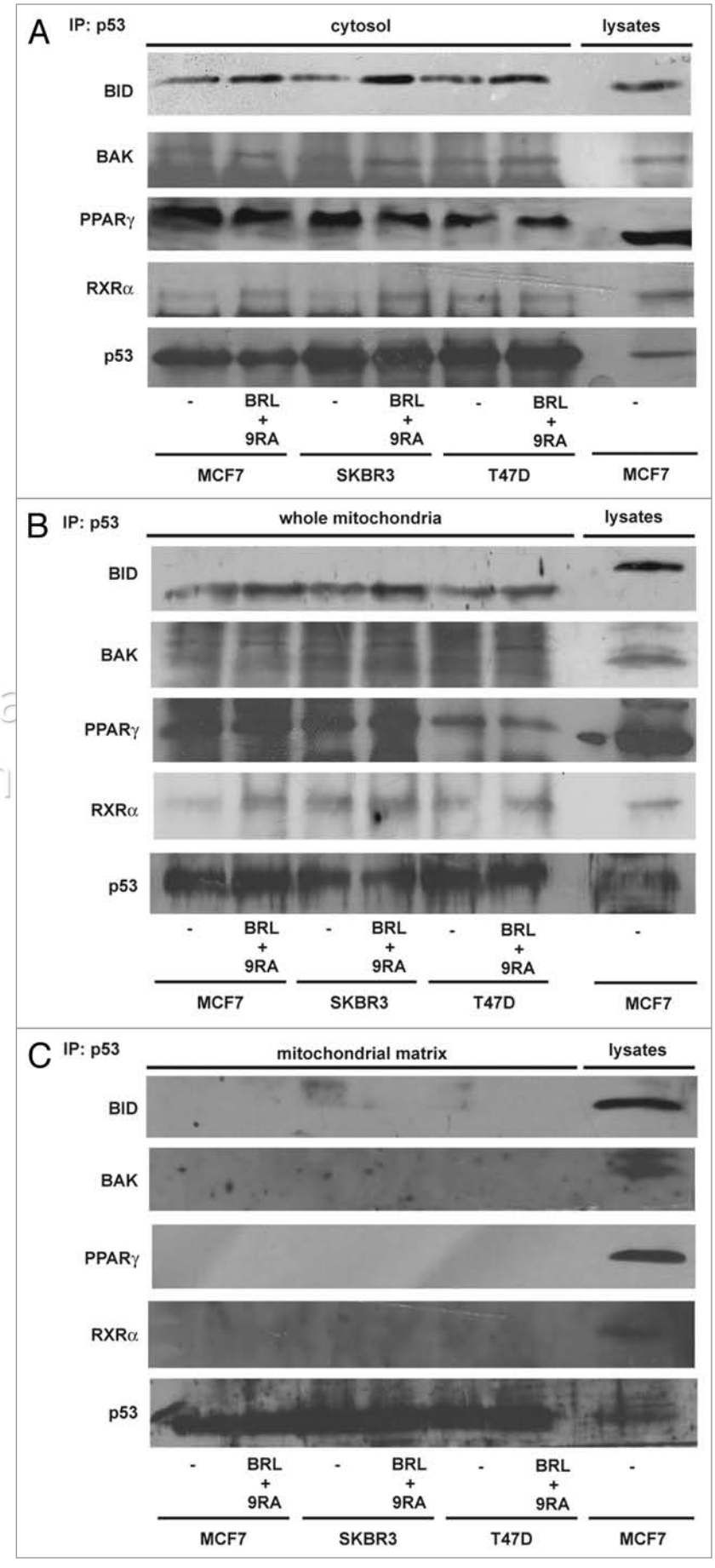

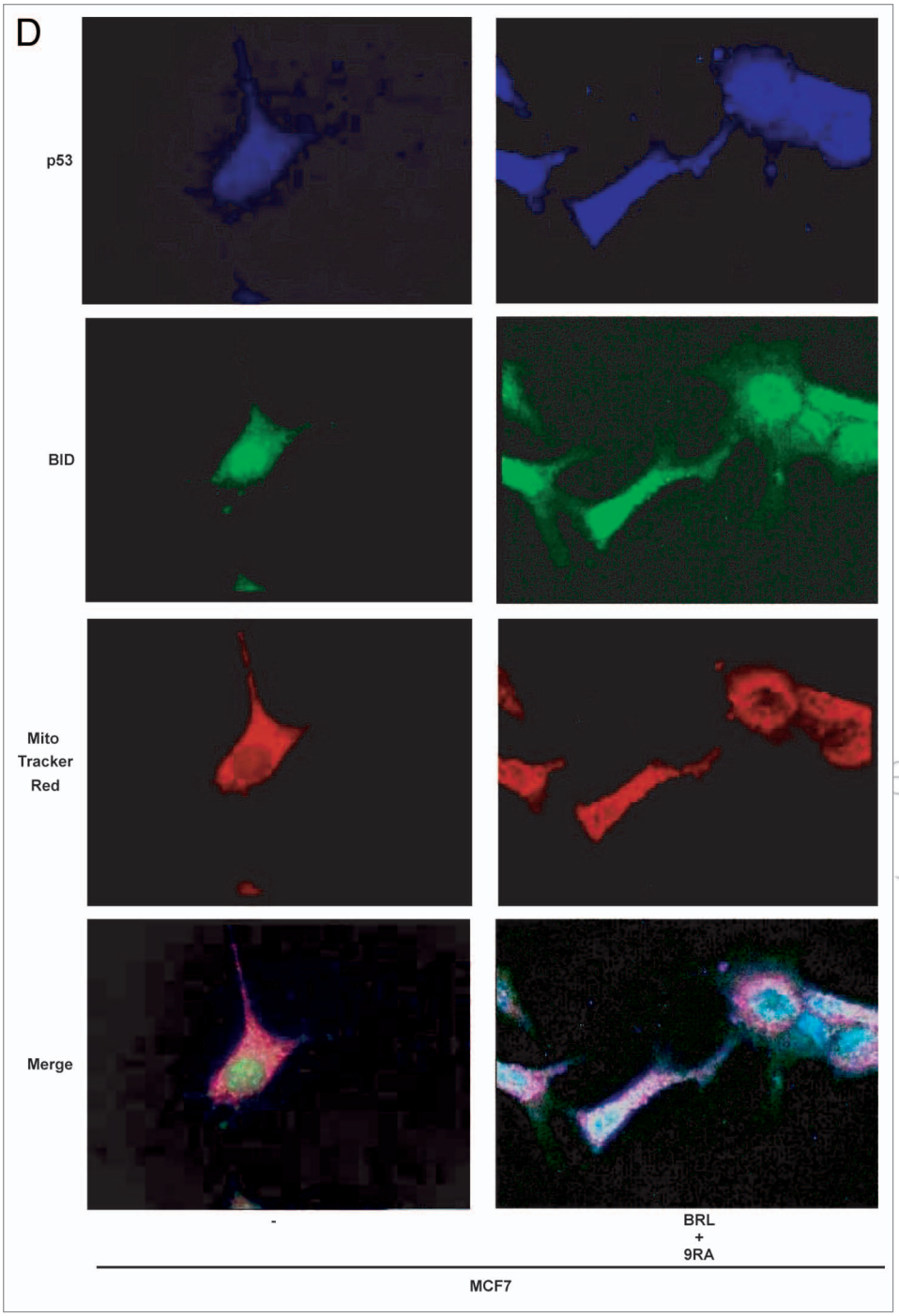

Figure 3D (For A–C, see previous page). Physical association between p53 and BID in breast cancer cells. (D) MCF7 cells untreated (-) or treated with BRL plus 9RA for 48 hours were incubated in MitoTracker Red dye. Cells were immunostained with p53 and BID and then examined by fluorescent microscopy. Blue, p53; green, BID; red, MitoTracker; merge of blue, green and red as expression of co-localization in mitochondria.

the mitochondrial membrane to inactivate Bcl-2 or activate Bax and Bak and to result in cytochrome *c* release.[12] The release of cytochrome *c* from mitochondria has been shown to promote the oligomerization of a cytochrome *c*/Apaf-1/caspase-9 complex that activates caspase-9, resulting in the cleavage of downstream effector caspases.[12] We showed the involvement of Bak protein as a component of a p53/Bid protein-protein interaction in breast cancer cells, hypothesizing that it contributes to form a large pore responsible for triggering apoptotic events.

Given the discovery that nanomolar concentrations of BRL and 9RA upregulate Bid expression in mitochondria, we sought to elucidate the role of Bid in the mitochondrial function of breast cancer cells.

Mitochondria, as a central point of oxidative metabolism, are a major source of intracellular reactive oxygen species (ROS), which cause, sequentially, cellular injury to DNA, protein and lipid peroxidation, followed by loss of cell membrane integrity and leading to cell death.[30] ROS, however, have also been implicated as second messengers in the apoptotic processes.[31] Under normal physiological conditions, cellular ROS generation is controlled by antioxidant enzymes and other small-molecule antioxidants.[32] We observed, upon combined treatment with PPARγ and RXR ligands, a significant reduction of GST enzymatic activity in mitochondrial extracts, which was no longer noticeable after knocking down Bid. These results highlight the crucial role played by Bid might provide a correlation between the mitochondrial dysfunction and the enhanced apoptotic responses of different breast cancer cells to PPARγ and RXR ligands.

The data described above providing new insight into the role of p53/Bid complex at the mitochondria in promoting breast cancer cell apoptosis upon low doses of PPARγ and RXR ligands address Bid as a potential target in the novel therapeutical strategies for breast cancer treatments.

Materials and Methods

Reagents. BRL 49,653 (BRL) was purchased from Alexis (San Diego, CA) and solubilized in DMSO. 9-cis retinoic acid (9RA) was obtained from Sigma-Aldrich (Milan, Italy). 9RA was prepared just before use (Sigma-Aldrich) and diluted into medium at the indicated concentration. All experiments involving 9RA were performed under yellow light, and the tubes and culture plates containing 9RA were

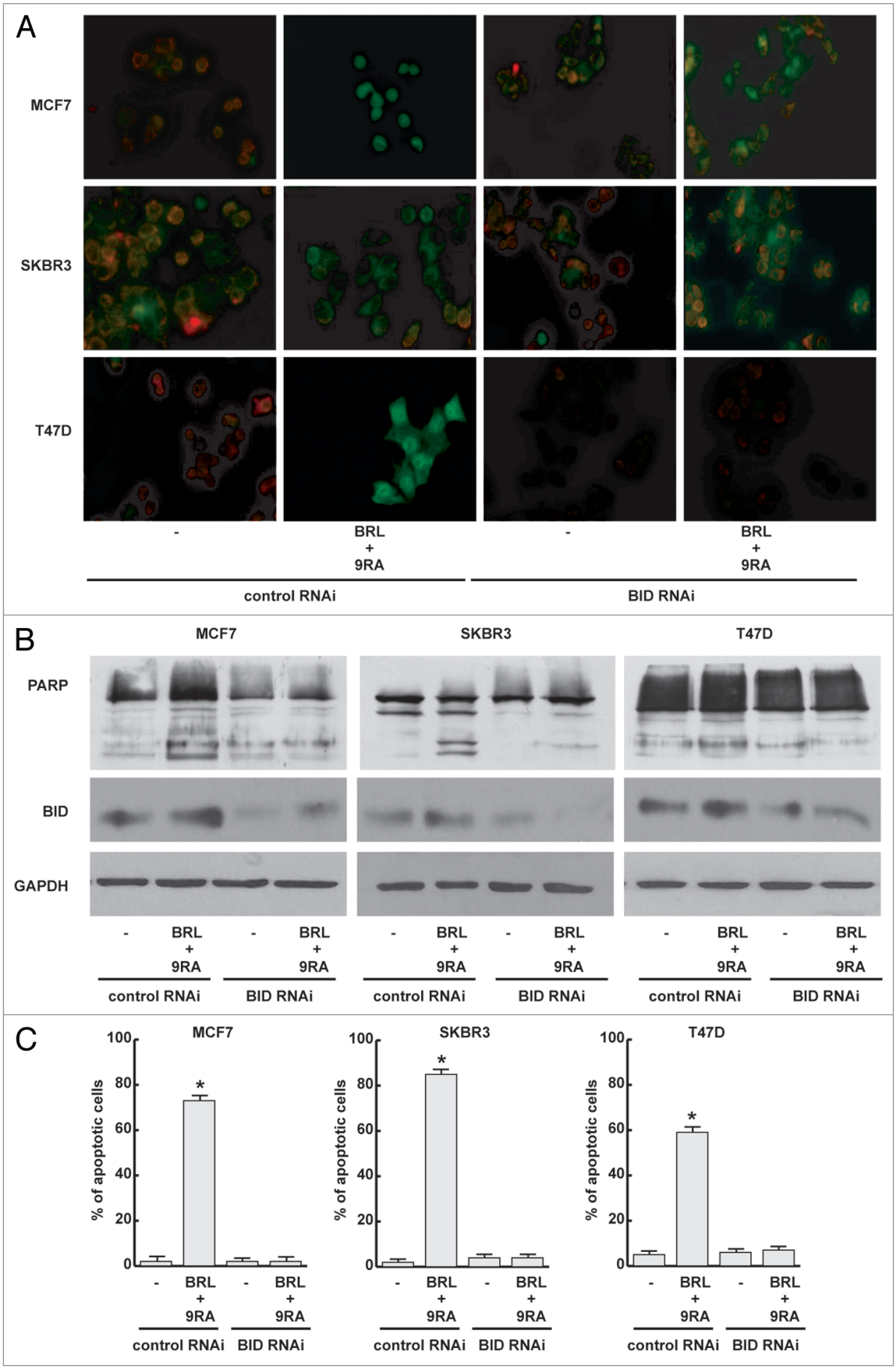

Figure 4. For figure legend, see page 2351.

Figure 4 (See opposite page). Knocking down BID abrogates apoptotic events in breast cancer cells. (A) MCF7, SKBR3 and T47D cells were transfected with control RNAi or with BID RNAi and treated for 48 hours as indicated. The results of JC-1 kit were examined by fluorescent microscopy. (B) Immunoblots of PARP and BID from total extracts of MCF7, SKBR3 and T47D cells transfected and treated as in (A). GAPDH was used as a loading control. One of three similar experiments is presented. (C) Cells were transfected as in (A) and treated for 72 hours as indicated. The histograms show the quantitative representation of data (mean ± SD) of three independent experiments performed in triplicates. *p < 0.05 combined-treated vs. untreated cells.

covered with aluminium foil. Cycloheximide (CX) was obtained from Sigma-Aldrich.

Plasmids. The human wild-type $p21^{WAF1/Cip1}$ promoter-luciferase (luc) reporter was a kind gift from Dr. T. Sakai (Kyoto Prefectural University of Medicine, Kyoto, Japan). As an internal transfection control, we co-transfected the plasmid pRL-CMV (Promega Corp., Milan, Italy), which expresses Renilla luciferase enzymatically distinguishable from firefly luciferase by the strong cytomegalovirus enhancer/promoter.

Cells. Wild-type human breast cancer MCF7 cells were grown in DMEM-F12 plus glutamax containing 5% new-born calf serum (Invitrogen, Milan, Italy) and 1 mg/ml penicillin-streptomycin (P/S). SKBR3 breast cancer cells were grown in RPMI 1640 without red phenol plus glutamax containing 10% fetal bovine serum (FBS) and 1 mg/ml P/S. T47D breast cancer cells were grown in RPMI 1640 with glutamax and red phenol containing 10% FBS, 1 mM sodium pyruvate, 10 mM HEPES, 2.5 g/L glucose, 0.2 U/ml insulin and 1 mg/ml P/S.

Immunoblotting. Cells were grown in 6 cm dishes to 70–80% confluence and exposed to treatments in 1% charcoal-treated (CT)-FBS as indicated. Cells were harvested in cold phosphate-buffered saline (PBS) and resuspended in total ripa buffer containing 1% NP40, 0.5% Na-deoxycholate, 0.1% SDS and inhibitors (0.1 mM sodium orthovanadate, 1% phenylmethylsulfonylfluoride or PMSF, 20 mg/ml aprotinin). Protein concentration was determined by Bio-Rad Protein Assay (Bio-Rad Laboratories, Hercules, CA). A 40 μg portion of total lysates was used for protein gel blotting, resolved on a 11% SDS-polyacrylamide gel, transferred to a nitrocellulose membrane and probed with an antibody directed against the p53 (cat#sc-126), $p21^{WAF1/Cip1}$ (cat#sc-756), PARP (cat#sc-7150), Bid (cat#sc-11423), anti-PPARγ (cat#sc-7196) and anti-RXRα (cat#sc-774) antibodies (Santa Cruz Biotechnology, CA). As internal control, all membranes were subsequently stripped (0.2 M glycine, pH 2.6, for 30 min at room temperature) of the first antibody and reprobed with anti-GAPDH antibody (cat#sc-25778, Santa Cruz Biotechnology). The antigen-antibody complex was detected by incubation of the membranes for 1 h at room temperature with peroxidase-coupled goat anti-mouse or anti-rabbit IgG and revealed using the enhanced chemiluminescence system (Amersham Pharmacia, Buckinghamshire UK). Blots were then exposed to film (Kodak film, Sigma). The intensity of bands representing relevant proteins was measured by Scion Image laser densitometry scanning program.

To obtain cytosolic and total mitochondrial fraction of proteins, cells were grown in 10 cm dishes to 70–80% confluence and exposed to treatments as for 48 h. Cells were harvested by centrifugation at 2,500 rpm for 10 min at 4°C. The pellets were suspended in 250 μl of RIPA buffer plus 10 μg/ml aprotinin, 50 mM PMSF and 50 mM sodium orthovanadate, and then 0.1% digitonine (final concentration) was added. Cells were incubated for 15 min at 4°C and centrifuged at 3,000 rpm for 10 min at 4°C. Supernatants were collected and further centrifuged at 14,000 rpm for 10 min at 4°C. The supernatant, containing cytosolic fraction of proteins, was collected, while the resulting mitochondrial pellet was resuspended in 3% Triton X-100, 20 mM Na_2SO_4, 10 mM PIPES and 1 mM EDTA, pH 7.2, incubated for 15 min at 4°C and centrifuged at 12,000 rpm for 10 min at 4°C. Alternatively, to provide matrix mitochondrial fraction of proteins, mitochondrial pellet was further solubilized in 6% of digitonine in RIPA buffer, for 10 min at 4°C then centrifuged at 14,000 rpm, 4°C, 10 min. The pellets (mitoplasts) were then lysed osmotically and centrifuged at 14,000 rpm 4°C for 10 min to discard the membrane residues and recover the soluble matrix content. Proteins of the mitochondrial and cytosolic fractions were determined by Bio-Rad Protein Assay (Bio-Rad Laboratories). Equal amounts of cytosolic and mitochondrial proteins (40 μg) were resolved by 11% SDS-PAGE, electrotransferred to nitrocellulose membranes and probed with antibodies directed against Bid, Bad (cat#sc-8044) and $BCL\text{-}X_L$ (cat#sc-7195) (Santa Cruz Biotechnology). For the internal loading, all membranes were stripped and reprobed with anti GAPDH (Santa Cruz Biotechnology) antibody.

Immunoprecipitation. 300 μg of mitochondrial and cytosolic proteins were incubated overnight with anti-p53 (cat#sc-126) or anti-Bid (cat#sc-135847) antibodies (Santa Cruz Biotechnology) and 500 μL of HNTG (immunoprecipitation) buffer [50 mmol/L HEPES (pH 7.4), 50 mmol/L NaCl, 0.1% Triton X-100, 10% glycerol, 1 mmol/L phenylmethylsulfonyl fluoride, 10 μg/mL leupeptin, 10 μg/mL aprotinin, 2 μg/mL pepstatin]. Immunocomplexes were recovered by incubation with protein A/G-agarose. The immunoprecipitates were centrifuged, washed twice with HNTG buffer and then used for protein gel blotting. Membranes were probed with anti-p53 (cat#sc-6243), anti-Bid (cat#sc-11423), anti-Bak (cat#sc-832), anti-Bax (cat#sc-7480), anti-PPARγ (cat#sc-7196) and anti-RXRα (cat#sc-774) antibodies (Santa Cruz Biotechnology).

Real-time (RT)-PCR. MCF7, SKBR3 and T47D cells were grown in 10 cm dishes to 70–80% confluence and exposed to treatments in 1% CT-FBS as indicated. Total cellular RNA was extracted using TRIZOL reagent (Invitrogen) as suggested by the manufacturer. The RNA sample was treated with DNase I (Ambion, Austin, TX), and purity and integrity of the RNA was confirmed both spectroscopically and electrophoretically. RNA was then reversed transcribed with High Capacity cDNA Reverse Transcription Kit (Applied Biosystems, Applera Italia, Monza, Milano, Italy). The evaluation of p53, $p21^{WAF1/Cip1}$ and the internal control gene 36B4 was performed using the RT-PCR method with the following primers: 5'-CCA GTG TGA TGA TGG TGA GG-3' (p53 forward) and 5-GCT TCA TGC CAG CTA

CTT CC-3 (p53 reverse), 5'-CTG TGC TCA CTT CAG GGT CA-3' (p21 forward) and 5'-CTC AAC ATC TCC CCC TTC-3' (p21 reverse), 5'-CTC AAC ATC TCC CCC TTC TC-3' (36B4 forward) and 5'-CAA ATC CCA TAT CCT CGT CC-3' (36B4 reverse) to yield, respectively, products of 190 bp with 18 cycles, 270 bp with 18 cycles and 408 bp with 18 cycles. The results obtained as optical density arbitrary values were transformed to percentage of the control (percent control) taking the samples from untreated cells as 100%.

Analysis of p53 and Bid gene expression was performed using Real-time reverse transcription PCR. cDNA was diluted 1:3 in nuclease-free water, and 5 μl were analyzed in triplicates by real-time PCR in an iCycler iQ Detection System (Bio-Rad) using SYBR Green Universal PCR Master Mix with 0.1 mmol/l of each primer in a total volume of 30 μl reaction mixture following the manufacturer's recommendations. Each sample was normalized on its GAPDH mRNA content. Relative gene expression levels were normalized to the basal, untreated sample chosen as calibrator. Final results are expressed as folds of difference in gene expression relative to GAPDH mRNA and calibrator, calculated following the ΔCt method, as follows:

Relative expression (folds) = $2^{-(\Delta Ctsample - \Delta Ctcalibrator)}$ where ΔCt values of the sample and calibrator were determined by subtracting the average Ct value of the GAPDH mRNA reference gene from the average Ct value of the analyzed gene. For p53, Bid and GAPDH the primers were: 5'-GCT GCT CAG ATA GCG ATG GTC-3' (p53 forward) and 5-CTC CCA GGA CAG GCA CAA ACA-3 (p53 reverse), 5'-CCA TGG ACT GTG AGG TCA AC-3' (Bid forward) and 5'-CTT TGG AGG AAG CCA AAC AC-3' (Bid reverse), 5'-CCC ACT CCT CCA CCT TTG AC-3' (GAPDH forward), 5'-TGT TGC TGT AGC CAA ATT CGT-3' (GAPDH reverse). Negative controls contained water instead of first strand cDNA.

Transient transfection assay. SKBR3 and T47D cells were transferred into 24-well plates with 500 μl of regular growth medium/well the day before transfection. The medium was replaced with 1% CT-FBS on the day of transfection, which was performed using Fugene 6 reagent as recommended by the manufacturer (Roche Diagnostics, Mannheim, Germany), with a mixture containing 0.5 μg of p21 promoter-luc plasmid and 10 ng of pRL-CMV. After transfection for 24 h, treatments were added in 1% CT-FBS, and cells were incubated for an additional 24 h. Firefly and Renilla luciferase activities were measured using the Dual Luciferase Kit (Promega).

RNA interference (RNAi). Cells were plated in 10 cm dishes with regular growth medium the day before transfection to 60–70% confluence. On the second day, the medium was changed with 1% CT-FBS without P/S, and cells were transfected with stealth RNAi targeted human Bid mRNA sequence -5'-UGC GGU UGC CAU CAG UCU GCA GCU C-3' (Invitrogen), with a stealth RNAi targeted human PPARγ mRNA sequence 5'-AGA AUA AUA AGG UGG AGA UGC AGG C-3' (Invitrogen), a stealth RNAi targeted human RXRα mRNA sequence 5'-UCG UCC UCU UUA ACC CUG ACU CCA A-3' or with a stealth RNAi-negative control (Invitrogen) to a final concentration of 100 nM using Lipofectamine 2000 (Invitrogen) as recommended by the manufacturer. After 5 h, the transfection medium was changed with complete 1% CT-FBS with P/S; in order to avoid Lipofectamine 2000 toxicity, cells were exposed to combined treatment and subjected to different experiments.

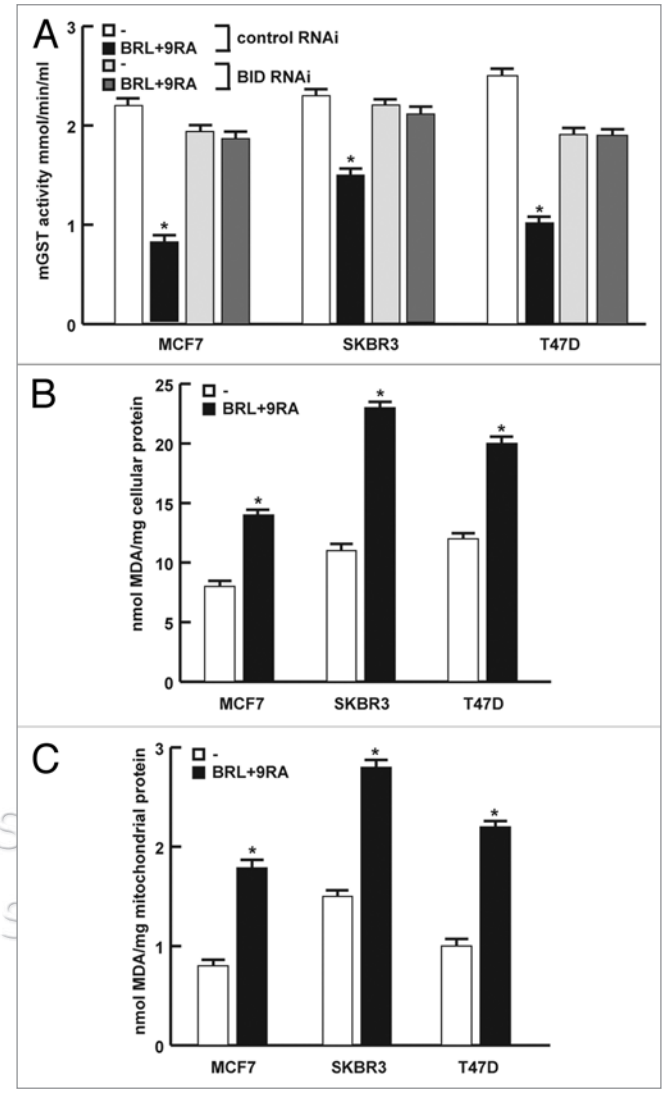

Figure 5. BRL and 9RA reduce glutathione S-transferase (GST) antioxidative enzyme activity and induce lipid peroxidation in breast cancer cells. (A) Glutathione S-transferase activity from mitochondrial extracts (mGST) of MCF7, SKBR3 and T47D cells transfected with control RNAi or with BID RNAi and treated for 24 hours as indicated. (B) Lipid peroxidation from total and (C) mitochondrial cell extracts of all breast cancer cells treated for 48 h as indicated. *p < 0.05 combined-treated vs. untreated cells. MDA, Malondialdehyde.

Immunofluorescence. MCF7 cells were plated in 6 cm dishes in complete growth medium. On the second day, the medium was changed with 1% CT-FBS, and cells were treated with BRL plus 9RA for 48 h. p53 and Bid staining was carried out using anti-p53 and anti-Bid primary antibodies followed by Alexa-fluo 350 (blue) and Alexa-fluo 488 (green) (Invitrogen) as secondary antibodies, respectively. Mitochondria were stained with MitoTracker mitochondrion selective probe (cat#MP07510,

Invitrogen) according to manufacturer's instructions. The images were acquired using fluorescent microscopy (Leica AF6000).

JC-1 mitochondrial membrane potential detection assay. Alteration of mitochondrial membrane potential was detected using the dye 5,5',6,6'-tetra-chloro-1,1',3,3'-tetraethylbenzimidazolyl-carbocyanine iodide (JC-1) as recommended by the manufacturer's instruction (Biotium, Hayward). MCF7, SKBR3 and T47D cells were grown in 10 cm dishes, transfected with control RNAi or Bid RNAi and then treated with BRL and 9RA for 56 h in 1% CT-FBS. Subsequently, cells were washed in ice-cold PBS and incubated with 10 mM JC-1 at 37°C in a 5% CO_2 incubator for 20 min in darkness. Subsequently, cells were extensively washed with PBS and analyzed by fluorescence microscopy. The red form has an absorption/emission maxima of 585/590 nm. The green monomeric form has absorption/emission maxima of 510/527 nm.

TUNEL assay. Apoptosis was determined by enzymatic labeling of DNA strand breaks using terminal deoxynucleotidyl transferase-mediated deoxyuridine triphosphate nick end-labeling (TUNEL). TUNEL labeling was conducted using APO-BrdU™ TUNEL Assay Kit (Invitrogen) and performed according to the manufacturer's instructions. Briefly, cells were trypsinized after treatments and resuspended in 0.5 ml of PBS. After fixation with 1% paraformaldehyde for 15 min on ice, cells were incubated on ice-cold 70% ethanol overnight. After washing twice with washing buffer for 5 min, the labeling reaction was performed using terminal deoxynucleotidyl transferase end-labeling cocktail for each sample and incubated for 1 h at 37°C. After rinsing, cells were incubated with antibody staining solution prepared with Alexa Fluor 488 dye-labeled anti-BrdU for 30 min at room temperature. Subsequently 0.5 mL of propidium iodide/RNase A buffer were added for each sample. Cells were incubated 30 min at room temperature, protected from light, analyzed and photographed by using a fluorescent microscope.

GST antioxidant enzyme activity and lipid peroxidation. To measure mitochondrial glutathione S-transferase (GST) activity, the mitochondrial suspension was used. Enzyme activity was detected according to the method provided by the manufacturer (Sigma Aldrich). To evaluate lipid peroxidation, cells were sonicated in PBS, and the crude homogenate was used. The level of lipid peroxidation in control as well as treated cell samples was assayed through the formation of thiobarbituric acid reactive species (TBARS) during an acid-heating reaction as previously described in reference 33. Briefly, the samples were mixed with 1 ml of 10% trichloroacetic acid (TCA) and 1 ml of 0.67% thiobarbituric acid (TBA) then heated in a boiling water bath for 15 min. TBARS were determined by the absorbance at 535 nm and were expressed as malondialdehyde equivalents (MDA) (nmol/mg protein) respect to cellular and mitochondrial.

Statistical analyses. Each datum point represents the mean ± SD of three different experiments. Statistical analysis was performed using ANOVA followed by Newman-Keuls testing to determine differences in means. $p < 0.05$ was considered as statistically significant.

Acknowledgments

We thank Dr. Maureen A. Kane for English revision.

Financial Support

This work was supported by AIRC, Foundation Lilli Funaro, MURST and Ex 60%.

Note

Supplemental materials can be found at:
www.landesbioscience.com/journals/cc/article/15917

References

1. Clarke AR, Purdie CA, Harrison DJ, Morris RG, Bird CC, Hooper ML, et al. Thymocyte apoptosis induced by p53-dependent and independent pathways. Nature 1993; 362:849-52.
2. Lowe SW, Schmitt EM, Smith SW, Osborne BA, Jacks T. p53 is required for radiation-induced apoptosis in mouse thymocytes. Nature 1993; 362:847-9.
3. Lowe SW, Bodis S, McClatchey A, Remington L, Ruley HE, Fisher DE, et al. p53 status and the efficacy of cancer therapy in vivo. Science 1994; 266:807-10.
4. El-Deiry WS. Insights into cancer therapeutic design based on p53 and TRAIL receptor signaling. Cell Death Differ 2001; 8:1066-75.
5. Caelles C, Helmberg A, Karin M. p53-dependent apoptosis in the absence of transcriptional activation of p53-target genes. Nature 1994; 370:220-3.
6. Haupt Y, Rowan S, Shaulian E, Vousden KH, Oren M. Induction of apoptosis in HeLa cells by trans-activation-deficient p53. Genes Dev 1995; 9:2170-83.
7. Ding HF, Lin YL, McGill G, Juo P, Zhu H, Blenis J, et al. Essential role for caspase-8 in transcription-independent apoptosis triggered by p53. J Biol Chem 2000; 275:38905-11.
8. Chipuk JE, Maurer U, Green DR, Schuler M. Pharmacologic activation of p53 elicits Bax-dependent apoptosis in the absence of transcription. Cancer Cell 2003; 4:371-81.
9. Chipuk JE, Kuwana T, Bouchier-Hayes L, Droin NM, Newmeyer DD, Schuler M, et al. Direct activation of Bax by p53 mediates mitochondrial membrane permeabilization and apoptosis. Science 2004; 303:1010-4.
10. Wei MC, Zong WX, Cheng EH, Lindsten T, Panoutsakopoulou V, Ross AJ, et al. Proapoptotic BAX and BAK: A requisite gateway to mitochondrial dysfunction and death. Science 2001; 292:727-30.
11. Wei MC, Lindsten T, Mootha VK, Weiler S, Gross A, Ashiya M, et al. tBID, a membrane-targeted death ligand, oligomerizes BAK to release cytochrome *c*. Genes Dev 2000; 14:2060-71.
12. Korsmeyer SJ, Wei MC, Saito M, Weiler S, Oh KJ, Schlesinger PH. Pro-apoptotic cascade activates BID, which oligomerizes BAK or BAX into pores that result in the release of cytochrome *c*. Cell Death Differ 2000; 7:1166-73.
13. Bonofiglio D, Cione E, Qi H, Pingitore A, Perri M, Catalano S, et al. Combined low doses of PPARgamma and RXR ligands trigger an intrinsic apoptotic pathway in human breast cancer cells. Am J Pathol 2009; 175:1270-80.
14. Levine AJ. p53, the cellular gatekeeper for growth and division. Cell 1997; 88:323-31.
15. Hansen R, Oren M. p53; from inductive signal to cellular effect. Curr Opin Genet Dev 1997; 7:46-51.
16. Oren M. Regulation of the p53 tumor suppressor protein. J Biol Chem 1999; 274:36031-4.
17. Chung SH, Onoda N, Ishikawa T, Ogisawa K, Takenaka C, Yano Y, et al. Peroxisome proliferator-activated receptor gamma activition induce cell cycle arrest via p53-independent pathway in human anaplastic thyroid cancer cells. Jap J Cancer Res 2002; 93:1358-65.
18. Hong J, Samudio I, Liu S, Abdelrahim M, Safe S. Peroxisome proliferator-activited receptor γ-dependent activation of p21 in panc-28 pancreatic cancer cells involves Sp1 and Sp4 proteins. Endocrinology 2004; 145:5774-85.
19. Bonofiglio D, Qi H, Gabriele S, Catalano S, Aquila S, Belmonte M, et al. Peroxisome proliferator-activated receptor-gamma inhibits follicular and anaplastic thyroid carcinoma cells growth by upregulating $p21^{Cip/WAF1}$ in a Sp1-dependent manner. Endocr Relat Cancer 2008; 15:545-57.
20. Murphy ME, Leu JIJ, George DL. p53 moves to mitochondria. A turn on the path to apoptosis. Cell Cycle 2004; 3:836-9.
21. Bonofiglio D, Aquila S, Catalano S, Gabriele S, Belmonte M, Middea E, et al. Peroxisome proliferator-activated receptor-gamma activates p53 gene promoter binding to the nuclear factor-kappaB sequence in human MCF7 breast cancer cells. Mol Endocrinol 2006; 20:3083-92.
22. Marchenko ND, Zaika A, Moll UM. Death signal-induced localization of p53 protein to mitochondria. A potential role in apoptotic signaling. J Biol Chem 2000; 275:16202-12.

23. Katsumoto T, Higaki K, Ohno K, Onodera K. Cell cycle dependent biosynthesis and localization of p53 protein in untransformed human cells. Biol Cell 1995; 84:167-73.
24. Mihara M, Erster S, Zaika A, Petrenko O, Chittenden T, Pancoska P, et al. p53 has a direct apoptogenic role at the mitochondria. Mol Cell 2003; 11:577-90.
25. Jiang P, Du WJ, Heese K, Wu M. The Bad Guy Cooperates with Good Cop p53: Bad is transcriptionally upregulated by p53 and forms a Bad/p53 complex at the mitochondria to induce apoptosis. Mol Cell Biol 2006; 26:9071-82.
26. Song G, Chen GG, Yun JP, Lai PB. Association of p53 with Bid induces cell death in response to etoposide treatment in hepatocellular carcinoma. Curr Cancer Drug Targets 2009; 9:871-80.
27. Sax JK, Fei P, Murphy ME, Bernhard E, Korsmeyer SJ, El-Deiry WS. BID regulation by p53 contributes to chemosensitivity. Nat Cell Biol 2002; 4:842-9.
28. Adams JM, Cory S. The Bcl-2 protein family: arbiters of cell survival. Science 1998; 281:1322-6.
29. Gross A, McDonnell JM, Korsmeyer SJ. BCL-2 family members and the mitochondria in apoptosis. Genes Dev 1999; 13:1899-911.
30. Pelicano H, Carney D, Huang P. ROS stress in cancer cells and therapeutic implications. Drug Resistance Updates 2004; 7:97-110.
31. Simon HU, Haj-Yehia A, Levi-Schaffer F. Role of reactive oxygen species (ROS) in apoptosis induction. Apoptosis 2000; 5:415-8.
32. Fruehauf JP, Meyskens FL Jr. Reactive oxygen species: A breath of life or death? Clin Cancer Res 2007; 13:789-94.
33. Ohkawa H, Ohishi N, Yagi K. Assay for lipid peroxides in animal tissues by thiobarbituric acid reaction. Anal Biochem 1979; 95:351-8.